Dissertation
submitted to the
Combined Faculties for the Natural Sciences and for Mathematics
of the Ruperto-Carola University of Heidelberg, Germany
for the degree of
Doctor of Natural Sciences

presented by

Dipl.-Ing. (FH) Ines Brückmann
born in: Heidelberg (Baden-Württemberg)

Effects of c-Myc overexpression in osteoblasts on bone homeostasis, sarcoma formation and dormant hematopoietic stem cell maintenance

Referees: Prof. Dr. Andreas Trumpp

Prof. Dr. Jan Lohmann

Submitted: 27. September 2012

Oral-examination: 22. November 2012

TABLE OF CONTENTS

LIST OF FIGURES

LIST OF TABLES

1 SUMMARY

The transcription factor c-Myc is an important proto-oncogene and its expression is induced by a variety of mitogenic signals promoting cell proliferation, cell growth and stem cell maintenance while concomitantely inhibiting terminal differentiation. In order to elucidate the role of c-Myc in the HSC niche, a doxycycline-inducible double transgenic *ColtTA;TreMyc* mouse model was used to conditionally overexpress human c-Myc in endosteal niche osteoblasts (mutant; mt). These mice display developmental bone disorders with signs of osteopetrosis. The animals developed thicker bones with concomitantly increased amounts of osteoblasts and osteoclasts. In addition the structure of the compact bone compartment was interrupted with cavernal structures, filled with ectopic bone marrow. qPCR analysis revealed that the expression of the cell cycle inhibitor $p57^{KIP2}$ was significantly lower in mutant osteoblasts, suggesting that c-Myc dependent down-regulation of the cell cylce inhibitor induced elevated cell proliferation of mutant osteoblasts resulting in a higher bone-turnover. Most strikingly, the elevated bone remodeling caused a fast reduction of dormant hematopoietic stem cells (dHSCs), known to harbor the most potent HSCs. BrdU-label retaining assays revealed similar turnover kinetics for dormant and homeostatic HSCs, both dividing every 58 days in mutant animals. These data suggest that dHSC are not maintained in mutant animals. Besides decreased numbers in dHSCs a simultaneous decrease of long- and short-term HSCs (LT-, ST-HSCs) was observed, while the number of more differentiated progenitor and mature cells did not differ between mutant and control mice. Interestingly, dHSC loss appeared to be compensated by elevated Bmi1 expression and down-regulated $p16^{INK4a}$ cell cycle inhibitor in cycling LT-HSCs in order to prevent their premature depletion. Interestingly, HSC differentiation capacity in mutant mice was not impaired and the bone marrow reconstitution ability of mutant HSCs after bone marrow transplantation was also normal. Notably, the proportion of LT- and ST-HSCs was significantly decreased in recipients of primary and secondary bone marrow transplantations, indicating that only the number but not self-renewal and differentiation capacities of HSCs were reduced in c-Myc overexpressing mice. Interestingly, unlike wild type HSCs, HSCs from double transgenic

animals could not be efficiently activated by the HSC activators dsRNA PolyI:C or lipopolysaccharide (LPS).

Strikingly, 26% of transgenic *ColtTA;TreMyc* animals developed osteosarcoma often associated with simultaneous lung and liver metastasis. Analysis of osteoblasts from tumor bearing mice revealed high similarities to human osteosarcoma, with the tumor osteoblasts displaying an immature osteoblastic phenotype with deregulated Wnt signaling and high expression of the tyrosine kinase receptor c-Kit. Interestingly it was recently shown that c-Kit is expressed in human osteosarcomas and that its expression negatively correlates with patient survival. Thus this mouse model system might be an interesting tool for further pre-clinical studies, as it is the first osteosarcoma model with spontaneous tumor development closely resembling human osteoblastic osteosarcoma. Finally, our model highlights the important cross-talk between endosteal osteoblasts, hematopoietic stem cells and tumorigenesis, which are also found deregulated in a variety of human bone marrow diseases. The mouse model generated and characterized in this work may facilitate to elucidate the complex molecular and cellular mechanisms operative in the diseased organism and may be used to the development of novel intervention strategies.

2 ZUSAMMENFASSUNG

Eines der wichtigsten Proto-onkogene im Menschen ist der Transkriptionsfaktor c-Myc. Die Expression von c-Myc wird durch eine Vielzahl mitogener Signale induziert und spielt eine wichtige Rolle in der Regulation von Zellteilung, Wachstum, terminaler Differenzierung und Stammzellerhaltung. Die genaue Funktion des Transkriptionsfaktors hängt dabei stark vom jeweiligen Zelltyp ab. Um die Funktion von c-Myc in ausgereiften Osteoblasten im Knochen genauer beschreiben zu können, verwendeten wir das transgene Mausmodell *ColtTA;TreMyc* (Mutante; mt), in dem die Expression von humanem c-Myc über den Collagen I Promotor reguliert wird. Durch die Überexpression von c-Myc kam es zunächst zu schweren Entwicklungsstörungen des Knochens mit Anzeichen von Osteopetrose, d.h. sichtbar verdickten Knochen mit einem erhöhten Anteil an Osteoblasten und Osteoklasten. Die kompakte Hartsubstanz der Knochen war jedoch völlig mit Knochenmarkeinschlüssen durchzogen und führte zur Erhöhung der Knochenbrüchigkeit. Verstärktes Ostenblastenwachstum und erhöhte Umbaufrequenz sind wahrscheinlich Folge der verminderten Expression des Zellzyklus-Inhibitors $p57^{KIP2}$. Interessanterweise führte diese verstärkte Knochenumstrukturierung zu einer drastischen Abnahme der potentesten Stammzellpopulation des hämatopoetischen Systems, der sogenannten ruhenden Stammzellen (dormant, dHSCs). Analyse der Zellteilungsrate zeigte, dass sich aktivierte und ruhende Stammzellen in den mutanten Mäusen im Schnitt nach 58 Tagen teilen, d.h dass im transgenen Mausmodell keine ruhenden Stammzellen mehr vorhanden sind. Dieser Verlust der dHSC Population ging mit einer erhöhten Expression von Bmi1 und gleichzeitiger Herunterregulierung des Zellzyklus-Inhibitors $p16^{INK4a}$ in LT-HSCs einher. Möglicherweise um so den stetigen Verlust der Zellen nach erneuter Zellteilung zu verhindern. Zusätzlich sind weniger homeostatische Stammzellen (LT-, ST-HSC) vorhanden, die sich auch nach Knochenmarkstransplantationen der HSCs in immunkomprimierte Mäuse widerspiegelte. Wohingegen keine Unterschiede in der terminalen Differenzierung vorlagen. Dies zeigt, dass allein die Anzahl der HSCs, jedoch nicht ihre Fähigkeit zur Selbsterneuerung und Differenzierungsfähigkeiten in den

transgenen *ColtTA;TreMyc* Mäusen beeinträchtigt waren. HSCs können in Stresssituationen wie bakteriellen oder viralen Infektionen schnell aktiviert werden, teilweise durch das Zytokin IFNα. Interessanterweise konnten Stammzellen von transgenen Mäusen weder durch die Injektion der dsRNA Poly-I:C, welches zur Produktion von IFNα führt, noch durch LPS Injektion aktiviert werden.

Zusätzlich entwickelten sich in 26% der transgenen Tiere Osteosarkome, die in Lunge und Leber metastasierten, und eine große Ähnlichkeit zu humanen Osteosarkomen aufwiesen. Insbesondere waren die Tumor-Osteoblasten genau wie in humanen Osteosarkomen undifferenziert und zeigten einige Eigenschaften unreifer Osteoblasten, sowie eine Deregulierung des Wnt-Signalweges und erhöhte Expression des Tyrosin-Kinase-Rezeptors c-Kit. Erst kürzlich wurde gezeigt, dass in humanen Osteosarkomen ein Zusammenhang zwischen c-Kit Expression und der Überlebensdauer der Patienten besteht. Zusammengefasst handelt es sich bei dem vorliegenden Maus-Modell um das erste Osteosarkom-Modell, in dem Tumore wie beim Patienten spontan entstehen. Es eignet sich daher gut als Testmodell zur Erforschung neuer Tumor-Therapien gegen Osteosarkome. Darüber hinaus ermöglicht das Mausmodell die genauere Analyse der hämatopoetischen Stammzell-Nische und der Interaktion zwischen Osteoblasten und HSCs, die in einer Vielzahl von humanen Erkrankungen gestört ist. Dadurch können Regulationsmechanismen und Krankheitsentstehung besser untersucht und moduliert werden.

3 Introduction

3.1 The Myc family of proto-oncogenes

Human c-Myc is a transcription factor that is involved in the regulation of about 10-15% of all human genes (Kim, et al., 2008; Li, et al., 2003; Coller, et al., 2000). In addition it is a major proto-oncogene, which is found deregulated in about 60% of human cancers e.g. breast, colon, lymphoma (Gómez-Casares, et al., 2012; Eilers, et al., 2008). The Myc family consists of three members, c-Myc, N-Myc and L-Myc, which share an overall homology of about 80%. Functionally the Myc proteins are transcription factors that bind the so-called E-Box (CACGTG) via a helix-loop-helix domain (Dang, et al., 1999; Lee and Reddy, 1999; Fisher, et al., 1992; DePinho, et al., 1987). In this group of transcription factors, c-Myc is the best characterized and was identified by Ivanov, et al., 1964 as a homolog of v-Myc, a viral inducer of leukemia in chicken (Atchley and Fitch, 1995). However c-Myc is not only a relatively weak transactivator, but also has other, not yet fully understood functions (Koch, et al., 2007). Activation of c-Myc occurs through mitogenic signals e.g. via Wnt. Upon binding of Wnt to its cellular receptors, a cellular complex including Dishevelled (Dsh) and Axin is formed, which then complexes with Adenomatous-polyposis-coli (APC). APC is normally bound to ß-catenin and is recruited to this complex only upon Wnt-signalling. Thus ß-catenin is set free, accumulates in the cytoplasm and then migrates to the nucleus where it induces the expression of c-Myc (Dang, et al., 1999).

While c-Myc occurs in most tissues and seems to be important for embryonic patterning, L-Myc was identified by Nau, et al., 1985 to associate with human small cell lung cancer (SCLC). N-Myc plays a pivotal role in embryonic development, especially during neurogenesis and is highly amplified in neuroblastoma (Knoepfler, et al., 2002; Stanton, et al., 1992; Kohl, et al., 1984; Schwab, et al., 1983).

Transcriptional functionality in Myc is controlled by interaction via a leucine zipper with the Myc-associated factor X (Max) (Blackwood and Eisenman, et al., 1991; Kato, et al., 1991). In the presence of Myc, the Myc-Max heterodimer activates transcription while in the absence of Myc, Max associates with the family of Mad proteins (Mad1, Mxi1 (Mad2), Mad3, Mad4 and Mnt) that functionally repress transcription (Quéva, et al., 1998; Ayer, et al., 1993; Zervos, et al., 1993). The Myc-Max complex mainly drives cell proliferation (Blackwood, et al., 1992; Littlewood, et al., 1990), while Max-Mad interactions show the opposite effect, and inhibit cell growth (Zhou, et al., 2001; Grandori, et al., 2000). This is mainly the reason for Max expression in resting and differentiated cell populations (Lüscher and Larsson, et al., 1999) (Figure 1).

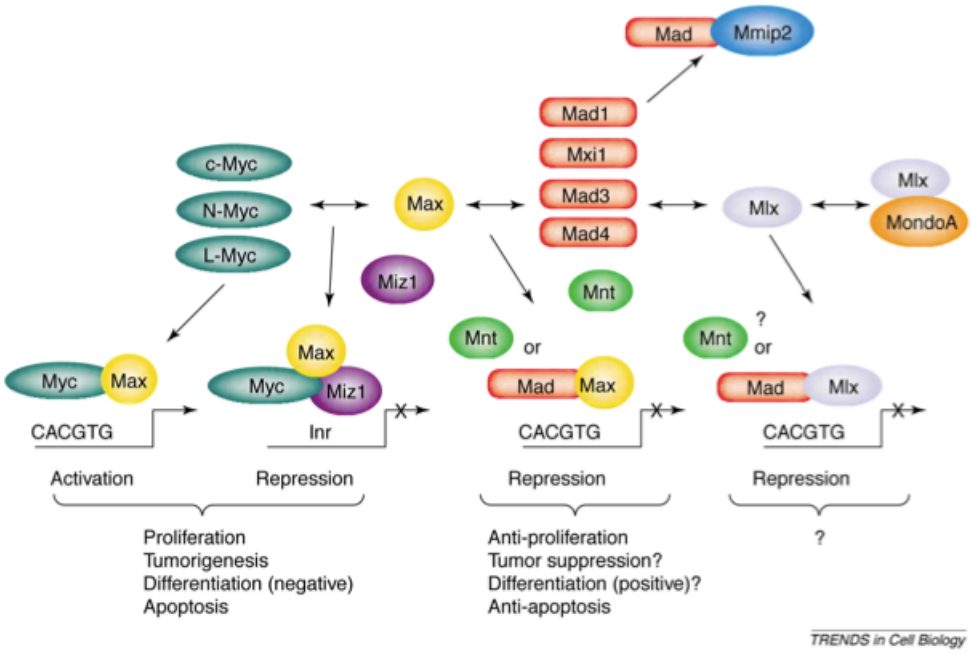

Figure 1: Model for Myc and Mad protein interactions
Overview of Myc and Mad protein interaction partners and their repressors. The Myc-Max heterodimer binds to E-Box sequence and results in transcriptional activation while the Myc-Max-Miz1 complex binds to initiator sequence elements (Inr) to repress Myc target gene expression. Either Mad-Max heterodimer or Mad-Mlx dimers repress transcriptional activity (Lüscher and Larsson, et al., 1999).

The biological roles of c-Myc are mainly focused on cell cycle control, apoptosis and differentiation, but are very complex as c-Myc deletion or ectopic expression has yielded many diverse effects (Eilers, et al., 2008; Adhikary and Eilers, 2005; Eisenman, et al., 2001) (Figure 2). Early experiments showed that deletion of one single c-Myc allele in RAT1 cells (rat fibroblasts) leads to a three-hour delay in S-phase entry, thus demonstrating the importance of c-Myc in cellular proliferation (Schmidt 1999). In contrast activation of c-Myc in serum-starved fibroblasts induces their entry into the cell cyle, indicating the central role that the proto-oncogene plays in cell cycle regulation. The tumorigenic potential of the proto-oncogene was highlighted in experiments, where c-Myc was overexpressed in lymphoid cells and the mice subsequently developed lymphomas. The influence of c-Myc on differentiation during endochondral ossification in the bone was impressively shown by Zhou, et al. The group showed, that c- and N-Myc expression is sequentially coordinated during cell proliferation and differentiation of the appropriate chondrocyte and osteoblast compartments, that are both important for limb skeletal development (Zhou, et al., 2011).

Myc is not only able to induce target gene expression but also to repress the transcription of down-stream target genes by interrupting the function of other transcriptional activators as Miz-1, NF-Y and SP-1 (Rottmann, et al., 2006; Herold, et al., 2002; Gartel, et al., 2001). Most importantly, cell growth and differentiation are among the best-studied cellular effects of Myc interactions. Therefore it is not surprising that some of the Myc target genes belong to cell cycle regulatory proteins like Cyclin D1, Cyclin D2, cyclin-dependent kinase 4 (CDK4) and the cell cycle inhibitors $p21^{CIP1}$ and $p15^{INK4b}$. By c-Myc dependent inhibition of the cell cycle inhibitor p21CIP1, damaged cells fail to arrest in G_1 (Adhikary and Eilers, 2005). Additionally down-regulation of the cell cycle inhibitor $p15^{INK4b}$ leads to the upregulation of Cyclin D1-CDK4/6 complex and promotes cell cycle progression in a TGFß-dependent manner and thereby influences cell differentiation (Warner, et al., 1999).

A

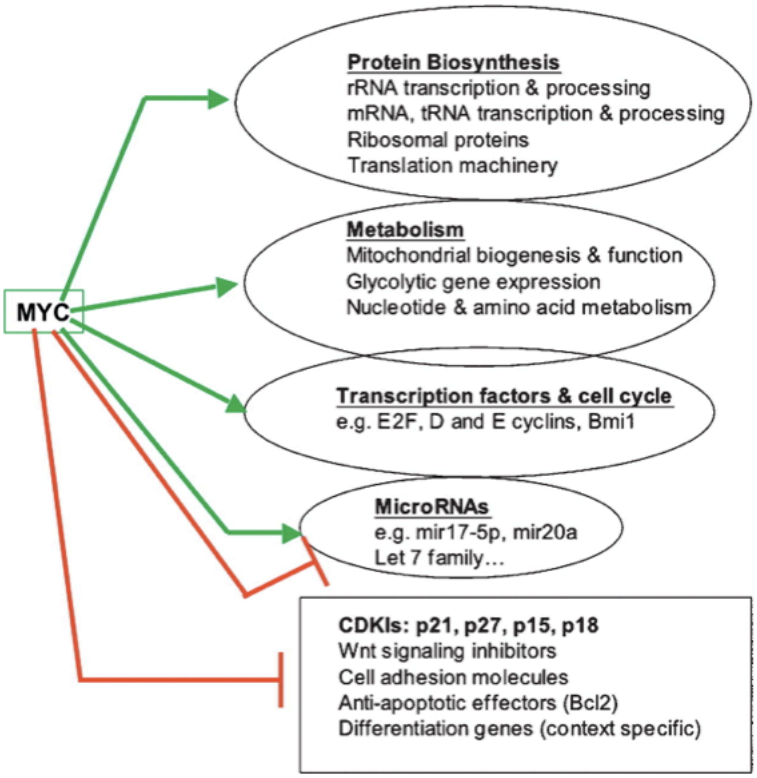

B

Table 1 | **Selected Myc target genes and their proposed function**

Target gene	Regulation	Pathway	Functional relevance	References
p21^{CIP1}	Down	DNA-damage response, APC pathway	Checkpoint failure, cell differentiation	21,57,91
p15^{INK4B}	Down	TGFβ pathway	Resistance to TGFβ-mediated proliferation arrest	55,56
ODC, RCL, HMGI/Y, PMTA	Up	Transformation of rat fibroblasts	Anchorage-independent growth	149–152
HDAC2	Up	APC pathway	Suppression of differentiation	153
CCND1, CCND2, CDK4	Up	Growth-factor response, proliferation of cerebellar neuronal precursors, skin carcinogenesis	G1 progression in response to mitogenic signals	93,99,154,155
E2F2	Up	Growth-factor-dependent proliferation	Required for Myc-induced proliferation	156
IRP2, H-ferritin	Up, down	Iron metabolism	Required for Myc-induced proliferation and transformation	4
LDHA	Up	Glycolysis	Required for Myc-induced transformation	101
N-cadherin, integrins	Down	Adhesion of stem cells to their niche in skin and bone marrow	Exit from the stem-cell compartment	20
SHMT	Up	C1 metabolism	Myc-induced proliferation and growth	105

Figure 2: Implication of Myc signaling
(A) Overview of deregulated Myc signaling pathways and its effect on cellular biology (Eilers, et al., 2008). (B) Selected Myc target genes (Adhikary and Eilers, 2005).

Notably, c-Myc expression is implicated in self-renewal, maintenance of stemness and differentiation. While c-Myc overexpression in hematopoietic stem cells (HSC) results in a loss of the stem cell pool, c-Myc loss leads to an accumulation of the HSCs in the bone marrow due to impaired engraftment capabilities with their surrounding niche cells (Laurenti, et al., 2008; Wilson, et al., 2004). In general, it seems that there is a correlation between cell proliferation and stem cell maintenance in a c-Myc dependent manner. Strikingly, Myc is dispensable in dormant HSCs while it becomes important in transient-amplifying (multipotent progenitors, MPPs) cell populations and is again no longer relevant in terminally differentiated cells. Hence Myc supports the proliferation of actively-dividing cells, as it is important for stem cell maintenance, pluripotency and self-renewal capacities in HSCs under homeostatic conditions (Smith, et al., 2010; Varlakhanova, et al., 2010; Laurenti, et al., 2009; Murphy, et al., 2005; Wilson, et al., 2004).

Myc was first discovered as a proto-oncogene in 1979 and furthermore its role in tumorigenesis was studied (Meyer and Penn, 2008). Activation of oncogenic Myc due to chromosomal translocation, overexpression, amplification and insertional mutagenesis. First insertional mutagenesis was discovered in plasmacytomas due to a recombination of the Myc locus and the immunoglobulin (Ig) heavy chain locus. Later, Adams and colleagues generated the *Eμ -Myc* mouse, which specifically develops B-cell lymphomas (Adams, et al., 1985). Myc is mainly implicated in Burkitt lymphomas and plasmacytomas, and deregulated in a variety of solid cancers e.g. hepato-cellular carcinomas, mammary tumors, colo-rectal cancer and head and neck cancer (Park, et al., 2005; Felsher, et al., 1999; Field and Spandidos, 1990). Interestingly, in human osteosarcomas c-Myc amplification was identified in about 8-16% of human patients (Ueda, et al., 1997).

3.2 Bone development

3.2.1 Bone structure

Bone itself does not only give bodies a shape, it is also a very important endocrine regulator and harbors the bone marrow, which is crucial for blood replenishment throughout the whole life. The body contains five different types of bones. The long bones e.g. femur, tibia, humerus, the short bones e.g. wrists and ankles, flat bones e.g. skull, ribs, sternum, sesamoid bones, and irregular bones like the hips and the spine.

The bone is one of the greatest reservoirs for calcium and phosphate ions and helps thereby to regulate the whole body ion metabolism. Bone is composed of different cell types: osteoblasts, osteoclasts and osteocytes that are embedded into bone matrix. This matrix mainly consists of calcium and phosphate ions that build hydroxyapatite crystals and about 30% of collagen (collagen I) fibers. Morphologically the bone can be distinguished into two important regions, the epiphysis and the diaphysis. The epiphysis is located at the top (proximal) and the bottom (distal) of a bone and builds a joint with another bone, while the part between the epiphyses is called diaphysis. Two types of bone are distinguished, the spongy bone in the epiphyses and in irregular bones, and the compact bone which forms the shaft along long bones and the outer layer. The very outer cell layer of a bone is the periosteum and the inner layer is composed of endosteal osteoblasts, and therefore called endosteum. These osteoblasts are of mesenchymal origin and produce the bone matrix, which is subsequently mineralized. Only about 10% of the mature osteoblasts remain as bone lining cells in the inner layer of the bone, while the rest terminally differentiates into osteocytes that are embedded into bone matrix and thereby build the compact structure of the bone. Bone remodeling occurs throughout life and depends not only on active bone elongation and growth, but is also affected by aging, body metabolism, repair and bone diseases. Osteoclasts are of hematopoietic origin and degrade the bone by enzymatic activity. Importantly, the bone is highly vascularized and possesses many nerve fibers that are located in Haversian canals to react fast in response to

endocrine signals. Bone caverns are inside the bone, where the bone marrow is homed and protected (Figure 3).

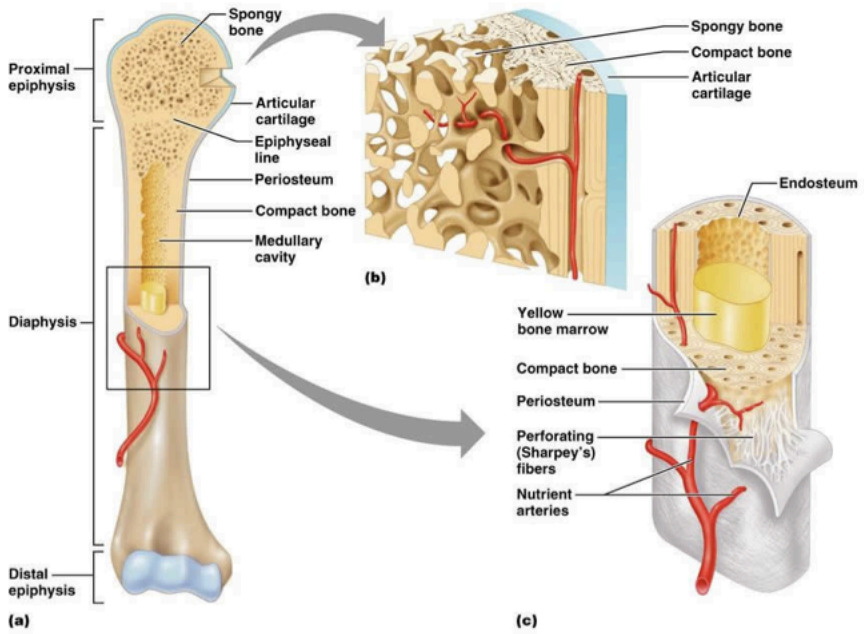

Figure 3: Bone composition
(a) Bone can be separated into two different areas, the proximal and distal epiphysis and the diaphysis. (b) The inner layer of the epiphyses is composed of spongy bone, while the shaft and the outer layer contains compact bone. (c) The inner cell layer of the bone is called endosteum, while cells on the outside form the periosteum. Nerve fibers and the vasculature are located in Haversian canals and the bone marrow is build in the bone marrow cavity, surrounded by the endosteum. Copyright © 2009 Pearson Education, Inc., publishing as Benjamin Cummings. Zitat nicht vollständig!

3.2.2 Bone formation

Bone development occurs in two different ways, endochondral ossification and intramembraneous ossification (Figure 4). During embryonic development bone is formed by intramembraneous ossification, a process where cells from the neural crest become mesenchyme at the sites where the bones will appear. With the help of the transcription factor Runt-related transcription factor 2 (RunX2; cbfa1) and growth factors, mainly bone morphogenic proteins (BMPs) that are important for the tissues architecture, the condensed mesenchymal cells differentiate along the osteoblastic lineages to form mature bone producing cells. In contrast, endochondral ossification involves cartilage formation first and then the replacement of cartilage by bone cells. This can be separated into five steps. In the first step, the mesenchymal cells differentiate into cartilage by Pax1 and Scleraxis, which are both transcription factors. In the second step another transcription factor Sox9 drives chondrocyte development and ends finally in the third step with highly proliferating chondrocytes that begin to form the bone shape. In the fourth step chondrocyte proliferation stops and chondrocytes start to increase their volume dramatically to become hypertrophic. Thereby the chondrocytes start to produce matrix that subsequently becomes mineralized. Finally, in the last step, the chondrocytes begin to die and form thereby the bone marrow cavity. Blood vessels are moving in and the cells that surrounded the cartilage cells start to differentiate into osteoblasts and bone matrix is produced. Subsequently, the dying cartilage cells are replaced by bone cells and thereby bone is formed. Upon bone matrix mineralization about 50-70% of osteoblasts undergo apoptosis while the rest either start to differentiate into osteocytes that are embedded into the bone matrix or become bone lining osteoblasts (Tamara, et al., 2006; Lynch, et al., 1994). These osteocytes mainly remain metabolically quiescent and do not show active cell proliferation.

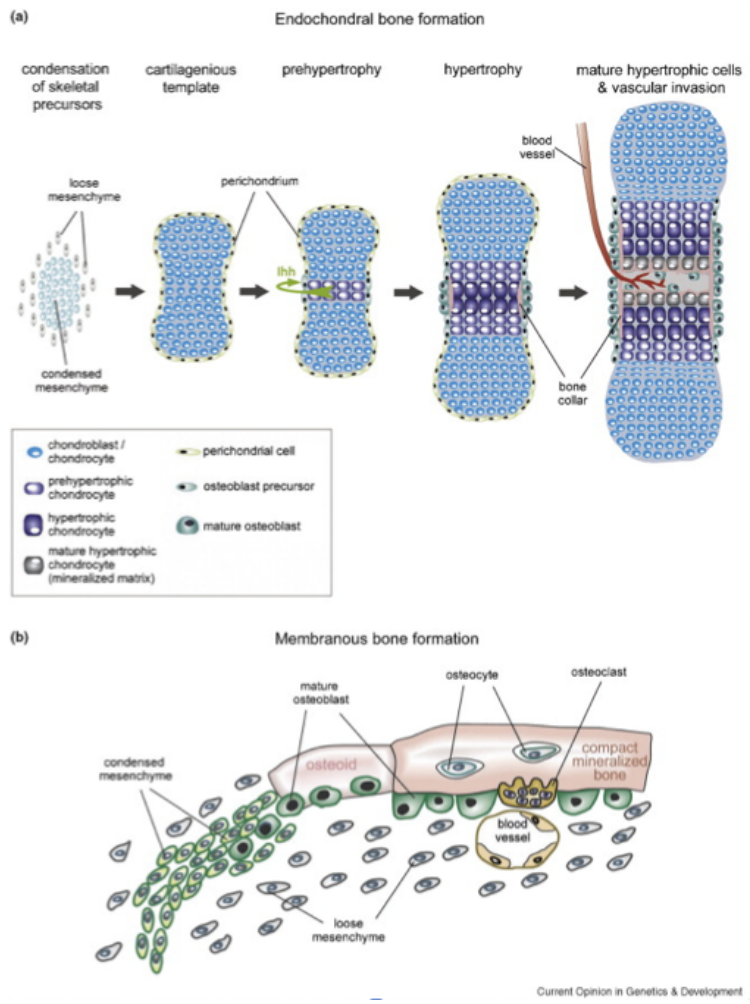

Figure 4: Mechanisms of endochondral and intramembranous bone formation
(a) Mechanism of endochondral bone formation by replacement of cartilage anlagen with osteoblasts. Through mesenchymal stem cell condensation the cartilagenious skeleton is formed. Hypertrophic chondrocytes are subsequently replaced by immigrating osteoblasts and the vasculature connects to the bone marrow cavity. (b) Scheme for membranous bone formation. Mesenchymal progenitors differentiate into osteoblasts that line up the bone. Upon mineralization, a proportion of osteoblasts differentiate into osteocytes that form the compact structure of the bone. Osteoclasts are involved in bone remodeling by degradation of bone matrix (Hartmann, et al., 2009).

3.3 Osteoblasts and osteoclasts are key players in the bone

Mesenchymal stem cells differentiate into osteoblasts by RunX2 expression, one of the master regulators of bone development. Osteoblasts generate bone, while osteoclasts degrade the bone to keep bone remodeling balanced under homeostatic conditions. Interestingly, even though hematopoietic stem cells generate osteoclasts through macrophage-colony stimulating factor (M-CSF) differentiation, osteoblasts have a great influence on osteoclast development too. The receptor activator of NFkB-Ligand (RANK-L) is expressed on the surface of osteoblasts and interacts with RANK, which is expressed on immature osteoclasts to induce osteoclastogenesis. Another receptor, which is expressed on osteoblasts is osteoprotegerin (OPG). This receptor functions as a decoy receptor for RANK-L, thereby negatively influencing osteoclastogenesis. And as mentioned above, osteoblasts also produce M-CSF that interacts with c-fms (M-CSFR; CD115) on the surface of immature osteoclasts to induce terminal osteoclast differentiation (Figure 5). This shows that osteoblasts can influence osteoclastogenesis and differentiation by a wide range of possibilities.

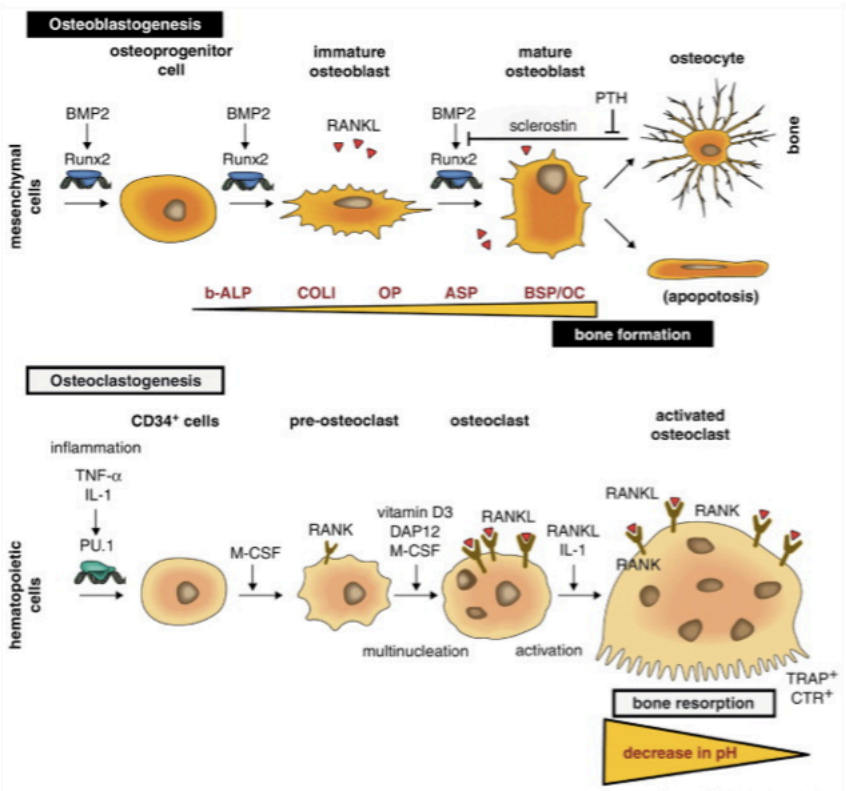

Figure 5: Osteoblastogenesis and Osteoclastogenesis
Upper row: Overview of osteoblastogenesis and osteoclastogenesis in the bone. Mesenchymal stem cells start to differentiate into osteoblasts upon RunX2 and BMP2 signaling. Mature osteoblasts either terminally differentiate into osteocytes or become apoptotic. Sclerostin produced by osteocytes negatively influences mature osteoblast synthesis and is inhibited by parathormone (PTH). Important genes expressed during the different stages of osteoblastogenesis are indicated as alkaline phosphatase (ALP), collagen I (Coll), osteopontin (OP), acidic bone sialoprotein (ASP), bone sialoprotein (BSP), osteocalcin (OC). Lower row: Osteoclastogenesis is induced upon hematopoietic cell differentiation from macrophage progenitors and is stimulated by inflammatory cytokines such as TNFa or IL-1 that induce Pu.1 (Pu-Box transcription factor) expression. Macrophage-colony stimulating factor (M-CSF) induces macrophage maturation to generate activated osteoclasts being tartrate-resistant acid phosphatase (TRAP+) and calcitonin receptor (CTR+) positive. RANK receptor on osteoclasts interacts with RANK-L from osteoblasts to induce HSC-independent osteoclast maturation through bone tissue (Monroe, et al., 2012).

3.4 Transcriptional control of osteoblast development

The main inducer of osteoblast differentiation is RunX2, which is highly expressed in osteoblasts, cartilage precursors and MSCs (Ducy, et al., 1997; Komori, et al., 1997; Otto, et al., 1999) (Figure 5). It was shown that RunX2 knockout (RunX2-/-) animals were not able to induce bone formation, however cartilage skeleton developed with delayed chondrocyte maturation (Otto, et al., 1997; Komori, et al., 1997). Haploinsufficiency of RunX2 causes a severe delay in bone formation and results in cleidocranial dysplasia (CCD), an autosomal dominant disorder. In contrast, overexpression of RunX2 in osteoblasts resulted in a terminal osteoblast differentiation block with a loss of bone mineralization and porous bones (Liu, et al., 2001). This demonstrated that RunX2 is important for early osteoblast differentiation and initiation of bone mineralization and normal bone development. These observations impressively show that RunX2 regulates the initiation of osteoblast development as well as it controls differentiation and terminal function of osteoblasts. Therefore it is not surprising that RunX2 binding sites were identified in many genes involved in osteoblast regulation (Xiao, et al., 2005; Thomas, et al., 2001; Zhang, et al., 2000; Javed, et al., 2000). Besides Retinoblastoma (pRb) (Thomas, et al., 2001), Lian, et al., furthermore identified that osteocalcin (OCN), one of the key players that control bone metabolism and formation, has three binding sites for RunX2, indicating the high relevance of RunX2 controlled osteoblast differentiation and functionality (Lian, et al., 2001). Simultaneously, bone morphogenic proteins (BMP) induce osteoblast and cartilage development and then sex-determining region Y Box 9 (Sox9) exclusively drives further chondrocyte development (reviewed Zelzer and Olsen, 2003).

Osteoprogenitors then differentiate through osterix (Osx) into immature osteoblasts. Since Osx is expressed in RunX2-/- animals but in contrast RunX2 is not expressed in Osx-/- animals, it is believed that Osx is downstream of RunX2 during osteoblast development (Hu, et al., 2004; Nakashima, et la., 2002). Osx-/- mice show normal cartilage development with full mineralization and the presence of terminally differentiated chondrocytes that indicate the importance of Osx in osteoblast differentiation (reviewed Harada and Rodan, 2003).

During osteoblast maturation the differentiation progress of an osteoblastic cell can be categorized by its marker expression. One of the expression markers that are expressed during early differentiation steps is alkaline phosphatase (ALP). ALP activity is important for proper bone mineralization and is mainly controlled by RunX2, BMP and Wnt signaling (Rawadi, et al., 2003; Beck, et al., 2000). Fedde, et al., showed that ALP-/- mice developed symptoms of hypophosphatasia as a consequence of hypomineralization (Fedde, et al., 1999). Upon further osteoblast maturation ALP expression fades. One of the most abundant proteins in the bone is collagen I. Collagen I is synthesized in mature osteoblasts to generate bone matrix that subsequently is mineralized with calcium to form the solid bone structure. Collagen I expression is a hallmark of a functional osteoblast. Lynch and colleagues observed in rat osteoblast tissue cultures that collagen I synthesis is attributed to final osteoblast maturation and is needed for mineralization of bone tissue (Lynch, et al., 1995).

Other proteins like osteopontin (OPN) and osteocalcin (OCN) are then synthesized in mature osteoblasts during active bone mineralization. Osteopontin is an important non-collagenous protein that is expressed in osteoblasts and osteoclasts respectively. Importantly, OPN has an effect on bone remodeling and homeostasis as it influences mineral deposition of the bone matrix and promotes osteoclastogenesis (Standal, et al., 2004; Yoshitake, et al., 1999). The influence of OPN on osteoclasts was shown by Yoshitake, et al., where in a mouse model system of osteoporosis, ovariectomy in OPN-/- deficient mice did not lead to an increase in osteoclast numbers (Yoshitake, et al., 1999). While OPN is only secreted in cells during active cell proliferation, OCN synthesis is only observed in mature osteoblasts in the post-proliferative phase (Lian and Stein, 1995; Hauschka, et al., 1989). OCN is the most important indicator for bone formation (Lian, et al., 1989). OCN deficient animals showed elevated bone formation capacity and bone mass without any effect on bone degradation (Ducy, et al., 1996). There exist two different forms of OCN - pre-OCN, which is unminerlized and mature OCN, which is the mineralized OCN. Unmineralized OCN is synthesized by mature osteoblasts and only in the presence of vitamin K, which is its cofactor. It binds to hydroxyapatite to generate the mineralized bone matrix. Excessive OCN is then released to the blood stream and functions as an endocrine regulator to influence bone formation by energy metabolism

(Ferron, et al., 2010 and 2008; Takeda and Karsenty, 2001). In a very last differentiation step osteoblasts differentiate to either osteocytes or become apoptotic (reviewed Franz-Odendaal, et al., 2006). About 50-70% of osteoblast-derived osteocytes are trapped in the mineralized bone matrix to generate compact bone, while the remaining non-apoptotic 10-20% of osteoblasts form the endosteum. Osteocytes mainly express sclerostin as a product of the SOST gene that negatively influences bone formation. Sclerostin is directly inhibited by parathormone (PTH), which is an inducer of bone formation (Keller, et al., 2005). On the other hand sclerostin interrupts intracellular Wnt signaling by binding to LRP5/6 receptor that actually induces differentiation of mature osteoblasts with a simultaneous block in osteoclastogenesis, thereby regulating bone mass and bone formation (reviewed Baron and Rawadi, 2007; Li, et al., 2006).

3.5 Key pathways influencing bone formation and degradation

3.5.1 Wnt signaling

Bone formation by osteoblast maturation and differentiation is tightly regulated and controlled by a number of pathways. One of the major pathways that influences bone metabolism is Wnt signaling. Wnt induces MSCs to differentiate towards osteoblastic cell lineages and promotes the maturation of pre-osteoblasts to mature osteoblasts. By expression of DKK-1, a direct Wnt antagonist, osteoclastogenesis is efficiently blocked, thereby positively influencing bone formation upon induced Wnt signaling. LRP5 and LRP6 are Wnt co-receptors and induce canonical Wnt signaling. Kato and colleagues showed that LRP5 knockout (LRP5-/-) mice have impaired bone formation and osteoblast proliferation, resulting in lower bone mass and matrix deposition (Kato, et al., 2002). In contrast in LRP5 (G171V) mutants, excess activity of the Wnt signaling pathway resulted in higher bone mass without an influence on the osteoclast compartment. Instead osteoblasts from transgenic animals revealed prolonged life-span and an increased mineralization capacity (Babij, et al., 2003). Many target genes can be used as a read-out for the functionality of the activated Wnt signaling pathway, however ß-Catenin and Axin2 seem to be the most significant ones. Interestingly, mice with conditional deletion of ß-Catenin

(ß-Catenin-flox) in osteoblasts, resulted in an early onset of osteoporosis, a severe bone disease with reduced bone mass and high risk for fractures. In contrast, conditional deletion of Adenomateous polyposis coli (Apc-flox), which normally degrades ß-Catenin complex, resulted in severe osteopetrosis. Osteopetrosis is characterized through an increase in bone mass with a high bone turnover as a consequence of impaired osteoclast activity. These results indicated the important role of ß-Catenin signaling in rather modulating osteoclastogenesis and its effect on bone development (Holmen, et al., 2005). Most interestingly, OPG, the decoy receptor for RANK-L that negatively influences osteoclastogenesis, was found to be a ß-Catenin target and loss of ß-Catenin in differentiated osteoblasts results in mice with osteopenia. Osteopenia implies low bone mass and high bone resorption by osteoclasts (Glass II, et al., 2005). In addition to APC, Axin2 belongs to the ß-Catenin degradation complex too and thereby regulates Wnt signaling in a negative feedback-loop (Jho, et al., 2002). Examinations on Axin2-/- mice showed that the animals had increased bone mass and elevated differentiation capacities with a simultaneous decrease in osteoclastogenesis (Yan, et al., 2009). Notably, even though Wnt signaling is a master regulator of bone development that influences osteoblast maturation, it primarily seems to act on osteoclastogenesis first, which in turn then influences osteoblast behavior as a secondary effect and results in a specific bone phenotype (Figure 6).

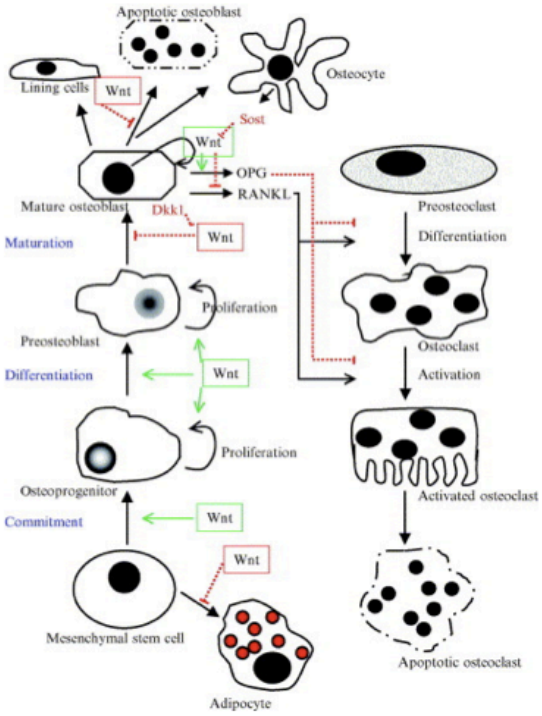

Figure 6: Wnt signaling in the bone
Wnt signaling positively influences mesenchymal stem cells (MSC) to differentiate towards osteoblastic lineages and drives the maturation of osteoprogenitors. In addition Wnt induces osteoprotegerin (OPG) expression in mature osteoblasts to prevent osteoclastogenesis. Wnt blocks MSC differentiation to adipocytes, inhibits final maturation of osteoblasts by upregulation of Wnt inhibitor dickkopf-1 (DKK-1) and prevents apoptosis of mature osteoblasts. Positive Wnt influence is indicated in green while negative regulation is shown in red (Baron, et al., 2006).

3.5.2 Transforming growth factor beta (TGFß) signaling

Bone morphogenic proteins (BMP) are involved in cell growth and differentiation, homeostasis and apoptosis (Chao and Chen, et al., 2005; Siegel and Massagué, 2003; Massagué, 2000). From eleven known BMP subtypes, six (BMP2-7) belong to the TGFß superfamily,. By binding to its receptor BMPR-2 induces activated SMAD signaling, which triggers the transcription of TGFß target genes, e.g. cell cycle inhibitors $p15^{INK4b}$, $p21^{CIP1}$, $p57^{KIP2}$ and RunX2 (Lee, et al., 2000). In general TGFß signaling cooperates with Wnt signaling in promoting osteoblast differentiation and maturation (Takeuchi, et al., 2010; Zhou, et al., 2004; Zhou, et al., 2003;). Mutations in BMPs and their inhibitors, e.g. sclerostin and noggin, result in skeletal disorders (Chen, et al., 2012).

3.5.3 Vitamin D and parathormone (PTH) signaling

Calcium is one of the major signal transducers throughout the body and relevant as second messenger or in cofactor signaling. One major component of the solid bone structure is hydroxyapatite, which is composed of calcium and phosphate ions. Therefore minerals highly influence bone metabolism. Two pathways mainly control the mineral metabolism in the body, the vitamin D and the parathormone (PTH) signaling cascades. Interstingly, Ono, et al., showed that constitutively active PTH and PTHR (receptor) in mature osteoblasts resembled the phenotype of animals with chronically elevated PTH serum levels. Mice showed increased bone mass due to suppression of osteocytic sclerostin (Ono, et al., 2006; Bellido, et al., 2005).

3.6 Osteosarcoma

Osteoblasts are cells that do no longer proliferate as much as their progenitors. While about 50-70% of osteoblasts finally differentiate to osteocytes, only about 10% form the inner layer of the bone and the rest starts to become apoptotic. This shows that the classical osteoblast becomes more and more quiescent during aging. Therefore it is not suprising that oncogenic transformation of mature osteoblasts happen mainly during active cell proliferation and cell growth, which is during skeleton develpment. In this phase most of malignant osteosarcoma develop. In general osteosarcoma form about 20% of all bone tumors and they are among the most frequent type of cancer developed in children and adolescent (Tang, et al., 2009; Clark, et al., 2007; Hayden, et al., 2006; Helman, et al., 2003). Osteosarcoma is therefore categorized into juvenile and adolescent osteosarcoma while a second peak arises in elderly patients (Mirabello, et al., 2009; Tang, et al., 2008) Most frequently patients suffer from lung metastasis, which is an indicator for poor prognosis and survival (Marina, et al., 2004; Bielack, et al., 2002; Gamberi, et al., 1998). Primarily, osteosarcoma arises in areas with active bone growth, like hips, femur, tibia, humerus, clavicula and mandibula and it seems that it is to be considered a differentiation disease. Most of the tumors show disruption of final differentiation steps in the maturation of osteoblasts and cell proliferation of osteoprogenitors (Haydon, et al., 2007; Thomas, et al., 2006) (Figure 7). Most frequently disruption of cell cycle regulators p53 and pRb were shown to be involved in osteosarcoma onset (Berman, et al., 2008; Walkley, et al., 2008; Sandberg, et al., 2003). Interestingly, c-Myc is amplified in about 8-16% of human patients (Ueda, et al., 1997). There are some risk factors that promote osteosarcoma onset, such as previous radiation therapy, hereditary retinoblastoma gene, Li-Fraumeni syndrome, Rothmund-Thomson syndrome, Werner syndrome, Bloom syndrome and Paget disease.

Basically osteosarcoma diagnosis in patients is not easy, as most of the patients suffer from pain and swelling, which happens quite often in children and adolescent patients. Therefore detection is based on mass or limb formation close to the bones, imaging tests (e.g. x-ray, MRI (magnet resonance imaging), CT-Scan), biopsy and pathology. Histological sectioning and staining then identifies osteosarcoma osteoblasts in tissues by malignant

osteoid production, which is uncalcified bone matrix. Therapy is therefore mainly based on surgery, chemotherapy, radiation therapy or the combination of all of them. Chemotherapy that is used these days includes methotrexate, doxorubicin, cisplatin, etoposide, ifosfamide, cyclophosphamide, epirubicin, gemcitabine and topotecan[1]. There exist some osteosarcoma specific markers that show prognostic value like ezrin (cytovillin, linked to cell motility and migration), S100A6 (cell proliferation and differentiation), Annexin2 (signal transduction and increases bone degradation) and CXCR-4 (C-X-C chemokine receptor-4; SDF1R (stromal derived factor 1 receptor); homing, chemoatractant) (Tang, et al., 2008). In addition c-Kit expression has been linked to stromal tumors, especially to gastro-intestinal stromal tumors (GIST) and is there expressed in a wide range on tumor cells. In osteosarcoma, it seems that c-Kit lacks prognostic value, however it opens new targeting opportunities (Adhikari, *et al.*, 2011; Ikeda, *et al.*, 2010; Judson, *et al.*, 2010; Sulzbacher, *et al.*, 2006; Entz-Werle, *et al.*, 2005; Matsuyama, *et al.*, 2005).

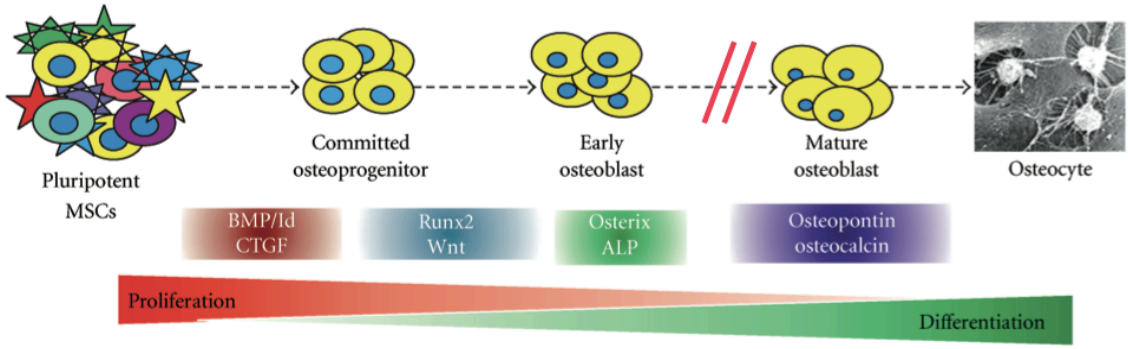

Figure 7: Hypothesis of human osteosarcoma development
Scheme of mesenchymal stem cell differentiation (MSC) into mature osteoblasts with important genes expressed in the appropriate osteoblast populations. Hypothesis of osteosarcoma development by a blockage in the final maturation step from early osteoblasts to mature osteoblasts that results in uncontrolled cell proliferation of immature osteoblastic cells (blockage is indicated by red lines). (Gene expressions: BMP = bone morphogenic protein with Id target genes; CTGF = connective tissue growth factor; RunX2 = Runt-related transcription factor 2) (Adapted Wagner, et al., 2011).

[1] http://sarcomahelp.org/osteosarcoma.html

3.7 Osteoblast – HSC interactions

Stem cells in general possess the ability to self-renew and differentiate into all the cells of a specific tissue. These cells are most important and therefore it is not surprising that the stem cells need to be protected and tightly controlled. In the bone marrow the hematopoietic stem cells (HSCs) serve as a continuous reservoir and replenish the cells of the hematopoietic system each day. Especially during injury the stem cells of the bone marrow and the periphery need to be activated within a short time. Therefore it is believed that HSCs are located in two different stem cell niches under homeostatic conditions - the endosteal and the perivascular niche in the trabecular region of the bone (Figure 8).

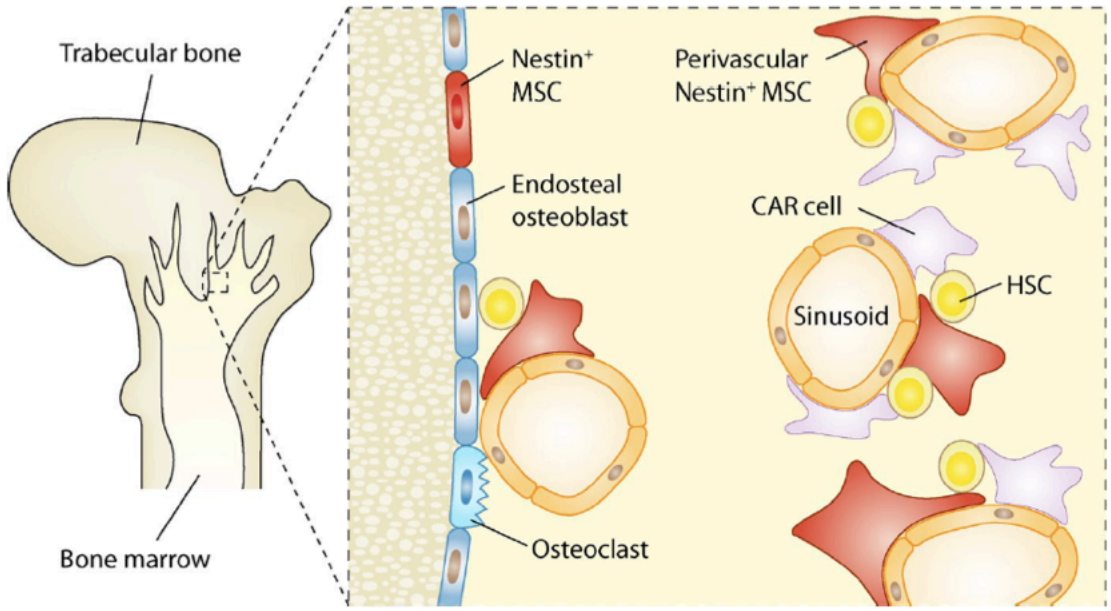

Figure 8: Lodgment of HSCs in the trabecular bone region
Hematopoietic stem cells (HSCs) are located close to endosteal niche osteoblasts and in the proximity of Nestin$^+$ mesenchymal stem cells (MSCs) and CXCL12-abundant reticular cells (CAR) that control HSC maintenance. HSCs are also found to be located close to sinusoids in the bone marrow (Ehninger and Trumpp, 2011).

It has previously been shown that HSCs are linked to mature endosteal osteoblasts and that these cells control HSC maintenance, differentiation and self-renewal capacities of HSCs (Méndez-Ferrer, et al., 2010; Wilson, et al., 2008; Yin and Li, 2006; Kiel, et al., 2005; Visnjic, et al., 2004; Calvi, et al., 2003; Zhang, et al., 2003; Nilsson, et al., 2001). Interestingly Visnjic, et al. showed that the specific deletion of osteoblasts (col2.3ΔTK) in mice resulted in extra-medullary hematopoiesis and a decrease in the number of hematopoietic stem and progenitors in the bone marrow (Visnjic, et al., 2004). Calvi and colleagues showed that in mice expressing activated parathormone and its receptor (PTH/PTHrP) on osteoblasts not only the osteoblast pool but also the HSC population were increased in a Notch dependent manner (Calvi, et al., 2003). Additionally, Zhang, et al., observed that by conditionally knocking out the bone morphogenic protein receptor type IA (BMPRIA) on osteoblasts, not only the amount of spindle-shaped N-Cadherin^{+} expressing osteoblasts (SNO cells) increases but also HSC numbers and thereby the niche size (Zhang, et al., 2003).

However not only osteoblasts were considered to be part of the HSC niche as many other cell types do have an impact on HSC regulations as well. Therefore it is likely that the niche contains several different cell populations that act in specific circumstances on HSC control and regulation. Recently, nestin-expressing mesenchymal stem cells (nestin^{+} MSCs) and CXCL12 abundant reticular (CAR) cells were shown to play crucial roles in controlling HSC maintenance and regulation (Nagasawa, et al., 2011; Méndez-Ferrer, et al., 2010). Interestingly, both cell populations also belong to the mesenchymal cell lineages like osteoblasts and show high similarities in their marker expressions. While CAR cells express high levels of CXCL12 and stem cell factor (SCF), nestin+ MSCs show in addition to nestin, a mesenchymal stem cell marker, high expression of markers that are related to HSC maintenance like Angiopoetin-1 (Ang-1), interleukin-7 (IL7), vascular cell adhesion protein 1 (VCAM, CD106) and osteopontin (OPN) (Lander, et al., 2012; Noll, et al., 2012; Ehninger and Trumpp, 2011; Méndez-Ferrer, et al., 2010; Sugiyama, et al., 2006) (Figure 9).

Furthermore, Yamazaki and colleagues identified nonmyelinated Schwann cells (glial cells) as regulators for HSC maintenance (Yamazaki, et al., 2011). They showed that denervation induces a decrease in TGFß expression with a simultaneous reduction of HSC numbers and increased HSC cycling. These observations are in line with earlier findings by Méndez-Ferrer, et al. 2008, where noradrenalin secretion down-regulates CXCL12 expression and thereby releases HSCs from their niche. Recently, leptin-receptor positive stromal cells were identified as crucial stem cell factor (SCF) producers, thereby promoting HSC maintenance (Lander, et al., 2012; Ding, et al., 2012). Leptin itself is a hormone produced by adipocytes to control and regulate energy metabolism in the body. It positively affects bone growth while inhibiting osteoclastogenesis and hence influences the HSC niche (Takeda, et al., 2002).

Lastly, macrophages were identified as major key players in controlling HSC fate. Winkler and colleagues showed that macrophage depletion in mice resulted in a loss of endosteal osteoblasts and a concomitant mobilization of HSCs to the periphery (Winkler, et al., 2010). Most importantly, Chow et al., 2011 observed that specific phagocyte depletion in mice results in a down-regulation of CXCL12 expression in nestin^{+} MSCs and to HSC migration to the peripheral blood (Chow, et al., 2011).

Osteoclasts are generated upon differentiation of monocytes into tissue-specific macrophages and are found in the bone marrow. Osteoclasts generation is regulated through the RANK-L/ RANK interaction and is therefore mainly controlled by osteoblasts. Interestingly, loss of osteoclast functionality was also linked to impaired HSC homing ability in mice (*oc/oc*) with impaired endochondral ossification. Lymperi, et al., 2011 observed similar results when they abolished osteoclast activity by bisphosphonate alendronate (ALN) treatment and detected a simultaneous decrease in the HSC pool (Lymperi, et al., 2011). These findings confirm the potential role of osteoclast functionality on HSC control and regulation.

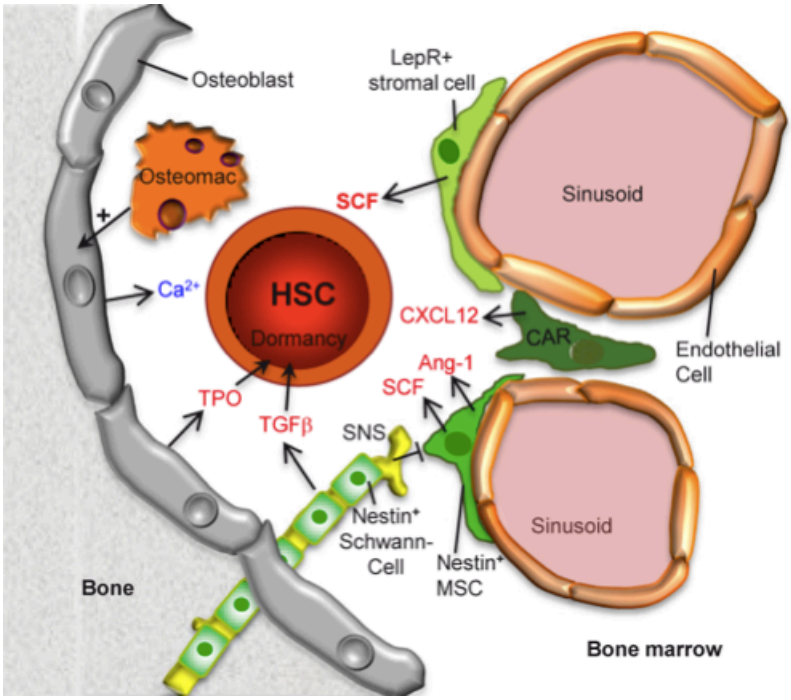

Figure 9: The hematopoietic stem cell niche
Localization of hematopoietic stem cells (HSCs) in their niche. Factors that control HSC maintenance are produced by different niche cells such as thrombopoietin (TPO) by osteoblasts, TGFß by Nestin^{+} Schwann cells, CXCL12 by CXCL12-abundant reticular cells (CAR), stem cell factor (SCF) mainly produced by Leptin-receptor^{+} (LepR) stromal cells and SCF angiopoetin-1 (Ang-1) from Nestin^{+} mesenchymal stem cells (MSCs). Osteomacs release calcium (Ca^{2+}) from the bone by degradation (Lander, et al. 2012).

3.8 Hematopoietic stem cells

To date murine hematopoietic stem cells that give rise to all the different cell types in the blood, are the best characterized stem cell population.. They are located at the trabecular region of the bone within the bone marrow of tibia, femur, hips, sternum and the spinal cord. Like other tissue stem cells they possess the ability to self-renew and differentiate throughout life (Weissman, 2000). Upon differentiation HSCs give rise to multi-potent progenitor cells (MPPs) and these in turn specifically differentiate into committed progenitor cells. These include common lymphocyte progenitors (CLPs), megakaryocyte erythroid progenitors (MEPs), granulocyte macrophage progenitors (GMPs) and common myeloid progenitors (CMPs). Subsequently the committed progenitor cell pools further differentiate into the various terminally differentiated cells, the erythrocytes, platelets, granulocytes, macrophages, lymphocytes (T- and B-cells) and natural killer cells (NK-cells) (Figure 10).

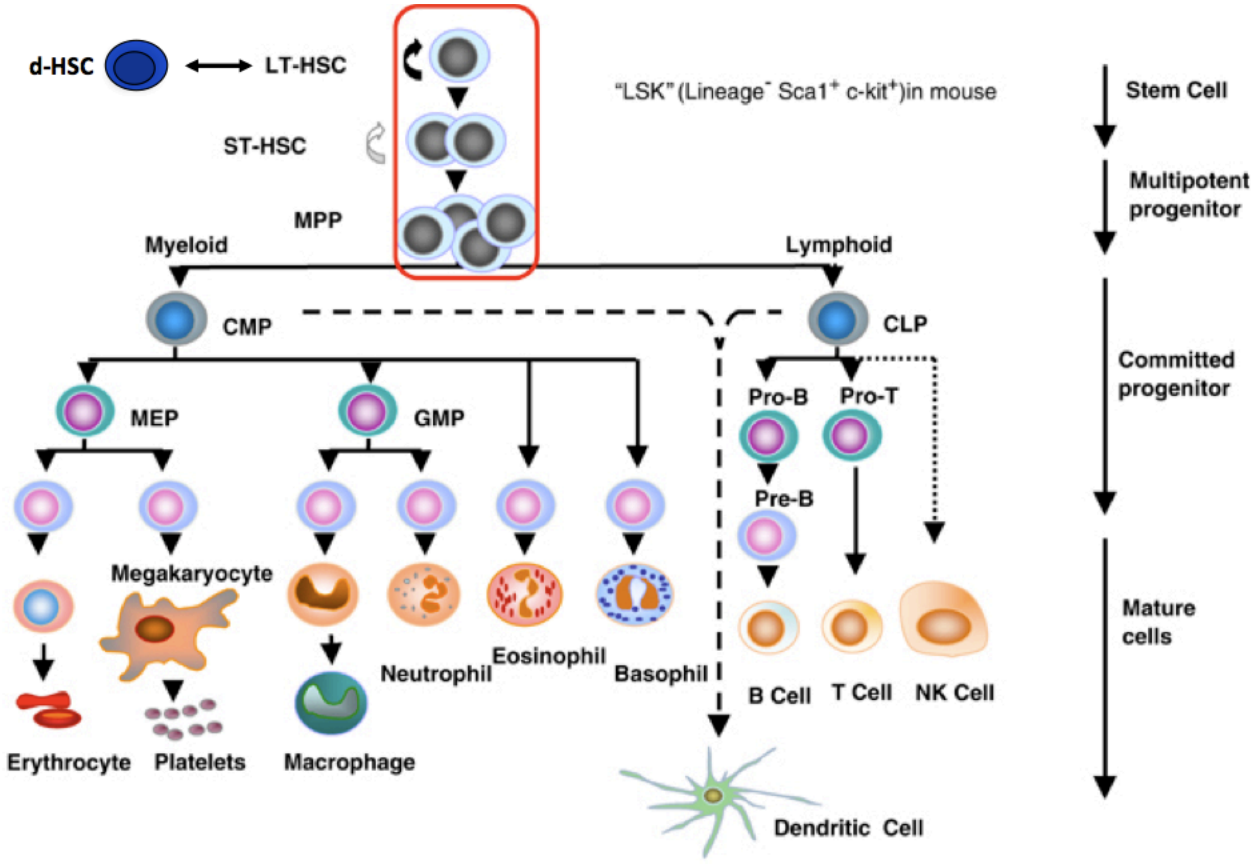

Figure 10: Hematopoietic hierarchy
Dormant stem cells (dHSCs) are on top of the hierarchy and develop into slow cycling long-term HSCs (LT-HSC) and short-term HSCs (ST-HSCs). These are subsequently differentiated into multipotent progenitors (MPPs) and then develop into committed myeloid (CMP) and lymphoid progenitors (CLP). CMPs differentiate to megakaryocyte-erythroid progenitors (MEPs) and granulocyte-macrophage progenitors which terminally differentiate into erythrocytes, platelets and macrophages. In contrast CLPs produce B- and T-cells, natural killer (NK) cells and dendritic cells. (Adapted Larsson, et al., 2005).

As there is an intimate relationship between hematopoietic stem and progenitor cells and their progenies, there are several cell surface markers used to distinguish the different cell populations in the bone marrow by flow cytometry. Several markers from the cluster of differentiation (CD) are used in combination with signalling lymphocyte activation molecule (SLAM) to identify the cells (Table 1).

Abbreviation	Population	Cell surface marker
Lin-	Lineage	CD4, CD8a, CD11b, Gr1, B220, Ter119
LSK	LSK	Lin^{-} Sca^{+} c-Kit^{+}
LSK SLAM	LSK SLAM	LSK $CD150^{+}$ $CD48^{-}$
ST-HSC	Short-term HSC	LSK $CD150^{+}$ $CD48^{-}$ $CD34^{+}$
LT-HSC mu	Long-term HSC murine	LSK $CD150^{+}$ $CD48^{-}$ $CD34^{-}$
CMP	Common myeloid progenitor	Lin^{-} $Sca\text{-}1^{-}$ c-Kit^{+} $CD34^{+}$ $CD16/32^{-}$
GMP	Granulocyte macrophage/ monocyte progenitor	Lin^{-} $Sca\text{-}1^{-}$ c-Kit^{+} $CD34^{+}$ $CD16/32^{+}$
MEP	Megakaryocyte erythroid progenitor	Lin^{-} $Sca\text{-}1^{-}$ c-Kit^{+} $CD34^{-}$ $CD16/32^{-}$
CLP	Common lymphoid progenitor	Lin^{-} $Sca\text{-}1^{low}$ c-Kit^{low} $CD127^{+}$
Granulocyte	Granulocyte	$Gr1^{+}$ $CD11b^{+}$
Erythrocyte progenitor	Erythrocyte progenitor	$CD71^{+}$ $Ter119^{-}$
Erythrocytic blasts	Erythrocytic blasts	$CD71^{+}$ $Ter119^{+}$
Erythrocyte	Erythrocyte	$CD71^{-}$ $Ter119^{+}$
T-cell	T-lymphocyte	$CD3^{+}$, $CD4^{+}$, $CD8a^{+}$
Pre-pro B-cell	Pre-pro B-cell	IgM^{-} $B220^{+}$
Immature B-cell	Immature B-cell	IgM^{+} $B220^{low}$
Mature B-cell	B-lymphocyte	IgM^{+} $B220^{+}$
Monocyte	Monocyte	$CD45^{+}$ $Gr1^{-}$ $CD11b^{low/-}$ $F/480^{-}$ $CD115^{+}$

Table 1: Overview of cell surface marker expression on cells of the hematopoietic lineages

3.8.1 Key signaling molecules for HSC functionality

3.8.1.1 Factors regulating self-renewal capacities

Even though HSCs possess highest self-renewal capacities, their functionality cannot be tested easily. It is still a major problem to handle the cells under *in vitro* conditions. However, the first experiments by Jacobsen, et al., 1949 demonstrated that mice that were given high doses of whole body irradiation suffered from hematopoietic failures and were not able to re-generate the cells of the bone marrow (Jacobsen, et al., 1949). Therefore bone marrow transplantations are used to quantify and evaluate HSC repopulating capacities *in vivo*.

The signals important for HSC self-renewal are still not completely unravelled yet, however telomerase was discovered to be important (Morisson, et al., 1996). HSC propagation *in vitro* is limited to about 3 days and even if cytokines that are known to maintain HSC functionality are added, the cells begin to proliferate and differentiate quite early. These cytokines include thrombopoetin (TPO), stem cell factor (SCF, c-KitL), IL-1, 3, 6, 11. Recently, Reya, et al., 2003 identified that overexpression of ß-Catenin increased the HSC pool *in vitro* and induced the expression of genes involved in HSC self-renewal like homeobox DNA binding protein 4 (HoxB4) or Notch1 (Reya, et al., 2003). In addition Perry and colleagues observed that double transgenic animals with an overexpression of ß-Catenin and a loss of the Phosphatase and Tensin homolog protein (Pten) showed an upregulation of the inhibitor of differentiation 2 (Id2) and the myeloid leukemia cell differentiation protein-1 (Mcl-1), an anti-apoptotic factor. This led to the maintenance of the HSC self-renewal capacity, however the differentiation abilities were lost (Perry, et al., 2011). The role of homeobox proteins was identified early on and was linked to self-renewal capacities of HSCs. This effect seems to be emphasized by TPO (Magnusson, et al., 2007; Beslu, et al., 2004; Kirito, et al., 2003) (Figure 11).

Another marker, which was shown to be important for HSC self-renewal maintenance is the B lymphoma Mo-MLV insertion region 1 homolog (Bmi1). Bmi1 belongs to the polycomb group and was shown to regulate $p16^{INK4a}$ and $p19^{ARF}$ cell cycle inhibitors by repressing both activities. Importantly, Bmi1 deficient (Bmi1-/-) mice showed normal expression of $p16^{INK4a}$ and $p19^{ARF}$ and resulted in a loss of self-renewing HSCs with impaired hematopoiesis (Oguro, et al., 2006; Park, et al., 2003). In addition it was shown that Bmi1 plays a major role in DNA repair mechanisms. Chagraoui, et al., 2006 observed chromosomal instabilities in HSCs of Bmi1-/- mice, leading to an accumulation of DNA damage upon impaired cell cycle control (Chagraoi, et al., 2006). Another important HSC self-renewal regulator is c-Myc. The transcription factor was shown to regulate HSC self-renewal and maintenance in a dose-dependent manner (Reavie, et al., 2010; Wilson, et al., 2008). Under physiologic conditions LT-HSCs exhibit low c-Myc expression, ST-HSCs and MPPs have high c-Myc levels while in contrast c-Myc expression in terminally differentiated cells is dispensable. While high c-Myc expression leads to a loss of HSC self-renewal capacities and an exhaustion of the stem cell pool as a consequence of normal cell proliferation, c-Myc deficiency leads to an accumulation of self-renewing HSCs that are no more able to differentiate (Wilson, et al., 2008).

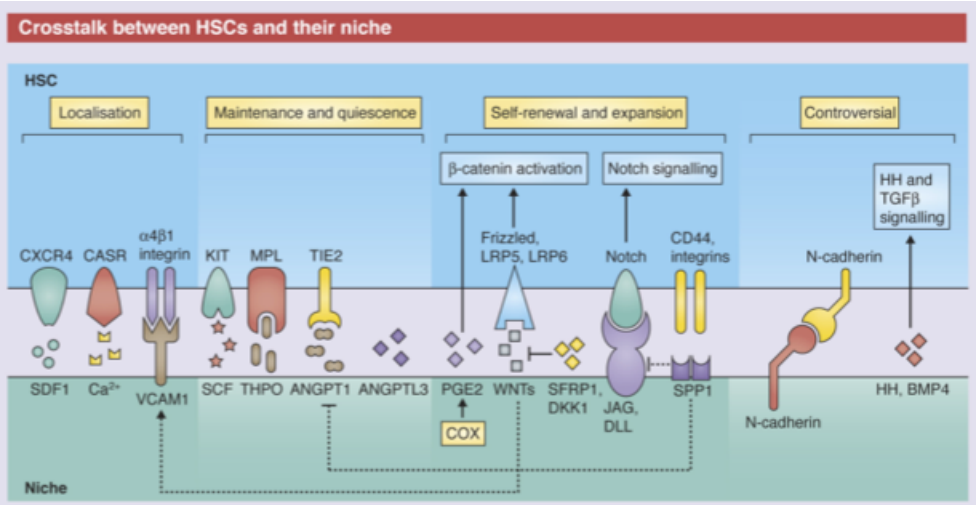

Figure 11: Overview of key signaling molecules of HSC - niche interactions
(Adapted Celso and Scadden, 2011)

3.8.1.2 Dormany and activation of HSCs

Interestingly, cell cycle analysis of stem cells from the hematopoietic system revealed that about 70-90% of LT-HSCs remain in G_0 while among more differentiated progenies the percentage of cells in G_0 decreases to about 10% (Pietras, et al., 2011; Passegué, et al., 2005; Wilson, et al., 2008). One of the first questions was therefore, whether cell cycle status of HSCs correlates with stemness and the HSCs` functional properties of self-renewal and differentiation. Most interestingly, Passegué and colleagues observed that all cells of the hematopoietic system that remain in G_0 possess long-term reconstitution capacities during bone marrow transplantation assays *in vivo* (Figure 12) (Passegué, et al., 2005). As the majority of LT-HSC populations were quiescent, the next question was then to check the frequency of cell divisons. Therefore label-retaining assays with 5-bromo-2'-deoxyuridine (BrdU) were performed *in vivo*. Initial BrdU treatment of mice ensured that all the cells are labeled, as BrdU incorporates into the DNA and is only diluted out upon cell divisions. Interestingly, only about 15% of LT-HSCs retained their BrdU label during a BrdU-free chase period of about 100 days, while 85% of these LT-HSCs became activated and lost their label. Mathematic modeling of the doubling times revealed that the 15% BrdU-psoitive LT-HSCs remained completely quiescent and that the cells only divide once within about 149 days and only about five times during a life circle of a mouse. In contrast activated HSCs cycle about every 30 days (van der Wath, et al., 2009; Wilson, et al. 2008). Serial bone marrow transplantation assays of the different HSC compartments revealed that these quiescent or dormant stem cells indeed possess the highest repopulating capacities. Therefore stem cell quiescence can be correlated to the highest stem cell functionality and thus identifies the most potent hematopoietic stem cells (Wilson, et al., 2008). It seems that these most potent stem cells serve as a stem cell reservoir for emergency cases as their metabolic activity is down-regulated and they are kept in quiescence (Trumpp, et al., 2010).

		3–4 wk		9–12 wk	
Phase	Cell #	Frequency reconstitution (#/total)	Average chimerism (range) engraftment type (#/reconstituted)	Frequency reconstitution (#/total)	Average chimerism (range) engraftment type (#/reconstituted)
LT-HSC					
G_0	10	57% (8/14)	1.1% (0.1–3.9%) M + L (8/8)	57% (8/14)	4.7% (0.3–15.2%) M + L (8/8)
	50	100% (5/5)	1.5% (0.1–5.8%) M + L (5/5)	100% (5/5)	5.7% (0.5–14.3%) M + L (5/5)
G_1	10	8% (1/12)	0.2% M only (1/1)	0% (0/11)	n/a
	50	50% (3/6)	4.2% (0.1–12.5%) M only (3/3)	0% (0/5)	n/a
S-G_2/M	10	0% (0/9)	n/a	0% (0/9)	n/a
	50	50% (3/6)	0.4% (0.2–0.7%) M + L (3/3)	33% (2/6)	0.35% (0.3–0.4%) M + L (1/2), L only (1/2)
KTLS HSC					
G_0	10	50% (6/12)	0.7% (0.1–1.2%) M + L (5/6), M only (1/6)	42% (5/12)	3% (0.2–10.6%) M + L (5/5)
	50	100% (4/4)	0.7% (0.1–1.2%) M + L (4/4)	100% (4/4)	2.9% (0.4–8.2%) M + L (4/4)
G_1	10	0% (0/10)	n/a	0% (0/10)	n/a
	50	25% (1/4)	0.3% M (1/1)	0% (0/4)	n/a
S-G_2/M	10	0% (0/10)	n/a	0% (0/10)	n/a
	50	20% (1/5)	0.6% M + L (1/1)	20% (1/5)	0.3% L only (1/1)

Figure 12: Quiescent LT-HSCs possess the highest engraftment capacities
Correlation between cell cycle status and reconstitution capacities of LT-HSCs (red) and KTLS HSCs (blue). As little as 50 cells in G_0 (quiescent) of the cell cycle of either LT-HSCs or KTLS HSCs showed 100% reconstitution after 3-4 weeks and 9-12 weeks post transplantation (Adapted Passegué, et al., 2005).

3.8.1.3 Factors controlling HSC dormancy

Under homeostatic conditions dormant HSCs are kept quiescent and divide only rarely (Wilson, et al., 2008). This already indicates that these stem cells need to be tightly controlled and regulated to prevent accidental activation of this important stem cell pool. Recently, some key signaling molecules have been identified that are crucial in controlling HSC dormancy and activation. To these factors belong molecules that are expressed directly in the HSC niche by cells, which stay in close interaction to dormant HSCs. One important cell adhesion interaction that controls HSC quiescence is the Angiopoetin-Tie system. Arai and colleagues demonstrated that HSCs that express the receptor tyrosine kinase Tie2 are quiescent and additional expression of angiopoetin1, the ligand for Tie2, in endosteal osteoblasts further increased HSC quiescence by binding HSCs to their niche (Arai, et al., 2004). In addition thrombopoetin (TPO), a hormone that regulates megakaryocyte differentiation, was shown to be involved in maintaining quiescence of HSCs. Transgenic wherein the the TPO receptor was knocked out, showed a reduction in the frequency of quiescent HSCs during aging in a TPO dependent manner (Arai, et al., 2009; Qian, et al., 2007; Yoshihara, et al., 2007).

The most potent regulators for HSC quiescence, self-renewal and differentiation are cell cycle associated genes that directly influence cell cycle entry and exit of these cells. During the last years several genetic mouse models have been establish to better understand the influence of cell cycle related genes on HSC maintenance and quiescence (Figure 13).

Category	Gene(s)	Genetic model	HSC cell cycle activity	Developmental stage	References
Cell-intrinsic mechanisms					
Cell cycle regulators	*pRb/p107/p130*	*Mx1-Cre* conditional deletion	Increased	Adult	Viatour et al., 2008
	CyclinD1/D2/D3	Triple knockout	Decreased	Fetal	Kozar et al., 2004
	Cdk4/6	Double knockout	Decreased	Fetal	Malumbres et al., 2004
	p21^{Cip1}	Knockout	Decreased or unchanged	Adult	Cheng et al., 2000a; van Os et al., 2007; Foudi et al., 2009
	p57^{Kip2}	*Mx1-Cre* conditional deletion	Increased	Adult	Matsumoto et al., 2011
	p27^{Kip1}/p57^{Kip2}	Double knockout; fetal liver HSC transplant	Increased	Fetal, Adult	Zou et al., 2011
	p18^{ink4c}	Knockout	Increased	Adult	Yuan et al 2004
Transcription factors	*p53*	Knockout	Increased	Adult	Liu et al., 2009
	p53	Hypermorphic allele	Decreased	Old	Dumble et al., 2007
	junB	*More-Cre* conditional deletion	Increased	Adult	Santaguida et al., 2009
PI3K pathway	*Pten*	*Mx1-Cre* conditional deletion	Increased	Adult	Yilmaz et al., 2006; Zhang et al., 2006
	Tsc1	Knockout	Increased	Adult	C. Chen et al., 2008
	Akt1/2	Double knockout	Decreased	Adult	Juntilla et al., 2010
	myr-Akt	Retroviral expression	Increased	Adult	Kharas and Gritsman 2010
	Foxo1/3/4	Triple knockout	Increased	Adult	Tothova et al., 2007
	Foxo3	Knockout	Increased	Adult	Miyamoto et al., 2007
Cell-extrinsic mechanisms					
Environmental factors	*Tpo*	Knockout	Increased	Fetal, Adult	Qian et al., 2007
	Ang-1	Retroviral expression	Decreased	Adult	Arai et al., 2004
	Kit	Hypomorphic allele	Increased	Fetal, Adult	Thorén et al., 2008
	Cxcr4	*Rosa$^{Cre-Ert2}$* conditional deletion	Increased	Adult	Nie et al., 2008
Developmental pathways	*Dkk*	*Col1α2.3*-driven transgene	Increased	Adult	Fleming et al., 2008
	Gli1	Knockout	Decreased	Adult	Merchant et al., 2010

Figure 13: Genetic mouse models that contributed to the understanding of cell cycle control in HSCs
(adapted Pietras, et al., 2011)

There are two important groups of cell cycle inhibitors, the CIP/KIP family and the INK4a/ARF family. The cyclin dependent kinase inhibitors (CDKI) of the CIP/KIP family, $p21^{CIP1}$, $p27^{KIP1}$ and $p57^{KIP2}$, are crucial to control G_1/S transition of a cell by inhibiting cyclinE-CDK2 complex and in addition inhibit the cyclinA/CDK2 complex in early S-Phase. The same family also controls cell quiescence by negatively regulating the cyclinD-CDK4/6 complex and by prevention of G_0 exit and G_1 entry. The INK4a/ARF family comprises four family members, $p15^{INK4b}$, $p16^{INK4a}$, $p18^{INK4c}$ and $p19^{INK4d}$. This family is especially important in arresting the cells in early G_1 phase by preventing Retinoblastoma (Rb) tumor suppressor phosphorylation under stress conditions. Recently, it has been shown that especially $p21^{CIP1}$ expression can be attributed to HSC cell cycle control during stress conditions (Pietras, et al., 2011; Foudi, et al., 2009; Cheng, et al., 2000a). For $p27^{KIP1}$ it was recently identified that the protein directly cooperates with p130 to actively repress cell cycle progression into G_1 phase of the cell cycle (Pippa, et al., 2012). However its impact on HSCs is rather low and deletion of $p27^{KIP1}$ resulted in an accumulation of the

progenitor compartment (Cheng, et al., 2000b). It has been shown that especially $p57^{KIP2}$ is highly important for keeping HSCs in quiescence (Tesio and Trumpp 2011; Pietras, et al., 2011; Matsumoto, et al., 2011). Matsumoto and colleagues observed that the specific deletion of $p57^{KIP2}$ in HSCs results in a severe defect in self-renewal capacities and induces cell cycle entry, which can be rescued by knock-in of $p27^{KIP1}$ into the $p57^{KIP2}$ locus (Matsumoto, et al., 2011). This highlights the important role of $p57^{KIP2}$ in controlling HSC quiescence. Furthermore it seems that the CIP/KIP family members are differentially expressed in the different hematopoietic cell compartments and contribute in different manners to cell cycle control and cell functionality (Figure 14) (Tesio and Trumpp, 2011).

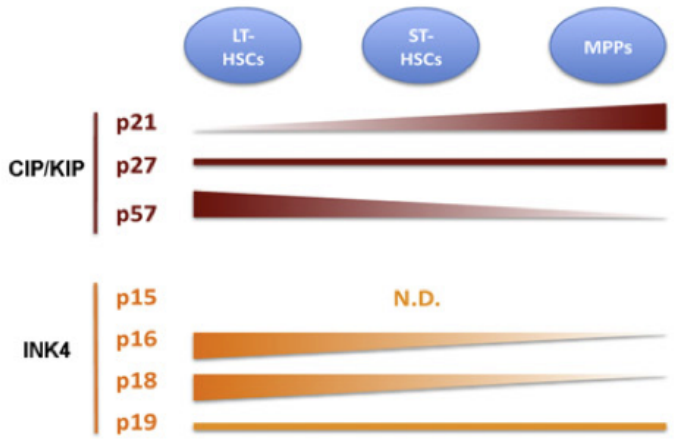

Figure 14: Expression level of cell cycle inhibitors depend on the hematopoietic stem cell type
Differences in the expression level of cell cycle inhibitors of the CIP/KIP and INK4a family in hematopoietic stem cell populations (LT-HSCs, ST-HSCs, MPPs) (Tesio and Trumpp, 2011).

Most interestingly, $p16^{INK4a}$ is only weakly expressed in HSCs and the deletion of this gene by interrupting the INK4a gene locus has only minor effects on HSC activity. This is mainly due to blocking of $p16^{INK4a}$ by the polycomb repressor Bmi1. In addition Bmi1 expression is low during cellular senescence when $p16^{INK4a}$ expression is increased. Notably, Bmi1 is a c-Myc target gene and was found to be involved in lymphoma onset by downregulating $p16^{INK4a}$ expression (Guney, et al., 2006; Van Lohuizen, et al., 1999). In contrast Bmi1-deficiency is lethal in adult animals as a consequence of a lack of self-renewal capacities of HSCs and an exhaustion of the HSC pool over time (Pietras, et al., 2011; Chagraoui, et al., 2011; Park, et al., 2003). Bmi1 has also been shown to block $p19^{ARF}$ expression, and it

thereby influences the p53 damage response pathway. Expression level of p18^{INK4c} directly correlates to HSC quiescence: in quiescent HSCs p18^{INK4c} is highly expressed, while little p18^{INK4c} expression identifies actively proliferating HSCs (Passegué, et al., 2005) (Figure 15).

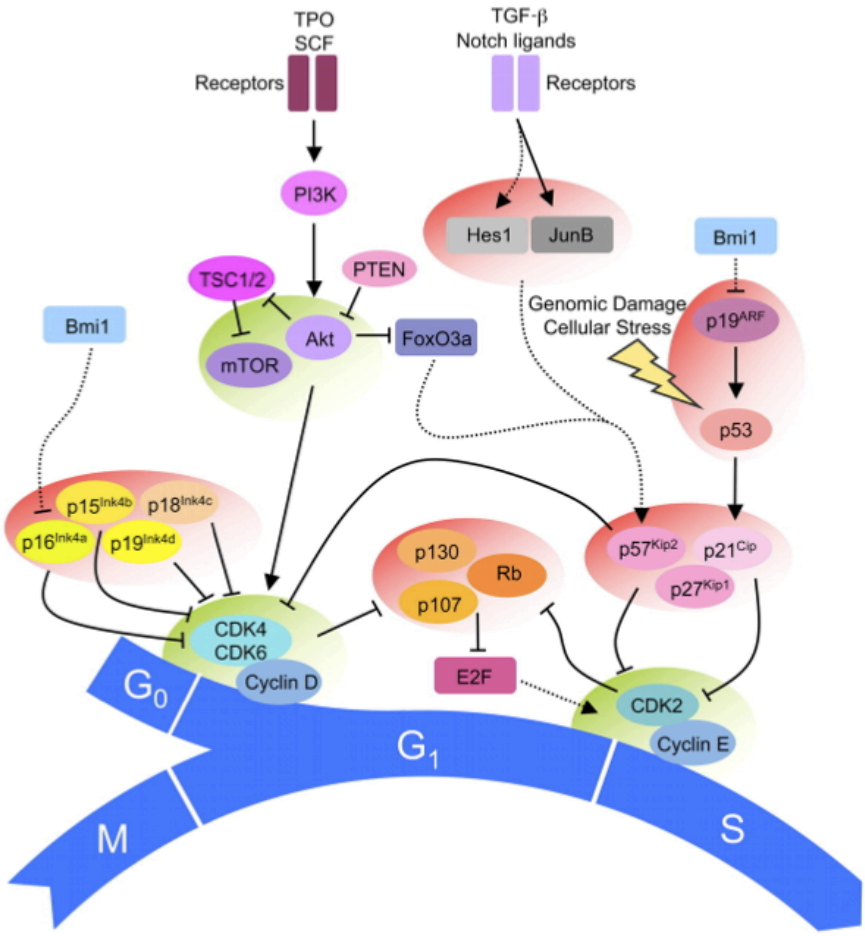

Figure 15: Cell cycle regulation of hematopoietic stem cells
Cell cycle inhibitors regulate cell cycle entry of hematopoietic stem cells (HSCs). The INK4 family with p15^{INK4b}, p16^{INK4a}, p18^{INK4c}, p19^{INK4d} blocks G_0/G_1 transition by CyclinD-CDK4/6 complex inhibition while the CIP/KIP family with p21^{CIP1}, p27^{KIP1}, p57^{KIP2} prevents G_1/S transition. Bmi1 physiologically represses p16^{INK4a} and under stress conditions prevents p19^{ARF} expression. (Pietras, et al., 2011)

3.8.1.4 Forced activation of dormant stem cells

Recently, our group and others showed that the quiescent stem cell pool can be actively pushed into cell cycle by interferon (IFN) treatment (Baldridge, et al., 2010; Essers, et al., 2009). Only a few hours after interferon administration *in vivo* dormant stem cells leave G_o and enter G_1 phase of the cell cycle (Trumpp, et al., 2010; Essers, et al., 2009). Notably, interferon treatment in animals leads to direct binding of interferon to its interferon receptor (INFR). Hence this causes further down-stream signaling and it seems that this correlates with an upregulation of the GPI-linker stem cell antigen (Sca-1), which seem to be crucial to induce cell proliferation in this process (Figure 16). In contrast *in vitro* treatment of HSCs and other cells with interferon results in an inhibition of cell proliferation. Importantly, interferon treatment does only lead to stem cell activation by induction of cell proliferation but not to a mobilization of the cells to the periphery (Essers, et al., 2009).

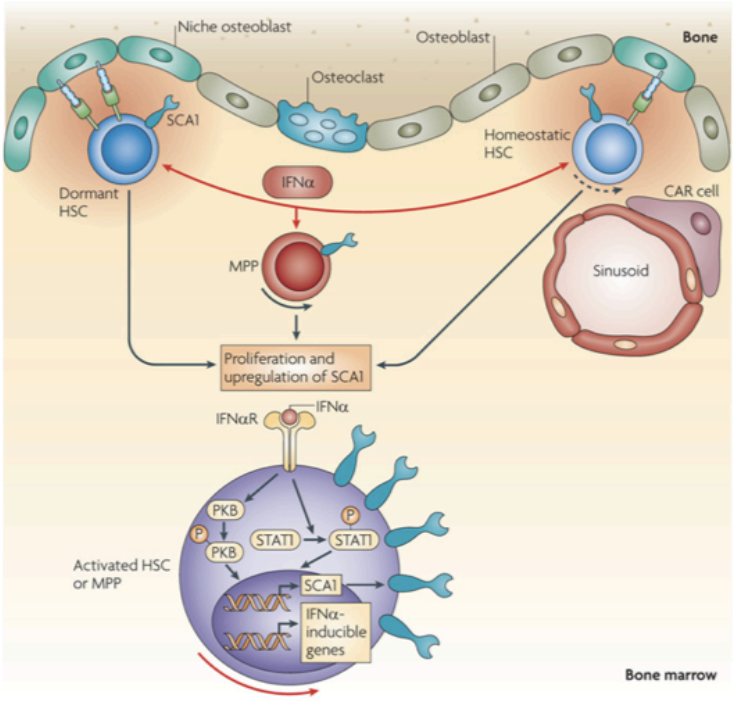

Figure 16: Activation of dormant stem cells by interferon
Interferon alpha (IFN**α**) leads to the activation of dormant hematopoietic stem cells (HSCs). IFN**α** signaling induces Stat1 expression that leads to the upregulation of stem cell antigen (Sca1) and the transcription of IFN-inducible target genes (Trumpp, et al., 2010).

Interferons in general comprise a large family of immune-response genes that are involved in cell growth regulation, anti-viral response and activation of the immune system (Doly, et al., 1998). In practice most often interferon treatment in animals is replaced by Polyinosinic:polycytidylic acid (PolyI:C; pI:C) as this efficiently mimics viral immune response and also leads to HSC activation. Another immune response inducer that activates dormant HSCs is the bacterial endotoxin lipopolysaccharide (LPS). Notably, all three types of immune response inducers have slightly different mechanisms that lead to intrinsic interferon production (Figure 17) (Trinchieri; et al., 2010). While IFN directly binds to the IFN_{α} receptor (IFNAR), LPS and pI:C induce intrinsic interferon production that subsequently activates interferon signaling upon binding to the IFNAR.

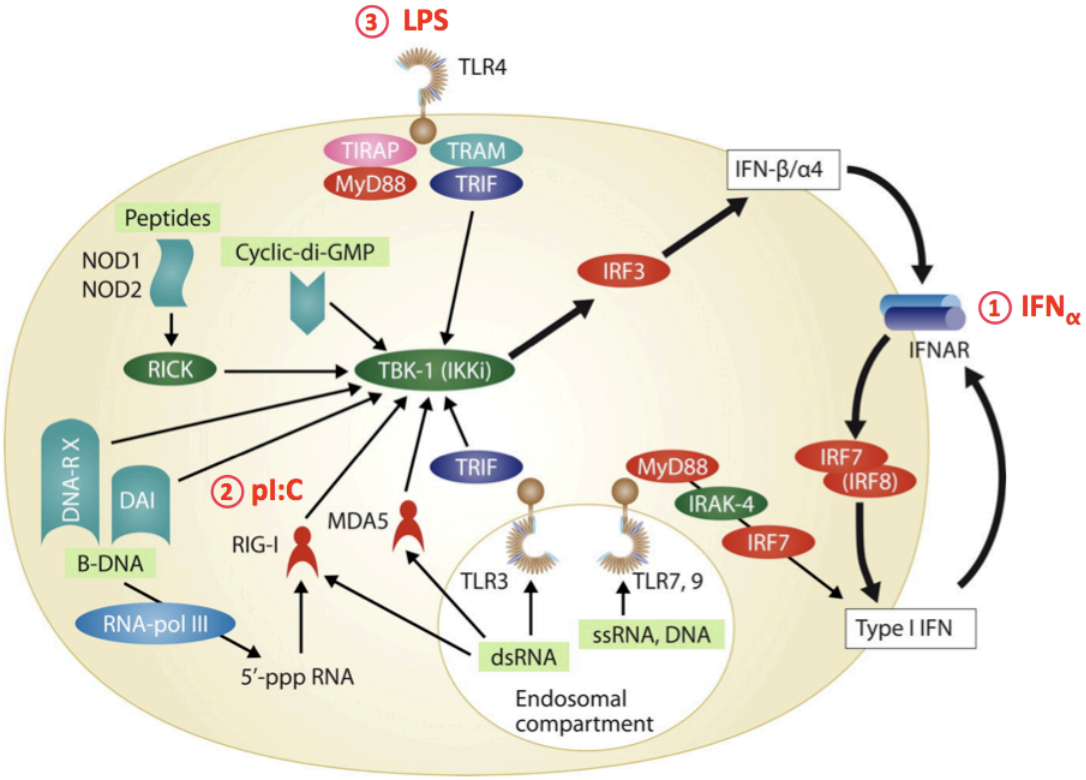

Figure 17: Toll-like receptor signaling cascades that induce interferon production in a cell
(1) Interferon alpha (IFNα) directly binds to the IFNA-receptor (IFNAR) on a cell and leads to induced interferon production. (2) Intrinsic toll-like receptor (TLR)-independent interferon production through PolyI:C (pI:C) that binds to helicase receptor retinoic acid inducible gene 1 (RIG-1) and melanoma differentiation-associated protein 5 (MDA5). (3) Lipopolysaccharide (LPS) TLR-4 dependent intrinsic interferon production (Adapted Trinchieri, et al., 2010).

Interferon signaling plays also an important role directly in the bone. It was recently shown that IFN_{γ} has two main effects in osteoclasts. It inhibits and simultaneously promotes osteoclastogenesis, while the net outcome triggers bone resorption (Gao, et al., 2007). The interaction of the RANK receptor on osteoclasts with RANK-L, which is secreted by osteoblasts, is crucial for osteoclast development (Monroe, et al., 2012; Wada,et al., 2006). However, RANK itself has no intrinsic enzymatic activity and needs for signal transduction other molecules, especially TNF-receptor associated factor 6 (TRAF6). Subsequently NFkB and Jun N-terminal kinase (JNK) signaling cascades are activated and induce AP-1 and NFATc target gene expression, which leads to further osteoclastogenesis by inducing the differentiation of pre-osteoclasts to functional mature osteoclasts. On the other hand TRAF6 signaling is also induced through Toll-like receptors (TLRs) and TLR4, 7 and 9 are expressed on osteoclasts. Importantly, the effect of TLR signaling in osteoclasts highly depends on the maturation status of the cells. In pre-osteoclasts TLR signaling inhibits final maturation, while in mature osteoclasts it promotes cell proliferation and osteoclastogenesis (Caetano-Lopes, et al., 2009; Takayanagi, et al., 2002) (Figure 18).

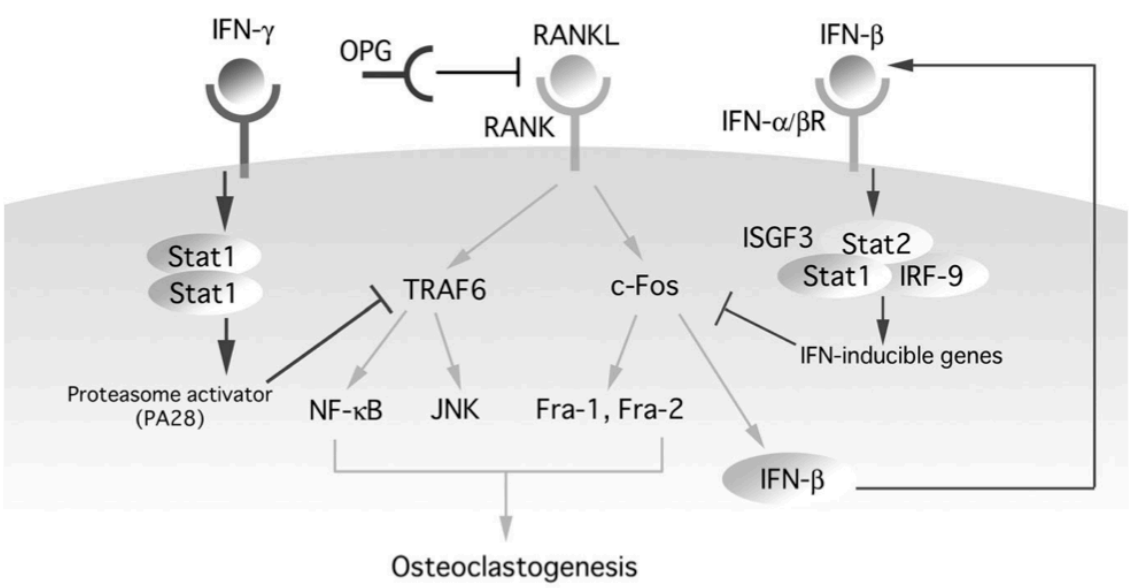

Figure 18: Effects of interferon signaling in osteoclasts
Interaction between RANKL and RANK leads to TRAF6 and c-Fos signaling induced osteoclastogenesis and interferon (IFNß) production in immature osteoclasts. IFNß negative feed-back loop induces the expression of IFN-inducible genes that slow down RANKL-RANK induced c-Fos signaling (Takayanagi, et al., 2002).

3.9 Generation of doxycycline-inducible *ColtTA;TreMyc* animals

Interestingly, our group recently showed that c-Myc is also involved in normal hematopoietic stem cell (HSC) maintenance and differentiation (Laurenti, et al., 2009; Wilson, et al., 2008). Osteoblasts are bone-lining cells that are part of the HSC niches and thus are involved in the regulation of HSCs. The aim of this work was to analyze the effect of c-Myc amplification in osteoblasts on bone development and its influence on HSCs.

In our laboratory an inducible transgenic mouse line for human c-Myc overexpression in mature osteoblasts had already been established (Jaworski and Trumpp, thesis 2009). Mice in which the expression of the tetracycline transactivator (tTA) was controlled by the osteoblast specific collagen I promoter (col1α1) was crossed with mice transgenic for the tetracycline response element (TRE) and oncogenic human c-Myc (MYC). The tissue specific col1α1 promoter regulated the expression of the tTA transactivator, which then in turn bound to TRE and induced Myc expression. Thus human c-Myc was selectively overexpressed in mature osteoblasts. Furthermore c-Myc expression could be repressed by doxycycline. Upon addition of doxycycline, an antibiotic of the tetracycline family, the antibiotic interacted with the tetracycline transactivator, thereby blocking TRE interaction and thus inhibiting c-Myc overexpression (Figure 19).

Initial studies had shown that c-Myc overexpression during embryonic development led to neonatal death of newborns as a consequence of bone developmental disorders (Jaworski and Trumpp, thesis 2009). In order to suppress this strong phenotype in embryos, doxycycline was added to the drinking water of the mouse matings until the weaning age of the newborns, thereby preventing human c-Myc overexpression in bone cells of the embryo. In three week old *ColtTA;TreMyc* (mutant, mt) mice human c-Myc overexpression was subsequently induced by the removal of doxycycline containing drinking water until this stage mutant mice showed normal development (Jaworski and Trumpp, thesis 2009).

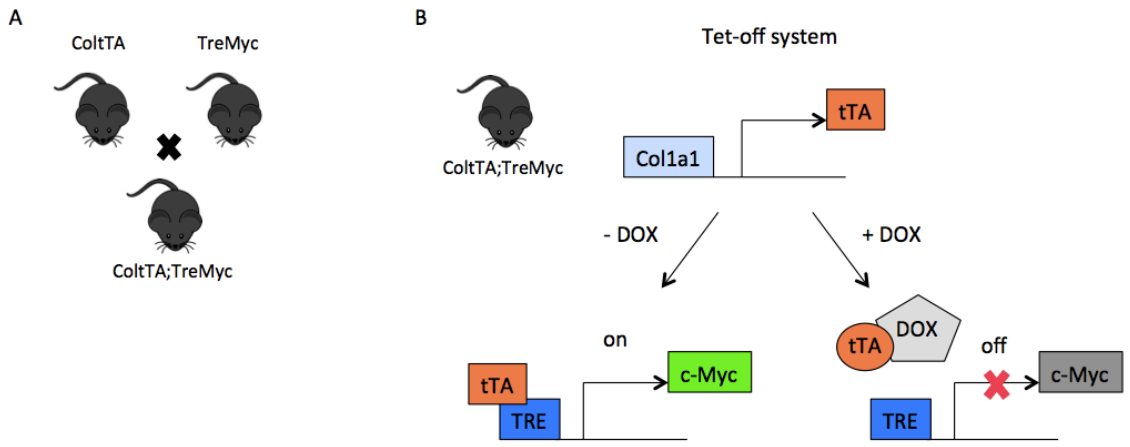

Figure 19: Generation of double transgenic *ColtTA;TreMyc* animals
(A) Transgenic mice with the osteoblast specific promoter collagen I (col1α1) and transgenic for tetracycline transactivator (tTA) are crossed with mice transgenic for the tetracycline response element (TRE) and oncogenic human c-Myc (MYC) to generate *ColtTA;TreMyc* littermates (mutant animals). (B) Doxycycline-inducible Tet-off system: human c-Myc expression is turned on in the absence of doxycycline (Dox) and it is repressed by doxycycline addition.

4 AIM

The human bone is an endocrine organ that is important beyond the simple task of providing a skeleton. Within the bones many complex processes take place such as the genesis and maintenance of the cells for the hematopoietic system or continuous bone remodeling. The effects of the human proto-oncogene c-Myc are cell dependent. Therefore the major aim of this thesis was to study the effect of human c-Myc overexpression in mature osteoblasts. In particular the following aspects should be analyzed:

- What effect has c-Myc overexpression on bone structure and morphology? It is known that bone development involves a complex interplay between bone-matrix generating cells, the osteoblast and bone-matrix degrading cells, the osteoclasts. In many human diseases this interplay is destroyed or impaired. Thus the morphological as well as molecular properties will be closely monitored in order to further elucidate the role of osteoblasts in the human bone.

- Can c-Myc overexpression induce tumor formation? c-Myc is a proto-oncogene that is involved in a great number of cellular processes and is frequently involved in human tumors. The aim of this work will be to determine, whether c-Myc overexpression in fact has a tumorigenic effect and to further characterize the tumors. As currently human osteosarcoma models are rare and very artifical, it will be interesting to see whether the *ColtTA;TreMyc* mouse model will be useful as an alternative.

- Does c-Myc overexpression in endosteal osteoblasts influence hematopoietic stem cells (HSCs)? Osteoblasts form an important part of the stem cell niche which is responsible for regulating the self-renewal and differentiation processes of the HSCs. The effects that c-Myc overexpression exerts on signalling pathways within the osteoblasts, will help to further elucidate the crosstalk between osteoblasts and the HSCs and also with other cells of the hematopoietic niche.

5 RESULTS

5.1 Validation of mouse alpha1(I)-collagen promoter specificity

Collagen is one of the most abundant proteins in mammals and is predominantly expressed in connective tissues and bones where it helps to stabilize these tissues. An abbreviated version of the collagen promoter is specifically activated during bone development (Marko, *et al.*, 2003; Dacquin, *et al.*, 2002). Since the 2.3-kb proximal fragment of the mouse alpha1(I)-collagen promoter was used in the transgenic mice, the specificity of this promoter in the transgenic mouse line was assessed. Therefore the mRNA expression levels of human c-Myc in the bone marrow and bones of mutant mice (Figure 20) were analyzed by quantitative real time PCR (qRT-PCR).

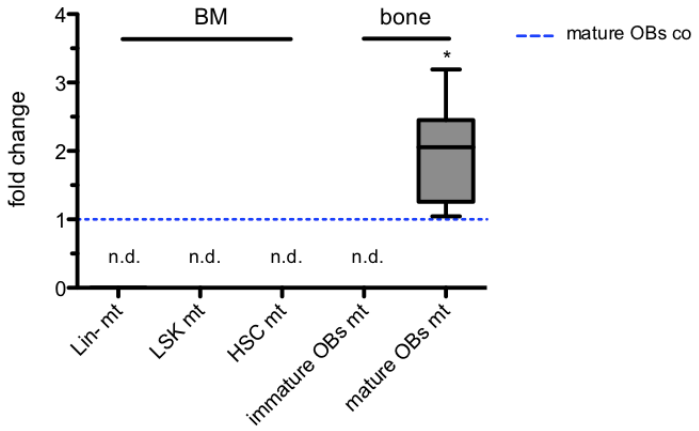

Figure 20: Human c-Myc mRNA expression in *ColtTA;TreMyc* animals is restricted to mature osteoblasts
Human c-Myc mRNA expression level in different cell compartments of the bone marrow (BM) and the bone of mutant 20-week old *ColtTA;TreMyc* animals detected by qRT-PCR (Lin- = lineage negative cells, LSK = Lin- Sca1$^+$ c-Kit$^+$, HSC = LSK CD150$^+$ CD48$^-$ CD34$^-$, immature OBs = CD45$^-$ CD31$^-$ Ter119$^-$ Sca-1$^+$ CD51$^+$, mature OBs = CD45$^-$ CD31$^-$ Ter119$^-$ Sca1$^-$ CD51$^+$). Expression levels are indicated as fold changes against healthy control mature osteoblasts (blue dotted line = mature OBs co) and normalized to SDHA and OAZ (n = 7, n.d. = not detectable).

Human c-Myc mRNA was only detected in mature osteoblasts of mutant animals, while it was not detectable in immature osteoblasts as well as in different cells of the hematopoietic system including lineage negative cells (Lin-), hematopoietic progenitors (LSK) and hematopoietic stem cells (HSC). Especially in control osteoblasts only very little human c-Myc expression could be detected due to high DNA sequence homology between mouse and human c-Myc. This analysis confirms that the collagen promoter is specifically activated in mature osteoblasts.

During embryogenesis the collagen promoter becomes active at embryonic day 14.5 (E14.5) as soon as bone development begins (Figure 2A). To further confirm that the expression of human c-Myc is indeed restricted to mature osteoblasts, histological sections of embryonic femurs from day E17.5 were performed. For this purpose the *ColtTA;TreMyc*;TreH2B-GFP mouse line (mt) was used, which expresses a fusion protein between histone H2B and GFP in addition to the c-Myc transgene. In addition for the purpose of control experiments the mouse line ColtTA;TreH2B-GFP (co) without any human c-Myc expression was used. The expression of both elements is controlled by the tetracycline response element (Gossen and Bujard, 1992). In this mouse line only cells with an active alpha1(I)-collagen promoter show GFP expression, indicating c-Myc overexpression in GFP-positive cells.

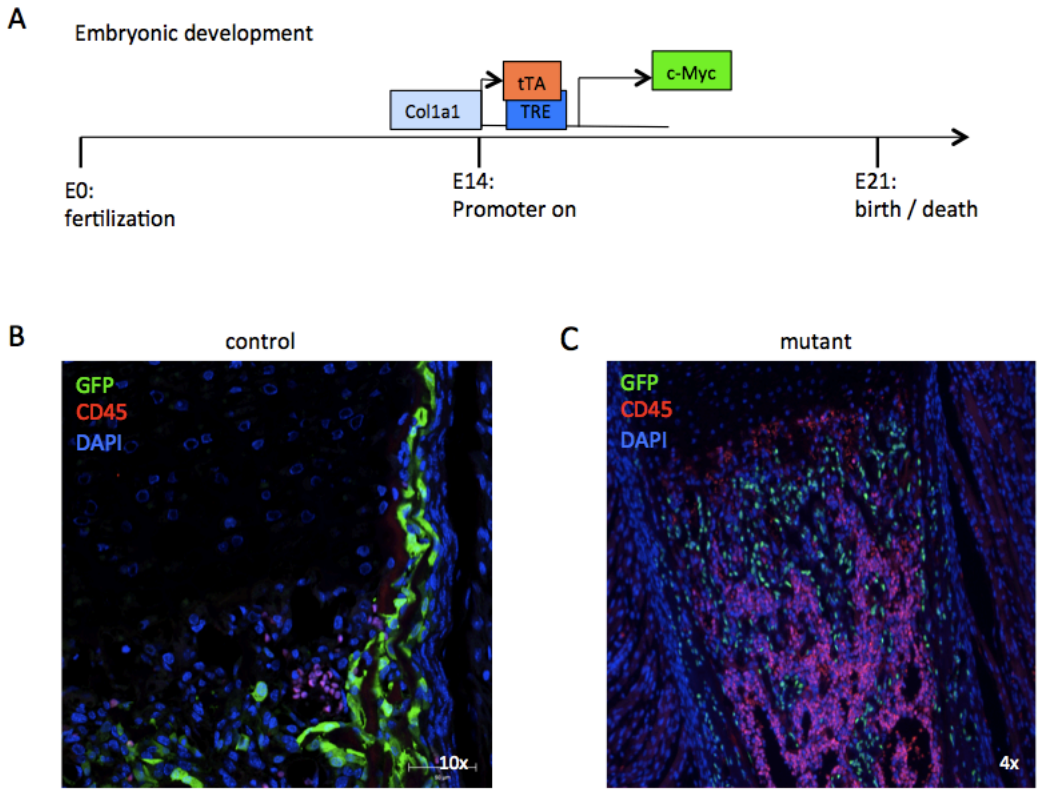

Figure 21: Collagen promoter specificity and the identification of GFP-positive osteoblasts by histology
Collagen promoter activity starts at embryonic day E14. In transgenic animals human c-Myc expression is turned on by interaction of the tetracycline-transactivator (tTA) with the tetracycline-responsive element (Tre) (A). CD45 expression in hematopoietic bone marrow cells (red) and GFP-positive expression in osteoblasts (grün) show collagen promoter specificity in control (B) and mutant (C) E17.5 femurs. Dapi is used as counterstaining.

Analysis of the histological sections demonstrated that GFP positive cells in the femur of control and mutant mice do not express the hematopoietic cell marker CD45 (Figure 21). This confirms the specificity of the collagen promoter as simultaneous GFP and c-Myc expression was strictly restricted to non-hematopoietic cells in mutant animals. In addition control animals showed promoter activity by GFP-expression without any c-Myc transgene correlation.

5.2 Histological analysis of transgenic *ColtTA;TreMyc* animals

It was previously shown that overexpression of human c-Myc in mature osteoblasts during embryonic development had a major influence on bone maturation as well as the life-span of the animals (Jaworski and Trumpp). After the specificity of the collagen promoter for mature osteoblasts had been demonstrated next I went on to elucidate the influence of c-Myc on bone development in adult animals. Therefore mice were treated with doxycycline containing drinking water until weaning age. Starting from three weeks of age, c-Myc expression was induced in mature osteoblasts. Bone morphology was analyzed in 20-week old animals. Strikingly *ColtTA;TreMyc* animals showed enhanced bone thickening and shorter bones (Figure 22B, left picture). Furthermore histological sections of demineralized femurs from 20-week old animals were performed.

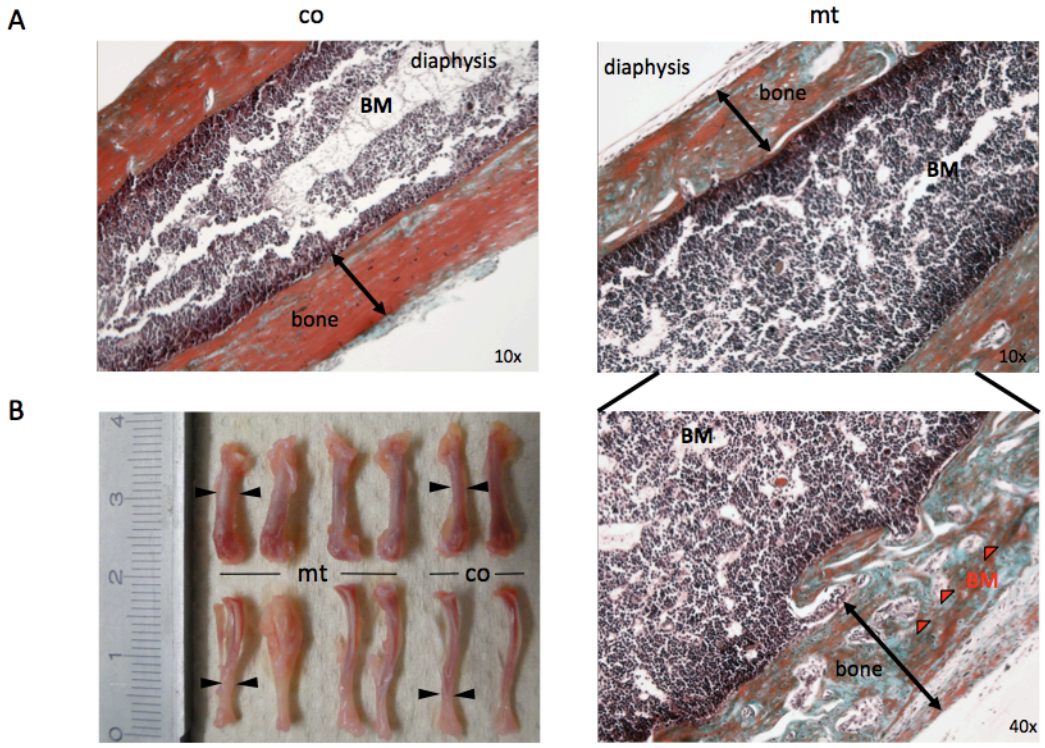

Figure 22: Irregular bone structure of *ColtTA;TreMyc* animals
Staining on decalcified paraffin sections indicates differences in bone thickness and bone structural organisation between control (co) and mutant (mt) femurs. Blue/green staining detects mineralized bone consisting mainly of collagen, produced by osteoblasts while pink/red staining highlights compact bone with mainly osteocytes; 10x magnification (A), 40x magnification (B, right picture). Differences in the phenotype of control and mutant bones of 20-week old animals in bone thickness and length (Black arrowheads = bone thickness, red arrowheads = bone marrow (BM) in mutant bone caverns).

The tissues were stained according to Masson Goldner staining and revealed that the mutant bones mainly consist of connective tissue. In contrast to control bones the compact bone structure seemed to be completely lost in mutant animals. The bones were thicker and exhibited irregular cavernous structures comprising bone marrow cells within the bone, thereby braking down the solid composition of a normal bone. Even though bones were partially demineralized for a short period of 4 days prior to the histological sections, the mutant bones still contained significant amounts of mineralized bone matrix, shown by collagen presence and green stained areas (Figure 22). In contrast, the control bone mainly consists of terminally differentiated osteocytes that are no more able to synthesize collagen and are only embedded into the bone matrix. Osteocytes are stained in pink. This indicates that the mutant bones contain significantly higher levels of collagen. Taken together these data suggest that there are more osteoblasts in mutant bones while in the bones of control animals contain more terminally differentiated osteocytes.

5.3 Analysis of the osteoblast compartment in *ColtTA;TreMyc* animals

5.3.1 Detection of mature osteoblasts by flow cytometry

To corroborate the findings of the histological sections, I next quantified the amount of osteoblasts present in the bones of control and mutant animals by flow cytometry. The gating strategy employed to identify osteoblast in the stroma is shown in Figure 5. First, hematopoietic cells were excluded based on CD45 and Ter119 positivity. Next, CD31 positive endothelial cells were excluded. Within the remaining population, mature and immature mesenchymal populations were defined by CD51 and Sca1. The osteoblast marker CD51 is also known as the vitronectin receptor or integrin alpha-V. In addition Sca1, the stem cell antigen, enabled to distinguish mature osteoblasts from more primitive cell populations in the stroma.

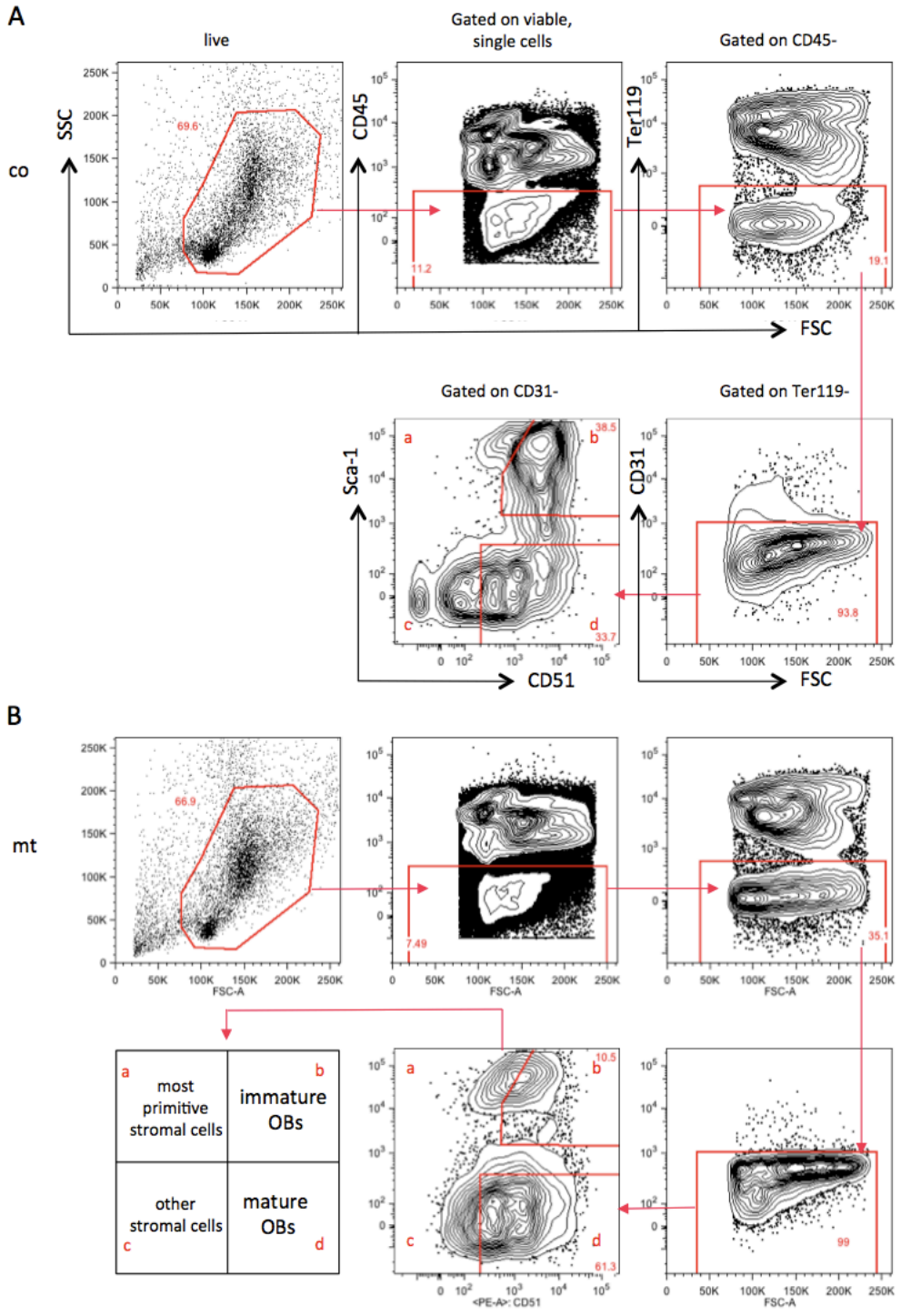

Figure 23: Identification of mature osteoblasts by flow cytometry

Representitive FACS plot indicates the gating strategy used to identify osteoblast populations from control (co) (A) and mutant (mt) (B) animals in the stromal compartment. Stromal cells can be separated into four groups as indicated: a = most primitive stromal cells CD45$^-$ CD31$^-$ Ter119$^-$ Sca-1$^+$ CD51$^-$, b = immature osteoblasts (OBs) CD45$^-$ CD31$^-$ Ter119$^-$ Sca-1$^+$ CD51$^+$, c = other stromal cells CD45$^-$ CD31$^-$ Ter119$^-$ Sca-1$^-$ CD51$^-$, d = mature osteoblasts (OBs) CD45$^-$ CD31$^-$ Ter119$^-$ Sca-1$^-$ CD51$^+$).

Mutant osteoblasts are phenotypically indistinguishable from control osteoblasts by FACS Figure 23). However quantification of the FACS data showed, that the percentage of osteoblasts was significantly increased in mutant animal. The increase was about two fold compared to control animals. In contrast the level of immature osteoblasts were not significantly different in control and mutant mice.

To confirm these observations, histo-morphometric analysis of skeleton measures was performed. Here the number of osteoblasts per bone perimeter is determined in histological sections. The analysis revealed about 15 osteoblast per bone perimeter in control animals, while in mutant mice the number of osteoblast was almost doubled to about 30. Thogether this indicates that c-Myc overexpression in osteoblasts results in increased numbers of mature osteoblast in *ColtTA;TreMyc* animals (Figure 24).

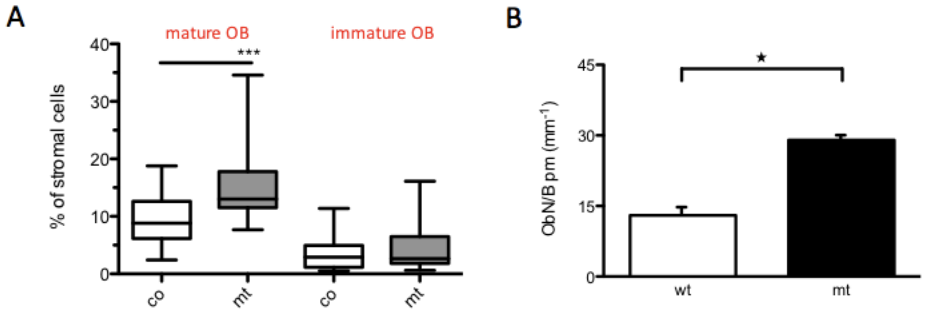

Figure 24: Quantification of stromal compartments reveals increased osteoblast numbers in transgenic animals
Box plot analysis indicates the percentage of mature osteoblasts ($CD45^-$ $CD31^-$ $Ter119^-$ $Sca\text{-}1^-$ $CD51^+$) and immature osteoblasts ($CD45^-$ $CD31^-$ $Ter119^-$ $Sca\text{-}1^+$ $CD51^+$) within stromal cells ($CD45^-$ $CD31^-$ $Ter119^-$) of ColtTA (co) and *ColtTA;TreMyc* (mt) animals (co: n = 21, mt: n = 30) (A). Histo-morphometric bone measurements comparing wt (control osteoblasts) to mt animals (ObN/B pm (mm^{-1}) = number of osteoblasts per bone perimeter, measured per mm) (wt = co: n = 6; mt: n = 6) (B).

5.3.2 Cell proliferation of mature osteoblasts

c-Myc controls the cell cycle and cell proliferation in a cell type specific manner. The previous set of experiments demonstrated that as a consequence of c-Myc overexpression in mature osteoblasts the percentage of osteoblasts in mutant animals is significantly increased. Therefore, I next assessed the cell proliferation rate of the mutant osteoblasts to see whether their increased proliferation accounts for the observed expansion. In addition the mRNA expression level of different cell cycle regulator genes was analyzed by qRT-PCR.

To analyze the cell proliferation rate of osteoblasts *in vivo,* a 5-Bromo-2-deoxy-uridine (BrdU) assay was performed. Therefore the animals were injected with BrdU intra-peritoneally 16-24 hrs before the analysis. While all cells take up BrdU, only actively proliferating cells incorporate the thymidine analogue BrdU into the DNA.

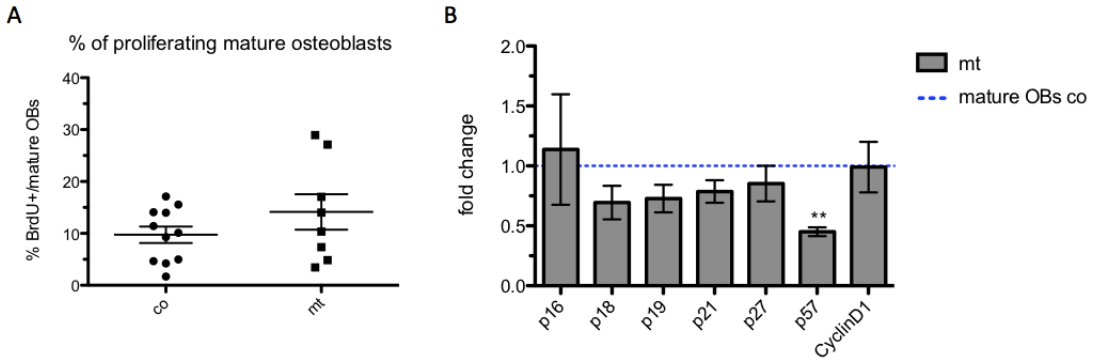

Figure 25: Cell proliferation and cell cycle regulators of mutant mature osteoblasts are impaired
Scatter plot analysis shows the percentage of $BrdU^+$ cells, representing the fraction of actively proliferating cells among mature osteoblasts (A). mRNA expression of different cell cycle regulators as determined by qRT-PCR. Expression values are normalized to SDHA and OAZ and fold changes of mutant osteoblasts are compared to mature osteoblasts of control animals (blue dotted line) (B) (n = 3 for p16 - p19; n = 10 for p21 – CyclinD1).

For FACS analysis stromal cells were gated for mature osteoblasts (for gating strategy compare Figure 23) and the percentage of actively proliferating osteoblasts was determined (Figure 25). No significant differences in the cell proliferation rates of control and mutant mature osteoblasts could be detected. Thus despite the role of c-Myc in promoting cell

cycle progression, the cell proliferation rate was only slightly increased in mutant osteoblasts (Figure 25, A). This confirms that the bone lining osteoblasts tend to be a more quiescent cell population compared to the hematopoietic cells where the proliferation rate, after a similar BrdU pulse, is usually about 30% (Kim, *et al.*, 2012; Hauge, *et al.*, 2001).

To gain more insight into the regulation of proliferation in osteoblasts, I next performed qRT-PCR analysis for several cell cycle regulators was performed on sorted mature osteoblasts (singlets, $CD45^-$ $CD31^-$ $Ter119^-$ $Sca\text{-}1^-$ $CD51^+$) from control and mutant animals. The cell cycle is tightly controlled by two groups of cell cycle regulators: the cyclins and the cyclin-dependent kinases (CDKs). Therefore qRT-PCR on Cyclin D1 and the CDKs of the cip/kip and the INK4a/ARF families was performed to better understand the cell proliferation behavior of c-Myc overexpressing osteoblasts.

The mRNA expression level of the cell cycle regulators $p21^{CIP1}$ and $p27^{KIP1}$ of the cip/kip family was unaffected by c-Myc overexpression (Figure 25, B). Also the expression for the CDKs $p15^{INK4b}$, $p18^{INK4c}$ and $p19^{INK4d}$ of the INK4a/ARF family was unchanged, while in contrast $p57^{KIP2}$ was significantly down-regulated in mutant osteoblasts. Previous work had identified a role of $p57^{KIP2}$ in retaining cells in G_1 phase of the cell cycle (Kim, *et al.*, 2008; Nishimori, *et al.*, 2001; Urano, *et al.*, 1999; Drissi, *et al.*, 1999). The down-regulation of $p57^{KIP2}$ might therefore drive c-Myc overexpressing osteoblasts into proliferation, even though this could not be confirmed by BrdU analysis. An explanation for the modified BrdU incorporation might be because incubation times were too short to see any significant effects. In contrast the observed increase in osteoblast numbers in transgenic animals as identified by histo-morphometric analysis and by quantitative flow cytometry (Figure 24) appears to corroborate the hypothesis that c-Myc induces cell proliferation.

5.3.3 Analysis of osteoblast maturation and differentiation

Interestingly, previous work had demonstrated that $p57^{KIP2}$ not only was involved in cell cycle regulation but also in promoting osteoblast differentiation. The down-regulation of $p57^{KIP2}$ might therefore also affect the balance between proliferation and differentiation. Therefore, as c-Myc has been described to have an influence on osteoblast differentiation, a next set of experiments was performed to assay genes involved in osteoblast maturation and differentiation. The differentiation of MSCs towards the osteoblastic lineage involves many intermediate steps including a variety of transcription factors and highlights the complexity of osteoblast cell maturation. Osteoblasts themselves are mature even though they possess the ability to finally differentiate into osteocytes.

In a first step the expression levels of differentiation markers were compared for immature and mature osteoblasts from non-manipulated regular C57BL/6 mice. As expected earlier the maturation of osteoblasts can be directly linked to the expression of specific genes (Wei, et al., 2012; Neve, et al., 2010; Franz-Odendaal, et al., 2006; Hauge, et al., 2001; Harada, et al., 1999; Ducy, et al., 1997). While in immature osteoblasts mRNA expression for Sca-1 was high and low for osteocalcin, the opposite was the case in mature osteosblasts.

QRT-PCR analysis of mature, mutant osteoblasts showed that in mutant osteoblasts collagen I production was increased as the gene encoding for collagen I synthesis is about 4-fold upregulated in mutant osteoblasts. This nicely corroborates the finding of histological sectioning and staining with Masson Goldner of mutant bones, where mutant femurs show more collagen presence as compared to control bones (Figure 22, green = collagen). Apart from collagen mutant osteoblasts seem to be unchanged in all the other markers and did not show significant changes compared to control osteoblasts. This indicates that c-Myc overexpression directly influences collagen I mRNA expression levels in mutant osteoblasts but none of the other maturation and differentiation markers.

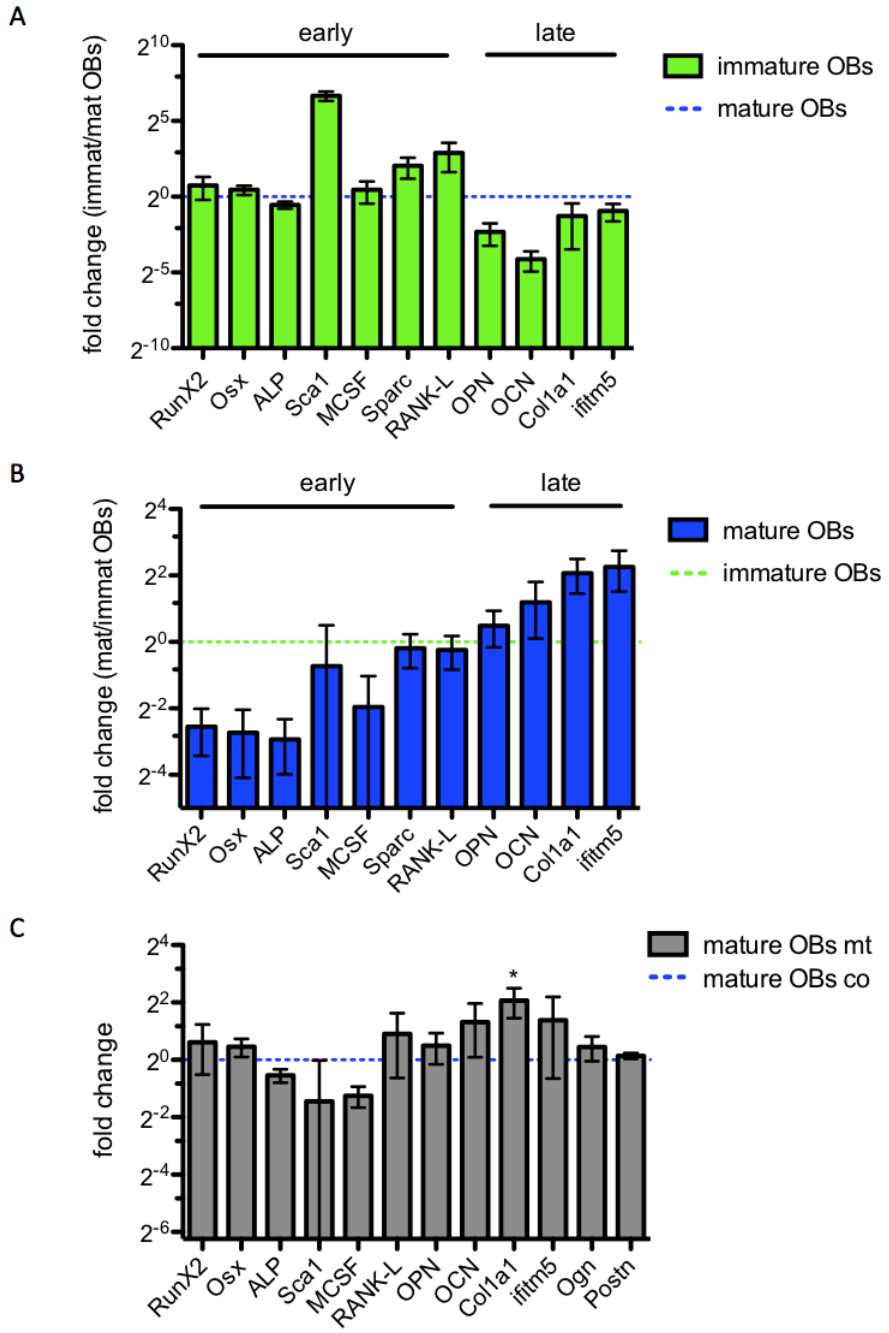

Figure 26: Analysis of osteoblast maturation genes shows elevated collagen expression in mutant osteoblasts
Early and late maturation marker expression of sorted immature osteoblasts ($CD45^-$ $CD31^-$ $Ter119^-$ $Sca\text{-}1^+$ $CD51^+$) (A) and mature osteoblasts ($CD45^-$ $CD31^-$ $Ter119^-$ $Sca\text{-}1^-$ $CD51^+$) (B) from C57BL/6 mice (RunX2, Sca-1, RANK-L, OCN: n=8; Osx, ALP, MCSF, Sparc, OPN, Col1a1, ifitm5: n = 4). Comparison of early and late maturation marker expression of mutant mature osteoblasts as fold changes against control osteoblasts (blue dotted line) (C). All genes are normalized to SDHA and OAZ. Expression values of early and late maturation marker in sorted mutant osteoblasts, represented as fold changes against mature osteoblasts from control animals (blue-dotted line) and normalized to SDHA and OAZ (RunX2, ifitm5: n = 7; Osx, OPN, MCSF, RANK-L, Sca-1: n = 4; Col1a1, Ogn, Postn: n =3; ALP, OCN: n = 5;) (C).
(RunX2 = runt-related transcription factor 2, Osx = osterix, ALP = alkaline phosphatase, Sca-1 = stem cell antigen, MCSF = macrophage colony stimulating factor, Sparc = osteonectin, RANK-L = receptor activator of nuclear factor kappa-B ligand, OPN = osteopontin, OCN = osteocalcin, col1a1 = collagen type I alpha 1, ifitm5 = interferon-inducible transmembrane protein 5; Ogn = osteoglycin; Postn = Periostin).

5.3.4 The Wnt signaling pathway in osteoblast maturation

Wnt signaling is a key pathway that plays a major role in embryogenesis and cell physiology and is frequently aberrant during tumorigenesis (Jeong, et al., 2012; Lai, et al., 2009; Taketo, et al., 2006; Glassil, *et al*., 2005; Moon, et al., 2004). In bone development the role of Wnt signaling is mainly to regulate the differentiation of osteoblast progenitors – the mesenchymal stem cells (MSCs) - to osteoblasts. Furthermore, Wnt signaling controls the final maturation step of pre-osteoblasts to functional mature osteoblasts. Thus I wanted to test whether c-Myc overexpression also affected Wnt-signaling in mutant osteoblasts. Therefore mRNA expression levels of genes involved in Wnt signaling were determined in sorted mutant osteoblasts by qRT-PCR.

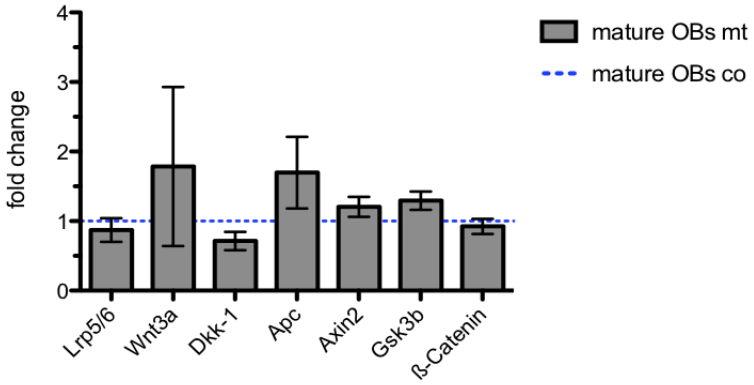

Figure 27: Expression level of genes involved in Wnt signaling are unchanged in mature osteoblasts
Fold changes represent the ratio between mutant osteoblasts against control osteoblasts (blue-dotted line) (normalized to SDHA and OAZ) (Lrp5/6 = LDL-receptor related protein 5/6, Wnt3a = wingless-type MMTV integration site family, DKK-1 = Dickkopf, Apc = adenomatous polyposis coli, Axin2 = axis inhibition protein2, Gsk3b = glycogen synthase kinase 3 beta) (Lrp5/6, Axin2, Gsk-3b: n = 7, DKK-1, Apc: n = 10, Wnt3a, ß-Catenin n = 14).

Interestingly, canonical Wnt signaling was not affected by human c-Myc overexpression in mature osteoblasts (Figure 27). None of the assayed genes showed any significant difference in the expression levels compared to mature control osteoblasts. This indicates that human c-Myc exerts no direct influence on Wnt activity in this important osteoblast differentiation pathway in mutant mature osteoblasts. However whether is has an influence on osteoprogenitors from *ColtTA;TreMyc* mutants still needs to be determined.

5.3.5 Transgenic animals show normal mineralization capacities in vitro

Taken together this indicates slight but significant effects of human c-Myc overexpression in mature osteoblasts as for example upregulated collagen I synthesis and $p57^{KIP2}$ down-regulation. I next analyzed whether c-Myc overexpression has any functional consequences in osteoblasts as a result of thickening of the bones.

Mineralization of the bone, the last step of osteoblast differentiation, can be easily assessed by von Kossa staining, which detects calcium deposition in tissues and organs by a silver nitrate reaction (Bonewald, et al., 2003). In bones, von Kossa staining indicates mineralized areas, showing the functionality of osteoblasts. However as the bone has to be demineralized for histological sections, von Kossa staining on mineralized bones of mutant and control animals was not possible. Osteoblasts from tibia and femur of control and mutant animals were isolated and cultured *in vitro* for 14 days followed by von Kossa staining.

The microscopic analysis revealed that mutant and control osteoblasts were equally able to produce mineralized bone material *in vitro* (Figure 28). Thus mutant osteoblatss possess normal mineralization properties.

Osteoblast functionality was tested independently by detection of alkaline phosphatase activity (ALP) (Miao, *et al.*, 2002). ALP expression starts in pre-osteoblasts and lasts until final differentiation to mature osteoblasts. The ALP staining of the mutant osteoblasts revealed no significant difference between control and c-Myc overexpressing osteoblasts (Figure 28). Thus mutant osteoblasts can be categorized as functional bone forming cells at least based on these findings *in vitro*. These results indicate that the human c-Myc overexpressing mature osteoblasts are functional. Therefore, the aberrant phenotype of the mutant bone (Figure 22) cannot be attributed to functional defects of osteoblasts.

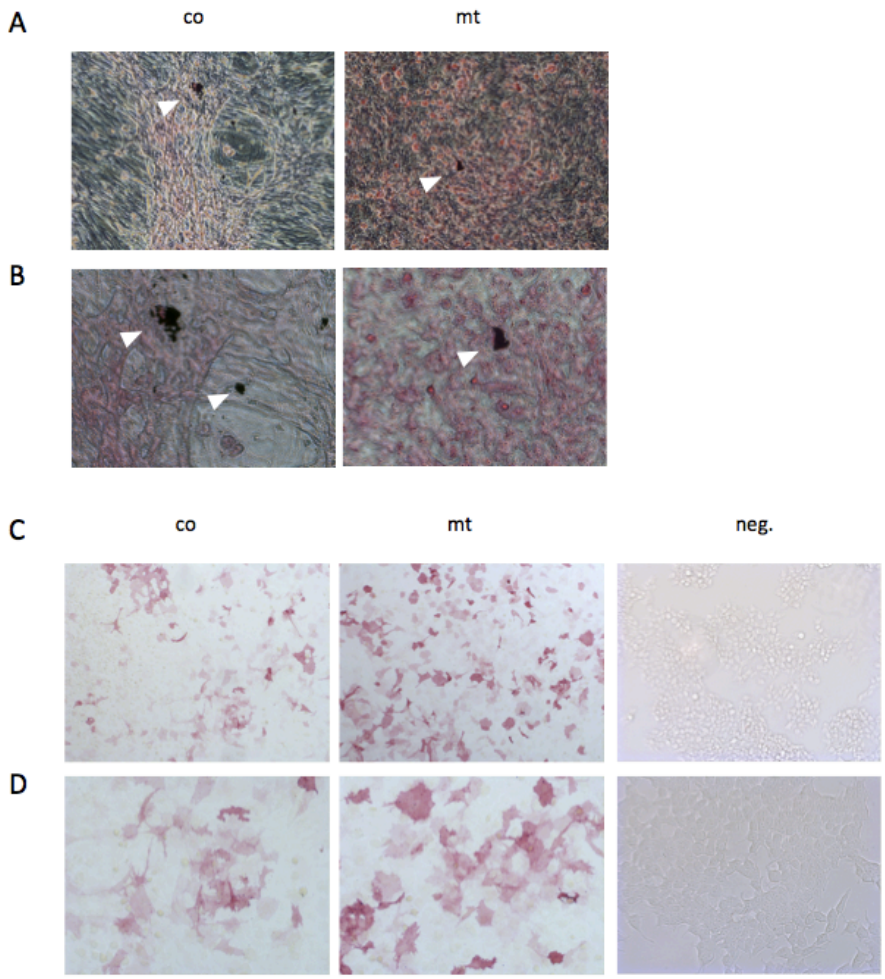

Figure 28: Mutant osteoblasts show normal mineralization capacity *in vitro*
Von Kossa staining on confluent osteoblast layers *in vitro* (left: control osteoblast culture (co), right: mutant osteoblast culture (mt). Arrowheads point out silver precipitations, 4x magnification (A), 10x magnification. (B). Alkaline phosphatase staining (ALP) on osteoblast cultures. Pink staining identifies ALP positive osteoblasts (co = control, mt = mutant, neg. = negative control, HEK 293 cells), 4x magnification (C), 10x magnification (D).

5.4 Analysis of the osteoclast compartment

5.4.1 Identification of osteoclasts by flow cytometry

Bone turnover is a strictly balanced process between bone formation and resorption. As I previously showed that the percentage of osteoblasts is significantly increased upon human c-Myc overexpression, I next investigated whether the number of bone resorbing cells, the osteoclasts, was simultaneously affected in transgenic animals as well (Figure 24). The number of osteoclasts in mutant animals was determined by gating on $CD45^{+}$ $Gr1^{-}$ $CD11b^{low/-}$ cell populations in the bone marrow to distinguish between immature osteoclasts ($F4/80^{-}$ $CD115^{+}$) and mature osteoclasts ($F4/80^{+}$ $CD115^{+}$) (Jacquin, *et al.*, 2005).

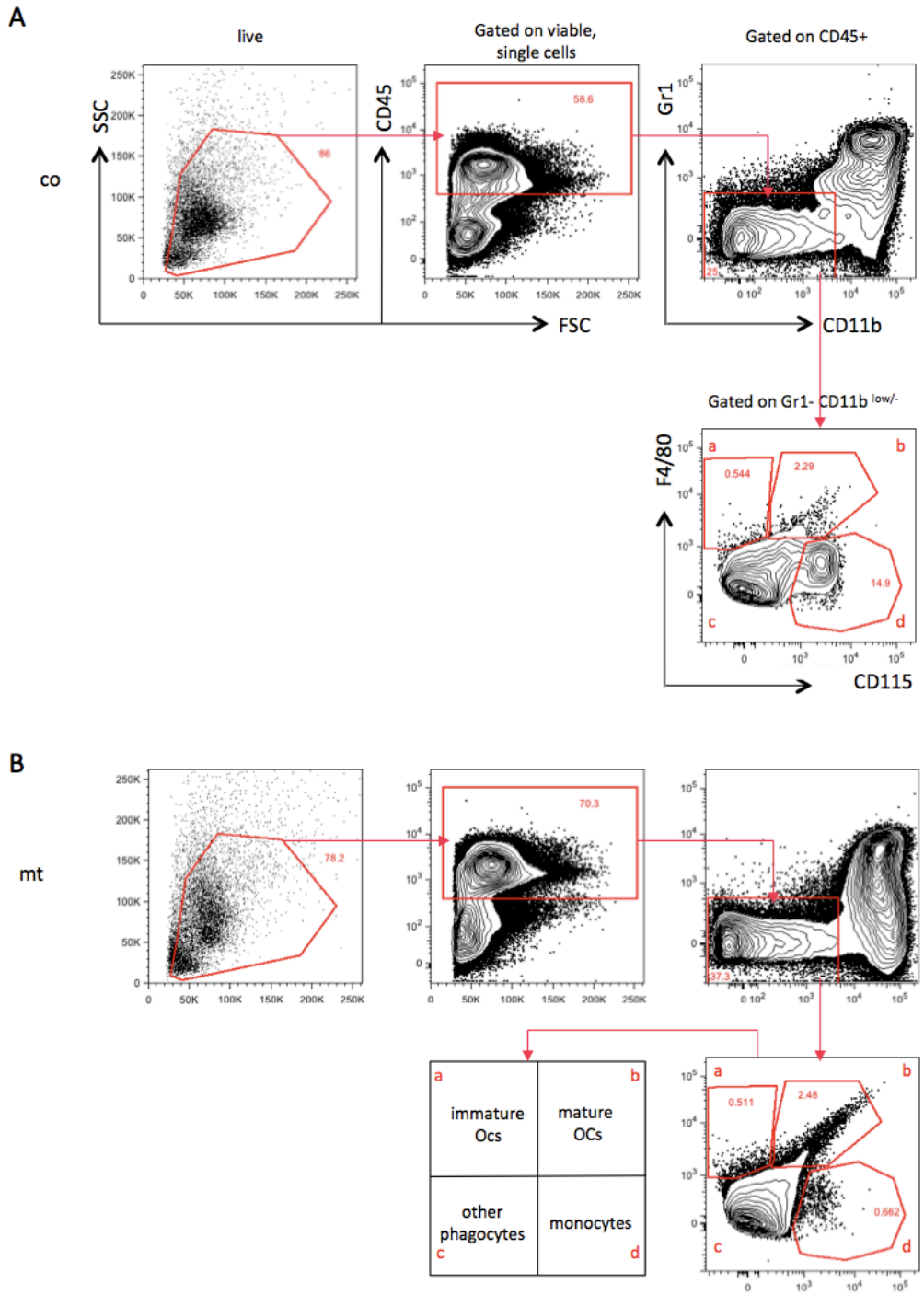

Figure 29: Gating strategy for the identification of osteoclasts by FACS
Representive FACS plot indicates osteoclast populations from control (co) (A) and mutant (mt) (B) animals in the bone marrow. Different sub-populations can be distinguished in phagocyte compartments as indicated (C) (a = immature osteoclasts $CD45^{+}$ $Gr1^{-}$ $CD11b^{low/neg}$ $F4/80^{+}$ $CD115^{-}$, b = mature osteoclasts $CD45^{+}$ $Gr1^{-}$ $CD11b^{low/neg}$ $F4/80^{+}$ $CD115^{+}$ c = other phagocytes $CD45^{+}$ $Gr1^{-}$ $CD11b^{low/neg}$ $F4/80^{-}$ $CD115^{-}$, d = monocytes $CD45^{+}$ $Gr1^{-}$ $CD11b^{low/neg}$ $F4/80^{-}$ $CD115^{+}$).

FACS analysis revealed no major differences in the osteoclast staining pattern between control and mutant bone marrow cells. When osteoclast populations were quantified, a slight increase in the number of mature osteoclasts was observed in mutant animals (Figure 30). However statistical analysis showed that this difference was not statistically significant. Notably, additional histo-morphometric analysis of the osteoclast numbers appeared to confirm the FACS analysis data. Here, the increase in osteoclast number was statistically significant. The increase in osteoclast numbers in mutant bones demonstrates that c-Myc overexpression in mature osteoblasts results in higher osteoblast and osteoclast numbers. Furthermore, these results are in line with the increased bone thickness in the transgenic animals and osteoclast numbers might be higher as a compensatory mechanism in response to imbalanced bone turnover.

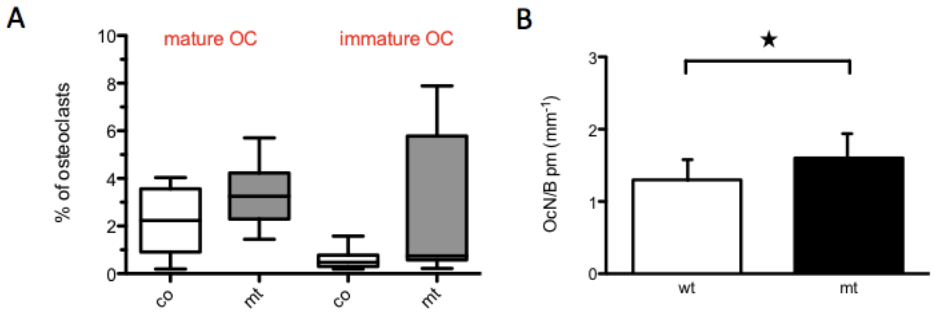

Figure 30: Osteoclast numbers are increased in transgenic animals
Box plot analysis indicates the percentage of mature and immature osteoclasts populations on phagocyte compartments in the bone marrow of control (co) and mutant (mt) animals (co: n = 10; mt: n = 9) (A). Analysis of histo-morphometric bone measurements comparing wt (control bone) to mt animals (OcN/B pm (mm^{-1}) = number of osteoclasts per bone perimeter, measured per mm) (wt = co: n = 6; mt: n = 6) (B).

5.4.2 *ColtTA;TreMyc* animals have normal osteoclastogenesis

Osteoclasts are derived from hematopoietic stem cells and are mainly generated by differentiation of circulating monocytes. Differentiation signals like interleukin-6 (IL-6), IL-1, macrophage-colony stimulating factor (M-CSF), receptor activator of NFkB ligand (RANK-L), osteoprotegerin (OPG) as well as transforming growth factor beta (TGFb) are produced by osteoblasts and induce differentiation of monocytes towards osteoclasts (Udagawa, et al., 1999; Yasuda, et al., 1999; Udagawa, et al., 1995). Thus osteoblasts control osteoclast differentiation. To further investigate whether c-Myc overexpression in osteoblasts influences synthesis of osteoclast differentiation factors, mRNA expression levels of these factors were evaluated by qRT-PCR.

Amongst osteoclast differentiation factors only OPG expression was significantly down-regulated. OPG is produced by mature osteoblasts and is a decoy receptor for RANK-L. Binding of RANK-L to OPG on stromal cells blocks functional crosstalk between RANK-L on osteoblasts and RANK on osteoclast precursor cells, affecting osteoclastogenesis. It is therefore possible that in mutant animals not the differentiation towards osteoclasts is affected but rather the control of osteoclastogenesis. In addition vitamin D repceptor (VDR) expression was 2.5-fold upregulated in mutant osteoblasts. Calcitriol (1,25$(OH)_2$D), a metabolic derivative of vitamin D, is generated in the kidney and stimulates osteoblasts. Osteoblasts in turn produce RANK-L which interacts with RANK and induces osteoclastogenesis. The newly formed osteoclasts resorb bone to mobilize calcium from the bone to the periphery. Taken together, upregulation of vitamin D leads to an increase in osteoclast formation, while at the same time the downregulation of OPG prevents inhibition of osteoclastogenesis. These observations are in line with the increase of osteoclasts in these animals (Figure 30, B).

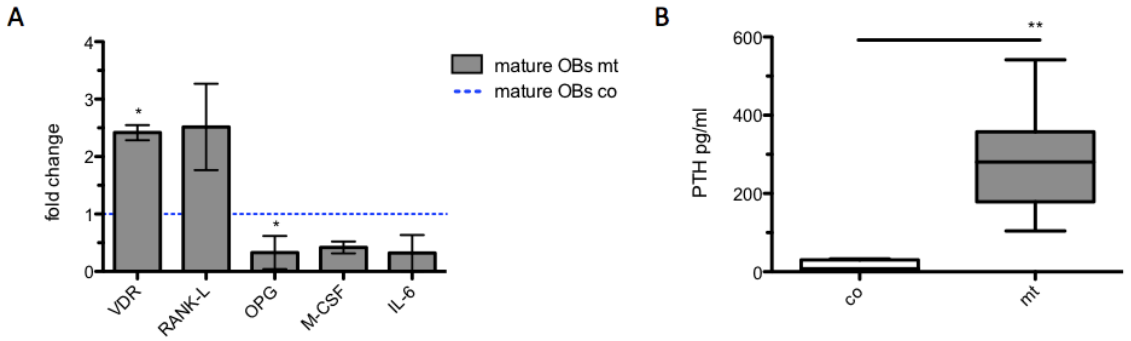

Figure 31: Elevated parathormone levels in mutant animals indicates imbalanced bone homeostasis
Expression values of mRNA osteoclast differentiation factors and vitamin D receptor (VDR) are represented as fold changes against control osteoblasts (blue dotted line). Values are normalized to SDHA and OAZ (VDR = vitamin D receptor, RANK-L = Receptor Activator of NF-kB ligand, OPG = osteoprotegerin, M-CSF = macrophage-colony stimulating factor, IL-6 = interleukin 6), (VDR, RANK-L, M-CSF: n = 4, OPG: n = 6, IL-6: n = 7) (A). Parathormone (PTH, parathyroid hormone) serum levels (pg/ml) in control (co) and mutant (mt) animals (n = 6) (B).

In addition, osteoclastogenesis is induced by parathormone (PTH). PTH is secreted by cells of the parathyroid gland and increases calcium serum levels. PTH increases vitamin D-Calcitriol levels and thus RANK-L expression is induced and on the other hand it binds to the PTH-receptor (PTHR) on osteoblasts again inducing RANK-L expression and thus positively influencing osteoclastogenesis. Therefore in a next step PTH concentrations were measured in the serum of control and mutant animals. PTH serum levels were significantly higher in transgenic animals, indicating a higher rate of osteoclast formation (Figure 31B). Taken together it seems that c-Myc overexpression in osteoblasts has a simultaneous effect on the osteoclast compartment and therefore keeps the ratio of osteoblasts to osteoclasts balanced, while leading to increased turnover of bone.

5.5 Tumorigenesis

5.5.1 Transgenic animals develop bone tumors

As demonstrated, upon overexpression of human c-Myc in mature osteoblasts, mice developed thicker bones but surprisingly mutant animals did not show health defects. However, with increased age (20-30 weeks) animals started to show signs of sickness such as loss of appetite and weight, weariness and faintness. In addition mice died earlier compared to ColtTA controls and most interestingly, the overall life span of transgenic *ColtTA;TreMyc* mice was dramatically reduced (mean survival of 120 days) compared to control animals (> 200 days) (Figure 32).

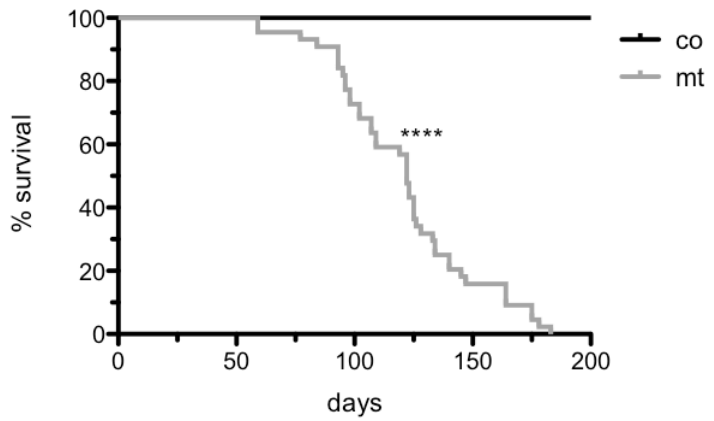

Figure 32: Transgenic *ColtTA;TreMyc* mice have a reduced life span
Survival curve of ColtTA (co) and *ColtTA;TreMyc* (mt) transgenic animals shows a mean survival time of mutant animals of about 120 days while control mice die > 200 days (co: n = 6, mt: n = 46).

While control animals are healthy at 200 days of age, double transgenic mice die on average after 120 days, starting as early as day 60. Therefore, 20-30 week old animals with signs of morbidity were dissected to get further insights into the cause of death.

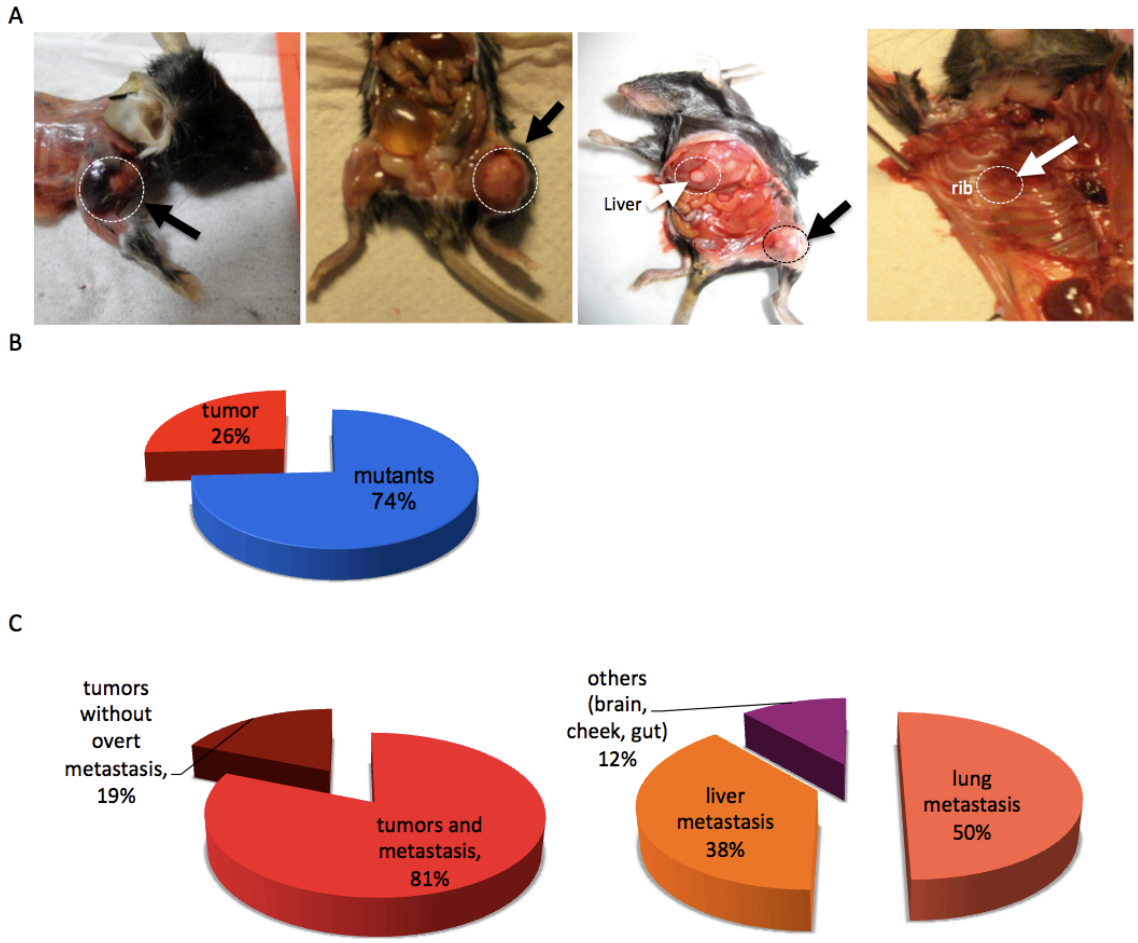

Figure 33: Tumor and metastasis formation in *ColtTA;TreMyc* animals
20-30 week old *ColtTA;TreMyc* animals develop tumors (black arrows) and metastases (white arrows) (A). Frequency of tumor development in transgenic animals (B), simultaneous tumor and metastasis formation and site of metastasis development (C) (n = 20).

In 76% of the cases *ColtTA;TreMyc* mice died with no clear death indication. Notably, it could have been due to the development of paralyzed hind legs and a dramatic weight loss due to reduced food intake.

Strikingly, the remaining 24% of double transgenic animals developed tumors (Figure 33). These tumors were always developed in close proximity to the bones e.g. mainly femur, tibia, mandibula, arms and hips. In addition, in 81% of tumor bearing animals, simultaneous metastasis formation was detected in lungs and liver (38%). Furthermore 12% of the mice developed metastasis in the brain, gut and cheeks or the rib cage.

To visualize the localization and the outgrowth of the tumors micro-CT imaging (small animal computer tomography) was performed on animal skeletons.

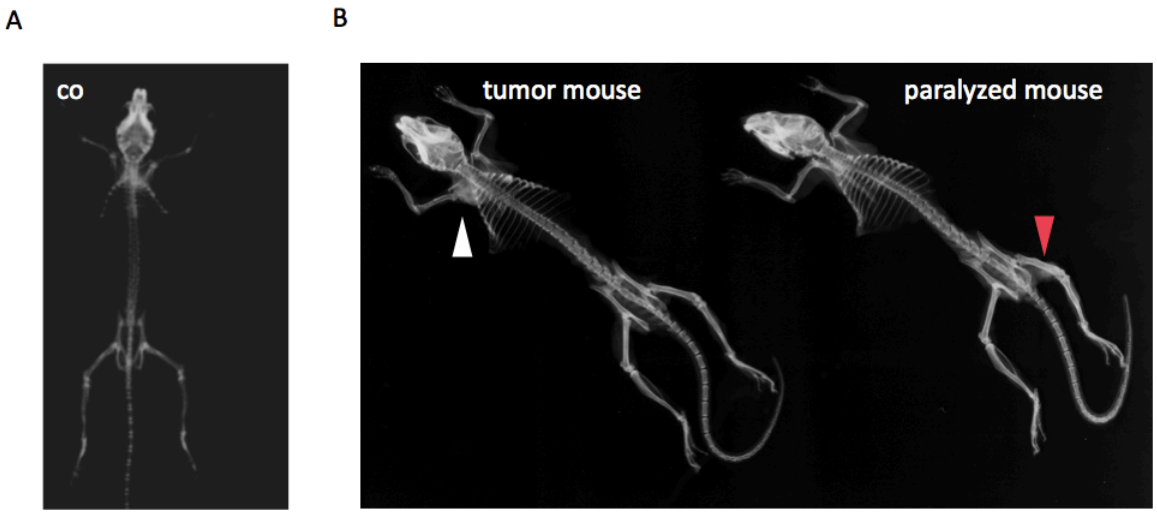

Figure 34: Micro-CT imaging of single and double transgenic mouse skeletons
X-ray image of a skeleton of a ColtTA control animal (A), a tumor-bearing *ColtTA;TreMyc* mouse (site of tumor development indicated with white arrowhead) and a ColTA;TreMyc mutant with paralyzed hind legs (indicated with red arrowhead) (B).

X-ray analysis with micro-CT scan clearly showed an effect of human c-Myc overexpression in mature osteoblasts on the skeleton of mutant animals (Figure 34). Again an overall increase in bone mass was noticed, confirming earlier results by histo-morphometric analysis of the bones and quantitative flow cytometry (Figure 24). Furthermore, the site of tumor development was clearly attributable and identified in more condensed areas in the x-rays. This suggests that the tumors definitely arose from bones.

Thus, overexpression of human c-Myc in *ColtTA;TreMyc* animals led to bone malformations and tumor development. As the only difference between *ColtTA;TreMyc* animals and controls is the overexpression of human c-Myc in mature osteoblasts, the cause of tumorigenesis is apparently the modified osteoblast compartment. To confirm human c-Myc overexpression in these tumors, its mRNA levels were analyzed in tumor cells and cells isolated from metastatic tissues by qRT-PCR.

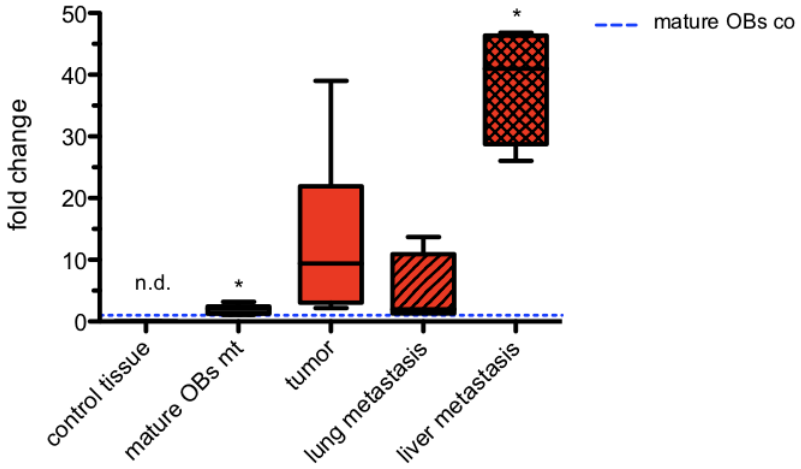

Figure 35: Human c-Myc mRNA expression in tumors and metastatic tissues
Box plot analysis indicate mRNA expression values of human c-Myc, shown in fold changes against control osteoblasts (blue dotted line) and normalized to SDHA and OAZ (n.d. = not detectable; control tissue: n = 3, mature OBs mt: n = 7, tumor: n = 6, lung and liver metastasis: n = 4).

Determination of human c-Myc mRNA expression in tumors and metastatic tissues showed very high expression levels in all samples. Especially tumors (10-fold increase compared to controls) and the metastatic liver tissues (40-fold) showed the highest expression levels of human c-Myc. Interestingly, human c-Myc expression levels in lung metastatic tissues were increased only to about the same extent as was human c-Myc expression in mutant mature osteoblasts (Figure 35). Taken together, human c-Myc was overexpressed in all tumorigenic tissues analyzed, indicating that the source of oncogenic transformation must have been the modified mature osteoblast.

5.5.2 ColtTA;TreMyc animals show metastatic osteosarcoma development

To further characterize the tumors and metastases histological sections and stainings were performed.

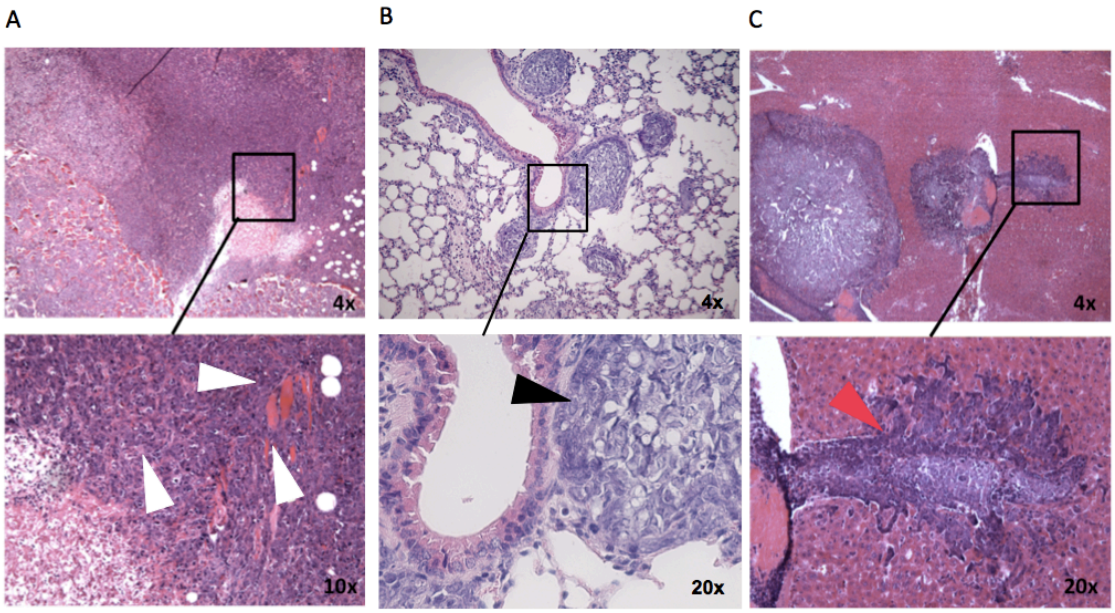

Figure 36: H&E staining of tumor and metastasis identifies malignant osteoid
H&E staining on histological sections of tumor (A), lung (B), liver (C) tissues. White arrowheads depict malignant osteoid in tumor tissue, black arrowhead exhibit lung metastasis, red arrowhead points out liver metastasis.

Histological sections revealed that the tumors had a heterogeneous appearance, while the metastases appeared to be more uniform. Interestingly, osteoid was identified in all the different histological sections. Osteoid is unmineralized bone matrix and normally synthesized by osteoblasts. Furthermore, it is a marker for active bone formation. The presence of malignant osteoid clearly categorized the tumors as osteosarcomas (Figure 36) (Schajowicz, et al., 1982). Especially in the tumors malignant osteoid was abundantly expressed, while its presence was lower in liver metastases and sparse in lungs.

The term osteosarcoma implies that the cell of origin is an osteoblast. Besides fibroblasts, osteoblasts are the main producers of collagen I which is most prominent in connective tissues and bone. Thus, in a next step the osteosarcomas were analyzed by immunofluorescence stainings against collagen I.

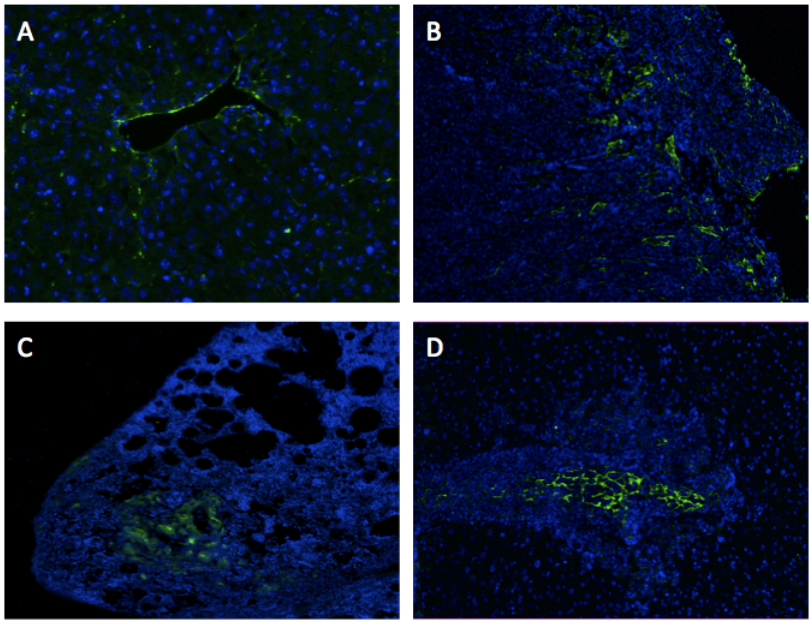

Figure 37: Collagen I expression in tumor and metastatic tissues
Immunofluorescence staining against Collagen I, in liver control tissue (A), tumor (B), lung metastatic tissue (C) and liver metastatic tissue (D). Tissues were counterstained with Dapi (green: Collagen I, blue: nuclei; 20x magnification)

Immunofluorescence staining of tumor and metastatic tissues revealed that collagen I was diffusely expressed in osteosarcoma sections and more centrally in metastatic tissues (Figure 37). In liver tissue from control mice collagen I expression was restricted to vessels, where fibroblasts and endothelial cells are present. In contrast, in liver and lung metastasis, collagen I was exclusively expressed in the middle of the metastasis. This confirms the presence of malignant osteoblasts, which are normally absent in lung and liver tissues. H&E staining had already revealed that osteosarcomas were more heterogeneous and therefore it was not surprising to detect collagen I expression in all parts of the tumors. Taken together, both osteosarcomas and metastatic tissues contained a high proportion of collagen I produced most likely by osteoblasts.

To quantify the portion of osteoblasts within these tumors flow cytometric analysis was performed on collagenase/dispase-digested tumors.

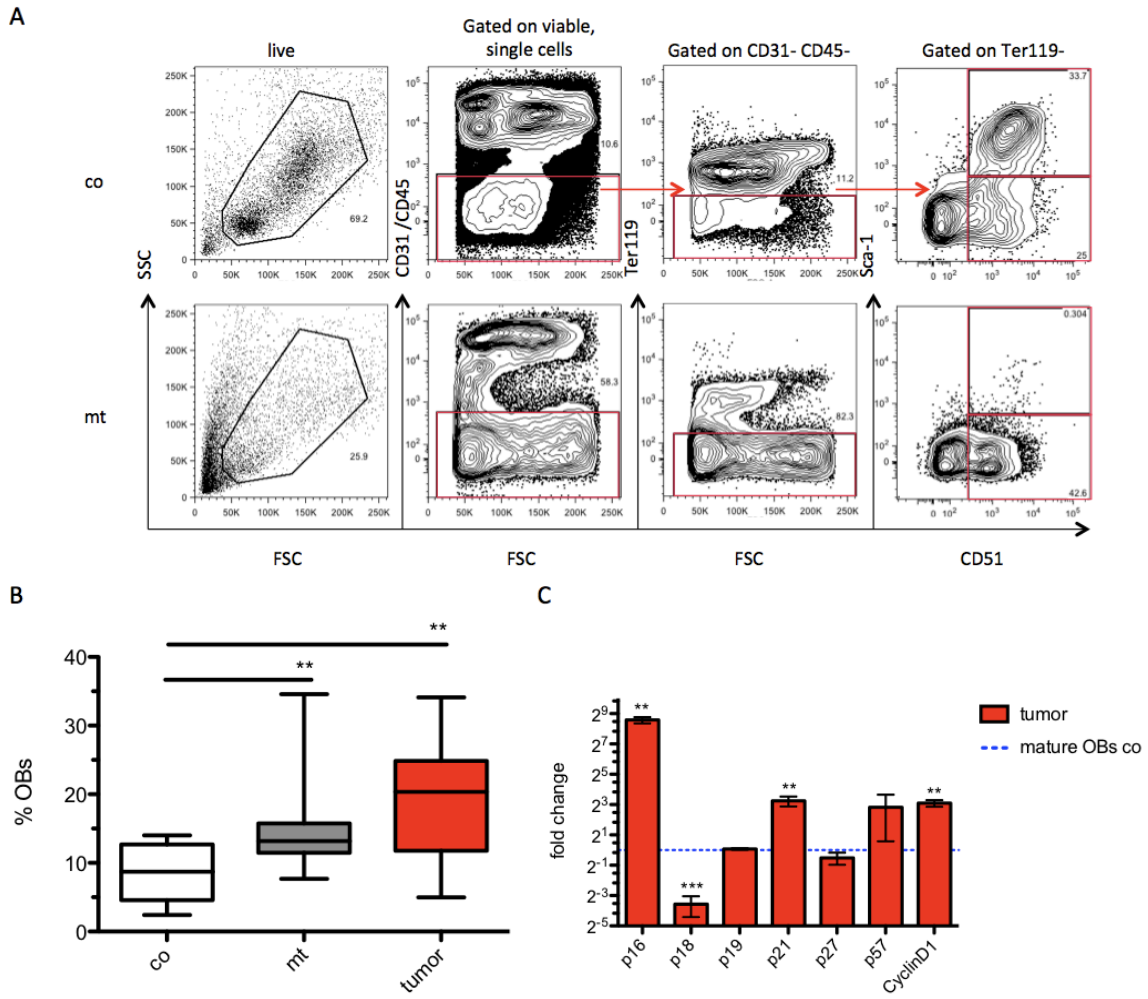

Figure 38: Tumors mainly contain osteoblasts and show impaired cell cycle regulation
Representitive FACS analysis indicates the gating strategy to identify osteoblast populations in control bones (co) and tumors within the stromal compartment. Cells are identified as mature osteoblasts ($CD45^-$ $CD31^-$ $Ter119^-$ $Sca\text{-}1^-$ $CD51^+$) and immature osteoblasts ($CD45^-$ $CD31^-$ $Ter119^-$ $Sca\text{-}1^+$ $CD51^+$) (A). Quantification of osteoblast populations within stromal cells by FACS (co: n=12, mt: n = 20, tumor: n = 22) (B). Fold changes of genes involved in cell cycle regulation of osteosarcoma cells against mature control osteoblasts (blue dotted line) and normalized to SDHA and OAZ (p16, p18, p19: n = 6, p21: n = 7, p27, p57, CyclinD1: n = 5).

Flow cytometry showed that the malignant osteosarcoma osteoblasts showed a very distinct expression pattern than normal osteoblasts. First of all the stromal compartment ($CD45^-$ $CD31^-$ $Ter119^-$ cells) seemed to be much bigger in osteosarcomas compared to

control osteoblasts. Interestingly, while control bones contained similar amounts of mature and immature osteoblasts the osteosarcomas almost exclusively showed the presence of mature osteoblasts (Figure 38, A). This was confirmed by quantification of the osteoblast compartment. Here tumors contained about 20% of mature osteoblasts (Figure 38, B). By comparison the stroma from normal bone contained only about 10% of osteoblasts. Taken together this indicates the presence of mature osteoblasts as the most prominent cell type in osteosarcomas.

Next, mRNA expression levels of cell cycle related genes were assessed by qRT-PCR. Therefore, mature osteoblasts were sorted from collagenase/dispase-digested tumors and mRNA expression values were analyzed. As expected, the expression of cell cycle related genes was deregulated in osteosarcoma cells (Figure 38, C). $p19^{INK4d}$ and $p27^{KIP1}$ did not show any differences in their expression compared to normal mature osteoblasts. In contrast, p18 showed a strong down-regulation while mRNA expression levels of $p16^{INK4a}$, $p21^{CIP1}$ and cyclinD1 were highly upregulated. Additionally $p57^{KIP2}$ expression was slightly elevated compared to controls. However, this was not significant. $p16^{INK4a}$ is a cell cycle dependent kinase that arrests the cells in G_1 phase, while $p21^{CIP1}$ blocks cell cycle progression in G_1/S transition. As cyclin D1 expression is simultaneously increased, this might indicate that $p16^{INK4a}$ is outcompeted and that therefore the cells are no longer arrested in G_1. This would in turn results in aberrant cell proliferation and tumor progression.

5.5.3 Malignant osteosarcoma osteoblasts are highly tumorigenic

Osteosarcomas are heterogeneous tumor cell populations, which do not solely consist of osteoblasts. Therefore it was hypothesized that aberrant cell proliferation was mainly linked to the predominating osteoblasts. However the tumor initiation capacity of these mutant mature osteoblasts was not proven yet. Thus, the tumorigenic potential of osteosarcoma cells was evaluated by xeno-transplantation assays *in vivo* in NOD scid IL2 receptor gamma chain knockout mice (NSG) mice. These are immuno-compromised mice that allow tumor cell growth *in vivo*.

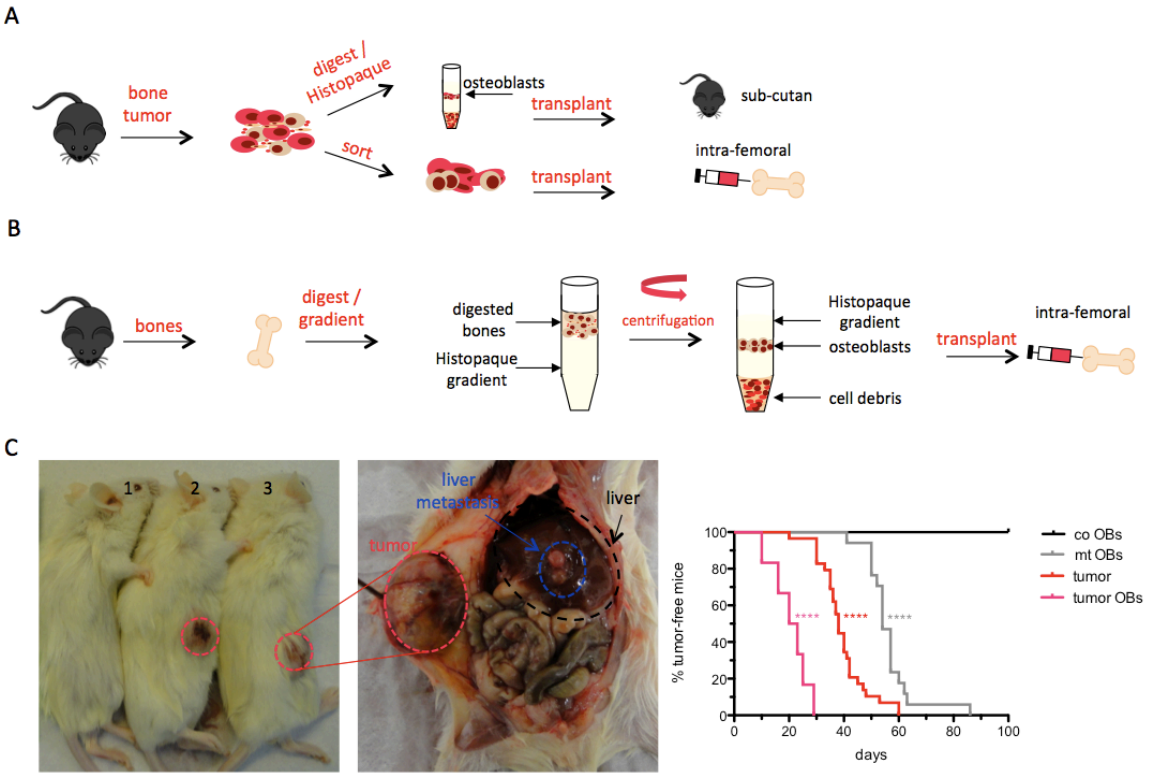

Figure 39: Xeno-transplantation of mouse osteosarcoma cells in NSG mice result in fast tumor growth and metastases formation
Experimental design of the tumor transplantation assay. Tumors are either directly transplanted sub-cutaneously or sorted for mature osteoblast markers and then injected intra-femorally (A). Mature osteoblasts are isolated from mouse bones and directly transplanted intra-femorally (B). Xeno-transplantation of primary mouse osteosarcoma cells in NSG mice and their tumor initiating potential (1 = negative control; 2, 3 = 10^6 mouse osteosarcoma cells injected; sub-cutaneous tumor of transplanted mouse osteosarcoma cells (red), liver metastasis (blue), normal liver tissue (black)). Kaplan-Meier curve of mice intra-femurally injected with osteoblasts from control bones (black), mutant osteoblasts (grey), bulk tumor (red) and 10^4 purified osteoblasts from tumor material (pink) (co OBs: n = 6, mt OBs: n = 17, tumor: n = 29, tumor OBs: n = 6) (C).

For xeno-transplantations tumor cells enriched for osteoblasts by sucrose gradient were injected sub-cutaneously into NSGs. Alternatively, tumor cells were sorted for osteoblast markers ($CD45^-$ $CD31^-$ $Ter119^-$ $Sca1^-$ $CD51^+$) and then transplanted intra-femorally (Figure 39, A). In addition, we performed experiments to address whether whether c-Myc overexpressing osteoblasts from mice with no apparent tumors, also displayed tumorigenic potential.

The xeno-transplantation of primary mouse osteosarcoma cells *in vivo* showed that the cells derived from the primary tumor were highly tumorigenic, as tumor formation was already detectable 14 days post transplantation. Interestingly, regardless of the site of transplantation, animals showed very fast tumor development, which were about 14 days for sub-cutaneous transplants and about 40 days for intra-femoral tansplantations (data not shown). Importantly, sub-cutaneously xeno-transplanted mice showed metastasis formation in various organs (liver and spleen). This indicates that mouse tumor osteoblasts possess a high metastasis initiating capacity (Figure 39, C).

Comparison of the xeno-transplantation experiments in a Kaplan-Meier survival curve demonstrated that all different malignant osteoblast populations had tumorigenic potential (Figure 39, C). The fastest tumor growth (20 days) was observed in animals, which were transplanted with purified osteoblasts from tumors. Transplantation of osteoblast enriched tumors resulted in a median growth phase of about 40 days. Most importantly, human c-Myc overexpressing osteoblasts from transgenic animals with non-overt tumor growth also led to tumor formation *in vivo*. Here, tumor development took more time and tumor growth was only observed about 60 days post transplantation. This illustrates the influence of c-Myc overexpression on the oncogenic potential of mature osteoblasts.

5.5.4 *In vitro* studies on osteosarcoma cells

5.5.4.1 Characterization of mouse osteosarcoma cells in vitro

As demonstrated, tumor development occurred in only about 26% of *ColtTA;TreMyc* transgenic mice and these mice died quickly after the tumor developed. Thus, the time for *in vivo* studies was limited. Thus, to characterize the osteosarcoma cells further, an *in vitro* approach was therefore applied and tissue cultures of malignant cells from mouse primary osteosarcomas were established (Figure 40).

Two different bone tumors (OS_1706tm and OS_9850tm) were excised from *ColtTA;TreMyc* mice and cultivated in tissue culture conditions. In addition a lung metastasis (OS_9850lung met) from an animal with a bone tumor was exised and cultured *in vitro*. The cells started to actively proliferate about 14 days after plating of the primary osteosarcoma cells *in vitro*. Light microscopic analysis of the tissue cultures showed no major morphological differences to commercially available cell lines such as mouse pre-osteoblastic cells (MC-3T3) and human osteosarcoma cell lines (SAOS-2, MG63) (Figure 40). This indicates that the digestion and fractionating method to enrich for osteosarcoma cells *in vitro* is a convenient system to establish osteosarcoma cell lines, without cross-contamination by other cell types. However, phenotypically healthy and malignant osteoblasts cannot be distinguished at this point.

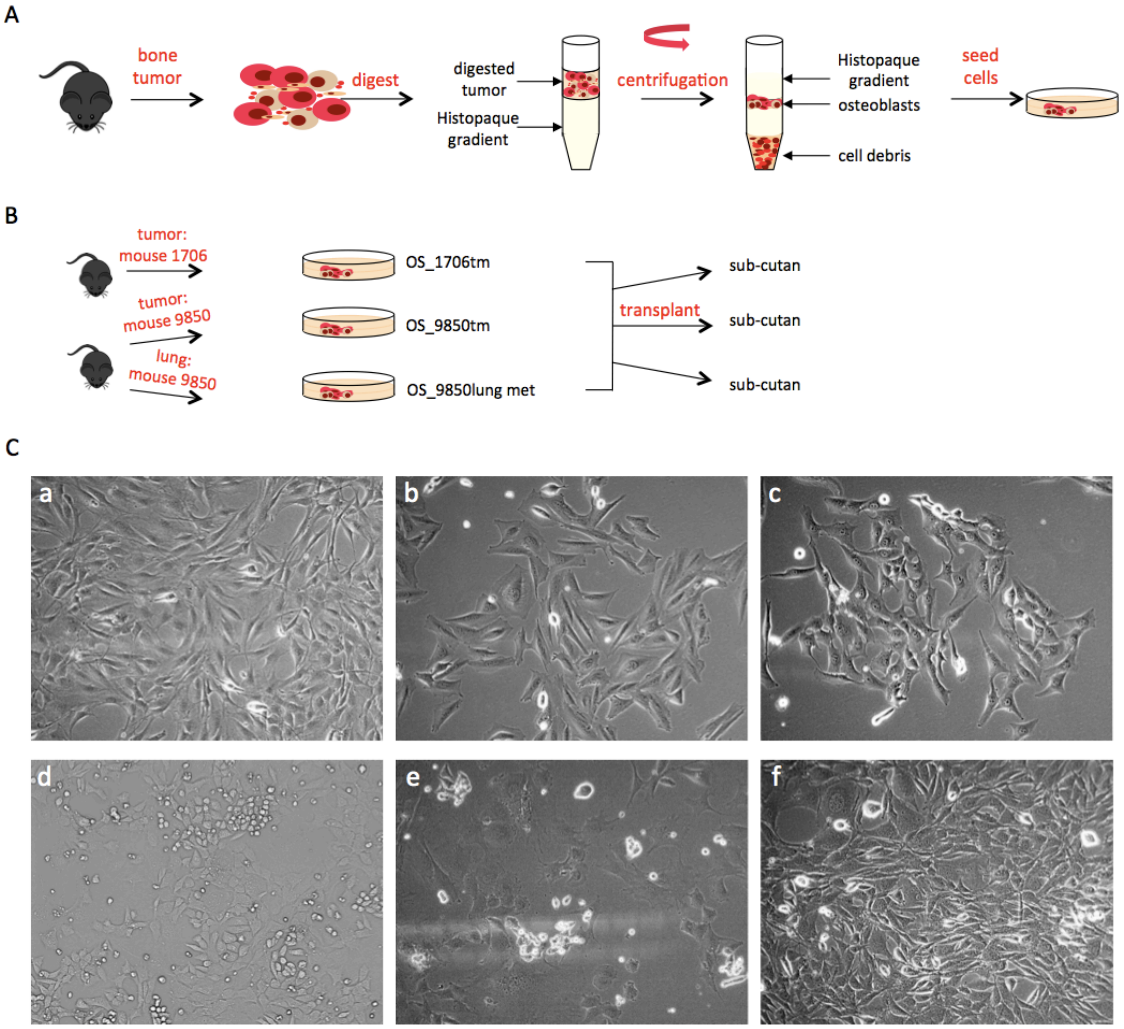

Figure 40: Establishment of primary osteosarcoma tissue culture
Bone tumors were exised from transgenic animals and purified with a sucrose gradient. The isolated osteoblasts were then seeded into tissue culture dishes (A). Establishment of xeno-transplantations with three different *in vitro* cultures: two primary osteosarcoma (tumor mouse 1706, 9850) and one lung metastasis (lung mouse 9850) (B). Light microscopic analysis shows osteosarcoma cell morphology: MC-3T3: mouse pre-osteoblastic cell line (a), human SAOS-2 (b), human MG63 (c), OS_1706tm, (d), OS_9850tm (e), OS_9850lung met (f), 10x magnification (C).

5.5.4.2 Osteosarcoma cells retain their tumorigenic potential in vitro

To check that the tumorigenic potential of the newly established osteosarcoma and metastasis cell lines was not altered, one million cells were transplanted sub-cutaneously into NSG mice and tumor development was monitored.

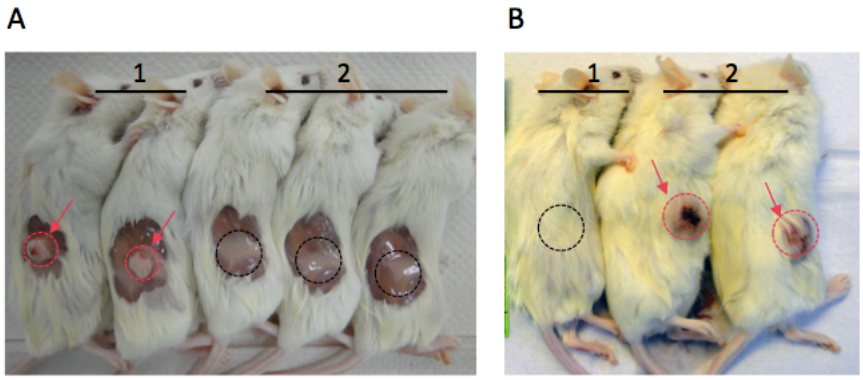

Figure 41: Osteosarcoma tissue cultures are highly tumorigenic
Tissue cultured osteosarcoma cell suspensions were sub-cutaneously transplanted into NSG mice. Red circle marks human SAOS-2 tumors (1), black circle marks mouse pre-osteoblast non-tumorigenic MC-3T3 transplants (2) (A), black circle indicates MC-3T3 negative control (1), red circle indicates mouse osteosarcoma transplants OS_1706tm (2) (B).

The tissue cultured osteosarcoma cells induced fast tumor growth *in vivo* (Figure 41). Cell lines (OS_1706tm, OS_9850tm, OS_9850lung met) showed sub-cutaneous tumor growth as early as 14 days after the transplantation. This was comparable to transplantations with the human osteosarcoma cell line SAOS-2, where tumor growth occurred in the same time frame. The mouse pre-osteoblastic cell line MC-3T3 was used as a negative control in these experiments and did not lead to tumor outgrowth. This indicated that the established *in vitro* cultures had preserved the tumorigenic potential of our newly established osteosarcoma cell lines under *in vitro* conditions.

5.5.4.3 Tissue culturing does not affect osteoblast behavior

In a second step, the purity of the established tissue cultures was analyzed by FACS. Flow cytometric analysisof the extracted and cultivated osteosarcoma cells revealed that *in vitro* culturing preserved very pure cell populations. The cells retained their typical marker expression and were therefore still identifiable as osteoblasts (Figure 42, A, B). Furthermore, the osteoblast cultures contained only a mixture of matureand immature osteoblasts, confirming that the extraction and cultivating methods used are highly specific for osteoblast enrichment *in vitro*.

However comparison of the expression profiles of the two primary osteosarcoma cell lines to the lung metastasis cell line showed a very distinct difference. The tumor cell line consisted almost exclusively of mature osteoblasts while the lung metastasis cell line comprised about 50% of mature and 50% of immature osteoblasts (Figure 42), C.

Next cells were screened for specific genes involved in osteoblast maturation and their mRNA expression levels were quantified (Figure 42, D). Not surprisingly, the tissue cultured osteosarcoma cells did not show any significant differences in their mRNA expression profiles compared to control osteoblasts. This further demonstrates that the *in vitro* conditions seemed to preserve the mature functional osteoblast status of the cells. This is in accordance with the finding that osteosarcoma cultures contained almost solely mature osteoblast populations.

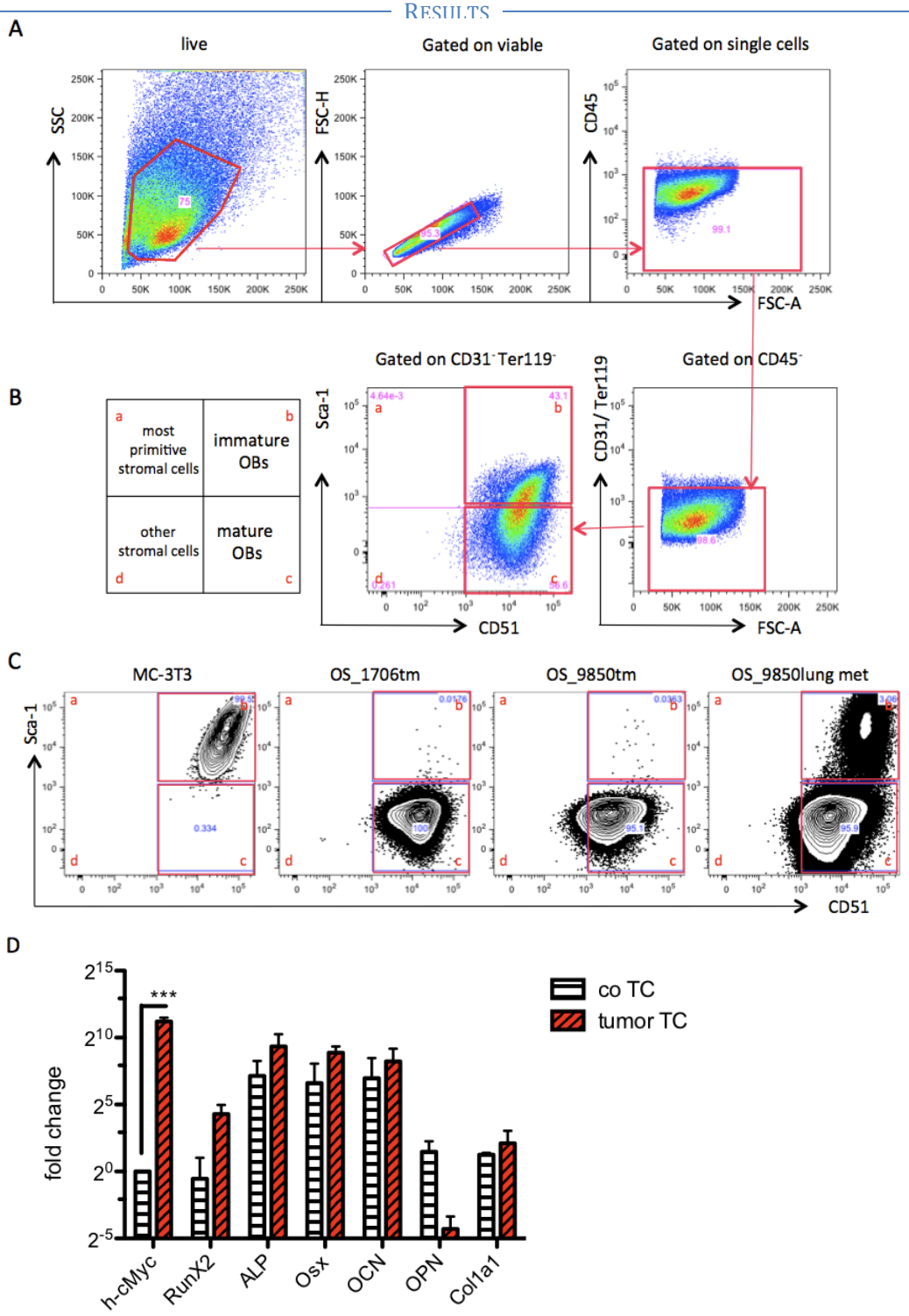

Figure 42: Osteosarcoma tissue cultures are highly enriched for osteoblasts
Detection of mature (CD45$^-$ CD31$^-$ Ter119$^-$ Sca1$^+$ CD51$^+$) and immature osteoblasts (CD45$^-$ CD31$^-$ Ter119$^-$ Sca1$^-$ CD51$^+$) in stromal cells under *in vitro* conditions (14 days post seeding). Gating strategy (A) and classification of stromal cells *in vitro* (B). Differences between pre-osteoblastic cells (MC-3T3) and osteosarcoma cells *in vitro* (OS_1706tm, OS_9850tm; OS_9850lung met). Cells are pre-gated on CD45$^-$ CD31$^-$ Ter119$^-$ fractions and identified as immature osteoblasts (Sca1$^+$ CD51$^+$) or mature osteoblasts (Sca1$^-$ CD51$^+$) (C), gene expression analysis of genes involved in osteoblast maturation indicated as fold changes of tissue culture tumor osteoblasts against control tissue culture osteoblasts. Control osteoblasts are indicated as fold changes against mean (h-cMyc: n = 6; all others: n = 4; not significant) (D).

Finally, cells were tested for their mineralization properties *in vitro*. For this purpose, cells were seeded into 6-well tissue culture dishes for 14 days and then stained by von Kossa staining to detect mineralized areas by silver nitrate precipitations. In comparison histological sections of osteosarcomas were analyzed. In contrast to bone material, preparation of this staining was possible, because osteosarcomas were less rigid and it was therefore possible to cut these tumors.

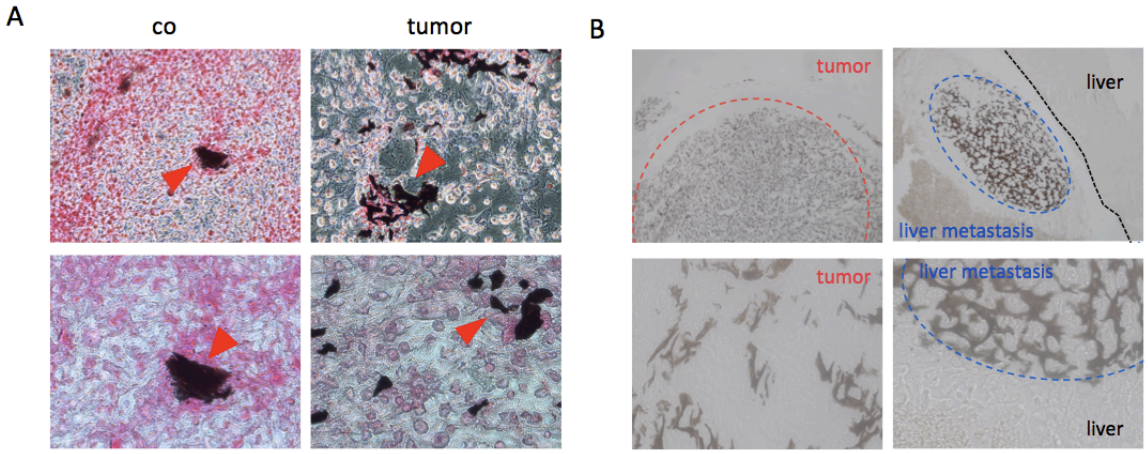

Figure 43: Osteosarcoma reveal calcium deposition
Von Kossa staining on confluent osteoblast layers *in vitro*: osteoblasts from control animals (co) and mouse osteosarcoma cell culture (OS_1706tm), arrowheads indicate mineralization by silver nitrate precipitations (upper row: 10x, lower row: 20x magnification) (A). Histological sections of a primary osteosarcoma sample (tumor 1706) and its liver metastasis. Mineralized areas are indicated by red line (tumor) and blue line (metastasis in liver tissue) (upper row: 4x, lower row: 10x magnification) (B).

Von Kossa staining showed that both the osteosarcoma cell lines (OS_1706tm, OS_9850tm data not shown) and histological sections of primary osteosarcoma samples (mouse number 1706; mouse number 9850 data not shown) and liver metastasis (to mouse number 1706) showed the mineralization properties of normal osteoblasts. Hence it seemes that osteoblasts in tumor tissue retained their osteoblast functionality under *in vitro* and *in vivo* conditions (Figure 43).

5.5.4.4 Establishment of an in vitro transplantation model for the characterization of metastasis initiation

In addition to osteosarcoma development, about 80% of transgenic animals simultaneously developed metastasis to the lung and liver. This has also been observed in human patients. Here, lung metastasis development has an influence on survival and prognosis of the disease (Osborne, et al., 2012; Kataoka, et al., 2012; Ta, et al., 2009; Longhi, et al., 2006;). Therefore, it is of great importance to further study metastasis initiation and to analyze the circulation of tumor cells in the blood stream with the long-term goal to pharmaceutically prevent engraftment of tumor cells in specific organs. Our osteosarcoma mouse model was thus used to establish a xeno-transplantation assay, in which tumor cells can be tracked after transduction with the luciferase gene (Figure 44).

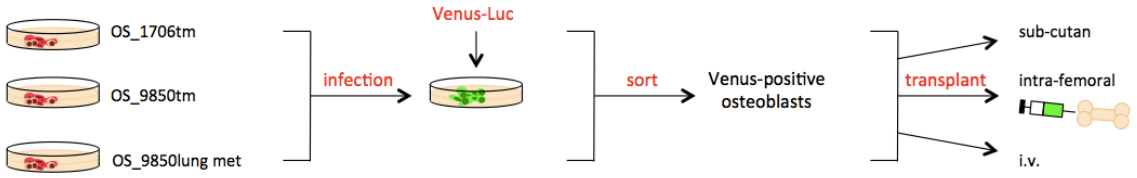

Figure 44: Flow diagram for tissue culture xeno-transplantations
The three different tissue cultures were infected with venus-luciferase double positive lenti-viral particles and sorted for osteoblast markers and venus-fluorescence. Cells were then transplanted either sub-cutaneously, intra-femorally or intra-veneously.

Bioluminescence imaging is one of the most sensitive assays used to track luciferase-positive living cells in luciferase-negative recipient animals. Therefore, established cell lines, OS_1706tm, OS_9850tm and OS_9850lung met, were infected with double-positive (venus-luciferase) lenti-viral particles (Figure 44) (compare supplementary data Figure 71). The luciferase positive cells were injected into NSG mice and monitored by bioluminescence imaging.

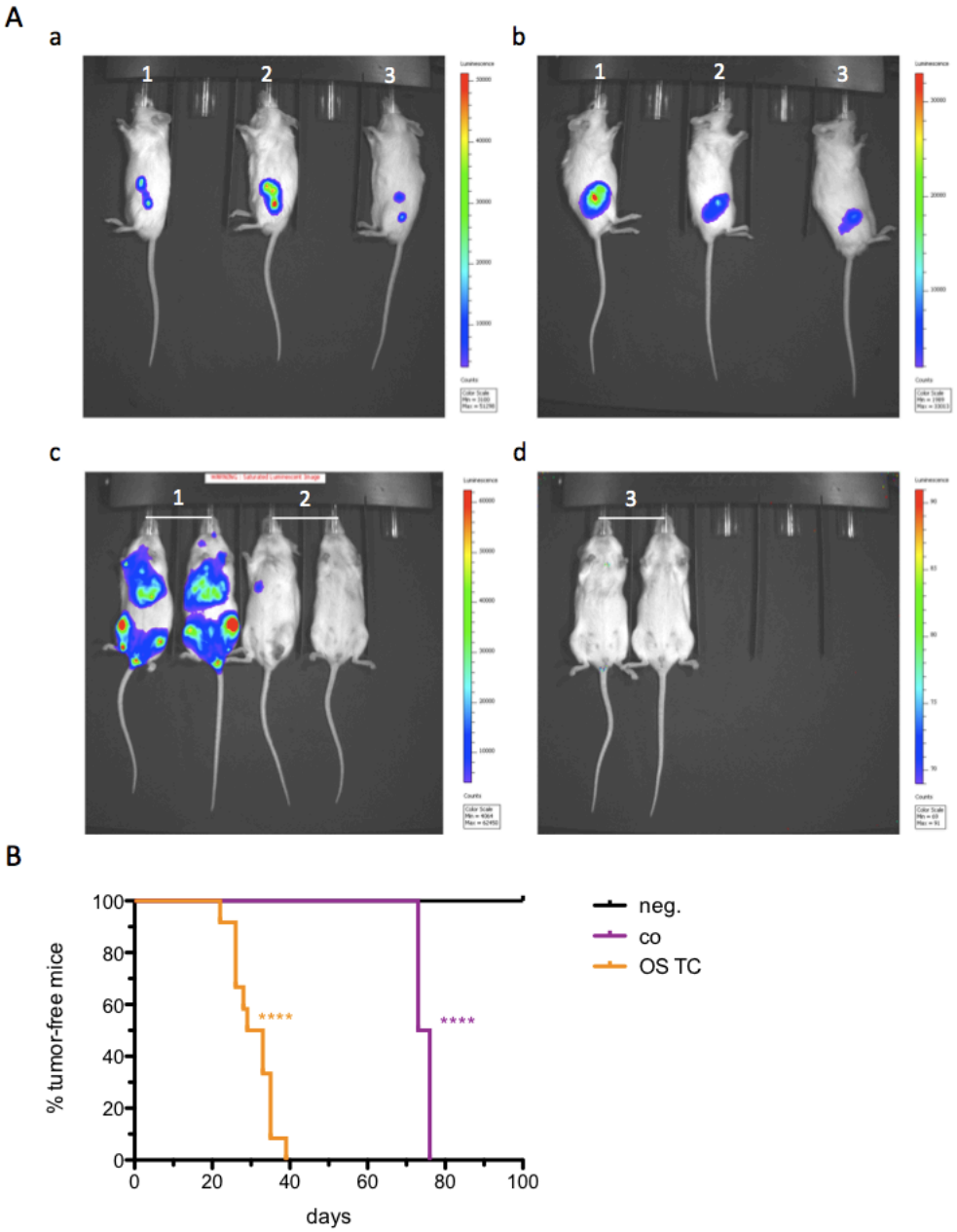

Figure 45: Luciferase transduced osteosarcoma tissue cultures are highly tumorigenic
NSG mice were transplanted with either $1x10^5$ infected luciferase-positive osteosarcoma or lung metastasis cells: sub-cutaneously (1: OS_1706tm, 2: OS_9850lung met, 3: OS_9850tm) (a), intra-femorally (1: OS_1706tm, 2: OS_9850lung met, 3: OS_9850tm) (b), intra-veneously ((1: OS_9850lung met, 2: OS_1706tm, 3: PBS negative control) (c/d). Measurements were carried out either 14 days (sub-cutan), 16 days (i.F.) or 18 days (i.v.) after the xeno-transplantation. Luciferase-positivity is indicated with a colour-scale (right bar) (A). Tissue culture cell lines were transplanted either sub-cutaneously, intra-veneously and intra-femorally and tumor growth monitored by bioluminescent imaging (orange line) (neg: negative control MC-3T3 cells n = 6, co: positive control SAOS-2 n = 4, OS TC = osteosarcoma and lung metastasis tissue culture cell lines n = 24) (B).

Bioluminescence imaging confirmed the earlier data (chapter 5.5.4.2: tumorigenic potential of cell lines) that the established cell lines possess high tumorigenic potential (Figure 45). All three different cell lines showed *in vivo* engraftment capacities, independent of the site of transplantation, while negative controls never showed any tumor development. Mice were generally sacrificed upon visible tumor growth or 3-6 weeks post transplantation. Post mortem analysis showed tumor development in sub-cutaneous as well as in intra-femoral transplantations in 100% of the cases. In addition about 80% of the animals developed metastasis to the lungs and the liver (data not shown), independent of the cell line used. Generally, mice injected i.v. showed metastasis to the lungs and liver. Interestingly animals intra-veneously transplanted with OS_9850lung met showed faster engraftment of the cells to the lungs and the liver. Intriguingly, our lung metastasis cell line colonized the bone marrow, which was never observed in osteosarcoma cell line transplantations. This highlights the close relationship between bone marrow and lung metastatic niches that seem to be the preferential targets for metastatic engraftments in other tumor types e.g. breast cancer and pancreatic cancer (Shiozawa, et al., 2011; Ibrahim, et al., 2010; Guise, et al., 2006; Strewler, et al., 2006; Kaplan, et al., 2006;).

Kaplan-Meier survival analysis revealed that osteosarcoma tissue cultures induce tumor growth within about 30 days while the control SAOS-2 cells developed tumors within about 75 days. In negative control transplantations with MC-3T3 cells tumor growth could never be observed.

This transplantation model can now be used as a system to study metastasis initiation and formation. Furthermore it can help to elucidate clonogenicity in osteosarcomas.

5.5.5 Osteosarcomas show normal osteoclastogenesis

The experiments thus far had shown that the osteosarcomas comprise large amounts of tumorigenic osteoblasts. This raised the question whether osteoclasts are present in osteosarcoma and to what extend. Therefore, histological sections and FACS stainings for osteoclast populations in the tumors were performed.

First, Tartrate-resistant acid phosphatase (TRAP) stainings were conducted on paraffin-embedded tissues to identify the enzymatic activity in osteoclast precursor cells and mature osteoclasts. Microscopic analysis of histological sections from osteosarcoma revealed that TRAP positive cells occurred all over the tumors with no preferential localization to specific areas within the tumors. Furthermore, bone located in the immediate vicinity of tumor growth was analyzed. In contrast to control bones, the amount of TRAP positive cells was much higher in tumor bones.

Next, flow cytometric analysis was used to identify and quantify osteoclast populations in the tumors. The tumors contained about 10% of mature osteoclasts (Figure 46). This amount was significantly higher in comparison to the 2-4% osteoclasts normally found in control or mutant bones. Thus it seemed that concomitantly with the large amount of osteoblasts within the osteosarcomas, the numbers of osteoclasts increased as well. This seemed to indicate that even though osteosarcoma showed a tumorigenic bone excess, the system tried to keep the balance between osteoblasts and osteoclasts.

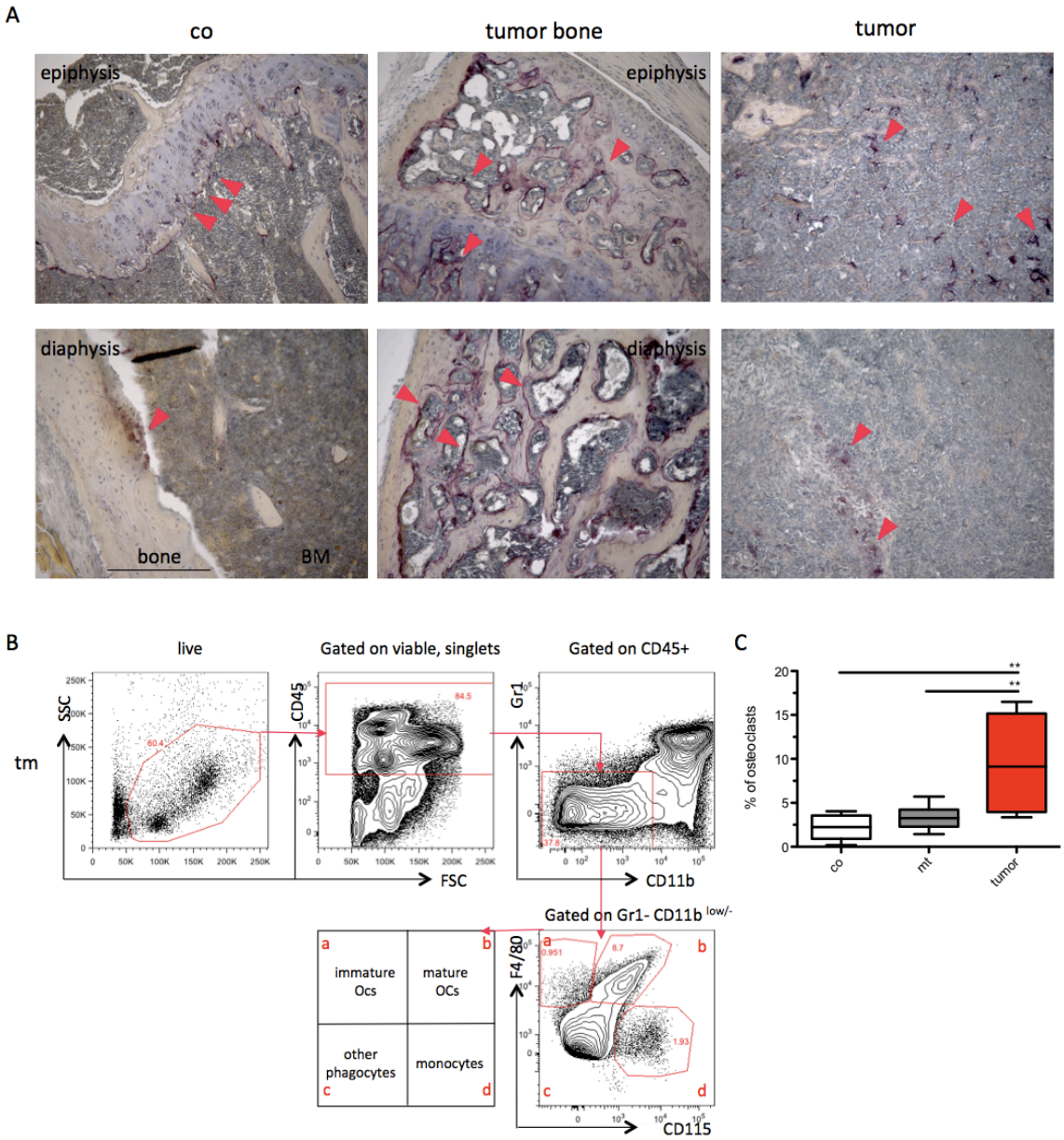

Figure 46: Osteosarcomas contain osteoclast populations

TRAP positively stained osteoclasts are indicated by red arrowheads in histological sections of control bone (co), tumor bone and tumors. (upper row: 10x magnification, lower row: 40x magnification) (A). Gating strategy to identify osteoclasts in osteosarcomas by FACS. Four different sub-populations are distinguished: immature osteoclasts ($CD45^+$ $Gr1^-$ $CD11b^{low/-}$ $F4/80^+$ $CD115^-$) (a), mature osteoclasts ($CD45^+$ $Gr1^-$ $CD11b^{low/-}$ $F4/80^+$ $CD115^+$) (b), other phagocytes ($CD45^+$ $Gr1^-$ $CD11b^{low/-}$ $F4/80^-$ $CD115^-$) (c), monocytes ($CD45^+$ $Gr1^-$ $CD11b^{low/-}$ $F4/80^-$ $CD115^+$) (d) (B). Box plot analysis shows the percentage of osteoclasts in phagocyte populations of control bones (co), mutant bones (mt) and tumors (co: n = 10, mt: n = 9, tumor: n = 5) (C).

Next, mRNA expression of genes involved in osteoclastogenesis were evaluated in osteosarcoma samples. Finally, the expression was compared to control osteoblasts.

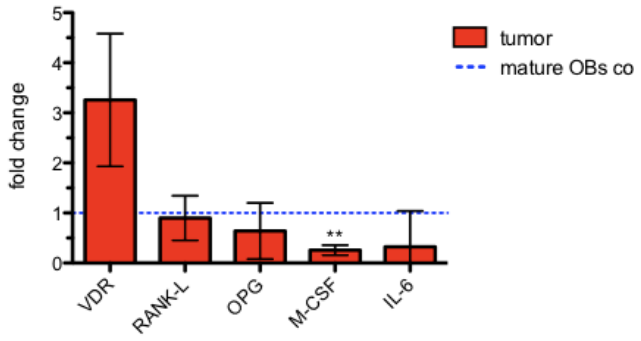

Figure 47: Osteosarcoma osteoblasts have reduced M-CSF expression
Fold changes of mRNA expression values against mature control osteoblasts, normalized to OAZ and SDHA (VDR: n = 3, RANK-L, OPG, M-CSF: n = 8, IL-6: n = 6).

Macrophage-colony stimulating factor (M-CSF) is one of the key compounds that drive osteoclastogenesis, and is released by osteoblasts. Thereby osteoblasts exert a big influence on osteoclasts differentiation (Fujita, et al., 2012; Fan, et al., 2001). The mRNA expression profile showed that M-CSF levels were significantly down-regulated in malignant osteoblasts compared to control mature osteoblasts (Figure 47). This might indicate that malignant osteoblasts have a defect compared to normal and c-Myc overexpressing osteoblasts (Figure 31). Interestingly, all the other regulators of osteoclastogenesis, RANK-L, OPG and IL-6, were not affected and expressed normally. In contrast vitamin D receptor (VDR) showed a slight increase in mRNA expression, although this was not statistically significant.

Bone remodeling can also be analyzed by measuring metabolic processes in peripheral blood of mutant and control mice. Thus, the concentration of proteins that play major roles in bone formation and degradation were evaluated in the serum of control, mutant and tumor-bearing mice by ELISA.

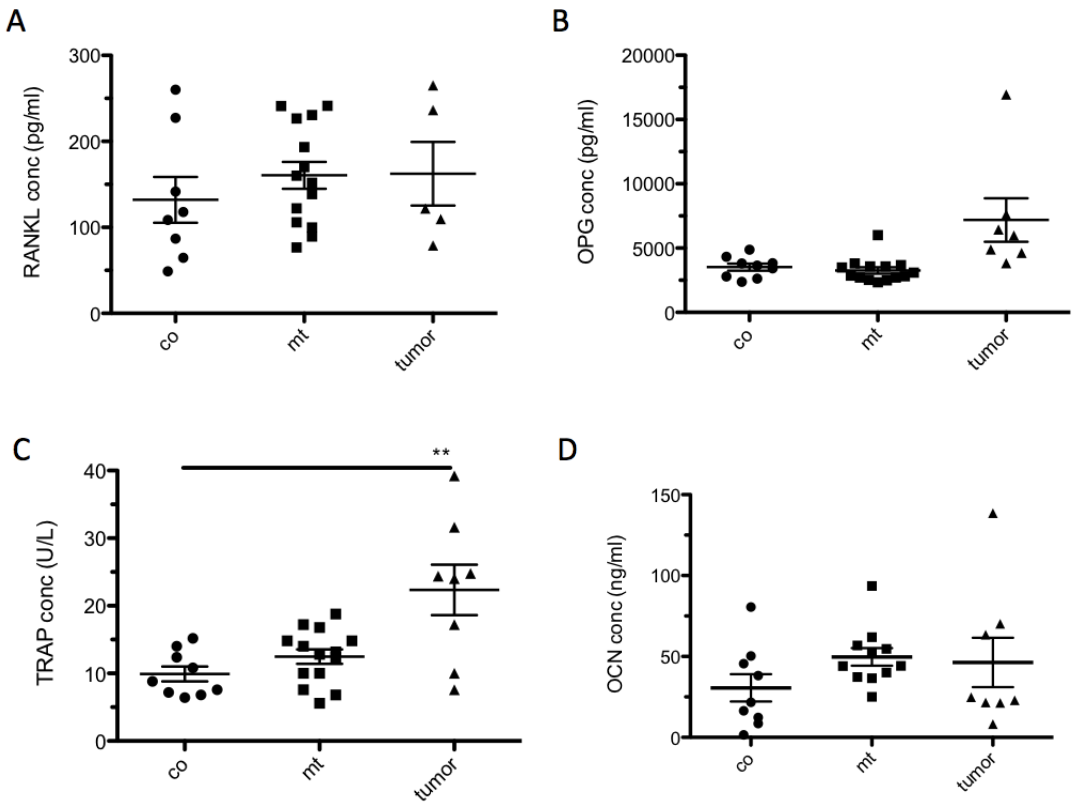

Figure 48: Tumor-bearing animals have increased bone remodeling
Serum analysis of control (co), mutant (mt) and tumor-bearing mice (tumor). RANKL (A), OPG (B), TRAP (C) and OCN (D) concentrations were measured by ELISA.

Comparison of proteins measured in the serum of control, mutant and tumor-bearing animals revealed that TRAP activity in the serum of osteosarcoma mice was about two-fold higher (22 U/L) compared to either control (10 U/L) or mutant (12 U/L) animals (Figure 48). This correlated with the observations made by histological TRAP staining (Figure 46) that demonstrated increased numbers of osteoclast populations in tumor bones and primary tumors. In contrast, protein concentrations of RANK-L, OPG and OCN did not differ in the serum of control, mutant and tumor-bearing mice. This is extremely interesting, as I had previously shown that OCN is highly expressed in mature osteoblasts and almost not detectable in osteosarcoma osteoblasts. OCN is essential for bone mineralization and energy metabolism, thereby functioning as an endocrine factor. Therefore it seems that OCN does not have an influence on the regulation of endocrine OCN metabolism in osteosarcoma mice.

5.5.6 Malignant osteoblasts fail to terminally differentiate

As demonstrated earlier, mutant osteoblasts have a mostly normal mRNA expression profile. Whether this was also the case in osteoblasts isolated from osteosarcomas was determined in the next step by qRT-PCR.

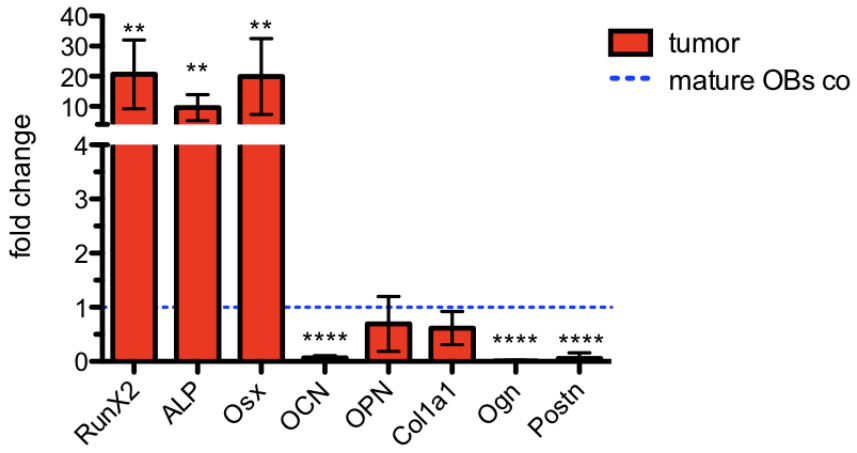

Figure 49: Osteosarcoma osteoblasts resemble the phenotype of immature osteoblasts
The mRNA expression is indicated as fold changes against control mature osteoblasts (blue dotted line). Early osteoblast differentiation markers are RunX2, ALP and Osx and late differentiation factors are OCN, OPN, Col1a1, Ogn and Postn (RunX2, OCN: n = 7, ALP, Osx, OPN: n = 3, Col1a1: n = 4,,Ogn, Postn: n = 6). Normalization to OAZ and SDHA.

Strikingly, qRT-PCR revealed increased mRNA expression of early bone maturation markers, RunX2, ALP, Osx in osteosarcoma cells. While ALP was 10-fold upregulated, RunX2 and Osx were expressed even higher and showed an increase of up to 20-fold in osteosarcoma osteoblasts compared to control mature osteoblasts. In contrast, genes that are normally expressed in terminally differentiated osteoblasts were significantly down-regulated, OCN, Ogn and Postn (Figure 49) and were hardly detectable anymore. In addition, OPN and Collagen were expressed normally and did not show any significant differences compared to normal controls. This seems to indicate that tumorigenic osteoblasts are trapped in a pre-mature osteoblast stage. Thus human c-Myc over-expression appears to induce oncogenic transformation of mature osteoblasts showing a pre-mature signature profile, probably by preventing final maturation and keeping the cells in an immature phase.

5.5.7 Osteosarcoma osteoblasts have deregulated Wnt signaling

Wnt signaling is one of the key pathways involved in osteoblast differentiation and maturation. The observed premature profile of osteosarcoma osteoblasts led to the hypothesis that Wnt signaling might be impaired in these cells. Thus, mRNA expression levels of genes involved in the canonical Wnt signaling pathway were analyzed by qRT-PCR.

Most interestingly, some of the genes involved in Wnt signaling were differentially expressed in osteosarcoma osteoblasts compared to control osteoblasts (Figure 50). Importantly, Wnt3a and ß-Catenin mRNAs were highly upregulated and showed a 40-fold increase in their expression level in osteosarcoma cells. In contrast, DKK-1, one of the major antagonists of Wnt3a, showed a simultaneous increase as well. Other genes involved in Wnt signaling like Lrp5/6, APC, Axin2 and GSK3b were not affected by c-Myc overexpression and showed normal expression levels. Thus c-Myc overexpression seems to have a major effect on canonical Wnt signaling, which is deregulated in osteosarcoma osteoblasts.

Wnt signaling is involved in many cellular processes and a list of Wnt target genes can be found online (http://www.stanford.edu/group/nusselab/cgi-bin/wnt/target_genes). Several genes involved in bone maturation and differentiation are regulated by the Wnt signaling pathway e.g. RunX2, DKK-1, Sox2, Sox9, OCN, E-Cadherin (E-Cadh, CDH-1). To assess the effect of upregulated Wnt signaling in osteosarcoma osteoblasts, in a next step the mRNA expression levels of these Wnt target genes were analyzed. While RunX2 and DKK-1 were 15-fold upregulated, Sox2, Sox9, OCN and E-Cad were significantly down-regulated in mouse osteosarcoma cells (Figure 50). These results are in line with earlier publications reporting deregulated expression of Wnt target genes (Luu, et al., 2004). Thus, human c-Myc affects the expression of genes that are regulated through the canonical Wnt signaling pathway in *ColtTA;TreMyc* induced osteosarcoma.

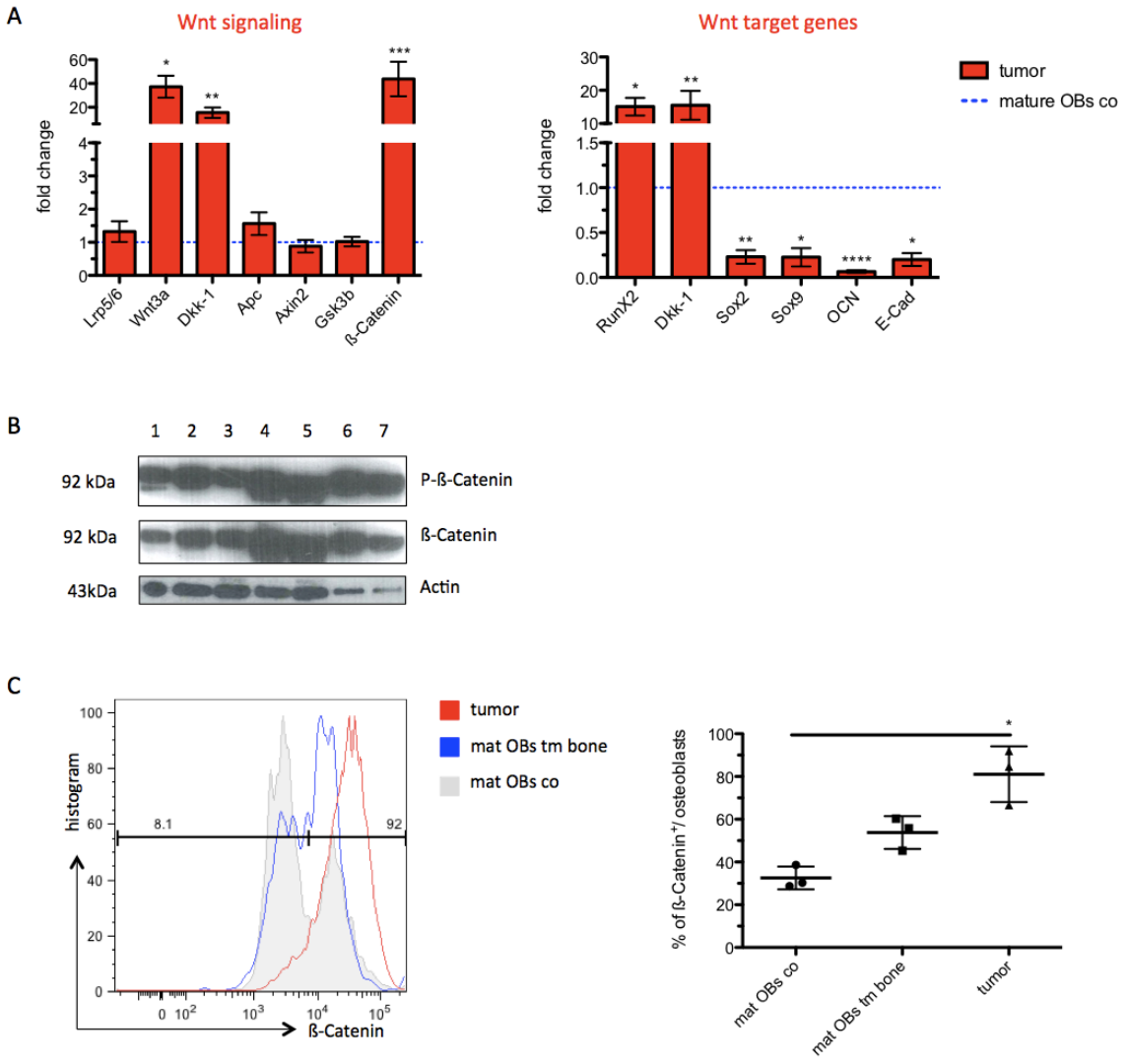

Figure 50: Deregulated expression of Wnt signaling genes in osteosarcomas
Evaluation of mRNA expression of genes involved in Wnt signaling. Expression values of Wnt signaling genes and Wnt target genes (A) are plotted in fold changes compared to control mature osteoblasts (blue dotted line) and normalized to SDHA and OAZ (Lrp5/6: n = 13, Wnt3a: n = 6, DKK-1: n = 11, Apc, Axin2, Gsk3b, ß-Catenin: n = 13, RunX2: n = 13, DKK-1: n = 11, Sox2: n = 10, Sox9: n = 13, OCN: n = 7, E-Cad: n = 7). Protein expression of phosphorylated and de-phosphorylated ß-Catenin protein in 300µg cell lysates and actin was used as a reference (1: control: MDA-MB231, 2: OS_1706tm, 3: OS_1706tm irradiated, 4: tumor_14715, 5: tumor_20928, 6: tumor_12888, 7: tumor_20691) (actin: 43kDa, phosphorylated and dephosphorylated ß-Catenin: 92kDa) (B). FACS plot analysis and quantification of ß-Catenin protein expression in tumor tissue (red), mature osteoblasts from tumor bones (blue) and mature control osteoblasts (grey). Cells are pre-gated on $CD45^-$ $CD31^-$ $Ter119^-$ (n = 3) (C).

Analysis of mRNA expression revealed that Wnt signaling gene ß-Catenin is significantly upregulated in osteosarcoma osteoblasts. ß-Catenin is an interesting protein as it is active in an unphosphorylated status and thus transmigrates from the cytoplasm to the nucleus where it starts to induce the transcription of Wnt target genes.

Therefore, I analyzed ß-Catenin phosphorylation status in order to check the activity status of the signaling pathway. However in western blot analysis using phospho-ß-Catenin-specific antibodies, no differences in bands detected by the phospho-antibody compared to bands detected by a total ß-Catenin antibody were observed. This indicates that almost all the ß-Catenin protein within the tumors is in a phosphorylated state. Thus, it was not surprising that even specific induction of phospho-ß-Catenin by irradiation of a tumor sample did not further increase its phosphorylation. In contrast, FACS analysis for ß-Catenin in tumor bone, osteosarcoma osteoblasts and control osteoblasts revealed that in tumor bone as well as in osteosarcoma osteoblasts ß-Catenin was expressed in 55% and 80% of the cells respectively. Thus, almost all of the osteosarcoma osteoblasts expressed this important signaling molecule while in control osteoblasts only about 25% of the cells stained ß-Catenin positive. This indicates that c-Myc overexpression in osteoblasts has a major influence on ß-Catenin regulation, most likely through the Wnt signaling pathway.

5.5.8 Aberrant p53 signaling in malignant osteoblasts

Tumorigenesis is a multi-step process where mutations of cell cycle regulators often lead to uncontrolled cell proliferation. pRb and p53 are master cell cycle regulators that control both, cell growth and cell death. p53 is inactivated and mutated in more than 50% of human cancers and is aberrantly expressed in about 20% of osteosarcomas. Therefore p53 expression levels were analyzed.

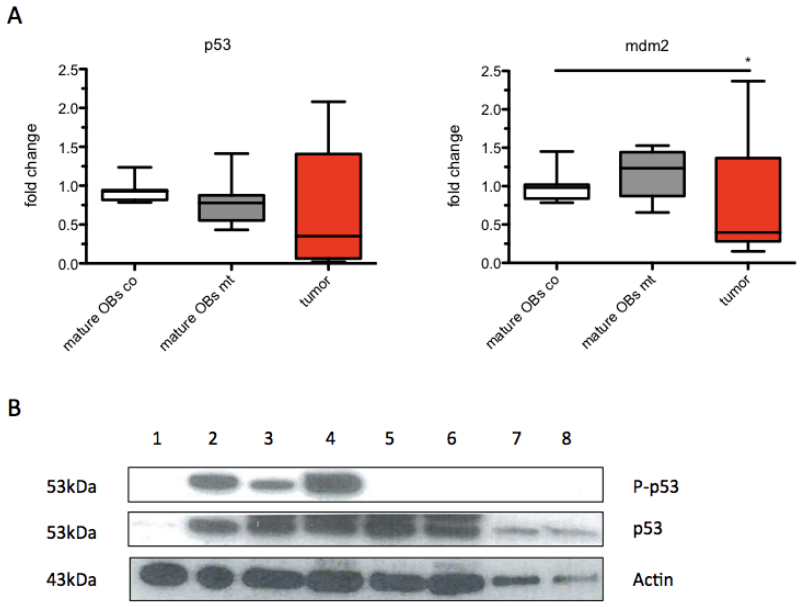

Figure 51: p53 activity is lost in osteosarcoma osteoblasts
Fold changes of p53 and mdm2 mRNA expression level in control, mutant and osteosarcoma osteoblasts (tumor). Expression levels are indicated as fold changes against control mature osteoblasts and normalized to SDHA and OAZ (p53: co: n = 9, mt: n = 8, tumor: n = 11; mdm2: co: n = 7, mt: n = 6, tumor: n = 19) (A). Protein expression of phosphorylated and de-phosphorylated p53 in 300µg cell lysates and actin was used as a reference (neg. control 1: K562, pos. control 2: MDA-MB231, 3: OS_1706tm, 4: OS_1706tm irradiated, 5: tumor_14715, 6: tumor_20928, 7: tumor_12888, 8: tumor_20691) (actin: 43kDa, phosphorylated and dephosphorylated p53: 53kDa) (B).

Analysis of control and mutant mature osteoblasts, as well as osteosarcoma osteoblasts demonstrated a slightly decreased expression of p53 in mutant and osteosarcoma osteoblasts (Figure 51). However this was not statistically significant. P53 activity is tightly controlled by mouse double minute 2 (mdm2) protein, which binds to p53 and thus blocks p53 activity. To test whether the regulation of p53 in mutant and osteosarcoma osteoblasts

was impaired, the expression level of mdm2 was analyzed. Evaluation of mdm2 mRNA expression level showed no significant difference between control and mutant osteoblasts. Osteosarcoma osteoblasts showed a markedly reduced mRNA expression level. However mdm2 and p53 expression varied greatly, making interpretations difficult (between 0.1-fold down-regulation to 2-fold upreguation). Here low p53 expression levels go along with low mdm2 levels resulting in little cell cycle inhibition in osteosarcoma osteoblasts. However, p53 protein activity also depends on the protein´s phosphorylation status. Therefore the phosphorylation status of p53 was analyzed by western blot.

Strikingly, western blot analysis of p53 protein expression of tissue cultured ostesosarcoma samples and primary tumors showed clear differences (Figure 51, B). Phosphorylated p53 was only detected in tissue-cultured osteosarcoma cells (lane 3, OS_1706tm) and MDA-MB231 (lane 2) cells. The latter one is a breast cancer cell line, which was used as a positive control. p53 phosphorylation can be induced by DNA damage induction through irradiation. As expected, irradiation of the osteosarcoma cell line (lane 4) resulted in increased p53 phosphorylation, indicating p53 functionality. In contrast all primary osteosarcoma samples showed normal p53 expression levels (lane 5-8) but did not show any p53 phosphorylation. This indicates that p53 protein activity is blocked in our mouse osteosarcoma mouse model.

5.5.9 Tyrosine kinase receptor c-Kit is upregulated in mouse osteosarcoma

Another protein often involved in oncogenic transformation of different tissues is the stem cell factor receptor c-Kit (CD117) (Chibon and Coindre, 2011; Adhikari, et al., 2010; Alava, et al., 2007). c-Kit is a membrane-bound receptor that dimerizes upon ligand binding and a subsequent auto-phosphorylation loop then triggers a c-Kit-specific intracellular signaling cascade. The receptor tyrosine kinase (RTK) c-Kit is frequently mutated in human cancers e.g. soft tissue sarcomas, gastro-intestinal stromal tumors and breast cancer. Therefore, its role in our osteosarcoma model was investigated. In a first set of experiments mRNA expression levels of c-Kit were tested by qRT-PCR.

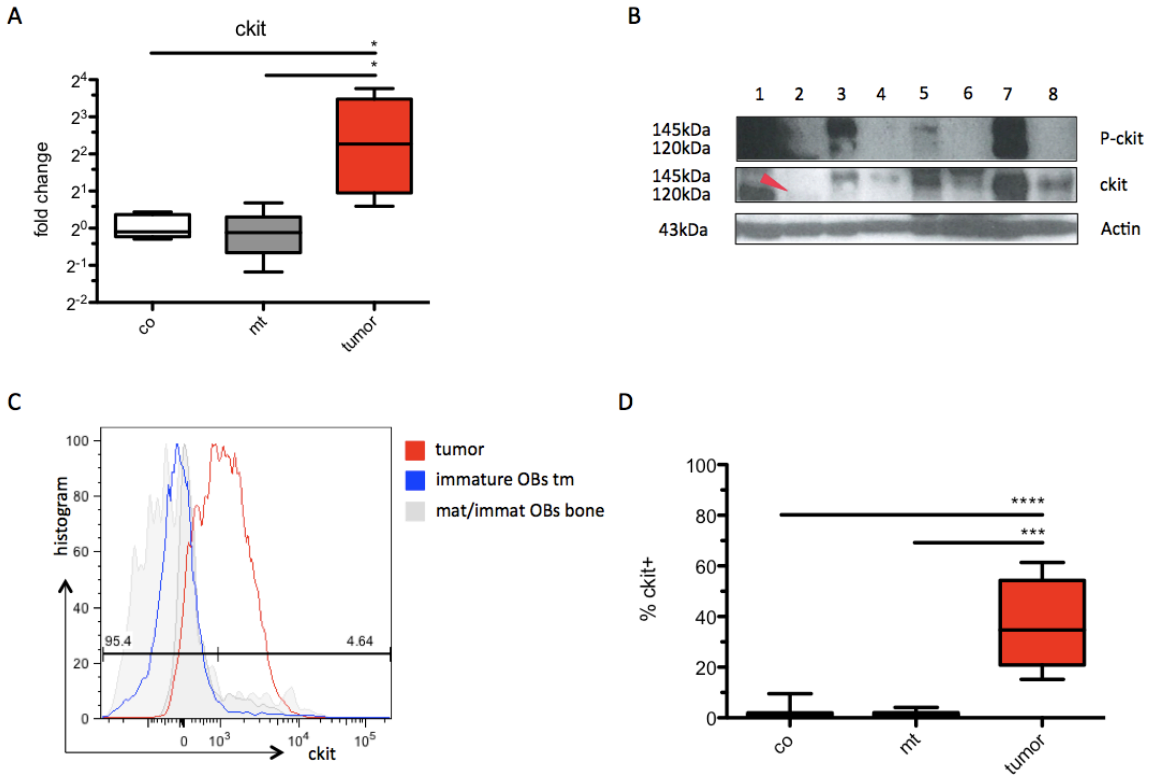

Figure 52: Increased c-Kit expression in osteosarcoma osteoblasts
Expression of c-Kit mRNA in control, mutant and osteosarcoma osteoblasts (tumor). Expression level are indicated as fold changes against control mature osteoblasts and normalized to SDHA and OAZ (co: n = 5, mt: n = 7, tumor: n = 6) (A). Protein expression of phosphorylated and de-phosphorylated c-Kit in 300µg cell lysates and actin as a reference control (pos. control 1: CCRF-HSB2, pos. control; 2: Jurkat, 3: tumor_20928, 4: tumor_20928 treated, 5: tumor_14715, 6: tumor_14715 treated, 7: tumor_15564, 8: tumor_15564 treated) (actin: 43kDa, phosphorylated and de-phosphorylated c-Kit: precursor: 125kDa, mature: 145kDa; arrowhead points out c-Kit precursor in non-induced Jurkat cells) (B). FACS analysis of c-Kit protein expression in tumor tissue (red), immature osteoblasts in tumor tissue (blue) and mature/ immature control osteoblasts (grey). Cells are pre-gated on CD45$^-$ CD31$^-$ Ter119$^-$ (n = 3) (C). Quantification of c-Kit expression by flow cytometry (co, mt: n = 10, tumor: n = 14) (D).

Comparison of c-Kit mRNA expression levels between control, mutant and osteosarcoma osteoblasts showed a 8-fold upregulation of c-Kit in osteosarcoma osteoblasts (Figure 52). To corroborate these findings, c-Kit expression was assayed by flow cytometry. Stromal cells from control and mutant bones as well as osteosarcomas were separated from hematopoietic cells by negative gating on $CD45^-$ $CD31^-$ $Ter119^-$ markers. In the stromal cell compartment the cells were further separated into mature (Sca-1^- $CD51^+$) and immature osteoblasts (Sca-1^+ $CD51^+$) and c-Kit expression was evaluated on both cell populations. Strikingly, osteosarcoma osteoblasts showed a significantly higher c-Kit expression compared to mature and immature osteoblasts from both control and mutant animals (Figure 52). More precisely, 40% of tumorigenic osteoblasts were c-Kit positive while only about 2% of control and mutant mature osteoblasts show c-Kit positivity. This nicely correlates with the upregulation of c-Kit mRNA expression and suggests a deregulated c-Kit signaling in osteosarcoma cells. Thus, in a next step the activity status of c-Kit receptor tyrosine kinase was tested by western blot.

In tumors c-Kit is frequently mutated resulting in spontaneous hyper-activity of the tyrosine kinase and leads to uncontrolled cell growth and proliferation. Thus analysis of the phosphorylation status of c-Kit indicates the degree of kinase activity and the functionality of the receptor. Analysis of total c-Kit protein expression by western blot showed that the mature 145kDa protein was expressed in all osteosarcoma samples. Precursors of c-Kit protein (120kDa) were only detectable in established cell lines used as a postitive control (lane 1: CCRF-HSB2 = human leukemia cell line). In contrast the T-cell line Jurkat (arrowhead, lane 2) expressed c-Kit only weakly and served as a negative control. Phosphorylated c-Kit was expressed in the positive control as well as in all primary tumor samples (lane 3, 5, 7). Specificity of the phospho-specific c-Kit antibody was tested by treating the samples with λ–phosphatase to remove phosphate residues at tyrosine 719 that was recognized by phospho-c-Kit antibody. c-Kit was phosphorylated at Tyr719 in all primary osteosarcoma samples, as phospho-specific c-Kit antibody detection occurred only in non-treated samples (lane 3, 5, 7).

A role of c-Kit in osteosarcoma onset and a correlation as a prognostic marker is discussed in the field and seems to be independent of c-Kit mutation status (Adhikari, *et al.*, 2011; Ikeda, *et al.*, 2010; Judson, *et al.*, 2010; Sulzbacher, *et al.*, 2006; Entz-Werle, *et al.*, 2005; Matsuyama, *et al.*, 2005). Nilotinib (Tasigna®, Novartis) is a specific c-Kit tyrosine kinase inhibitor, which is currently employed in cancer patients. Thus, we next tested the effect of Nilotinib treatment on osteosarcoma cell proliferation was tested *in vitro*. Osteosarcoma tissue culture cell lines (OS_1706tm, OS_9850tm, OS_9850lung met) and freshly isolated primary osteosarcoma cells (20928tm, 20691tm, 1706 s.c. tm_1/2) were incubated and then treated with different Nilotinib concentrations up to 10 µM for 72hrs and subsequently cell proliferation rate was determined in comparison to untreated controls.

Nilotinib treatment of osteosarcoma tissue cultures as well as of mouse primary osteosarcoma cells revealed an overall effect of the drug on cell proliferation *in vitro* (Figure 53). All the primary tumors showed a higher sensitivity to Nilotinib compared to tissue culture cell lines. In detail Nilotinib treatment of primary osteosarcoma samples resulted in successful inhibition of cell proliferation in all four tumors. In contrast cell line OS_1706tm seemed not to respond to Nilotinib treatment. Cell line OS_9850tm and the lung metastasis tissue culture OS_9850lung met showed decreased cell proliferation rates upon treatment and responded more sensitively. These results suggest that c-Kit signaling plays a major role in mouse osteosarcoma cell proliferation. In the future it will be interesting to evaluate the effect of Nilotinib treatment on osteosarcoma formation *in vivo*.

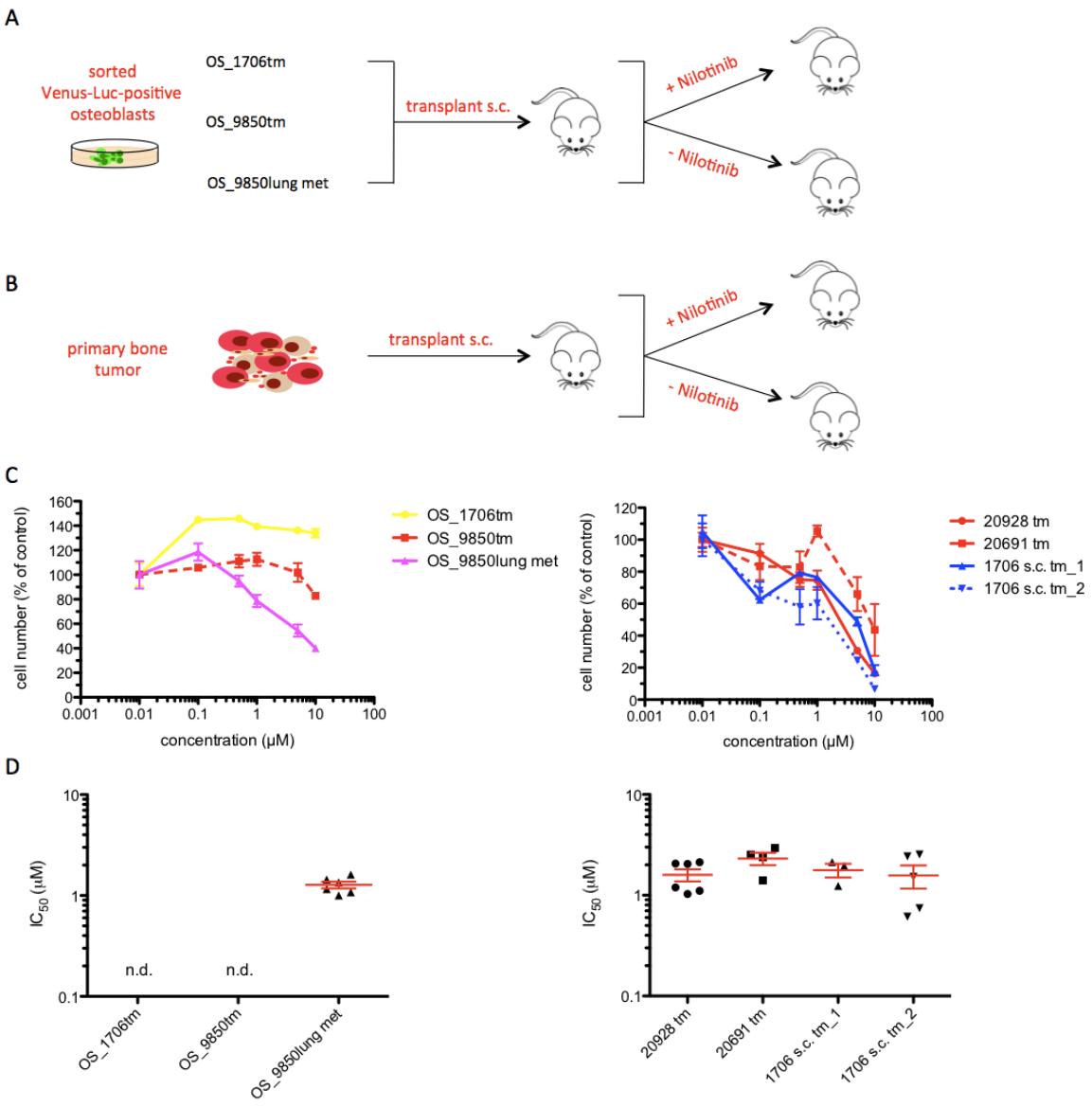

Figure 53: Primary osteosarcoma cell growth is inhibited by Nilotinib treatment *in vitro*
Experimental set up of Nilotinib (TKI) treatment in vitro. Osteosarcoma tissue culture cell lines (A) or mouse primary bone tumors (B) were plated and treated with Nilotinib for 72hrs. Consequence of Nilotinib treatment on cell proliferation *in vitro*. Osteosarcoma cell lines (OS_1706tm, OS_9850tm, OS_9850lung met) or primary osteosarcoma samples (20928tm, 20691tm, 1706 s.c. tm_1, 1706 s.c. tm_2) were treated with different doses of Nilotinib for 72hrs. Cell proliferation rate is normalized against untreated controls (C). Inhibitory concentration (IC_{50}) of Nilotinib on different osteosarcoma tissue cultures and primary osteosarcoma cells (D) (n = 3; n. d. = not detectable).

5.6 Osteoblast – HSC interaction

5.6.1 Hematopoietic stem cell populations are decreased in *ColtTA;TreMyc* animals

Mature osteoblasts either differentiate terminally into osteocytes to build solid bone or remain as osteoblasts to form the endosteum. A presumably small proportion amongst the latter ones, tightly interact with hematopoietic stem cells and are involved in forming a homing place for HSCs – the HSC niche. Thus osteoblasts play a major role in controlling growth and differentiation of HSCs. I used the *ColtTA;TreMyc* mouse model to test what effect c-Myc overexpression had on HSCs and to better understand how osteoblasts regulate the HSC niche.

In a first step hematopoietic stem cells and progenitor populations in the bone marrow of control and mutant animals were analyzed by FACS analysis. For progenitor cell identification, first, differentiated cell populations in the bone marrow were excluded by gating on lineage negative cells (Lin^-) and in a next step, cells staining positive for c-Kit and Sca-1 were selected (Lin^- c-Kit^+ Sca-1^+; LSK). Multipotent progenitor cells (MPPs) of HSCs were then identified within the LSK population by gating on the SLAM markers, $CD150^+$ and $CD48^-$. Long-term HSCs (LT-HSC; LSK $CD150^+$ $CD48^-$ $CD34^-$) and short-term HSCs (ST-HSC; LSK $CD150^+$ $CD48^-$ $CD34^+$) were then identified by CD34 expression.

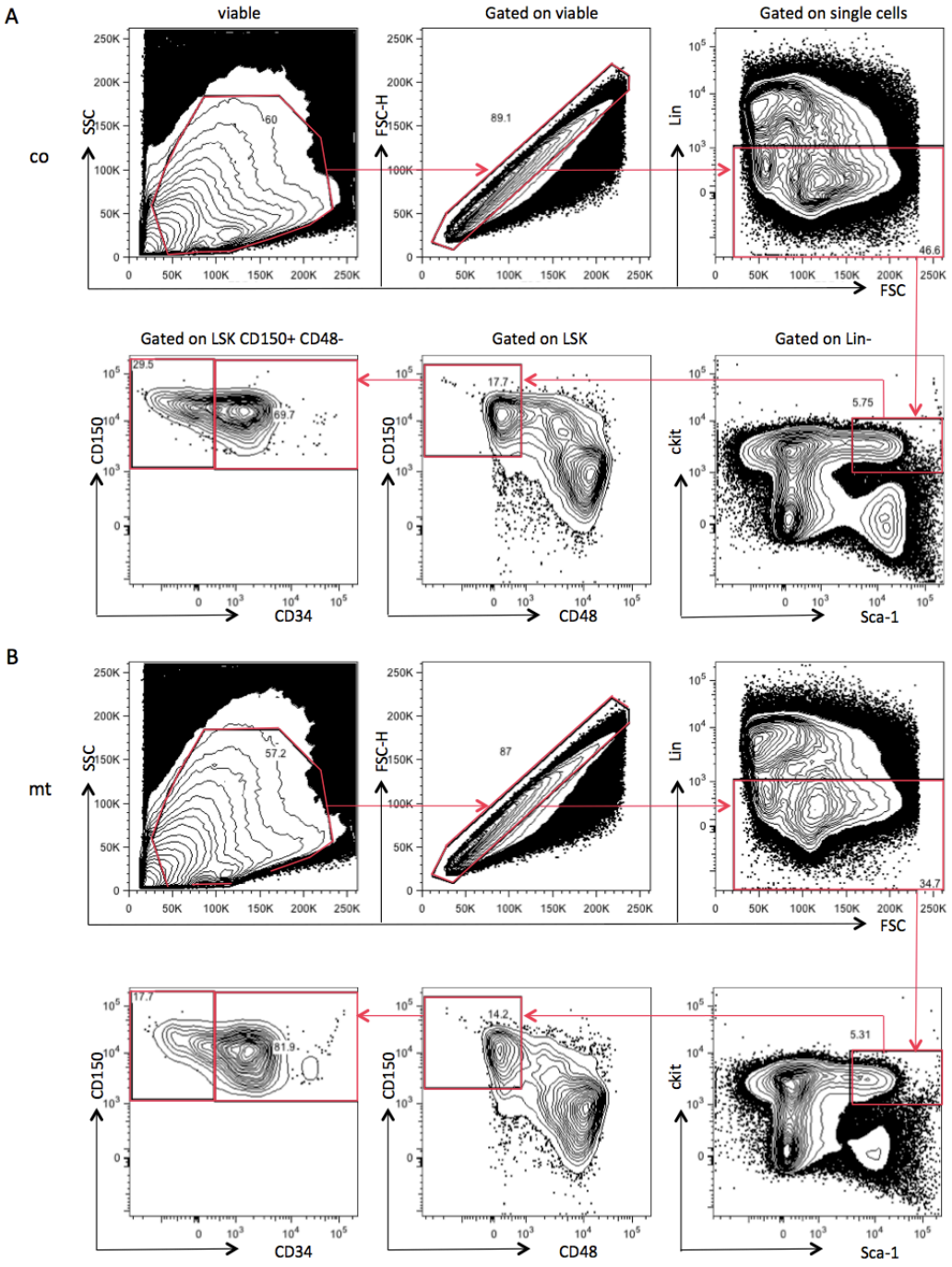

Figure 54: Gating strategy for the detection of hematopoietic cell populations
Identification of hematopoietic stem and progenitor cells in the bone marrow of control (A) and mutant (B) animals. Hematopoietic progenitors are identified as LSK population (Lin$^-$ c-Kit$^+$ Sca-1$^+$), MPPs (LSK CD150$^+$ CD48$^-$), long-term HSCs (Lin$^-$ c-Kit$^+$ Sca-1$^+$ CD150$^+$ CD34$^-$) and short-term HSCs (Lin$^-$ c-Kit$^+$ Sca-1$^+$ CD150$^+$ CD48$^-$ CD34$^+$).

Flow cytometry analysis revealed no obvious differences in the expression pattern of cell surface antigens between HSCs of control and mutants (Figure 54). In a next step, the different cell populations in the bone marrow were quantified (Figure 55).

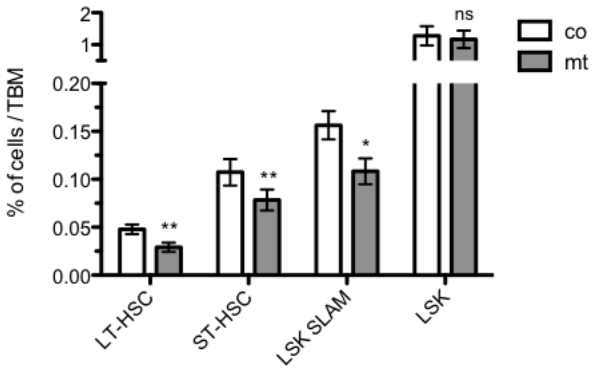

Figure 55: Decreased hematopoietic stem and progenitor compartments in mutant animals
Quantification of hematopoietic stem and progenitor populations in the bone marrow of control (co) and mutant (mt) animals (LT-HSC: long-term HSC, ST-HSC: short-term HSC) (n = 19).

Strikingly, the portion of LT-HSCs and ST-HSCs as well as MPPs (LSK SLAM) from mutant animals was reduced compared to cells from control animals. In contrast LSK cells, the least primitive HCS progenitor cells, did not differ between mutant and control animals. Interestingly, the most significant reduction in cell numbers was observed in the portion of LT- and ST-HSCs in mutant animals. Taken together these first observations indicate that human c-Myc overexpression in mature osteoblasts has a major effect in transgenic animals. This indicates that the osteoblast – HSC interaction is modified in *ColtTA;TreMyc* animals.

5.6.2 Long-term hematopoietic stem cells from *ColtTA;TreMyc* animals possess normal differentiation capacities

The identification of significantly less stem and progenitor cells in transgenic animals raised the question whether lineage differentiation was affected as well. During blood maturation HSCs differentiate into multipotent progenitors and these cells then mature into specific cell lineages in the bone marrow and the blood e.g. granulocytes, B-cells, T-cells, erythrocytes. To quantify the percentages of committed progenitor cell populations and terminally differentiated blood cells the bone marrow of control and mutant animals was analyzed by flow cytometry.

The committed progenitor cell populations in the bone marrow can be separated into common lymphoid progenitors (CLPs), megakaryocyte/ erythrocyte progenitors (MEPs), granulocyte/ macrophage progenitors (GMPs) and common myeloid progenitors (CMPs) (Figure 56, A, B). Quantification of these lineage commited progenitor cells in the bone marrow revealed no differences between control and mutant animals. Furthermore, when terminally differentiated cells were quantified, no difference between control and mutant cells was observed (Figure 56, C). These results demonstrate that the reduced numbers of HSCs did not have an influence neither on lineage commitment nor on terminal differentiation of bone marrow cells. This indicates that the differentiation capacities of HSCs were not affected in transgenic *ColtTA;TreMyc* animals. To get further insight into HSC regulation in *ColtTA;TreMyc* mice, cell cycle analysis was performed using Ki67/Hoechst FACS analysis (
Figure 57).

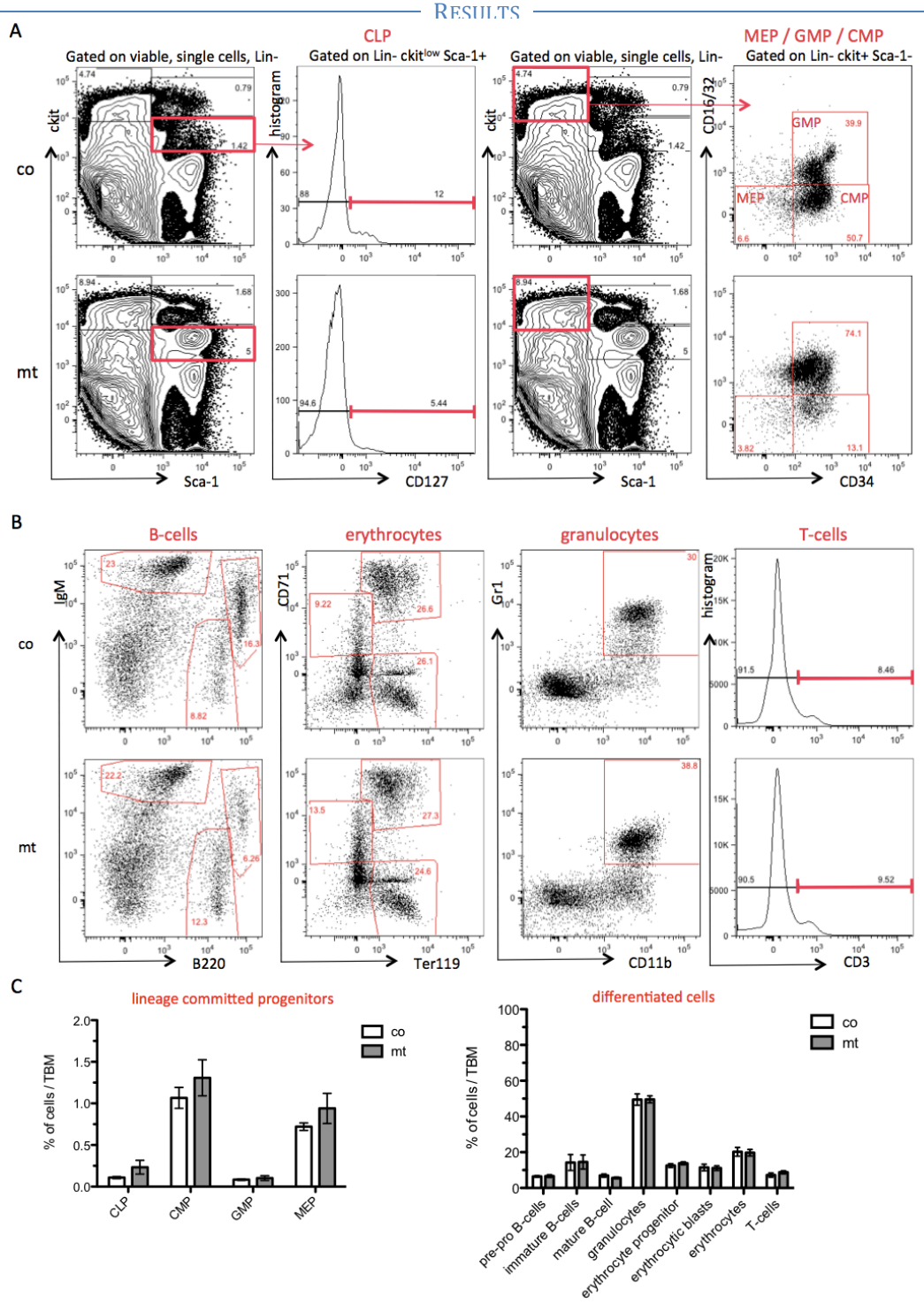

Figure 56: Identification of committed progenitor and terminally differentiated cells in the bone marrow
Committed lineage progenitors were identified as CLPs (Lin- c-Kitlow Sca-1+ CD127+), MEPs (Lin- c-Kit+ Sca-1- CD16/32- CD34-), GMPs (Lin- c-Kit+ Sca-1- CD16/32+ CD34+) and CMPs (Lin- c-Kit+ Sca-1$^-$ CD16/32$^-$ CD34$^+$) (A). Terminally differentiated cells were identified as immature B-cells (IgM$^+$ B220^{low}), pro-pre B-cells (IgM$^-$ B220$^+$), mature B-cells (IgM$^+$ B220$^+$), erythrocyte progenitors (CD71$^+$ Ter119$^-$), erythrocytic blasts (CD71$^+$ Ter119$^+$), erythrocytes (CD71$^-$ Ter119$^+$), granulocytes (Gr1$^+$ CD11b$^+$), T-cells (CD3$^+$) (B). Quantification of lineage committed progenitors and terminally differentiated cell fractions in the bone marrow of control (co) and mutant (mt) animals (CLP co: n = 9, CMP co: n = 12, GMP/ MEP: co: n = 6, CLP: mt: n = 8, CMP: mt: n = 11, GMP/MEP: mt: n = 5; differentiated cells: co: n = 12, mt: n = 11

5.6.3 Cell cycle genes are de-regulated in mutant long-term hematopoietic stem cells

The determination of the cell cycle status of LT-HSCs, ST-HSCs and LSK cells revealed no significant between control and mutant animals (Figure 57). There was a slight increased number of cells in G_0 in hematopoietic stem and progenitor cells from mutant animals but this did not reach statistical significance. In addition cell cycle distribution did not differ between mutant and control animals. Interestingly, mRNA expression profiles of LT-HSCs from control and mutant animals showed a very distinct down-regulation of the $p16^{INK4a}$ cell cycle inhibitor. Simultaneously a slight increase in Cyclin D1 and Bmi-1 mRNA was identified in these cells as well. Bmi-1 is an oncogene that is essential for self-renewal of HSCs and blocks cell cycle progression by inhibiting $p16^{INK4a}$ expression (Pardal., et al., 2005; Park, et al., 2003; Jacobs, et al., 1999). Therefore cells are retained in G_0 as the transition between G_0 and G_1 is blocked. Thus the upregulation of Bmi-1 fits very well to the observed down-regulation of $p16^{INK4a}$ and further correlates with the increased expression of Cyclin D1.

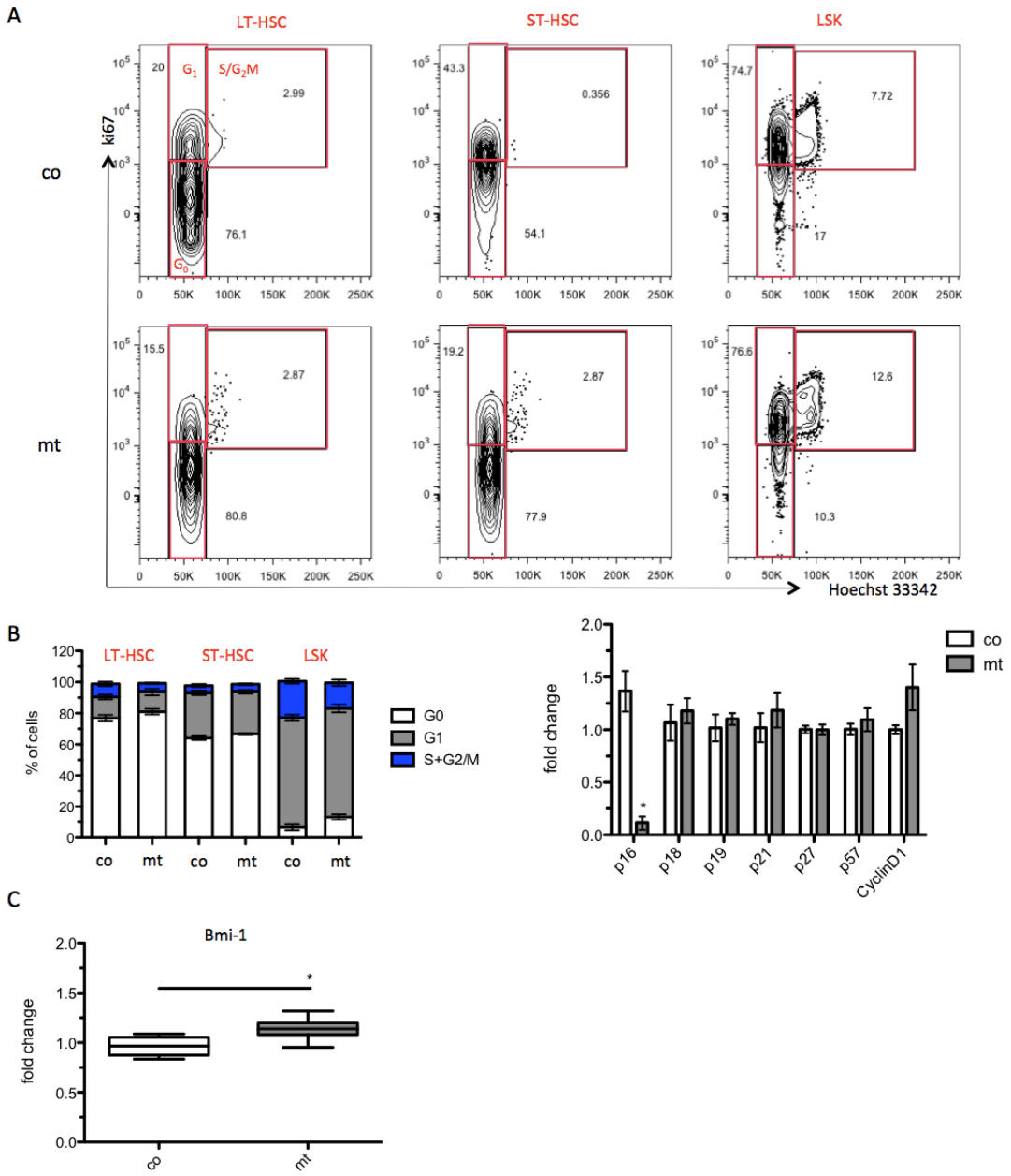

Figure 57: LT-HSCs from mutant animals have impaired cell cycle associated gene expression
(A) Cell cycle profile of hematopoietic stem and progenitors of control (co) and mutant (mt) animals. (B) Cell cycle distribution of hematopoietic stem and progenitor cells of control and mutant animals. (C) Fold change of Bmi-1 (B lymphoma Mo-MLV insertion region 1 homolog) mRNA in LT-HSCs of controls and mutants. Cells are normalized to SDHA and OAZ (n = 6; Bmi1: n = 8).

5.6.4 c-Myc overexpression in osteoblasts from transgenic animals leads to loss of label retaining long-term hematopoietic stem cells

The results so far had shown that the numbers of LT-HSCs were decreased in mutant animals and that expression of several cell cycle regulators was affected in these animals. Notably, our group recently discovered a cell population within the LT-HSCs that are even more quiescent and undergo cell division only a few times during the life span of a mouse (Wilson, et al., 2008). In the next step these so-called dormant HSCs were analyzed in *ColtTA;TreMyc* animals.

To identify dormant HSCs *in vivo*, a label-retaining assay with Bromo-deoxy-uridine (BrdU) was performed. For this purpose mice were given BrdU with the drinking water for 10 days in order to label all dividing cells with BrdU. After this pulse-period, BrdU administration was stopped and a chase period of 100 – 120 days followed, during which only the actively cycling cells lose their BrdU label. The remaining BrdU label-retaining cells (LRCs) were then identified by flow cytometry (Figure 58, A).

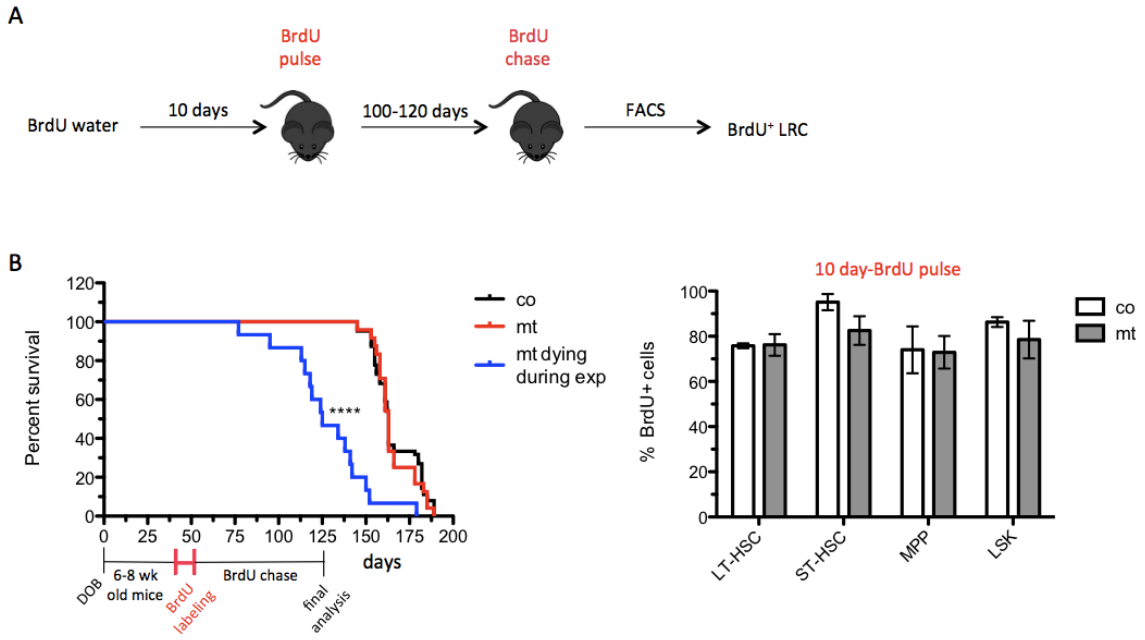

Figure 58: Overview of the set-up of the BrdU-LRC assay
Schematic scheme of long-term BrdU labeling of animals to identify dormant BrdU positively label-retaining cells by FACS (A). Effect of BrdU treatment on mouse viability over time of control (co) and mutant (mt) animals. Mutant animals, which were dying during the experiment are indicated in blue (co, mt: n = 28, mt dying during experiment n = 13). (B). FACS analysis of BrdU-positivity in bone marrow cells after initital BrdU labeling of 10 days (n = 3).

First, the effect of BrdU treatment on mouse survival was assayed. Kaplan-Meier survival analysis indicated no effect on animal survival as a consequence of 10-day BrdU labeling between control and mutant mice (Figure 58). As expected about one third of all mutant animals died prematurely due to bone malignancies (compare Figure 32, chapter 1.5.1 Transgenic animals develop bone tumors). Both groups of surviving animals showed normal behavior and survival statistics were identical for treated and non-treated mice. Therefore BrdU was non-toxic to transgenic and control animals.

Subsequently the initial BrdU-labeling efficiency was determined by fluorescence-coupled antibody staining against BrdU. At the end of the ten-day BrdU pulse animals were sacrificed and numbers of BrdU positive bone marrow cells were quantified by FACS (Figure 58). The analysis revealed an initial BrdU labeling of about 80%, which did not differ significantly among LT-HSCs, ST-HSCs, MPPs and LSK cells.

Finally, after a chase period of 105 days the animals were sacrificed and the percentage of BrdU label retaining cells in the bone marrow was assessed by flow cytometry.

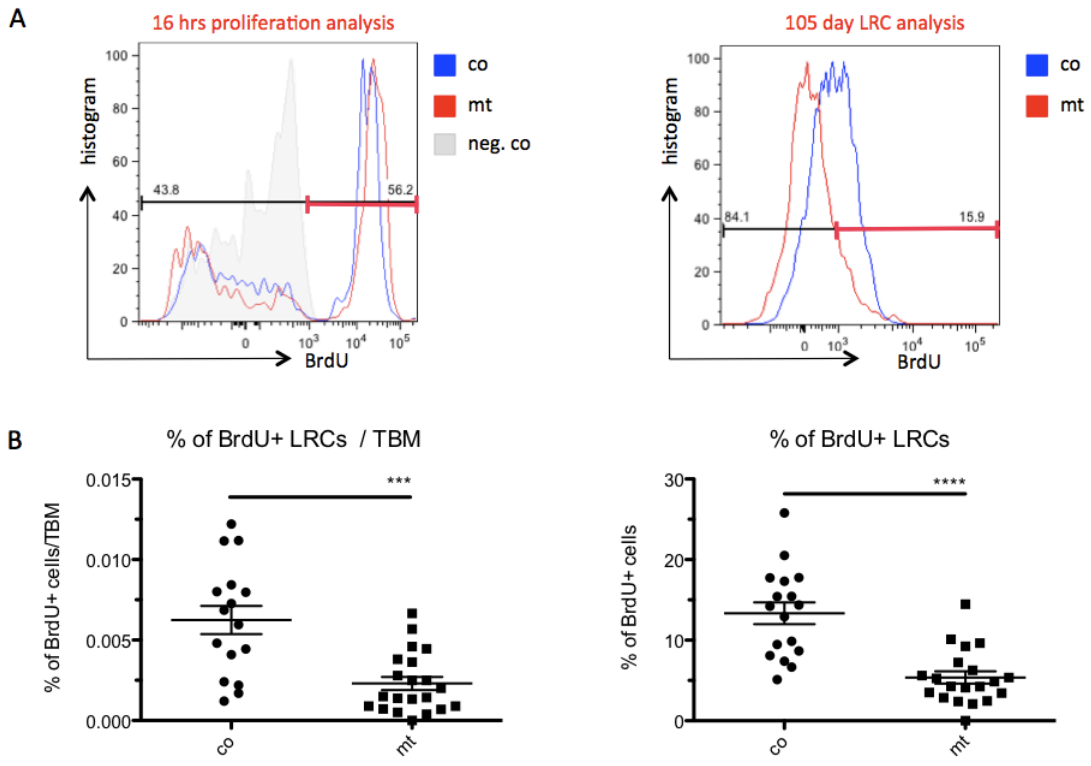

Figure 59: Dormant HSCs are lost in transgenic animals
Identification of BrdU-positively labeled LT-HSCs by FACS. Either 16 hrs post BrdU injection for a proliferation analysis (A, left) or 105 days post BrdU pulse to measure dormant HSCs (A, right). Cells were pre-gated on LSK CD150^{+} CD48^{-} CD34^{-} and then analyzed for their BrdU staining. BrdU positive cells were subsequently quantified (B).

In the next step a proliferation analysis on LT-HSCs was performed, by injecting BrdU into mice and analyzing LT-HSCs 16hrs post injection. Actively proliferating cells were then identified as BrdU positive cells. These experiments revealed equal proliferation rates of LT-HSCs in control and mutant animals (Figure 59). Normally the percentage of BrdU-LRCs is quite low and only about 15% of LT-HSCs are dormant (Trumpp, et al., 2010; Essers, et al., 2009; Wilson, et al., 2008). Most surprisingly, transgenic *ColtTA;TreMyc* animals had significantly less BrdU-LRCs compared to control animals. Indeed BrdU incorporation analysis revealed that in mutant animals the percentage of BrdU-LRCs within the LT-HSCs was reduced to about 5% and about 14% in control animals.

Initial BrdU labeling assays had shown that LT-HSC populations were equally labeled in control and mutant animals (Figure 58, B). Thus the loss of BrdU-LRCs in double transgenic animals must happen within the 105 days chase period. To further elucidate this, in a next step, a BrdU time course experiment was started. For this purpose, cells were again labeled with BrdU for 10 days and the percentage of BrdU positive cells in the bone marrow was monitored by FACS analysis during the chase period.

For the BrdU time course experiment control and double transgenic animals were sacrificed after 10, 30, 75, 105 and 125 days of chase and analyzed for their BrdU content. Strikingly, after 75 days already, the percentage of mutant $BrdU^+$ LT-HSCs was significantly reduced in *ColtTA;TreMyc* animals (Figure 60, A). This difference was observed for the remainders of the experiment and reached its maximum at 105 days post BrdU labeling. This indicates that mutant *ColtTA;TreMyc* animals do lose their BrdU label faster compared to control mice.

With the BrdU time course experiment HSC doubling times were calculated by the percentage of remaining BrdU in a cell at a given time point and analyzed over time. The HSC turnover in mutant and control animals was modeled using a 2-population fit model (Figure 60, B, C).

As expected the model showed that activated HSCs in control mice lose their label much faster than the dormant HSC population. In fact the model suggests that the activated HSC self-renew every 54 days while the dormant HSCs divide only once every 139 days. This fits well to the data published by Wilson, *et al.*, 2008. In contrast modeling of the BrdU positive HSCs in mutant animals revealed that all LT-HSCs self-renew within 58 days. This suggests that all HSCs in *ColtTA;TreMyc* animals are actively cycling and these mice do not maintain dormant HSCs.

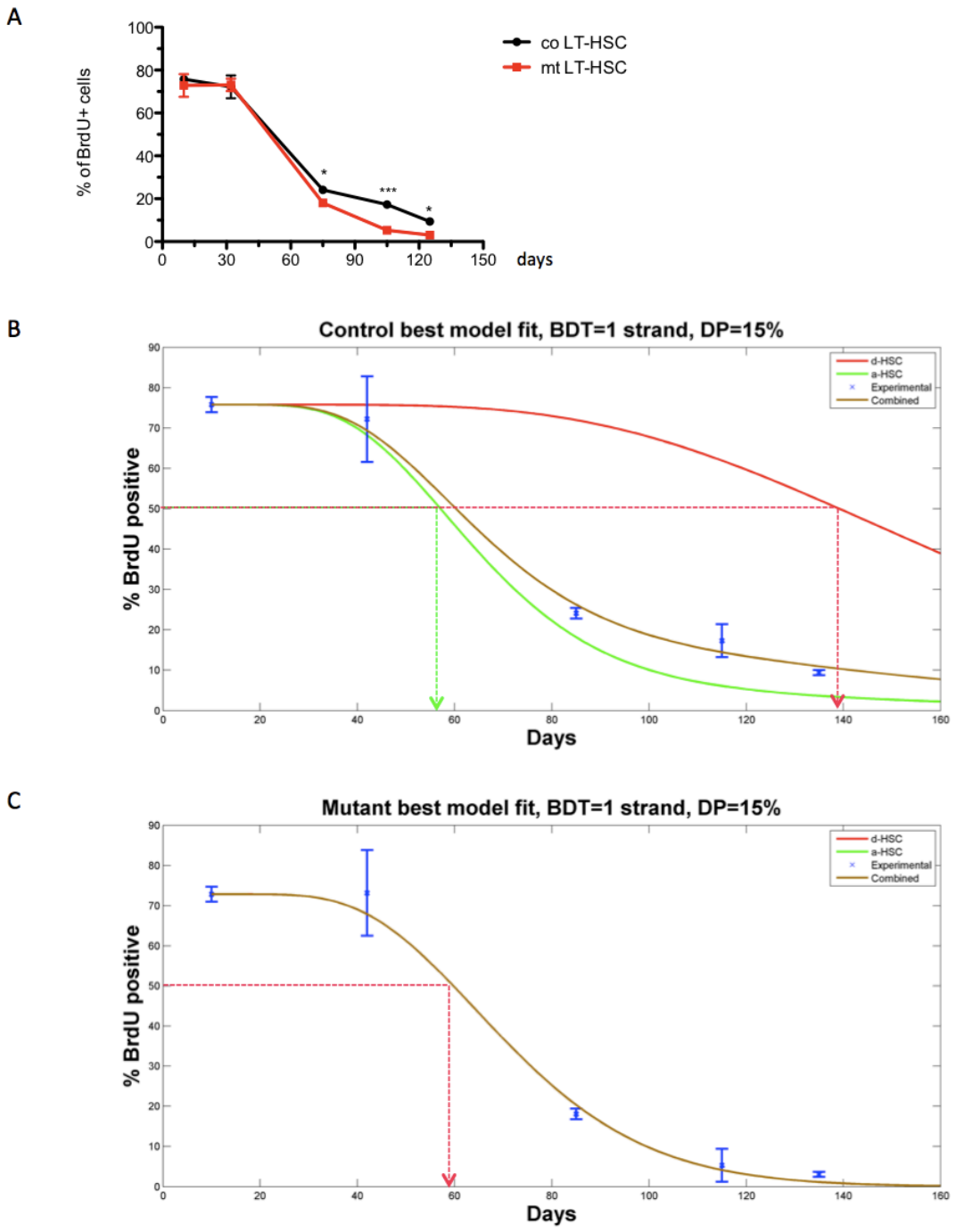

Figure 60: Mutant animals show LRC-loss over time
Time course of control (co) and mutant (mt) LRCs and BrdU loss over time during a BrdU chase period of 125 days (10 days: n = 3, 30 days: n = 4, 75 days n = 6, 105 days: n = 7, 125 days: n = 3) (A). Mathematic 2-population modeling of dormant HSC doubling time and BrdU loss over time in control (doubling time: every 54 days in aHSC and 139 days in dHSCs) (B) and mutant animals (equal doubling time of aHSCs and dHSCs every 58 days) (C) (sensitivity of the assay: BDT: BrdU detection threshold = 1 DNA strand out of 80 strands is positively labelled; estimated DP: dormant population 15%; arrows indicate HSC doubling time; LRC = label retaining cell).

5.6.5 Differentiation capacities of LT-HSCs from mutant animals are unchanged in transplantation assays *in vivo*

Most strikingly, the BrdU time course experiment revealed a loss of dormant HSCs in mutant animals. Dormant hematopoietic stem cells are the most competent stem cells that possess the ability to continuously replenish the blood system over time while ST-HSCs have only a limited self-renewal capacity. To corroborate these findings, in a next step, hematopoietic stem cell transplantations were performed to check self-renewal capacities in a functional assay.

For this purpose bone marrow from control and mutant animals was intra-veneously transplanted into sub-lethally irradiated NSG mice and the chimerism analyzed 25-30 weeks post transplantation. CD45 is the common leukocyte antigen, which is expressed on all hematopoietic cells and exists in two different isoforms, CD45.1 and CD45.2. Donor cells from control ColtTA and mutant *ColtTA;TreMyc* animals express a mixture of CD45.1 and CD45.2 while the recipient NSG animals only possess CD45.1 antigen. Therefore it is possible to exactly identify donor cells in recipient animals by fluorescent-coupled antibody staining for CD45.2, as these cells can only be derived from donor animals.

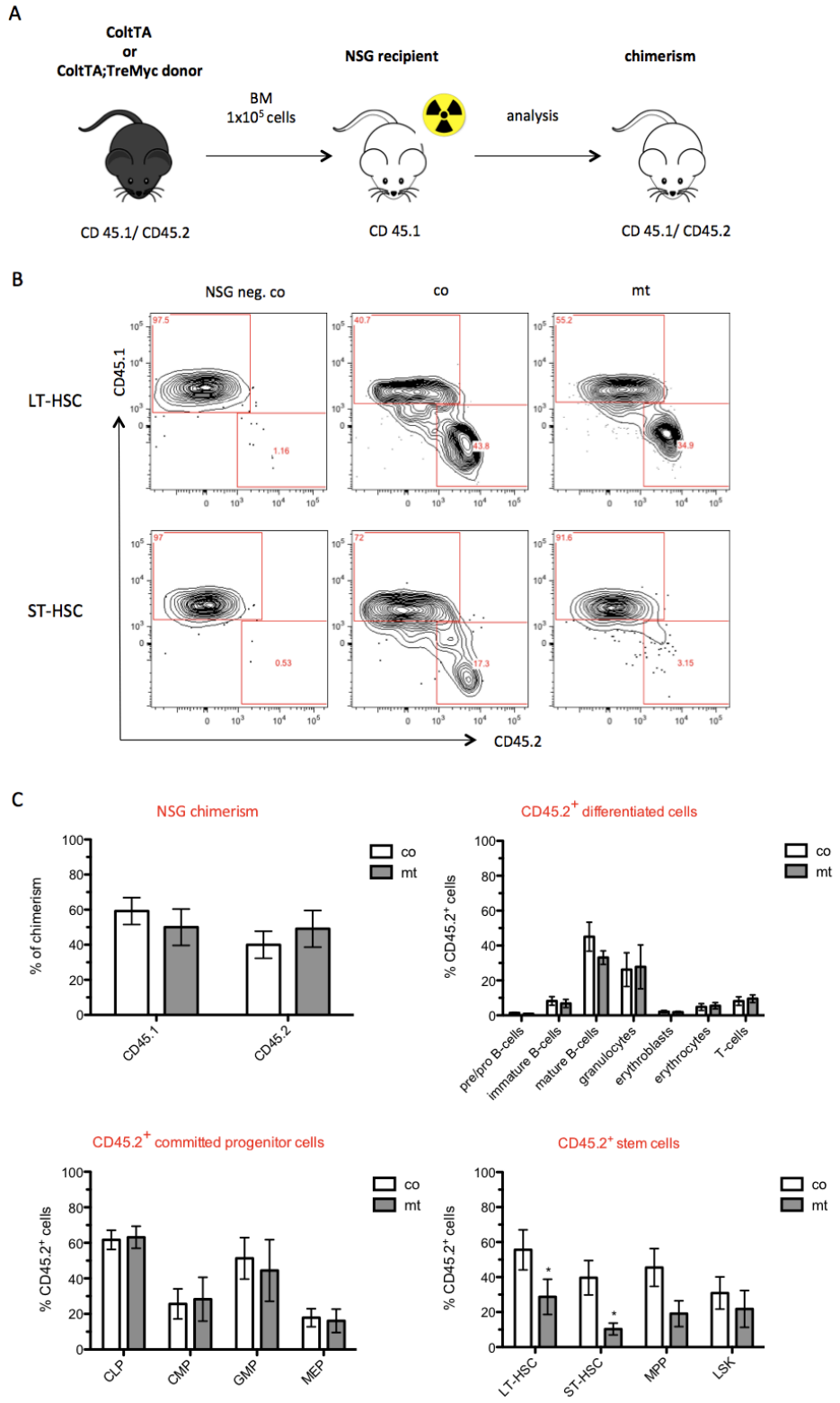

Figure 61: Mutant primary bone marrow chimeras show less LT- and ST-HSCs engraftment
Bone marrow (BM) of control or mutant donor mice was intra-veneously transplanted into sub-lethally irradiated NSG recipient animals and the chimerism analyzed 25-30 weeks post transplantation (A). FACS gating scheme to detect donor (CD45.2 positive) LT- and ST-HSCs in chimeras (B). Quantification analysis of CD45.2$^+$/CD45.1$^+$ chimerism, differentiated cell populations, hematopoietic progenitors and stem cell populations in chimeras (C).

Analysis of the bone marrow from chimeric animals revealed no differences in engraftment capacities of bone marrow between control and mutant animals (Figure 61). In both cases the percentage of the engrafted CD45.2 cell population was about 50%. This indicated that the mutant animals do possess stem cells with the same engraftment capacities as control animals. Furthermore, quantification analysis of CD45.2 positive differentiated cell populations (B-cells, T-cells, granulocytes and erythrocytes) showed no differences between control and mutant animals. Neither did the percentages of the committed progenitor populations (CLPs, GMPs, CMPs and MEPs) in recipient animals differ between controls and mutant animals. Taken together, this indicates that the differentiation capacities of HSCs are similar between control and mutant animals. However, quantification of engrafted short- and long-term HSCs revealed that the number of CD45.2 positive HSCs was significantly reduced in chimeras injected with bone marrow from mutant mice compared to those animals injected with control bone marrow. While chimeras, transplanted with cells from control animals had about 55% of CD45.2 positive LT-HSCs, only about 30% of LT-HSCs were identified in chimeras from mutant animals. In addition, analysis of ST-HSCs showed, that in chimeras from control animals 40% of ST-HSCs were CD45.2 positive while the percentage was reduced to 10% in chimeras from mutant mice. Also analysis of the CD45.2 positive multi-potent progenitor (MPP) compartments revealed a difference between control and mutant animals in the chimera experiments but this was not statistically significant. Taken together this data confirms, that *ColtTA;TreMyc* animals possess less LT- and ST-HSCs in their bone marrow compared to ColtTA control animals (Figure 55). This supports the hypothesis that the mutant osteoblasts have a major effect on the hematopoietic stem cell compartment.

To corroborate these findings, secondary bone marrow transplantations from first line generated chimeras, were performed. Therefore, bone marrow from control and mutant chimeras was transplanted again into sub-lethally irradiated NSGs. In secondary chimeras the chimerism was then analyzed 25-30 weeks post transplantation by FACS analysis.

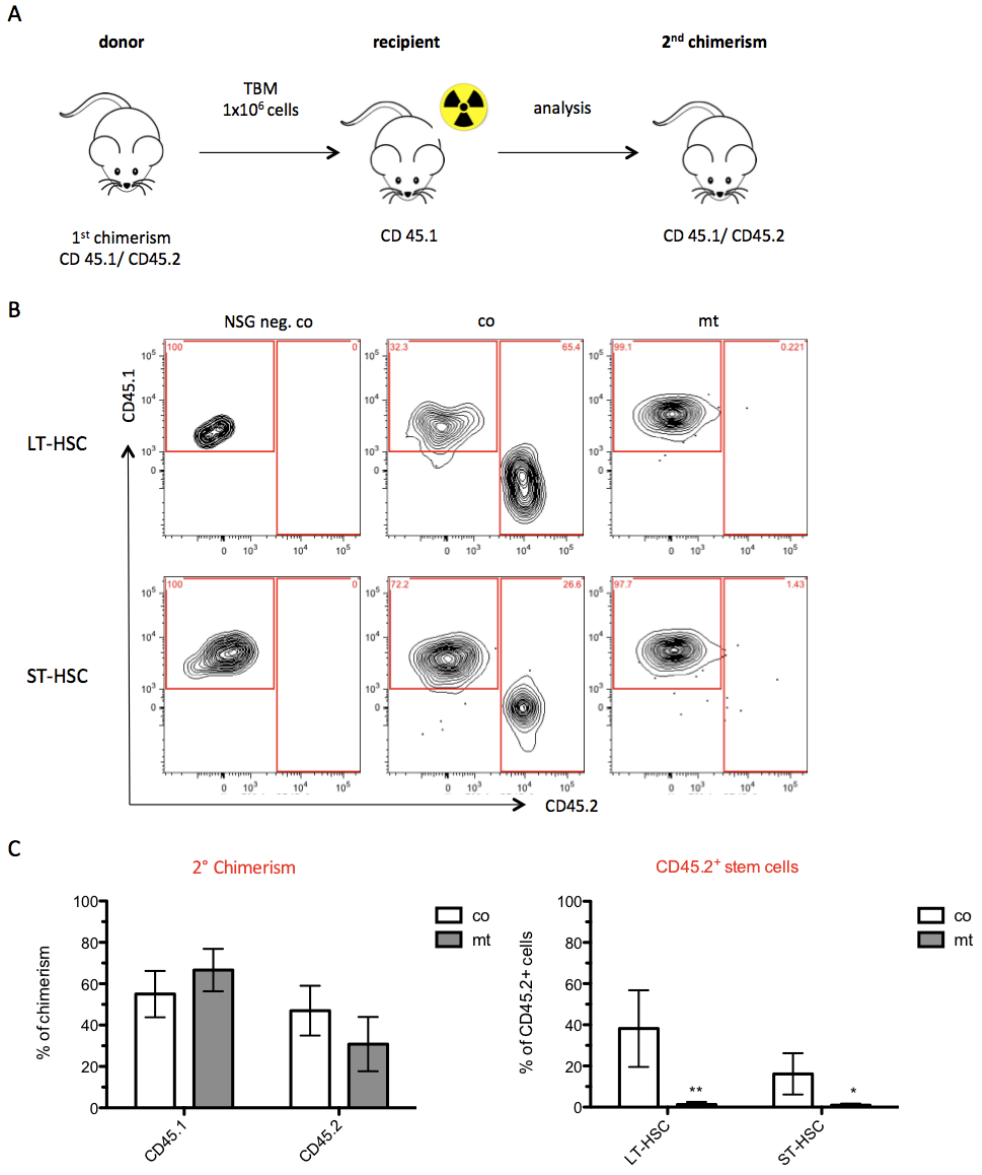

Figure 62: Mutant secondary bone marrow chimeras have almost no LT- and ST-HSC engraftment
(A) Bone marrow (BM) of control or mutant primary chimeras was intra-veneously transplanted into sub-lethally irradiated NSG recipient animals to generate secondary chimeras and the chimerism analyzed 25-30 weeks post transplantation. (B) FACS gating scheme to detect donor (CD45.2 positive) LT- and ST-HSCs in chimeras. (C) Quantification analysis of CD45.2$^+$/CD45.1$^+$ chimerism and stem cell populations in secondary chimeras.

Interestingly FACS analysis of the bone marrow of secondary chimeras revealed already a difference in engraftment capacities of control and mutant primary bone marrow transplants (Figure 62). While control secondary chimeras contained about 45% CD45.2 positive cells, the mutant secondary chimeras only contained about 30% CD45.2 hematopoietic cells. Most importantly, differences in the percentages of CD45.2 positive LT- and ST-HSCs were observed again. Secondary chimeras from control animals comprise about 40% LT-HSC and 20% ST-HSC populations. In contrast, the analysis of secondary chimeras from mutant animals showed, that almost no CD45.2 positive LT- and ST-HSCs were present. This fits well to the initial finding that primary mutant generated chimeras showed decreased numbers of LT- and ST-HSCs. As expected, the secondary chimeras confirmed again, that the transplanted bone marrow from the mutant primary chimeras contained less stem cells. All together this confirms, that mutant *ColtTA;TreMyc* animals do have decreased numbers of long- and short-term HSC populations and supports the mathematical modeling of the BrdU experiment that suggested no dormant HSCs are present in these animals while the differentiation capacities of HSCs are unchanged.

5.6.5.1 Forced cell cycle activation is impaired in LT-HSCs from *ColtTA;TreMyc* animals

5.6.5.2 Polyinosinic:polycytidylic acid (poly I:C) treatment of *ColtTA;TreMyc* animals does not lead to cell cycle activation

These experiments showed that the c-Myc overexpression in osteoblasts in *ColtTA;TreMyc* animals had a distinct influence on hematopoietic stem cells. Most importantly, it led to the drastic loss of dormant stem cells, indicating that mature osteoblasts play a major role in the hematopoietic stem niches. Upon specific external signals like injury or infection, hematopoietic stem cells are activated and mobilized to help the body react fast to stress situations. Therefore I analyzed whether HSCs derived from double transgenic animals still showed functional activation in response to stress. Recently our group could show that interferon alpha (IFN**α**) leads to hematopoietic stem cell activation and proliferation (Essers, et al., 2009). IFN**α** production in the mouse can be induced by injection of Polyinosinic:polycytidylic acid (poly I:C, pIC), a double stranded mRNA that mimics viral infections. In a first set of experiments the effect of pIC treatment on hematopoietic stem cells from control and mutant animals was therefore evaluated.

Normally, upon pIC stimuli hematopoietic stem cells are quickly activated and pushed out of G_0 into cell proliferation. However, HSCs from double transgenic *ColtTA;TreMyc* animals did not show complete cell cycle activation upon pIC treatment. About 60% of LT-HSCs in mutant mice remained in G_0 while only 20% of LT-HSCs remained quiescent in control animals (Figure 63). Interstingly, a similar result was observed when ST-HSCs were analyzed from control and mutant animals. While about 25% of ST-HSCs from control mice were still present in G_0, in mutant mice, about 50% of ST-HSCs remained in G_0.

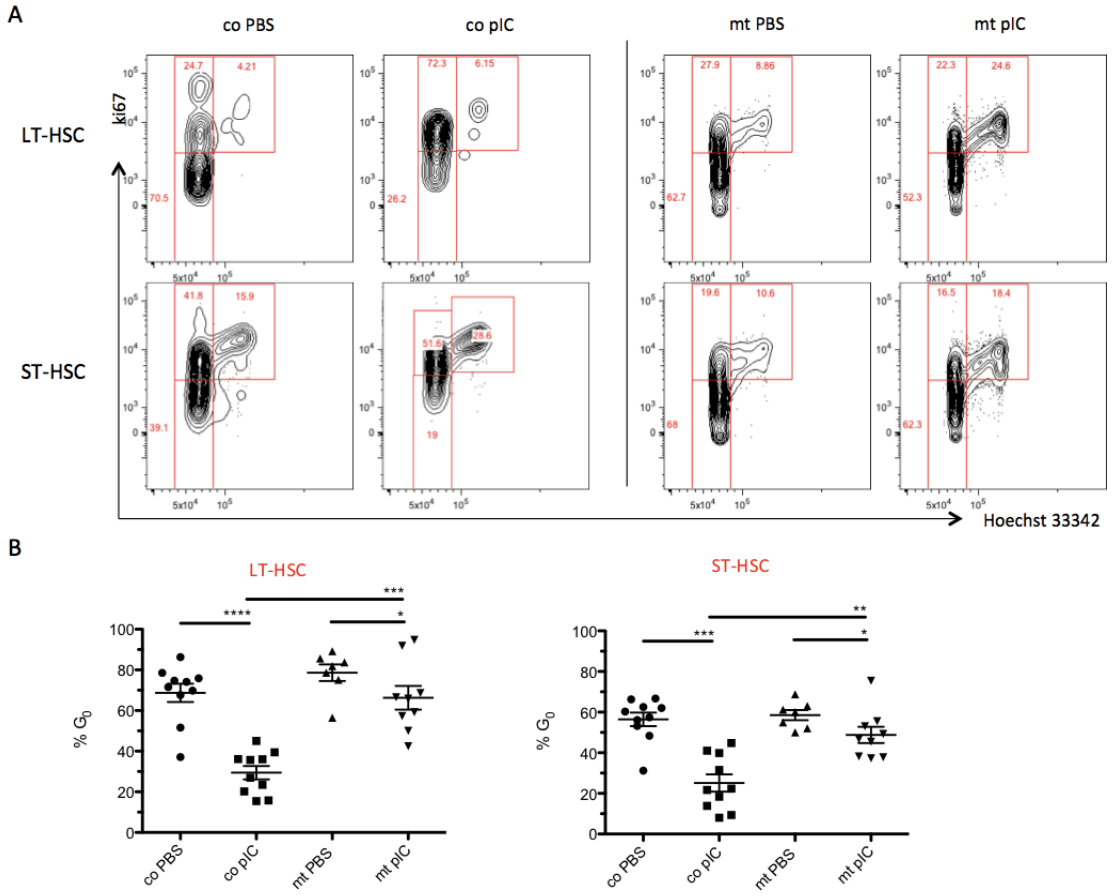

Figure 63: Hematopoietic stem cells from mutant animals are not efficiently activated upon PolyI:C treatment
Cell cycle analysis of control (co) and (mt) LT- and ST-HSCs before and 16 hrs after pIC treatment (A) and quantification of cells in G_0 of the cell cycle (B).

5.6.5.2.1 Interferon alpha treatment leads to complete cell cycle activation of HSCs from *ColtTA;TreMyc* animals

These observations indicated that manipulated osteoblasts influenced HSC behavior upon pIC stimuli. In a next step IFNα was directly administered to control and mutant animals to test whether the effects was based on interferon responsiveness of HSCs.

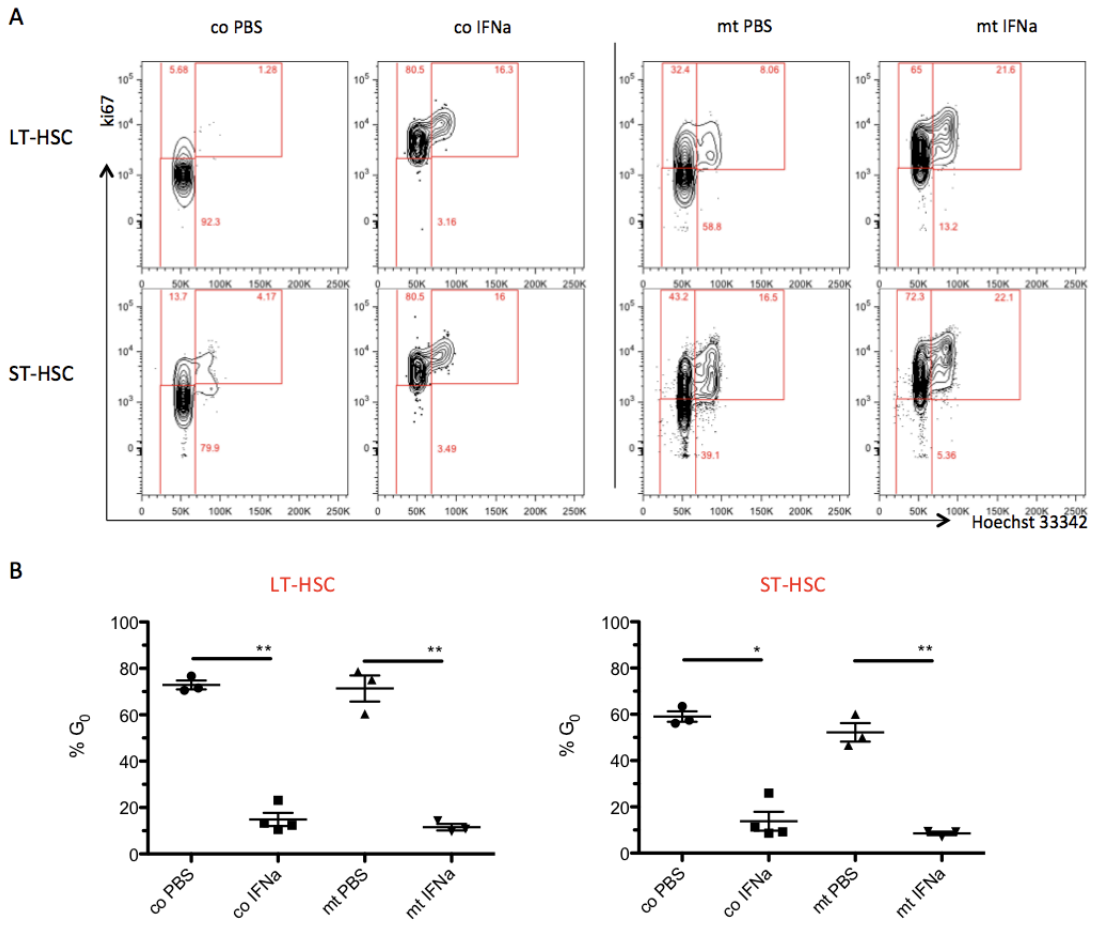

Figure 64: Normal IFNa-induced activation of hematopoietic stem cells from *ColtTA;TreMyc* mutants
Cell cycle analysis of control (co) and (mt) LT- and ST-HSCs before and 16 hrs after IFNa treatment (A) and quantification of cells in G_0 of the cell cycle (B).

Surprisingly, LT-HSCs from both control and mutant animals showed complete cell cycle activation and G_1 entry when cells were analyzed 16hrs post IFNα treatment (Figure 64). In detail, about 70% of quiescent LT-HSCs from control and mutant mice were in G_1, while only about 15% of cells were left in G_0 after IFNα treatment. Additionally, only about 10% of ST-HSCs from mutant and control animals were still in G_0 upon interferon treatment and thereby the ST-HSC population was almost completely activated. This indicated that LT- and ST-HSCs from mutant animals can be normally activated upon IFNα treatment.

Taken together these findings indicate that the manipulated human c-Myc overexpressing osteoblast seem to have an influence on normal hematopoietic stem cell activation upon pIC treatment, while this effect was no longer seen upon treatment of IFNα. One explanation for this observation might be that often treatment with IFNα binds directly to its receptor on HSCs, thereby circumventing indirect IFNα production via osteoblasts.

5.6.5.3 Lipopolysaccharide (LPS) treatment of *ColtTA;TreMyc* animals does not influence cell cycle profile of LT- and ST-HSCs

To strengthen this hypothesis mice were injected with lipopolysaccharide (LPS) next. LPS activates HSCs by an indirect mechanism. LPS induces CD14 expression on monocytes and then CD14 interacts with the Toll-like receptor 4 (TLR4) on HSCs. This leads to NFkB activation and the production of pro-inflammatory cytokines via TRIF/TRAM as well as intrinsic interferon production via MyD88 signaling. The TLR4 dependent pathway seems to be more important to efficiently activate HSCs as TLR4 knockout mice (TLR4-/-) fail to activate HSCs while IFN receptor knockout mice (IFNR-/-) show normal HSC activation upon LPS treatment. Therefore I hypothesized that upon LPS treatment *ColtTA;TreMyc* mice should show normal HSC activation.

Interestingly, LPS treatment did not lead to HSC activation in double transgenic *ColtTA;TreMyc* animals and showed instead the opposite effect as expected (Figure 65). While about 80% of control LT-HSCs were quiescent before LPS application, upon treatment with low-doses of LPS, only about 50% of cells remained in G_0, while the rest of the cells were pushed into active cell proliferation. In contrast about 80% of LT-HSCs from mutant animals remained in G_0 upon LPS administration. Thus, LPS induced TLR4 signaling to activate HSCs was not functional in *ColtTA;TreMyc* mice. The reason for this is still unclear and could be based on changes in TLR4 signaling pathway in HSCs or due to impaired interferon production as a consequence of c-Myc overexpression in osteoblasts and their effect on main interferon cell producers. More likely it could be due to slightly decreased monocyte populations that were observed in mutant animals (data not shown).

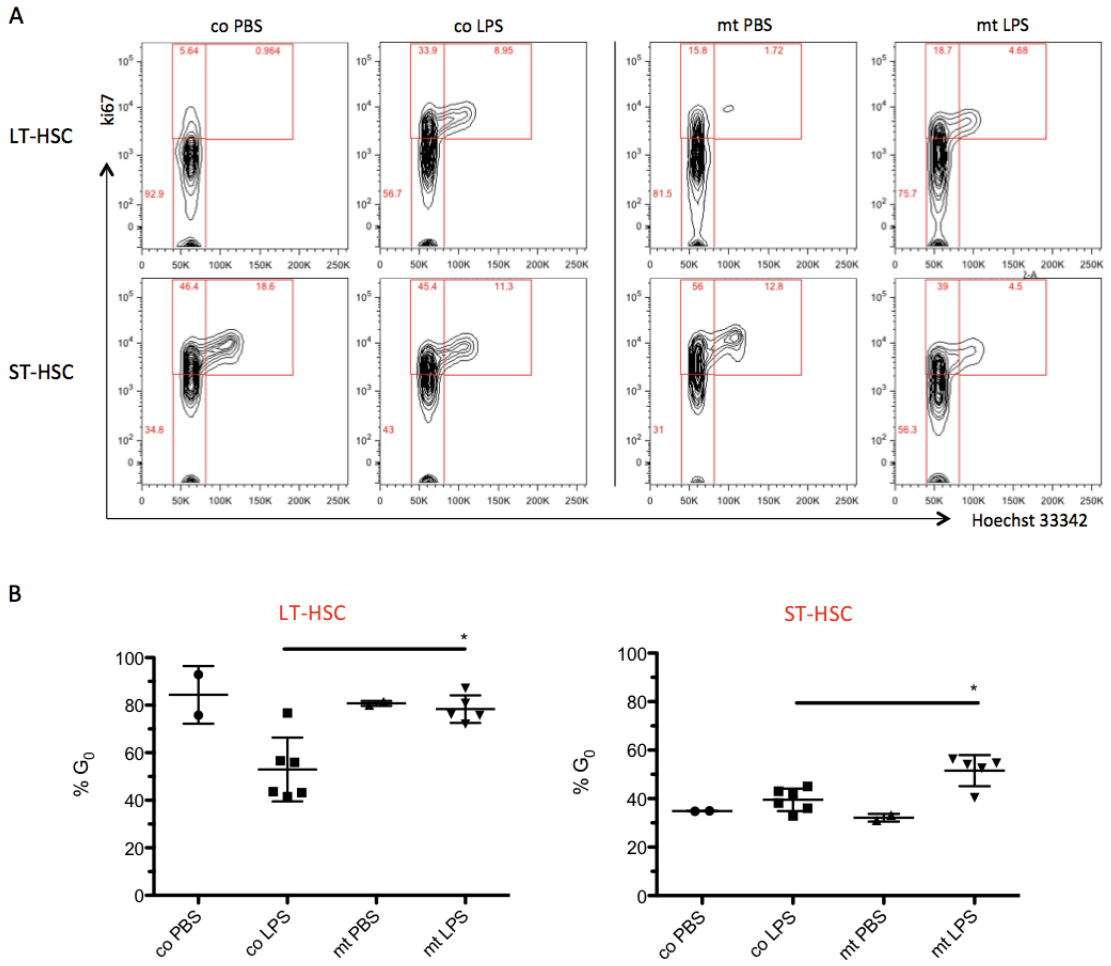

Figure 65: Hematopoietic stem cells from mutant animals are not efficiently activated through LPS treatment
Cell cycle analysis of control (co) and (mt) LT- and ST-HSCs before and 16 hrs after LPS treatment (A) and quantification of cells in G_0 of the cell cycle (B).

5.6.5.4 Aberrant intrinsic interferon production in *ColtTA;TreMyc* animals

To gain insight into IFN-dependent HSC activation the expression of proteins involved in TLR-independent signaling pathways were analyzed in mutant and control osteoblast and HSCs. Therefore mice were treated with pIC, which triggers interferon production through TLR3 signaling which in turn binds to the cytoplasmatic receptor retinoic acid inducible gene 1 (RIG-I) and IFN inducible helicase 1 (IFIH-1) and associates with mitochondrial anchored CARD adaptor (IPS-1) to activate IFN expression.

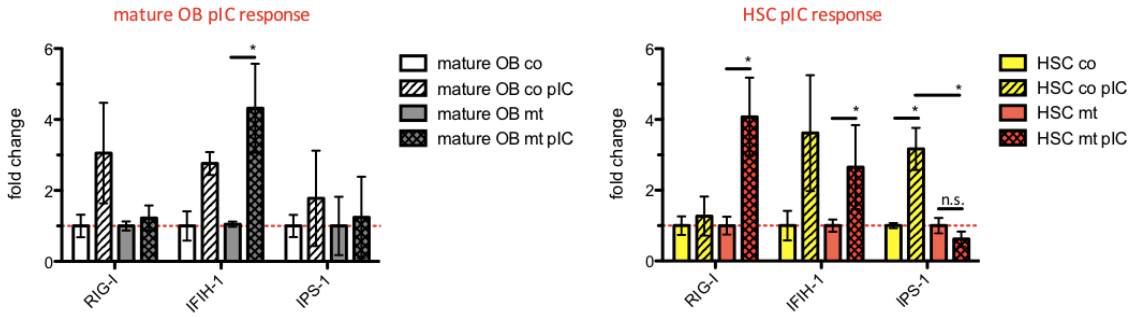

Figure 66: Impaired PolyI:C mRNA response in LT-HSCs from mutant animals
The mRNA expression is represented as fold changes of IFN-response genes in either mutant mature osteoblasts or LT-HSCs compared to controls and untreated samples, normalized to OAZ and SDHA (n = 3).

In response to pIC injection, RIG-I and IPS-1 mRNA expression was only slightly increased in both, control or mutant osteoblasts (Figure 66). However, the RNA sensor IFIH-1 was highly increased in control (3-fold) and mutant (4-fold) osteoblasts in response to pIC treatment. The difference in IFIH-1 expression was the only significant difference between osteoblasts from control and mutant animals. This difference is probably insufficient to explain the incomplete HSC activation in mutant mice.

Nevertheless, HSC activation was impaired in response to pIC as well as LPS treatment of double transgenic *ColtTA;TreMyc* mice. Therefore, expression of RIG-I, IPS-1 and IFIH-1 was checked in LT-HSCs from control and mutant animals before and after pIC treatment. In control LT-HSCs a simultaneous increase in expression of IFIH-1 and IPS-1 were observed. Furthermore a minor increase in RIG-I expression was noticed as well.

Unexpectedly, the response to pIC treatment in LT-HSCs from mutant animals differed significantly to LT-HSCs from controls. Again upon pIC treatment IFIH-1 expression rose sharply similar to the expression of RIG-I. In both cases the expression increased 3-4 fold. In contrast IPS-1 expression, which was increased in HSCs of control mice, was unchanged in mutant HSCs and even slightly down-regulated upon pIC treatment. This indicates that the pIC induced activation of HSCs is only partially working. In the first steps of pIC signaling the RNA helicases RIG-I and IFIH-1 seem to work properly, however subsequent signal transduction seem not to be functional in LT-HSCs from mutant animals.

5.6.6 Gene expression profile of LT-HSCs from *ColtTA;TreMyc* animals reveals differences in DNA replication genes in

To get more insight into the molecular differences between control and mutant long-term HSCs, in a next step, micro array analysis was performed from both cell populations. Therefore LT-HSCs from ColtTA and *ColtTA;TreMyc* animals were sorted and their mRNA expression profile was analyzed.

Symbol	fold change mt/co (log)	Definition	Function
Zcchc14	0,38	zinc finger, CCHC domain containing 14 (Zcchc14), mRNA.	
F830002E14Rik	0,35		
9530005P22Rik	0,34		
LOC381095	-0,89		
Cdc45l	-0,73	cell division cycle 45 homolog (S. cerevisiae)-like (Cdc45l), mRNA.	DNA replication
Apc	-0,53	Adenomatosis polyposis coli	loss of quiescence
2010111I01Rik	-0,53	C9orf3 chromosome 9 open reading frame 3	metabolism
Pprc1	-0,47	peroxisome proliferative activated receptor, gamma, coactivator-related 1 (Pprc1), mRNA.	metabolism
Xab1	-0,46	XPA binding protein 1 (Xab1), mRNA.	DNA repair
Thra	-0,45	thyroid hormone receptor alpha	
Matn4	-0,43	matrilin 4 (Matn4), mRNA.	ECM interaction
2410072D24Rik	-0,42	Psma8 proteasome (prosome, macropain) subunit, alpha type, 8	
B230217N24Rik	-0,40	Hspa13 heat shock protein 70 family, member 13	
Smug1	-0,38	single-strand selective monofunctional uracil DNA glycosylase (Smug1), mRNA.	DNA repair
A530016E13Rik	-0,38		
2010107H07Rik	-0,37	PREDICTED: RIKEN cDNA 2010107H07 gene (2010107H07Rik), mRNA.	
Imap38	-0,35	Gimap1 GTPase, IMAP family member 1	
Slc15a2	-0,35	Slc15a2 solute carrier family 15 (H+/peptide transporter), member 2	metabolism
Mlf1	-0,35	myeloid leukemia factor 1 (Mlf1), transcript variant 1, mRNA.	cell cycle arrest
Aatk	-0,34	apoptosis-associated tyrosine kinase (Aatk), mRNA.	growth arrest / apoptosis

Table 2: Short list of genes differentially expressed in mutant LT-HSCs of ColtTA;TreMyc animals
Log2 fold changes of a short list of genes differentially expressed in mutant LT-HSCs compared to control LT-HSCs. Upregulated genes are represented in orange while down-regulated are indicated in blue. Light orange and light blue indicates genes where no function was known.

Comparison of the gene expression profiles between LT-HSCs from ColtTA control and *ColtTA;TreMyc* mutant animals revealed that the overall difference in gene expression patterns between control and mutant LT-HSCs was rather low. This was not unexpected as the previous experiments had demonstrated that there were no major differences in LT-HSC differentiation or cell proliferation between mutant and control mice. Interestingly, however most of the genes that were differentially expressed in mutant and control mice, were down-regulated in LT-HSCs derived from *ColtTA;TreMyc* mice. Further analysis revealed that many of these genes are involved in cell cycle regulation and play roles in DNA replication, repair and cell metabolism. Only one gene was found to be upregulated,

namely the zinc finger CCHC domain 14 (Zcchc14), which is normally an interaction molecule that builds tandems with DNA, RNA or proteins. For example, Cdc45, the gene that is most strongly downregulated, is a replication factor that belongs to the CMG complex (Cdc45, MCM, GINS) and participates in the DNA replication machinery (Makarova, et al., 2012). In addition, Xab1 and Smug1 are enzymes for DNA repair mechanisms and were down-regulated in mutant LT-HSCs. This is interesting, as it might indicate that DNA replication and repair are impaired in mutant LT-HSCs. This would suggest that cell cycle control in mutant LT-HSCs is already impaired through the loss of important cell cycle check points that prevent cell proliferation of damaged cells.

Strikingly analysis of the differentially expressed genes also identified genes that had previously been described as important in HSC maintenace. Most interestingly, Adenomatous polyposis coli (Apc) was differentially expressed and down-regulated in mutant LT-HSCs. Notably, Wang, et al. had observed a block in early differentiation of erythropoiesis in Apc-heterozygous mice. Furthermore they could show that LT-HSCs from these mice had reduced repopulating capacities (Wang, et al., 2010). In addition these mice frequently developed myelodysplastic syndrome (MDS) (Lane, et al., 2010; Wang, et al., 2010). Another gene, that was strongly downregulated in LT-HSCs from *ColtTA;TreMyc* mice was Matrilin-4. Matrilin-4 is an extracellular matrix protein and is a member of the matrilin family. Matrilin-1 and matrilin-3 are expressed in skeletal tissues, while matrilin-2 and matrilin-4 are widely expressed throughout the body (Ko, et al., 2004). This is of special interest, as this might indicate that the interaction between HSCs and their niche is impaired due to the down-regulation of matrilin-4 extra-cellular matrix protein in LT-HSCs of mutant animals.

6 Discussion

Recently our group and others have demonstrated a pivotal role of c-Myc in maintenance, differentiation and development of hematopoietic stem cells (HSC) (Holien, et al., 2012; Laurenti, et al., 2008; Wilson, et al., 2008; Hoffmann, et al., 2002). Both, c-Myc deletion and induced c-Myc overexpression leads to dramatic phenotypes in mice. Deletion of Myc blocks the differentiation of HSCs into differentiated cells and leads to an accumulation of HSCs in the bone marrow. In contrast overexpression of c-Myc in HSCs induces increased proliferation of the long-term HSCs (LT-HSC), a HSC subpopulation that normally cycles only rarely. Here, the number of hematopoietic progenitor cells increases, while terminal differentiation is completely blocked (Wilson, et al., 2008).

Differentiation and self-renewal of stem cells is in large parts controlled by the surrounding cell populations, the so-called stem cell niche. Two different types of HSC niches have been previously described in the bone marrow: the endosteal niche, close to endosteal osteoblasts and the vascular niche, close to sinusoids. Besides nestin$^+$ MSCs, CAR (CXCL-12-abundant reticular cells) cells, leptin receptor$^+$ perivascular stromal cells (Lepr) cells and GFAP$^+$ nonmyelinating Schwann cells (glial cells), macrophages and N-cadherin$^+$ osteoblasts, osteoblasts and osteoclasts have been implicated in the HSC niche and appear to control HSC maintenance and differentiation (Ding, et al., 2012; Ehninger and Trumpp, 2011; Yamazaki, et al., 2011; Lévesque, et al., 2010; Wilson, et al., 2008; Zhu, et al., 2007; Nagasawa, et al., 2006; Zhang, et al., 2003; Calvi, et al., 2003). As the role of c-Myc is known to be cell-specific, we tested how ectopic overexpression of c-Myc in mature osteoblasts in the HSC niche affects the differentiation capabilities and self-renewal of HSCs. Furthermore as osteoblasts are heavily involved in bone formation, we also assessed whether c-Myc overexpression in osteoblasts leads to any overt bone phenotype in mice.

6.1.1 Human c-Myc overexpression in osteoblasts leads to an osteopetrosis-like phenotype in mice

Human c-Myc overexpression in mature osteoblasts of mice was achieved, using an inducible tet-off system and the collagen I (2.3kDa ColtTA) promoter, which is specific for mature osteoblasts. c-Myc overexpression was generally induced in three-week old double transgenic *ColtTA;TreMyc* mice. To evaluate the effects of c-Myc overexpression in osteoblasts, in a first step the bones of the animals were analyzed macro- and microscopically. Mutant animals exhibited significantly thicker and shorter bones. Histological sections revealed that the bone architecture was perturbed, as there was no clear separation between compact, solid bone and the bone marrow. In contrast compact bone formed extensions and cavities, and the bone marrow was partially localized in the brittle structures of the bone. Even though the bones were thicker, they were easily breakable and very fragile.

As osteoblasts are the major bone forming cells, a specific bone phenotype was expected in transgenic *ColtTA;TreMyc* animals. In order to gain insight into this phenotype, the bone stromal cells were analyzed by FACS. Here we found that the number of mutant osteoblasts was significantly increased to about 15%, compared to 9% in control animals. Additionally, osteoclast numbers were also increased. Interestingly in human osteopetrosis patients the number of osteoblasts and osteoclasts are frequently elevated as well. Osteopetrosis is a severe human bone disease, in which the bone formation rate is higher than bone resorption by osteoclasts, due to a currently not fully understood impairment in osteoblast differentiation and osteoclast function (Lo Iacono, et al., 2012; Stark, et al., 2009; Tolar, et al., 2004). In the ColtTA mouse model it is not entirely clear, whether ostoclasts are fully functional. While tartrate-resistant acid phosphatase (TRAP) staining suggests the presence of at least osteoclast progenitors and that the cells are partially functional, a proof of complete osteoclast functionality requires further investigation eg. Cathepsin K expression (Rodan, et al., 2001; Vanaanen, et al., 2000).

During osteoblast development, MSCs differentiate into pre-osteoblasts, that are characterized by high Runt-related transcription factor 2 (RunX2) and osterix (Osx) expression (Wu, et al., 2011; Zhou, et al., 2010; Karsenty, et al., 2007; Zelzer, et al., 2003). Upon external signalling, 50 – 70% of osteoblasts undergo apoptosis while the rest start to differentiate into osteocytes that are finally embedded into the bone matrix (Manolagas, et al., 2000; Parfitt, et al., 1990). It has been suggested that osteocytes form some sort of mechano-sensor, that controls the activity of osteoblasts and osteoclasts (Bonewald, et al., 2011; Winkler, et al., 2003). Previous work demonstrated that the transcription factor N-Myc, which is closely related to c-Myc, controls mesenchymal stem cell differentiation and proliferation in embryonic bone (Charron, et al., 1992), while c-Myc is involved in osteoblast and chondrocyte differentiation (Piek, et al., 2009; Karsenty, et al., 2007). In addition Zhou and colleagues have shown that while early osteoprogenitor populations possess high c-Myc expression levels, terminally differentiated osteocytes only express low c-Myc levels (Zhou, et al., 2011).

In the ColtTA,TreMyc mouse model this suggests that ectopic expression of c-Myc in mature osteoblasts inhibits their terminal differentiation into osteocytes. There are several lines of evidence that support this hypothesis. Masson-Goldner staining of the mutant bones revealed that the bone mainly consists of collagen. Collagen synthesis is performed by osteoblasts and indicates unmineralized bone matrix. In addition mRNA expression analysis revealed that collagen I expression was upregulated by mutant osteoblasts. Osteocytes however are embedded into mineralized bone matrix. This is achieved by calcium deposition and correlates to the progress of mineralization, therefore suggesting less osteocyte presence and pronounced proliferation of mature osteoblasts. Notably, the mutant bones showed a higher porosity than control bones, as detected by H&E staining. This is in agreement with the decreased number of osteocytes that fill up the lacunae and generate compact bone and less mineralization of the bones (Koshla, et al., 2012; Clarke, et al., 2008)

While these findings suggest that osteocyte numbers are reduced in ColtTA,TreMyc mice, the question regarding cause-and-effect remains unanswered. Does c-Myc directly block the development of osteoblasts to osteocytes by blocking important signaling pathways eg.

calcification (Zhou, et al., 2011) or sclerostin production by osteocytes (Wijenayaka, et al., 2011)? An alternative explanation for a reduction of osteocytes could be, that the mineralization of the osteoid in mutant bones is defective as osteocyte development is coupled to the mineralization of the bone. This line of reasoning is supported by the finding that vitamin D receptor is apparently upregulated in mutant osteoblasts as evidenced by qRT-PCR. This suggests elevated vitamin D signaling and is in agreement with the finding of increased PTH levels in mutant animals. It is known that PTH induces osteolysis through increased osteoclast activity and subsequently leads to calcium deposition from the bone to the blood stream. This would in turn result in a loss of minerals in the bone and thereby loss of bone mineralization. Reduced bone mineralization would in turn mean a reduced signaling to osteoblasts to differentiate into osteocytes.

In conclusion the present results suggest that c-Myc overexpression in mature osteoblasts induces a strong bone phenotype characterized by increased osteoblast levels. It is therefore tempting to speculate that terminal differentiation of osteoblasts into osteocytes is blocked. Whether this occurs directly through the known effects of c-Myc on differentiation or indirectly due to incomplete mineralization of the osteoid remains to be determined (Figure 67).

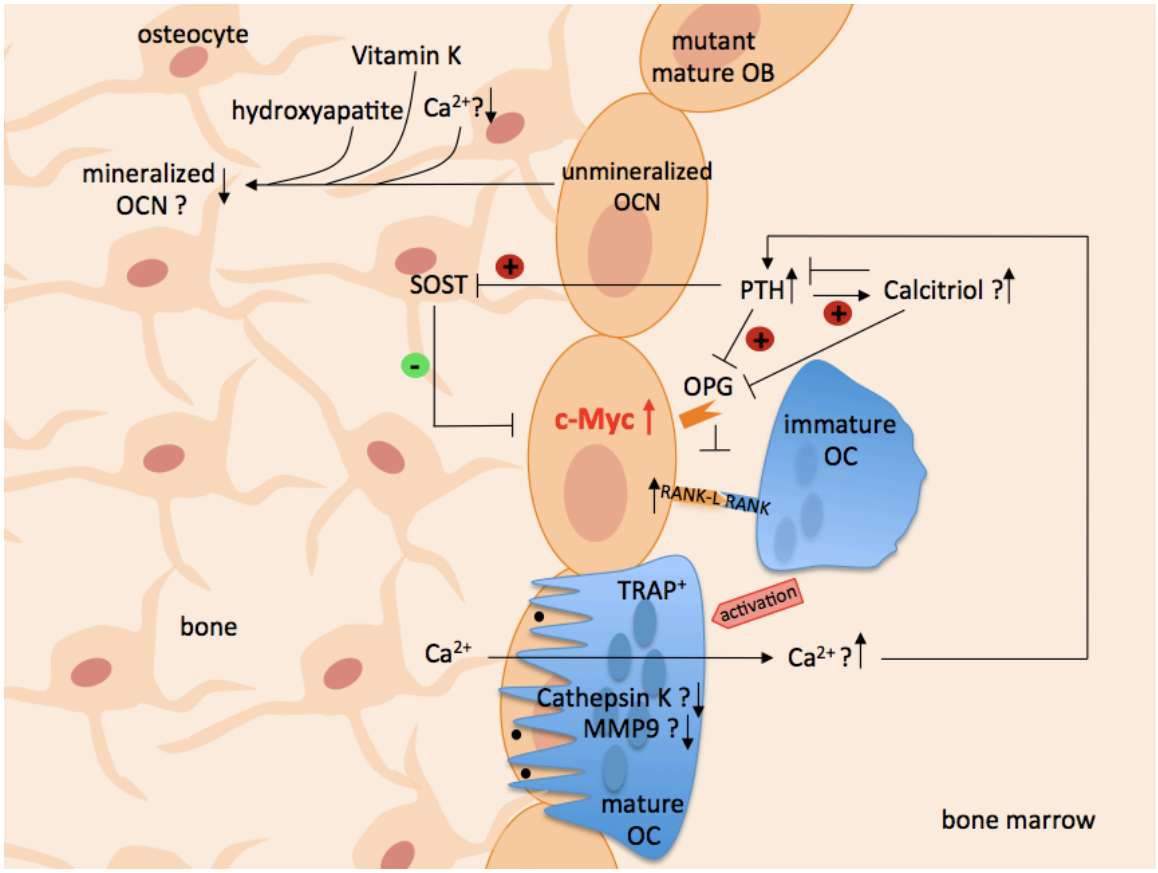

Figure 67: Mutant mature osteoblasts negatively influence osteocytes and bone mineralization
Human c-Myc overexpression in mature osteoblasts (mutant, OB) induces an upregulation of parathormone (PTH) that blocks sclerostin (SOST) synthesis in osteocytes. Upregulated PTH induces calcium release (Ca^{2+}) from the bone to the plasma and simultaneously blocks osteoprotegerin (OPG) expression from mature osteoblasts thereby not negatively influencing RANK-L / RANK induced osteoclastogenesis. Bone matrix formation relies on mineralization of pre-osteocalcin (unmineralized OCN) produced by mature osteoblasts that binds to hydroxyapatite with the help of the co-factor vitamin K and free calcium ions. High bone-turnover in mt osteoblasts might indicate impaired function of mature osteoclasts (OC) and decreased bone degradation rate by insufficient cathepsin K or matrix metallopeptidase 9 (MMP9) expression.

6.1.2 Human c-Myc overexpressing osteoblasts lead to osteosarcoma formation

The second interesting observation in the *ColtTA;TreMyc* mouse model was, that about 26% of the double transgenic mice spontaneously developed tumors. Based on the presence of osteoid within these tumours, they were classified as osteosarcomas.

Generally, human osteosarcoma development can be grouped into two main categories, pediatric osteosarcomas and adult osteosarcomas (Janeway, et al., 2012; Molyneux, et al., 2010; Benjamin, et al., 2009; Helman, et al., 2003). Pediatric osteosarcomas are the most frequent tumors in children and adolescents (with an average age of 15 – 20) and they primarily develop in the regions of fast growing bone e.g. femur, tibia and humerus. In contrast adult osteosarcomas mainly develop as secondary disease in elderly patients, as a consequence of primary bone disorders e.g Paget´s disease, osteoporosis or osteoarthritis (Geller, et al. 2010; Whyte, et al., 2006). Importantly, c-Myc is amplified and overexpressed in 8-16% of pediatric and adult osteosarcomas (Bayani, et al., 2003; Tarkkanen, et al., 1999; Ladanyi, et al., 1993).

Similar to human osteosarcoma in the *ColtTA;TreMyc* mice, tumor formation occurred mostly in femurs, tibia, mandibular and the clavicular. While this closely resembles the pediatric form of osteosarcoma, these tumors developed in about 30-60 week old mice. Moreover in most mice, even those without tumor development, a distinct bone phenotype, characterized by paralyzed hind legs, was observed. This in turn resembles more the adult osteosarcoma phenotype.

Histological and FACS analysis of the osteosarcoma demonstrated that osteoblasts and osteoclasts were present in tumors. Quantification of these cells showed that their levels were elevated compared to normal bone and that the majority of cells within osteosarcoma were osteoblasts. Again this finding correlates well with observations in human tumors, which mainly contain osteoblasts that produce malignant osteoid. Interestingly, in tumor-bearing mice, the development of metastasis in lung and liver was observed. Again this

reflects closely the disease progression in patients, where metastases mainly spread to the lungs (Namlos, et al., 2012; Osaki, et al., 2011; Luu, et al., 2005).

In order to determine how the tumor osteoblasts differ from non-tumor osteoblasts from ColtTA,TreMyc mice, in the next step the expression level of genes involved in osteoblast development was assayed by qRT-PCR analysis.

Gene	Expression level in osteosarcoma osteoblasts	Expression level in *ColtTA;TreMyc* osteoblasts
RunX2	↑	–
Osx	↑	–
ALP	↑	–
Collagen	↓	↑
OCN	↓	–
Osteoglycin	↓	–
Periostin	↓	–
Genes involved in Wnt signaling		
Wnt3a	↑	–
ß-Catenin	↑	–
DKK-1	↑	–
Cyclin D1	↑	–
RunX2	↑	–
E-cadherin	↓	n.d.
Sox2	↓	n.d.
Sox9	↓	n.d.

Table 3: Overview of differentially expressed genes in human c-Myc overexpressing osteoblasts and osteosarcoma osteoblasts
Comparison of differentially expressed genes of osteoblast maturation and Wnt signaling in osteosarcoma osteoblasts and human c-Myc overexpressing osteoblasts. Upregulated genes are indicated with red arrows and down-regulated with blue arrows (n.d. = not determined).

Several aspects of these results are of particular interest:

- Markers for early, immature osteoblasts were significantly increased. Most importantly RunX2 expression was 20-fold elevated in tumor osteoblasts in comparison to controls. RunX2 is a master regulator of osteoblastogenesis and expressed early in pre-osteoblasts, thereby leading mesenchymal stem cell (MSC) differentiation towards osteoblast lineage maturation (Karsenty, 2000). The role of RunX2 in bone development has been demonstrated by the work of Komori, et al., 1997 and Otto, et al., 1997 who showed that RunX2-/- mice completely lack ossification. RunX2 is a transcription factor that possesses a Runt DNA binding domain and interacts with hypophosphorylated pRb to control osteoblast cell proliferation together with cyclin D1 (Martin, et al., 2011). It belongs to the Runt family of proteins, which have been shown to play a role in tumorigenicity of many human cancers, e.g. in leukemia onset, by loss of function mutations in the RunX1 gene (Perry, et al., 2002).

- Markers for mature osteoblasts were strongly down-regulated. Osteocalcin (OCN) expression in the tumor osteoblasts was reduced by about 50-fold. OCN expression is one of the hallmarks of mature osteoblasts and necessary for the generation of a functional bone matrix. It is a non-collagenous protein that interacts with hydroxyapatite to generate a functional bone matrix, and in addition a very good indicator for bone formation. Previous studies had shown that mice deficient for OCN show elevated bone formation capacity without an impairment of bone resorption (Ducy, et al., 1996).

Taken together these data suggest, that the tumour osteoblasts from *ColtTA;TreMyc* mice are trapped in an immature pre-osteoblastic stage of maturation. This nicely correlates with human osteosarcoma, where also osteosarcoma cells are unable to fully differentiate into terminally differentiated human osteoblasts (Shimizu, et al., 2011; Yoshikawa, et al., 1997).

As demonstrated initially, c-Myc expression is induced through mitogenic signals of the Wnt signalling pathway. Notably, the Wnt pathway is frequently affected in human cancers and has already been demonstrated as a ready target for cancer treatment in osteosarcoma (Vijayakumar, et al. 2011; Iwao, et al., 1999), hepato-cellular carcinoma (La Coste, et al., 1998), melanoma (Rubinfeld, et al., 1997) and prostate cancer (Voeller, et al., 1998). However, the effects of Wnt-signalling on Myc is no one-way street and recently an effect of overexpressed c-Myc on the Wnt pathway has been described in breast cancer cells. Gene expression studies revealed, that Dickkopf-1 (DKK-1) and secreted frizzled-related protein 1 (SFRP1), two of the most potent repressors of Wnt signalling, were repressed in c-Myc overexpressing cells (Cowling 2007). In addition Wnt is known to play a major role in bone development. It directly forces mesenchymal stem cells (MSCs) to differentiate towards the osteoblast lineage and furthermore prevents osteoclastogenesis by inducing an upregulation of OPG, a negative regulator of osteoclastogenesis, during mature osteoblast differentiation.

Analysis of the Wnt-signaling pathway revealed some interesting results. First of all, Wnt3a and ß-catenin were upregulated in tumour osteoblasts. This suggests increased Wnt-signalling in these cells. Nicely in line with these observations is the upregulation of early osteoblast marker RunX2, as RunX2 is known to be a Wnt target gene (Luu, et al., 2004; Nelson, et al., 2004; Barker and Clevers, 2000). Surprisingly the Wnt antagonist DKK-1 was strongly upregulated as well. DKK-1 interacts with the transmembrane protein LRP5/6 on the cell membrane and competes for LRP5/6 with the Wnt-receptor (Hoeppner 2009). In earlier studies upregulation of DKK-1 had been associated with the induction of bone resorption and osteolysis (Yao, et al., 2011; Guo, et al., 2010; Qiang, et al., 2008; Fujita, et al. 2007; Rodda and McMahon, 2006). Interestingly DKK-1 expression has frequently been reported in multiple myeloma or hormone-resistant breast tumors (Forget 2007), while as mentioned above in some cases c-Myc overexpression led to repression of DKK-1. It is known that Wnt-signaling is repressed by DKK-1 in bone maturation during the differentiation from immature osteoblasts to mature osteoblasts. This suggests that DKK-1 seems to be physiologically upregulated as Wnt-signaling is elevated in osteosarcoma osteoblasts that resemble an immature osteoblast phenotype. Currently, it is this unclear

how DKK-1 works in the context of tumor development and how in *ColtTA;TreMyc* osteosarcomas the DKK-1 overexpression can be explained.

In addition Cyclin D1 was strongly overexpressed in tumor osteoblasts. Cyclin D1 is a known Wnt target gene and is involved in cell cycle control, especially in G1/S transition ((Alberts 2002). Elevated Cyclin D1 level are known to contribute to cancer progression, metastasis development and invasion by driving cell cycle progession (Besson, et al., 2004). This demonstrates an influence of the Wnt signaling on cell-cycle control. Therefore expression levels of other cell cycle control genes were analyzed in the osteosarcoma osteoblasts. Interestingly, I observed an increase in $p16^{INK4a}$ and $p21^{Cip1}$ expression and a simultaneous decrease of cell cycle inhibitor $p18^{INK4c}$. $p21^{Cip1}$ is a protein belonging to the CIP/KIP family of cyclin-dependent kinases inhibitors (CKI) that directly binds to the Cyclin E-CDK2 complex. In contrast $p16^{INK4a}$ belongs to the INK4 (Inhibitors of CDK4) family. $p16^{INK4a}$ prevents cell cycle progression and entry of cells into G_1/S transition by directly blocking the Cyclin D-CDK4/6 complex during the G_1 phase of the cell cycle. Most importantly, $p18^{INK4c}$ expression was down-regulated in tumor osteoblasts. This indicates elevated cell cycle entry of osteosarcoma osteoblasts from G_0 to G_1. In addition, Latres, et al., 2000 found that loss of $p18^{INK4c}$ seems to be associated with neoplasia. Taken together these data suggest that in the mouse osteosarcoma osteoblasts cell cycle entry and progression is enhanced by upregulation of Cyclin D1 and down-regulation of $p18^{INK4c}$. For $p21^{Cip1}$ a role in protection against apoptosis has been discussed (Bulavin et al. 1999). This might explain why this cell-division blocking CKI is overexpressed in osteosarcoma cells.

Interestingly, osteosarcoma development is frequently associated with a loss of tumor suppressors as p53, mdm2 or pRb (Tang, et al., 2008). Especially loss of p53 protein expression in the bone seems to be important for osteosarcomagenesis, independently of concomitant pRb loss (Berman, et al., 2008; Walkley, et al., 2008; Overholtzer, et al., 2003; Guo, et al., 1996). Analysis of the expression level of p53, mdm2 and pRb in tumor osteoblasts revealed that in all cases, expression levels were unchanged in comparison with control osteoblasts. Interestingly however, when protein expression of p53 was analyzed directly through Western blot, no p53 protein could be seen. This suggests that either synthesized p53 is rapidly degraded, or that p53 mRNA is not translated into protein.

Recent reports have suggested p53 mRNA translation is regulated by alternative transcripts (Candeias et al., 2006), which might explain the present result. Interestingly the loss of functional p53 nicely reflects findings in human osteosarcomas where p53 is lost in about 50% of cases (Miller, et al., 1990; Mulligan, et al. 1990).

Tumorigenesis in general is a multi-step process wherein several genes or signaling pathways need to be de-regulated (Knudson, et al., 2001). Uncontrolled cell proliferation occurs when initially quiescent or slowly growing cells enter the cell cycle and when, additionally in a secondary event, tumor suppressor genes are lost or mutated. In the context of *ColtTA;TreMyc* mice, the enforced c-Myc expression already represents the first step in this progression towards tumor development, as the c-Myc overexpressing osteoblasts are actively pushed into cell division. This increased cell cycle activity in turn, renders the cells more prone to mutations, amplifications or deregulations in general. Not surprisingly, human osteosarcoma occurs often in children and adolescent where during growth, bone cells are undergoing cell division with a very high frequency. The *ColtTA;TreMyc* mouse model therefore nicely correlates with human osteosarcoma patient situation. Mouse osteosarcoma development occurs at the same sites of active bone growth as in humans e.g. femur, tibia, hips, knee, humerus, mandibular and clavicular. In addition mice develop these tumors spontaneously during life, which highly resembles human osteosarcoma disease. Furthermore the mouse model shows in addition, that about 80% of these tumor-bearing animals develop further metastasis to lungs and liver similar to the findings in humans.

Although osteosarcoma is one of the most common cancers in children there are only few animal models available that mimic human osteosarcoma. Walkley, et al., 2008 generated conditional Osx-Cre^{+} p53$^{fl/fl}$ and Osx-Cre^{+}pRb$^{fl/fl}$ mutant mice, to specifically delete p53 and pRb respectively in osteoprogenitors, and induced osteosarcomagenesis within about 120 to 370 days. Overexpression of the c-fos oncogene in mice also resulted in osteosarcoma induction within about four weeks post induction (Wang, et al., 1995). In contrast, Khanna, et al. 2001, used osteosarcoma cell lines to induce tumor development in xeno-transplantations. In addition, Llombart-Bosch, et al., 1988 showed successful engraftment of primary human osteosarcoma into Nude mice. Finally, as early as 1964,

Kelloff, et al., 1994 isolated virus from an osteosarcoma-bearing mouse and successfully induced new osteosarcoma engraftment by viral infection of mice. All these models therefore either eliminate cell cycle control genes, or induce tumour growth directly by the injection of tumor cells or the expression of oncogenes. Thus currently there is no model that closely mimics the multistep process observed in human osteosarcoma patients. The *ColtTA;TreMyc* model is therefore very interesting as it for the first time mimics some of the key features of human osteosarcomas:

- In 8-16% proportion of human patients c-Myc is overexpressed
- Tumour and metastasis formation occur in similar places as in patients.
- Only a small percentage of mice develop tumors, probably due to the need of a second independent mutation in regulatory pathways.

Osteosarcoma in general is one of the cancers that are hard to detect. The disease in patients is most frequently detected by patients themselves, when they spontaneously develop strong bone pain, swelling and fractures of bones. Some genetic factors lead to increased risk to develop osteosarcomas e.g. changes in retinoblastoma gene, Paget´s disease, Li-Fraumeni syndrome, Rothmund-Thomson syndrome and others. Therapy is mainly based on surgery, chemotherapy, radiation therapy or all in combination. Many conventional chemotherapeutics are based on an inhibition of DNA replication and patients are treated with methotrexate, doxorubicin, cisplatin, etoposide, ifosfamide, cyclophosphamide, epirubicin, gemcitabine and topotecan or combinations of different agents (Jaffe, 2009; Ferguson, et al., 2001). However, predictive markers are still elusive in osteosarcomas. In our mouse model system, osteosarcoma osteoblasts did show a very high expression of tyrosine-kinase receptor c-Kit, which interestingly is upregulated in a variety of human sarcomas. These include especially gastro-intestinal stromal tumors (GIST), soft tissue sarcomas and Ewing´s sarcoma (Scotlandi, et al., 2003; Hornick, et al., 2002; Tuveson, et al., 2001). Furthermore, Wei, et al., 2008 observed a correlation between c-Kit expression in osteosarcoma patients and their survival. Nilotinib is one of the TKIs that specifically target c-Kit, and I therefore first screened the inhibitory effect of Nilotinib treatment on our mouse osteosarcoma cell lines and primary mouse osteosarcoma samples *in vitro*. The study revealed that Nilotinib treatment successfully

inhibits primary osteosarcoma cell growth, while cell lines were more resistant to Nilotinib treatment. This could be due to the fact that cell lines do only weakly express c-Kit while it is highly upregulated in primary tumors *in vivo*. Therefore it is highly interesting to test, whether *in vivo* TKI treatment of osteosarcoma mice inhibits tumor growth and thereby shows a link between c-Kit expression and proliferation. McGary, et al., 2002 shows the inhibitory effects of STI571 (Gleevec, Novartis) treatment, which inhibits mainly Bcr-Abl and c-Kit, on osteosarcoma cell line xeno-graft mouse model. However, in this study no complete growth inhibition occurred during a 6-week treatment period. While it was already shown that c-Kit is not a prognostic marker in osteosarcoma (Sulzbacher, et al., 2007), it is still important to test whether c-Kit positive tumors can be treated by combinational TKI treatment.

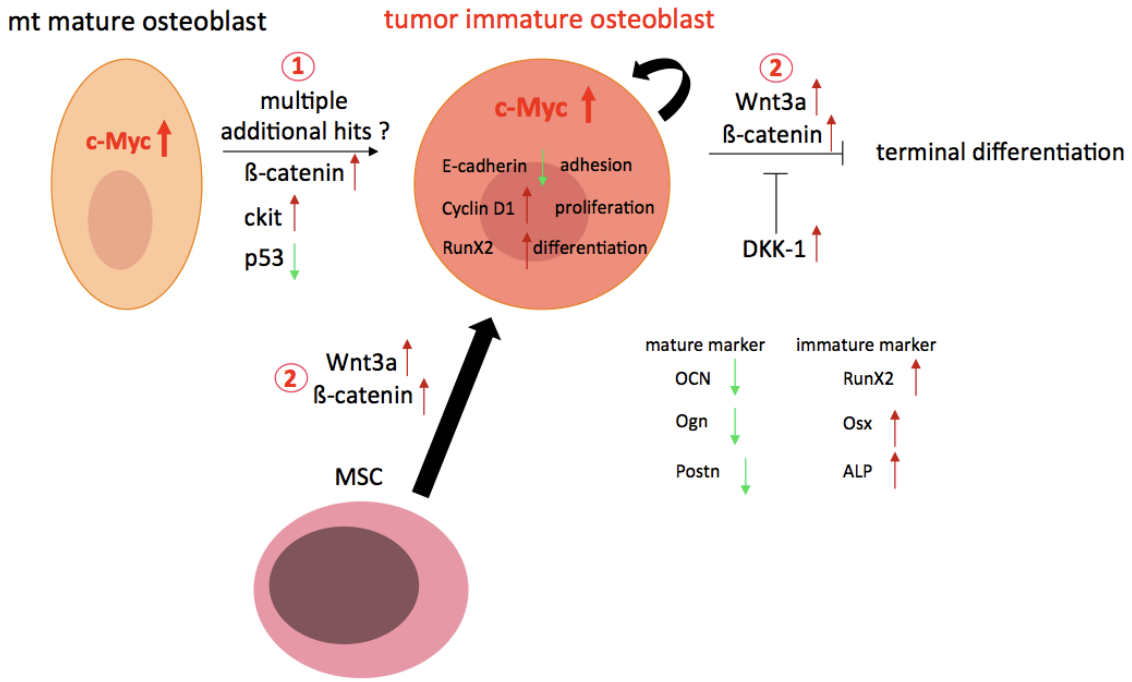

Figure 68: Immature osteosarcoma osteoblasts show elevated Wnt signaling in *ColtTA;TreMyc* animals
Hypothetic tumorigenesis of human c-Myc overexpressing osteoblasts (mt mature osteoblasts) into osteosarcoma osteoblasts (tumor immature osteoblast) with an immature expression signature in *ColtTA;TreMyc* animals. (1) In addition to human c-Myc overexpression multiple secondary hits e.g. ß-Catenin and c-Kit upregulation and p53 loss seem to drive osteosarcomagenesis. Osteosarcoma osteoblasts express markers of immature osteoblasts (upregulation of RunX2, Osx, ALP and down-regulation of osteocalcin (OCN), osteoglycin (Ogn) and periostin (Postn)). Therefore c-Myc represses terminal differentiation of osteosarcoma osteoblasts. (2) Deregulated Wnt signaling prevents terminal differentiation in osteosarcoma osteoblasts (up: Wnt, ß-Catenin, DKK-1). Human c-Myc overexpression in tumor osteoblasts leads to an upregulation of Wnt3a and ß-Catenin expression. Mesenchymal stem cells (MSC) differentiate faster into osteoblasts. Transcription of Wnt target genes effect tumor osteoblast behavior: less cell adhesion by E-cadherin down-regulation, enhanced cell proliferation by upregulation of cell cycle gene Cyclin D1 and loss of terminal differentiation by upregulation of RunX1, a master regulator for differentiation of early osteoblasts.

6.1.3 Influence of overexpression of human c-Myc in osteoblasts on the HSC niche

In numerous publications it has been shown that osteoblasts play a major role as a crucial part of the hematopoietic stem cell niche in the bone (Celso, et al., 2011; Lévesque, et al., 2010; Wilson, et al., 2008; Zhu, et al., 2007; Nagasawa, et al., 2006; Zhang, et al., 2003; Calvi, et al., 2003). Besides osteoblasts, nestin-positive MSCs, CAR cells (CXCL-12-abundant reticular), macrophages and nonmyelinated Schwann cells were identified to be part of the HSC niche (Ehninger and Trumpp, 2011; Yamazaki, et al., 2011; Méndez-Ferrer, et al., 2010; Arai, et al., 2005; Suda, et al., 2005; Zhang, et al., 2003; Calvi, et al., 2003). In several mouse models, manipulation of niche cells led to an impairment in the HSC compartment (Mercier, et al., 2012). Most interestingly, Fleming, et al. identified a loss of HSC quiescence by niche-associated overexpression of DKK-1 in osteoblasts (Fleming, et al., 2008). In addition, N-cadherin (Cdh2) deletion in murine osteoblasts did not lead to any alterations and effects in the hematopoietic stem cell compartment, putting in question, whether N-cadherin expression in osteoblasts play any role on the HSC niche (Bromberg, et al., 2012).

I therefore took a closer look at the HSC niche in *ColtTA;TreMyc* mice. Interestingly I found that the most important HSC population, the dormant HSCs had been lost in *ColtTA;TreMyc* animals. Dormant HSCs had only been discovered relatively recent, as a rarely dividing cell population that represents an HSC reservoir that is activated in cases of injury or infection (Takizawa, et al., 2011; Essers, et al., 2009; Foudi, et al., 2008; Wilson, et al., 2008). Dormant HSCs divide only about 5 times during the life time of a mouse, and can be detected as they retain their label in the BrdU-LRC assay. Long-term analysis of the *ColtTA;TreMyc* mice revealed that by day 70 already, mutant animals have a reduced amount of LRCs. Analysis at day 105 to 125 showed a similar trend. In fact at these time points the number of dormant HSCs was even further reduced.

To better understand this observation, the data was subjected to mathematic modeling based on a 2-population model. Mathematical modeling of HSC doubling times in mutant animals indicate that the dormant and activated HSC compartment have identical doubling times. This strongly suggests that mutant animals do not possess dormant HSCs. In addition FACS analysis of the stem and progenitor compartment furthermore revealed a significant decrease in the amount of LT-HSCs, ST-HSCs and multipotent progenitors (MPPs). The loss of dormant HSCs in mutant animals can be explained in two different ways. One is, that due to the severe bone malformations the *ColtTA;TreMyc* mice do not provide a stable niche environment for dormant HSCs. The alternative explanation suggests that the dormant HSCs are lost over time due to a loss of cell division. Previous experiments by Jaworski, had shown, that human c-Myc overexpression in mature osteoblasts during embryonic development leads to a loss of HSCs in the bone marrow and instead leads to extra-medullary hematopoiesis in the spleen (Jaworski and Trumpp, thesis 2009). A similar mechanism might occur when c-Myc overexpression is induced in adolescent or adult mice. Interestingly though, I could never observe increased HSC levels in the spleen of adult *ColtTA;TreMyc* mice. However, to better understand whether the absence of dormant HSCs was also reflected in the more active LT and ST-HSCs, bone-marrow chimeras were generated. In these experiments bone marrow from either mutant *ColtTA;TreMyc* or control ColtTA animals was transplanted into NSGs and engraftment of the HSCs as well as their differentiation capacities were evaluated. Here I found that in transplantations with mutant bone marrow lower percentages of LT- and ST-HSC engrafted in comparison to control bone marrow. This effect was even more striking in secondary transplantation assays, where hardly any LT- and ST-HSCs were left in mutant chimeras. In contrast the differentiation capacities of the HSCs were apparently unaffected as no difference in lineage-committed progenitors and differentiated cell populations could be observed between control and mutant animals.

Taken together this data suggests that as a consequence of the loss of dormant HSCs the remaining LT-HSC and ST-HSC pool is exhausted over time due to regular cell division, as the HSC pool is not replenished by dormant HSCs. This hypothesis is further strengthened by the fact that no differences in differentiated cells were observed between mutant and control chimeras. Thus it is not due to impaired differentiation capacities that HSC numbers are decreased in the mutant mice.

Finally what these experiments suggest is, that overexpression of human c-Myc exclusively in mature osteoblasts, has major effects on the dHSC population in mutant animals. This suggests that the mature osteoblasts do have a major impact on controlling the hematopoietic stem cell pool and its maintenance under homeostasis.

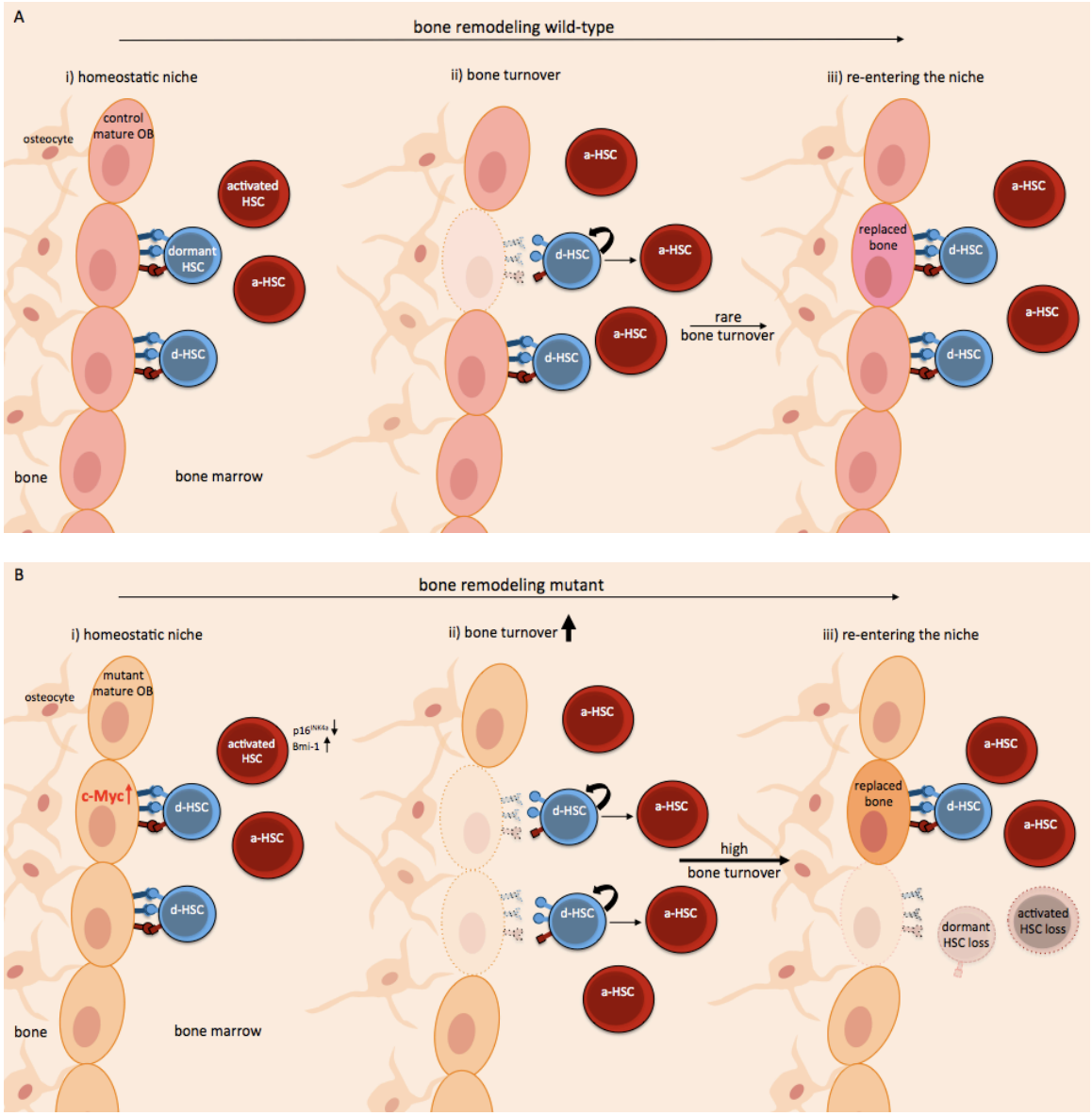

Figure 69: Mutant osteoblasts lead to a loss of dHSCs and reduced numbers of hematopoietic stem and progenitors
(A) In ColtTA control animals the bone marrow comprises normal hematopoietic stem and progenitor cells (activated HSCS (aHSCs)) and dormant HSCs (dHSCs). (i) Under homeostatic conditions the dHSC is quiescent and located in its endosteal niche (control mature osteoblasts). (ii) During bone turn-over control osteoblasts are replaced by newly synthesized bone and dHSCs leave their niche and become activated. (iii) Re-entering of dHSCs into their niche by relocation to replaced bone. (B) In ColTA;TreMyc mutant animals, already (i) under homeostatic conditions the activated HSCs show elevated expression of Bmi1 and decreased expression of $p16^{INK4a}$ cell cycle inhibitor. (ii) Mutant osteoblasts have a high bone-turnover and dHSCs are more frequently pushed out of their niche. (iii) dHSCs show decreased re-entering into their niche as a consequence of high mutant osteoblasts replacement. Therefore dHSCs and stem- and progenitors are decreased over time.

Previously, our group had described that the dormant hematopoietic stem cells can be activated by mimicking applied stress conditions through the injection of interferon alpha (IFNα) (Essers, et al., 2009). Interferon alpha is normally secreted as a result of bacterial or viral infection. Essers et al. showed that by injection of the ds-RNA polyinosine-polycytidylic acid (poly(I:C) or by injection of bacterial LPS, secretion of INFα and activation of dormant HSCs could also be achieved. Interestingly, in *ColtTA;TreMyc* mice neither pIC treatment nor LPS injection led to HSC activation while in both experiments control HSCs were normally activated. In contrast direct injection of IFNα induced dormant HSC activation even in *ColtTA;TreMyc* mice. This indicates that in mutant mice the IFNα receptor is present and functional and that signaling pathways downstream of IFNα are not affected. Comparing the signaling pathways upstream IFNα that lead to the cytokine´s secretion, it is interesting to note that the responses to pIC and LPS are very similar. The dsRNA pIC interacts with the toll-like receptor 3 (TLR3), which in turn activates Trif (TIR-domain-containing adapter-inducing interferon-β). In contrast LPS binds to TLR4 and transmits the activation signal through Trif and TIRAP (TIR-domain containing adaptor protein). Both pathways end then in the same signaling cascade that involves NFkB and AP-1 signaling to produce type I IFNs and inflammatory cytokines.

Interferons are secreted by a large number of cells such as leucocytes, moncytes and fibroblasts. In monocytes and macrophages IFNα activation occurs mainly through TLR4-mediated signaling. Thus the lack of HSC activation in mutant mice could be due to reduced macrophage functionality or due to reduced intrinsic IFN production in these cells. Chang, et al. previously demonstrated that macrophages have a major impact on the HSC niche. In addition the group showed that macrophage ablation in Macrophage Fas-Induced Apoptosis (MAFIA) transgenic mice led to osteoblast reduction and HSC mobilization (Chang, et al., 2008). Furthermore Winkler, et al., observed a strong correlation between macrophage deletion, and as a consequence decreases in osteoblast numbers with a simultaneous HSC loss in the bone marrow (Winkler, et al., 2010). These data suggest a strong interplay between HSCs, osteoblasts and macrophages/monocytes in the HSC niche. It is therefore tempting to speculate that the interaction of the c-Myc overexpressing osteoblast with the niche macrophage somehow stops TL3/4 mediated IFNα signaling and thereby prevents HSC activation in *ColtTA;TreMyc* mice.

An alternative explanation could be based on the influence that osteoblasts exert on the development of macrophages and osteoclasts from HSCs. The myeloid progenitor develops either into macrophages or into osteoclasts. Osteoclastogenesis is regulated by secretion of RANK-L from the neighboring stroma or osteoblasts. The c-Myc overexpressing osteoblasts in *ColtTA;TreMyc* mice could, in a yet undetermined manner, influence either macrophage or osteoclast development and lead to cells with impaired functionality. A role of osteoclasts on HSC activation has been demonstrated as osteoclast-secreted Cathepsin K cleaves the cytokine CXCL12 (SDF-1), one of the key factors responsible for HSC maintenance in the bone marrow. Thus osteoblast-mediated defects either in the TL3/4 signalling pathways of macrophages or osteoclasts might therefore explain the loss reactivity towards pIC and LPS stress signals in *ColtTA;TreMyc* mice.

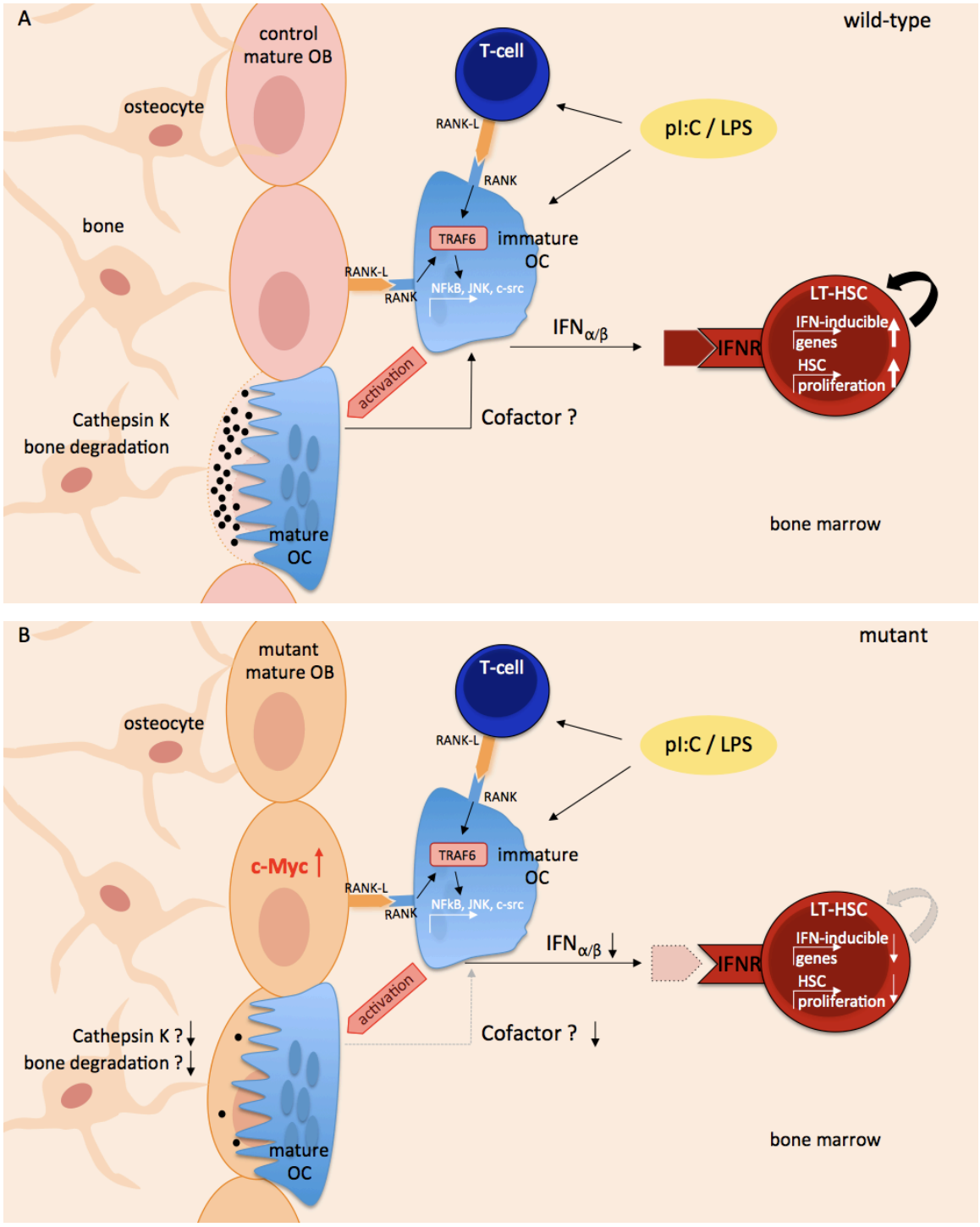

Figure 70: Mutant osteoblasts prevent LT-HSC activation by poly(I:C) and LPS respectively
(A) In wild-type animals PolyI:C (pI:C) or lipopolysaccharide (LPS) treatment induces T-cell activation that activates TRAF6 signaling in immature osteoclasts through RANK-L / RANK interaction. Subsequently interferon production (IFNα/ß) is induced and leads to IFN-signalling in long-term hematopoietic stem cell (LT-HSCs) upon IFN-receptor (IFNR) binding. LT-HSCs become activated and start to proliferate. (B) In mutant animals impaired mature osteoclast functionality prevents IFN-synthesis in immature osteoclasts, thereby preventing pI:C / LPS-induced LT-HSC activation and cell proliferation.

6.1.4 Outlook

In the course of this work I have closely characterized the effects of c-Myc overexpression in mature osteoblasts and demonstrated that the *ColtTA;TreMyc* mouse model is a useful model system for future work.

In one aspect the mutant mice can be used to further analyse the effects of an imbalance in the osteoblast / osteoclast ratio. The osteopetrosis-like phenotype that is characterized by unmineralized bone matrix and its connection to osteoblast and osteoclast development will help to better understand human bone aberrations in the future. Furthermore the mouse model serves as an ideal model system to further study human osteosarcoma. Up until now, all mouse models for osteosarcoma rely on the induction of bone tumor development through highly artifical means. The *ColtTA;TreMyc* mouse model is the first mouse wherein tumor forms spontaneously. Most likely tumor development in these mice is dependent on multiple additional mutations in an important signalling pathway, similar to the events in patients. The tumor and metastasis in the mutant mice closely resemble human osteosarcoma. Thus the *ColtTA;TreMyc* mice are ideally suited to further analyse tumor onset, development and also to study further therapeutic options for the treatment of this disease.

A further interesting aspect of the *ColtTA;TreMyc* mouse model is, that it offers the possibility to better study and understand the effects that the osteoblast has on the hematopoietic stem cell niche. As I could show in this work the osteoblasts do not only exert an influence directly on the HSCs but also on other cells within the niche, such as osteoclasts. In future work these interactions can be analyzed in more detail, as only a few, very defined changes in the gene expression pattern were observed in comparison to control mice. Taken together the *ColtTA;TreMyc* mouse model offers a lot of possibilities for future work to study the role of osteoblasts in bone and tumor development and its function in the hematopoietic system.

7 Material & Methods

7.1 Animals

Animals were maintained in accordance with the German Law for the Protection of Animals and the National Institute of Health (Guidelines for Care and Use of Laboratory Animals with the licence numbers G159/08 and G-99/12). All animals were kept under specific pathogen-free (SPF) conditions and housed in individually ventilated cages (IVC) at the animal facility at German Cancer Research Center. Animals used in all the experiments were between 20 and 30 weeks of age. Different conditions from this are noted in the text.

ColtTA;TreMyc mouse lines were generated previously (Jaworski and Trumpp, thesis 2009) and animals used in the experiments were generated by crossing ColtTA control animals with TreMyc mice. Animal matings were continuously kept under doxycycline treatment (2mg/mL) in the drinking water. Prolonged doxycycline treatment on newborns was continued until mice were 3-weeks of age (weaning age). *ColtTA;TreMyc* animals are on a mixed background C57BL/6 - S129.

NOD scid gamma (NSG; NOD.Cg-Prkdcscid Il2rgtm1Wjl/Sz) were purchased from The Jackson Laboratory.

7.2 BrdU treatment

BrdU was purchased from Sigma and dissolved in water with a concentration of 1g/ L and a final concentration of 5% glucose. Solution was substituted to mice drinking water for 10 days and changed ones a week. For BrdU proliferation assay and as a positive control for

BrdU-LRC analysis mice were intra-peritoneally injected with a 1.8mg / ml BrdU solution in PBS and cells isolated and analyzed 16 hrs after BrdU treatment.

7.3 Genotyping of mice

Animals were tagged with numbered ear marks and DNA from tail biopsies was extracted in Direct Lysis buffer and the addition of proteinase K (PeqLab). Primers were designed with Roche Assay Designing software and used with 10 µM. Genotyping PCR was conducted in 10x Invitrogen Buffer with either final concentrations of 10% DMSO ($^{++}$) or 10% Triton-X100 ($^{+}$) and 10mM dNTPs and 1 µL lysed DNA. Annaeling temperature of 60°C was used and DNA amplified with 35 cycles.

Primer	Sequence
3′-ColtTA^{++}	5′-CTC TGC ACC TTG GTG ATC-3′
5′-ColtTA^{++}	5′-GCT GCT TAA TGA GGT CGG-3′
3′-TreMyc^{+}	5′-TTT GAT GAA GGT CTC GTC GTC C-3′
5′-TreMyc^{+}	5′-TAG TGA ACC GTC AGA TCG CCT G-3′

Table 4: List of genotyping primer

7.4 Osteoblast isolation

Osteoblasts were isolated from 20 – 30 week old animals by dissecting femurs, tibia and the spinal cord. Briefly, bones were crushed and the bone marrow discarded. Subsequently, bone chips were digested with a 20 min. three-step digestion protocol by using trypsin (Invitrogen), collagenase P (Roche) and dispase (Roche) in aMEM (Invitrogen) supplemented with 10% fetal bovine serum (tet-System approved FBS, Clontech) in digest 2 and 3 and 25mM Hepes and 1M calcium-chloride. Osteoblast enrichment was conducted by gradient centrifugation in Histopaque-1083 (Invitrogen) and cells were then either plated into 10cm tissue culture dishes or used for flow cytometry or fluorescence cell sorting.

7.5 Bone marrow isolation

In general bone marrow was isolated from tibia, femurs and spinal cord. In brief, bones were crushed and bone marrow harvested in RPMI (Invitrogen) supplemented with 2% FCS (Gibco) and then centrifuged. Cell numbers were determined by automated cell counts with a ViCell (Beckman Coulter) and differentiated cells either removed by lineage depletion (Lin-) or $1x10^6$ bone marrow single cells stained directly with specific antibodies. Lineage depletion was carried out by incubation of the bone marrow with rat anti-mouse monoclonal lineage specific antibodies, CD4 (GK1.5), CD8a (53.6.7), B220 (RA3-6B2), Gr1 (RB6.8C5), Ter119 (Ter119), CD11b (M1/70). Antibody-bound cells were then removed from bone marrow by incubation with sheep anti-rat IgG-coated dynabeads (superparamagnetic polystyrene beads, Invitrogen) and separated with a magnet. Centrifugation was conducted at 4°C, 1600 rpm and 5 min. in Eppendorf 5810r centrifuges and washing steps were carried out with PBS supplemented with 2% FCS.

7.6 Chimera generation

Recipient NSG donor mice (CD45.1) were sub-lethally irradiated with 2.5 Gy 24 hours before chimera generation. Donor ColtTA control and *ColtTA;TreMyc* mutant animals (CD45.1 / CD45.2 mixture) were sacrificed, hind legs removed and the bone marrow isolated. Bone marrow was counted with a ViCell and $1x10^7$ cells per 1 ml RPMI (Invitrogen) incubated with 1:30 diluted hybridoma AT83 anti-mouse-Thy1.2 antibody (T-cell depletion). In a next step rabbit complement (1:10) and Dnase I (1:50 / 3 ml media) were added and then cells were counted again to get a final cell concentration of $1x10^5$ cells / 100 µL in PBS. T-cell depleted $1x10^5$ cells / 100 µL in PBS from ColtTA controla and *ColtTA;TreMyc* mutant animals were then intra-veneously injected into NSG recipient animals in triplicats. Bone marrow of primary chimeras was analyzed 25-30 weeks post transplanation and additionally secondary chimeras were generated.

For secondary chimera set-up, $1x10^6$ bone marrow cells from primary ColtTA and *ColtTA;TreMyc* chimeras were transplanted intra-veneously into sub-lethally irraded

(2.5Gy) NSG recipient animals following same protocol as for primary chimera generation. Also here, bone marrow of secondary chimeras was analyzed 25-40 weeks post transplantation.

7.7 Fluorecent cell sorting and flow cytometric analysis

Antibodies used in the experiments were titrated prior use. All antibodies were purchased from eBiosience. For osteoblast cell sorting cells were incubated with the following antibody mixture, pacific blue-CD45 (3-11), APC-CD31 (390), APC-Ter119 (Ter119), PE-Cy5-Sca-1 (D7), PE-CD51 (RMV-7) and cell surface staining was performed in PBS supplemented with 2% tet-free FCS for 30 min. on ice. For hematopoietic stem cell identification cell were stained with lineage cocktail antibodies, fluorescently coupled to PE-Cy7, CD4 (GK1.5), CD8a (53.6.7), B220 (RA3-6B2), Gr1 (RB6.8C5), Ter119 (Ter119), CD11b (M1/70), AF700-CD34 and PE-CD34 (RAM 34), PE-CD48 and pacific blue-CD48 (HM48.1), PE-Cy5-CD150 (TC15-12F12.2), AF400-Sca-1 and APC-Sca-1 (D7), APC-eFluor780-c-Kit (2B8). Hematopoietic progenitors were additionally identified with PE-CD127 or PE-Cy5 or APC (A7R34), pacific blue-CD16/32 or PE (93). Specific differentiated cell stainings and detection of chimerism in the bone marrow were achieved by incubation with APC-CD3 (17A2), FITC-CD45.1 (A20), AF-700-CD45.2 or pacific blue (104).

For cell cycle analysis intra-cellular cell staining was performed after regular cell surface staining. Cells were then fixed with cytofix/cytoperm following traders instructions (BD Heidelberg). Cells were then incubated with FITC-ki67 (BD) for at least one hour on ice and before flow cytometry additionally 5 -10 min. stained with Hoechst33342 (Invitrogen). For BrdU stainings, cells were fixed and permeabilized with cytofix/cytoperm following traders instructions and then incubated with DNase I (BD) for one hour at 37°C and then intra-cellularly stained with APC-BrdU (BD) antibody.

FACS was performed on either a BD LSR II or BD LSR Fortessa while FACS cell sorting was performed on BD Aria machines. Identification of cell populations with corresponding cell surface markers are indicated in (Table 5).

Abbreviation	Population	Cell surface marker
Lin-	Lineage	CD4, CD8a, CD11b, Gr1, B220, Ter119
LSK	LSK	Lin^{-} Sca^{+} c-Kit^{+}
LSK SLAM	LSK SLAM	LSK $CD150^{+}$ $CD48^{-}$
ST-HSC	Short-term HSC	LSK $CD150^{+}$ $CD48^{-}$ $CD34^{+}$
LT-HSC	Long-term HSC	LSK $CD150^{+}$ $CD48^{-}$ $CD34^{-}$
CMP	Common myeloid progenitor	Lin^{-} Sca-1^{-} c-Kit^{+} $CD34^{+}$ $CD16/32^{-}$
GMP	Granulocyte macrophage/ monocyte progenitor	Lin^{-} Sca-1^{-} c-Kit^{+} $CD34^{+}$ $CD16/32^{+}$
MEP	Megakaryocyte erythroid progenitor	Lin^{-} Sca-1^{-} c-Kit^{+} $CD34^{-}$ $CD16/32^{-}$
CLP	Common lymphoid progenitor	Lin^{-} Sca-1^{low} c-Kit^{low} $CD127^{+}$
Granulocyte	Granulocyte	$Gr1^{+}$ $CD11b^{+}$
Erythrocyte progenitor	Erythrocyte progenitor	$CD71^{+}$ $Ter119^{-}$
Erythrocytic blasts	Erythrocytic blasts	$CD71^{+}$ $Ter119^{+}$
Erythrocyte	Erythrocyte	$CD71^{-}$ $Ter119^{+}$
T-cell	T-lymphocyte	$CD3^{+}$, $CD4^{+}$, $CD8a^{+}$
Pre-pro B-cell	Pre-pro B-cell	IgM^{-} $B220^{+}$
Immature B-cell	Immature B-cell	IgM^{+} $B220^{low}$
Mature B-cell	B-lymphocyte	IgM^{+} $B220^{+}$
Osteoclast progenitor	Osteoclast progenitor	$CD45^{+}$ $Gr1^{-}$ $CD11b^{low/-}$ $F/480^{+}$ $CD115^{-}$
Mature osteoclast	Osteoclast	$CD45^{+}$ $Gr1^{-}$ $CD11b^{low/-}$ $F/480^{+}$ $CD115^{+}$
Monocyte	Monocyte	$CD45^{+}$ $Gr1^{-}$ $CD11b^{low/-}$ $F/480^{-}$ $CD115^{+}$
Primitive stromal cell	Stromal cell progenitor	$CD45^{-}$ $CD31^{-}$ $Ter119^{-}$ Sca-1^{+} $CD51^{-}$
Immature osteoblast	Immature osteoblast	$CD45^{-}$ $CD31^{-}$ $Ter119^{-}$ Sca-1^{+} $CD51^{+}$
Mature osteoblast	Osteoblast	$CD45^{-}$ $CD31^{-}$ $Ter119^{-}$ Sca-1^{-} $CD51^{+}$

Table 5: Identification of cell populations in the bone and the bone marrow by cell surface markers

7.8 RNA isolation

All RNA preparations were performed with Arcturus RNA Isolation kit (Arcturus). Just briefly cells were directly lyzed in 100 µL cell lysis buffer and RNA isolated following manufacturer´s instructions. RNA was isolated with 11 µL cell extraction buffer and either used for RNA micro-array or for c-DNA synthesis.

7.9 Reverse Transcription

All RNA samples were transcribed with SuperScript VILO cDNA synthesis kit (Invitrogen), following manufacturerer´s instructions. Synthesized cDNA from LT-HSCs was diluted in a 1:4 ratio while all the other samples were diluted 1:8 with ultra-pure water (Gibco) before qRT-PCR analysis.

7.10 Quantitative real-time PCR

Genomic DNA sequence was obtained from Genbank and primers were designed by using Roche Assay Designing software. Quantitative real-time PCR was performed on a Roche Light Cycler 480 PCR machine with ABI Power SYBR Green mastermix (Applied Biosystems). All reactions were performed in triplicats in 96-well plates with a final volume of 20 µL per reaction. The PCR program was uniquely designed and all samples were run with 50 cycles beginning with denaturation 95 °C 10 min, acquisition for 45 s at 60 °C and a continuous acquisition with 0.11 °C/s, ranging from 65 °C to 95 °C and finalized at 40 °C for 5 min. Results were analyzed by using Roche Light Cycler Software. Data was normalized to the house-keeping genes OAZ and SDHA. All primers were validated for the appropriate cp range and DNA specificity before used in the analysis of qRT-PCR (Table 6).

Gene target	Forward primer (5′-3′)	Reverse primer (5′-3′)	Eff.
OAZ	TTTCAGCTAGCATCCTGTACTCC	GACCCTGGTCTTGTCGTTAGA	2,041
SDHA	AAGTTGAGATTTGCCGATGG	TGGTTCTGCATCGACTTCTG	1,978
hu c-Myc	CGGAACTCTTGTGCGTAAGG	TGATTGCTCAGGACATTTCTGT	1,860
p16	GGGTTTTCTTGGTGAAGTTCG	TTGCCCATCATCATCACCT	1,793
p18	AAATGGATTTGGGAGAACTGC	AAATTGGGATTAGCACCTCTGA	1,990
p19	AATGTGACCCAAGGCCACT	TTTCCTCTTTTGTTGACAAGTAACC	1,986
p21	TCCACAGCGATATCCAGACA	GGACATCACCAGGATTGGAC	2,114
p27	GAGCAGTGTCCAGGGATGAG	TCTGTTCTGTTGGCCCTTTT	1,976
p57	GAAGGACCAGCCTCTCTCG	GAAGGACCAGCCTCTCTCG	1,954
CyclinD1	GAGATTGTGCCATCCATGC	CTCCTCTTCGCACTTCTGCT	1,982
RunX2	CGAGACCAACCGAGTCATTT	ACGCCATAGTCCCTCCTTTT	2,001
ALP	ACTCAGGGCAATGAGGTCAC	TCACCCGAGTGGTAGTCACA	2,000
Osx	TCTCCATCTGCCTGACTCCT	GGACTGGAGCCATAGTGAGC	1,696
OCN	GCGCTCTGTCTCTCTGACCT	ACCTTATTGCCCTCCTGCTT	1,840
OPN	GCTTGGCTTATGGACTGAGG	AGGTCCTCATCTGTGGCATC	1,708
Col1a1	CAGTCGCTTCACCTACAGCA	GACTGTCTTGCCCCAAGTTC	1,870
Ogn	GGAATTAAAGCAAACACATTCAAA	TTTCTGGTAAATTAGGAGGCACA	2,183
Postn	AAGCTGCGGCAAGACAAG	TCAAATCTGCAGCTTCAAGG	2,495
Lrp5/6	CATGGACATCCAAGTGCTGA	TTGTCCTCCTCGCATGGT	1.938
Wnt3a	CTTAGTGCTCTGCAGCCTGA	GAGTGCTCAGAGAGGAGTACTGG	2,041
DKK-1	CTTCAAAAATATATC	ACACCAAAGGA	2,059
APC	CATGGACCAGGACAAAAACC	GAACACACACAGCAGGACAGA	2.138
Axin2	GAGAGTGAGCGGCAGAGC	CGGCTGACTCGTTCTCCT	2.034
GSK3ß	CAGTGGTGTGGATCAGTTGG	AATTTGCTCCCTTGTTGGTG	1,986
ß-Cat	TGCAGATCTTGGACTGGACA	AAGAACGGTAGCTGGGATCA	1,978
VDR	AACCCCTCATAAAGTTCCAGGT	CTGTACCCCAGGTCGGTCT	1,775
RANK-L	AGCCATTTGCACACCTCAC	CGTGGTACCAAGAGGACAGAGT	1,782
OPG	GTTTCCCGAGGACCACAAT	CCATTCAATGATGTCCAGGAG	1,927
M-CSF	GGTGGAACTGCCAGTATAGAAAG	TCCCATATGTCTCCTTCCATAAA	1,870
IL-6	GCTACCAAACTGGATATAATCAGGA	CCAGGTAGCTATGGTACTCCAGAA	2,000
Sox2	GGACTTCTTTTTGGGGGACT	CAGATCTATACATGGTCCGATTCC	2,127
Sox9	TATCTTCAAGGCGCTGCAA	TCGGTTTTGGGAGTGGTG	2,052
E-Cad	ATCCTCGCCCTGCTGATT	ACCACCGTTCTCCTCCGTA	1,962

Mdm2	AGGGCACGAGCTCTCAGAT	TCTCCTTCAAAAGAGTCTGTATCG	2,000
p53	ACGCTTCTCCGAAGACTGG	AGGGAGCTCGAGGCTGATA	1,977
Sca-1	TGGATTCTCAAACAAGGAAAGTAAGA	ACCCAGGATCTCCATACTTTCAATA	1,996
c-Kit	GGAGCCCACAATAGATTGGTAT	CACTGGTGAGACAGGAGTGG	2,000
RIG-I	GAGAGTCACGGGACCCACT	CGG TCT TAG CAT CTC CAA CG	1,940
IFIH-1	TGATGCACTATTCCAAGAACTAACA	TCTGTGAGACGAGTTAGCCAAG	2,040
IPS-1	ATGAGGTCGGCCACACAC	TGGGATGGACTGAGATGGAC	1,983
Bmi-1	AAACCAGACCACTCCTGAACA	TCTTCTTCTCTTCATCTCATTTTTGA	2,201

Table 6: List of qRT-PCR Primer

7.11 Micro array analysis

Micro array analysis was performed at DKFZ Genomics & Proteomics Core Facility with Illumina MouseRef-6 v2.0 Expression BeadChips (Illumina, San Diego). RNA quality was analyzed and quantified on the Agilent Bioanalyzer 2100. Samples with sufficient RNA amount (> 3ng, > 500pg/ µL) and quality (RIN > 7) were amplified with Ovation PicoSL WTA system and labeled with Encore BiotinIL Module (NuGen) and then hybridized. Insufficient samples (< 500pg/ µL or < 3ng) were first amplified, using NuGen Amplicon kit.

7.12 Histology

7.12.1 Paraffin embedding

Freshly isolated bones and organs were rinsed in PBS and then fixed in 4% paraformaldehyde (Sigma) over night at 4°C. Bones were additionally decalcified for 4 days with 0.4 M PBS-EDTA. Tissues were then dehydrated with 70%, 80%, 95%, 100% ethanol, xylol and finally embedded into paraffin. For histological sectioning tissues were cut into 7 µm cuts and for staining procedures rehydrated with xylol, 100%, 80%, 70%, 50% ethanol.

7.12.2 Hematoxylin and Eosin staining

Tissue cuts were rehydrated and then rinsed in distilled water. Freshly filtered hematoxylin (Sigma) was added for 10 min at then slides rinsed in tap water for 10 min. Sections were next dehydrated with 70% and 100% ethanol and then cytoplasm was stained with freshly filtered eosin (Sigma) for 45 s and then in Entellan (Merck) embedded.

7.12.3 Tartrate-resistant acid phosphatase staining

Osteoclast staining was performed with Trap staining kit following manufacturers instructions (Sigma, 387A). Counterstaining was performed with Weigerts hematoxylin (Sigma).

7.12.4 Masson Goldner staining

Masson Goldner trichrome staining was performed following manufacturers instructions (Merck #1.00485.0001) and sections were counterstained with Weigerts hematoxylin (Sigma).

7.12.5 Von Kossa staining

For silver staining, sections were rehydrated to water, then placed in 1% silver nitrate solution and incubated for up to 3 hours under a 100 watt bulb. After intensive washing with distilled water, slides were incubated in 5% sodium thiosulfate for 5 min to remove un-reacted silver. Counterstaining was performed with nuclear fast red (Sigma), then slides were dehydrated and mounted in Entellan.

7.12.6 Alkaline Phosphatase Staining

ALP staining was performed with ALP staining kit (Stemgent #00-0009) following manufacturers instructions.

7.12.7 Immunofluorescence

Paraffin sections were rehydrated to water and then incubated in target retrival solution (citrate buffer, pH 6.0, Dako #S1700) for 20 min at 100°C. Then samples were chilled at room temperature and then blocked with 10% goat serum (Invitrogen) in PBS (blocking buffer) for 1hour at room temperature. Primary antibody incubation was performed over night at 4°C and administered in blocking buffer. Secondary antibody incubation was added for 1 hour incubation at room temperature in the dark. Then DAPI mounting medium was used for counterstaining (Invitrogen # P-36931). Image acquisitions were performed with either a laser scanning microscope (Zeiss, LSM700) or a light microscope (Leica SFL100).

7.12.8 Histomorphometry

Mouse skeletons were prepared by removal of skin, muscles and inner organs and then skeletons were rinsed in PBS. Skeletons were then fixed in neutral phosphate-buffered formalin over night, next overtaken into 80% ethanol and shipped for histomorphometric bone analysis.Histomorphometric analysis of bones were performed by Dr. Johannes Keller in the group of Professor Dr. Michael Amling at Universitätsklinikum Hamburg-Eppendorf, Institut für Osteologie und Biomechanik.

7.13 Western blot

For protein analysis cells or tissues were lyzed in 1x RIPA buffer (Cell Siganling) supplemented with proteinase inhibitor cocktail (Thermo Scientific #78430) and then protein concentration was measured with BCA kit (Pierce #23225). Proteins with 300 µg were loaded into Mini-Protean TGX precast gels (Biorad) and blottet on cellulose nitrate paper. Western blots were developed with SuperSignal West Pico (Pierce #34079) and x-ray paper (Fuji-film IX50). Antibodies used for western blot are indicated in Table 7.

Antibody	Dilution	Protein band	company
Actin	1:1000	43 kDa	Abcam #ab3280
ß-Catenin	1:1000	92 kDa	Cell Signaling #9582
Phospho-ß-Catenin	1:1000	92 kDa	Cell Signaling #9587
p53	1:1000	53 kDa	Abcam #ab26
Phospho-p53	1:500	53 kDa	Abcam #ab1431
c-Kit	1:100	120kDa/ 145kDa	Cell Signaling #3074
Phospho-c-Kit	1:100	120kDa/ 145kDa	Cell Signaling #3391

Table 7: List of western blot antibodies

7.14 ELISA

Mouse plasma was diluted in a 50% ratio with sample buffer from the PTH ELISA kit (Immutopics, #60-2700) and incubated for three hours on an orbital shaker (200 rpm). All other steps were performed in accordance with manufacturers instructions. OCN, Trap, RANK-L and OPG ELISAs were performed by Dr. Johannes Keller in the group of Professor Dr. Michael Amling at Universitätsklinikum Hamburg-Eppendorf, Institut für Osteologie und Biomechanik.

7.15 Tyrosine Kinase Inhibitor treatment

Nilotinib (Tasigna, Novartis) was a kind gift from Dr. Ingmar Bruns, Universitätsklinikum Düsseldorf, Klinik für Hämatologie, Onkologie und Klinische Immunologie, Arbeitsgruppe Prof. Dr. Rainer Haas. Nilotinib was administered *in vitro* in a dose dependent manner. For *in vitro* treatment Nilotinib was dissolved in DMSO to make a 10 mM stock solution. Then serial dilutions were made in DMSO to obtain final dilutions (10 µM; 5 µM; 1 µM; 0.5 µM; 0.1 µM) and osteosarcoma cell lines were treated for 72 hrs. Then cells were analyzed for their cell proliferation rate by using Promega Cell Titer Glo reagent according to manufacturers instructions (#G7570).

7.16 Interferon alpha treatment

Interferon alpha (IFNa) stock solution 10.000 U in PBS per mouse and is applied sub-cutaneously, 16 hrs before the analysis.

7.17 Polyinosinic:polycytidylic acid treatment

Polyinosinic:polycytidylic acid (polyI:C; pIC) stock solution with 1.8 mg/ml in PBS is administered intra-peritoneally with 200 µl per 20 g mouse. Animals are sacrificed and analyzed 16 hrs post injection.

7.18 Lipopolysaccharide treatment

Normally lipopolysaccharide (LPS) is injected intra-peritoneally with 5 µg per mouse and animals are analyzed 16 – 24 hrs post injection. For low dose treatment animals were injected with only 0.5 µg per mouse and analyzed 16 hrs post injection.

7.19 *In vitro* infections

Second generation lentivirus production was done with pSPAX2 and pMD2.G plasmids. pSPAX2 contains the CAG promoter and expresses the proteins necessary for viral particle packaging. pMD2.G plasmid encodes for the envelope for viral production. The pV2-Luc (MEF-1) plasmid contains both, the luciferase and venus insert (see map, xxx). Cells were infected with a viral titer of 2,3 x 10^8 PFU/ml.

7.20 Bioluminescence imaging *in vivo*

D-Luciferin (Caliper Life Sciences) was dissolved in PBS as a 15 mg/ml stock solution and kept at 4°C in the dark. For *in vivo* imaging 10 µL/ g of mouse body weight were given intra-peritoneally 5-10 min before measuring. The animals were anesthetized with 4.5% isofluorane in oxygen and maintained at 1.5% isofluorane in oxygen. Analysis was done in a heated camera chamber using Living Imaging software, according to manufacturer's instructions (Xenogen, IVIS 200, CALIPER).

7.21 Statistics

GraphPad Prism (GraphPad Sofware) was used to set-up graph analysis. All graphs show the mean value and the standard deviation (SD) and were performed by Prism. To determine statistical significance, usually unpaired two-tailed t-tests were performed and in several cases, when different experimental groups were compared in addition the mean value was plotted with the standard error of the mean (SEM). In all the cases statistical significance was plotted with *** (< 0.001; extremely significant), ** (0.001 to 0.01; very significant), * (0.01 to 0.05; significant), ns (> 0.05; not significant).

8 SUPPLEMENTARY

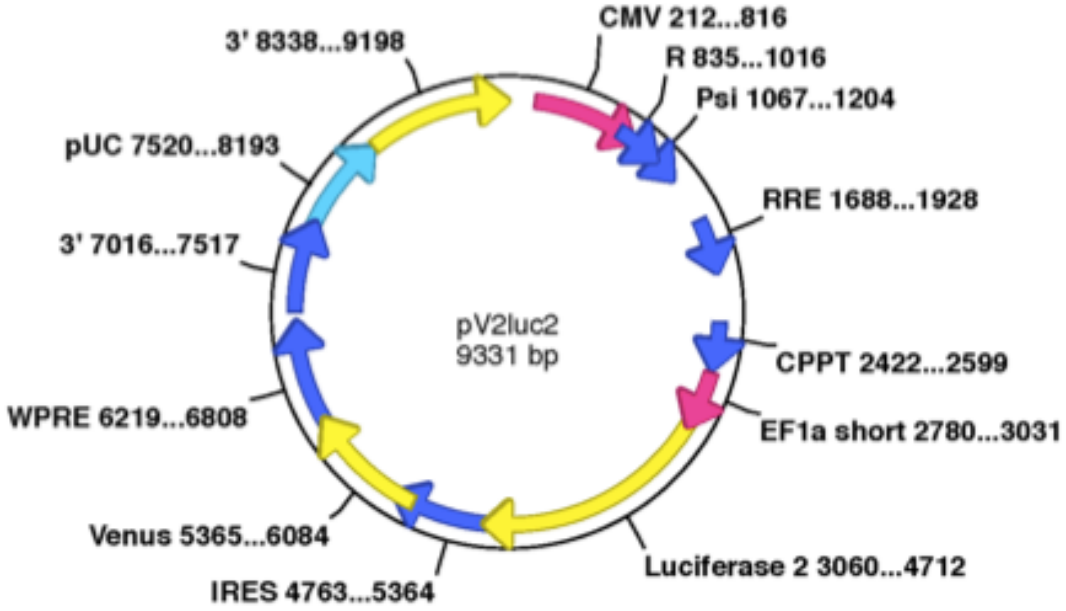

Figure 71: Vector map pV2luc2

9 Abbreviations

BM	Bone marrow
BrdU	5-Bromo-2-deoxyuridine
CAR	CXCL12-abundant reticular cell
c-Kit	v-kit Hardy-Zuckerman 4 feline sarcoma cellular homologue
c-Myc	Cellular myelocytomatosis homologue
DKK-1	Dickkopf-1
E14.5	Embryonic day 14.5
FACS	Fluorescence-activated cell sorting
GFP	Green fluorescent protein
HSC	Hematopoietic stem cells
IFN	interferon
LPS	lipopolysaccharide
LRC	Label retaining cell
Mdm2	Murine double minute 2
MSC	Mesenchymal stem cell
N-Myc	Neuroblastomaamplified myelocytomatosis homologue
OB	osteoblast
OCN	osteocalcin
P30	Post-natal day 30
P53	Tumor protein 53
pIC	Polyinosinic:polycytidylic acid (PolyI:C)
RunX2	Runt-related transcription factor 2
Sca-1	Stem cell antigen 1
SOST	sclerostin
Wnt	Wingless INT-1

10 BIBLIOGRAPHY

.

Adamson, E. D. (1987). "Oncogenes in development." Development **99**(4): 449-471.

Adhikary, S. and M. Eilers (2005). "Transcriptional regulation and transformation by Myc proteins." Nat Rev Mol Cell Biol **6**(8): 635-645.

Aizawa, T., S. Kokubun, et al. (1999). "c-Myc protein in the rabbit growth plate. Changes in immunolocalisation with age and possible roles from proliferation to apoptosis." J Bone Joint Surg Br **81**(5): 921-925.

Alberts, B. J., Alexander Lewis, Julian Raff, Martin Roberts, Keith Walter, Peter (2002). Molecular Biology of the Cell.

Arai, F., A. Hirao, et al. (2004). "Tie2/angiopoietin-1 signaling regulates hematopoietic stem cell quiescence in the bone marrow niche." Cell **118**(2): 149-161.

Arnsdorf, E. J., P. Tummala, et al. (2009). "Non-canonical Wnt signaling and N-cadherin related beta-catenin signaling play a role in mechanically induced osteogenic cell fate." PLoS One **4**(4): e5388.

Baccala, R., K. Hoebe, et al. (2007). "TLR-dependent and TLR-independent pathways of type I interferon induction in systemic autoimmunity." Nat Med **13**(5): 543-551.

Baena, E., M. Ortiz, et al. (2007). "c-Myc is essential for hematopoietic stem cell differentiation and regulates Lin(-)Sca-1(+)c-Kit(-) cell generation through p21." Exp Hematol **35**(9): 1333-1343.

Baldridge, M. T., K. Y. King, et al. (2010). "Quiescent haematopoietic stem cells are activated by IFN-gamma in response to chronic infection." Nature **465**(7299): 793-797.

Baldridge, M. T., K. Y. King, et al. (2011). "Inflammatory signals regulate hematopoietic stem cells." Trends Immunol **32**(2): 57-65.

Barker, N. and H. Clevers (2000). "Catenins, Wnt signaling and cancer." Bioessays **22**(11): 961-965.

Baron, R., G. Rawadi, et al. (2006). "Wnt signaling: a key regulator of bone mass." Curr Top Dev Biol **76**: 103-127.

Basu-Roy, U., E. Seo, et al. (2012). "Sox2 maintains self renewal of tumor-initiating cells in osteosarcomas." Oncogene **31**(18): 2270-2282.

Beck, G. R., Jr., B. Zerler, et al. (2000). "Phosphate is a specific signal for induction of osteopontin gene expression." Proc Natl Acad Sci U S A **97**(15): 8352-8357.

Behrens, A., W. Jochum, et al. (2000). "Oncogenic transformation by ras and fos is mediated by c-Jun N-terminal phosphorylation." Oncogene **19**(22): 2657-2663.

Berman, S. D., E. Calo, et al. (2008). "Metastatic osteosarcoma induced by inactivation of Rb and p53 in the osteoblast lineage." Proc Natl Acad Sci U S A **105**(33): 11851-11856.

Blank, U., G. Karlsson, et al. (2008). "Signaling pathways governing stem-cell fate." Blood **111**(2): 492-503.

Blyth, K., F. Vaillant, et al. (2006). "Runx2 and MYC collaborate in lymphoma development by suppressing apoptotic and growth arrest pathways in vivo." Cancer Res **66**(4): 2195-2201.

Bodine, P. V. (2008). "Wnt signaling control of bone cell apoptosis." Cell Res **18**(2): 248-253.

Bonewald, L. (2011). "The holy grail of high bone mass." Nat Med **17**(6): 657-658.

Bonewald, L. F. and M. L. Johnson (2008). "Osteocytes, mechanosensing and Wnt signaling." Bone **42**(4): 606-615.

Bonnet, N., S. J. Conway, et al. (2012). "Regulation of beta catenin signaling and parathyroid hormone anabolic effects in bone by the matricellular protein periostin." Proc Natl Acad Sci U S A **109**(37): 15048-15053.

Bouchard, C., S. Lee, et al. (2007). "FoxO transcription factors suppress Myc-driven lymphomagenesis via direct activation of Arf." Genes Dev **21**(21): 2775-2787.

Boxer, L. M. and C. V. Dang (2001). "Translocations involving c-myc and c-myc function." Oncogene **20**(40): 5595-5610.

Boyce, B. F. and L. Xing (2008). "Functions of RANKL/RANK/OPG in bone modeling and remodeling." Arch Biochem Biophys **473**(2): 139-146.

Boyle, W. J., W. S. Simonet, et al. (2003). "Osteoclast differentiation and activation." Nature **423**(6937): 337-342.

Buddingh, E. P., S. E. Ruslan, et al. (2012). "Intact interferon signaling in peripheral blood leukocytes of high-grade osteosarcoma patients." Cancer Immunol Immunother **61**(6): 941-947.

Bulavin, D. V., N. D. Tararova, et al. (1999). "Deregulation of p53/p21Cip1/Waf1 pathway contributes to polyploidy and apoptosis of E1A+cHa-ras transformed cells after gamma-irradiation." Oncogene **18**(41): 5611-5619.

Caetano-Lopes, J., H. Canhao, et al. (2009). "Osteoimmunology--the hidden immune regulation of bone." Autoimmun Rev **8**(3): 250-255.

Calandra, T. and T. Roger (2003). "Macrophage migration inhibitory factor: a regulator of innate immunity." Nat Rev Immunol **3**(10): 791-800.

Candeias, M. M., D. J. Powell, et al. (2006). "Expression of p53 and p53/47 are controlled by alternative mechanisms of messenger RNA translation initiation." Oncogene **25**(52): 6936-6947.

Chagraoui, J., J. Hebert, et al. (2011). "An anticlastogenic function for the Polycomb Group gene Bmi1." Proc Natl Acad Sci U S A **108**(13): 5284-5289.

Charron, J., B. A. Malynn, et al. (1992). "Embryonic lethality in mice homozygous for a targeted disruption of the N-myc gene." Genes Dev **6**(12A): 2248-2257.

Chen, G., C. Deng, et al. (2012). "TGF-beta and BMP signaling in osteoblast differentiation and bone formation." Int J Biol Sci **8**(2): 272-288.

Chen, H., K. Kolman, et al. (2012). "p53 and MDM2 are involved in the regulation of osteocalcin gene expression." Exp Cell Res **318**(8): 867-876.

Chow, A., D. Lucas, et al. (2011). "Bone marrow CD169+ macrophages promote the retention of hematopoietic stem and progenitor cells in the mesenchymal stem cell niche." J Exp Med **208**(2): 261-271.

Clarke, B. (2008). "Normal bone anatomy and physiology." Clin J Am Soc Nephrol **3 Suppl 3**: S131-139.

Cole, M. D. and S. B. McMahon (1999). "The Myc oncoprotein: a critical evaluation of transactivation and target gene regulation." Oncogene **18**(19): 2916-2924.

Coller, H. A., C. Grandori, et al. (2000). "Expression analysis with oligonucleotide microarrays reveals that MYC regulates genes involved in growth, cell cycle, signaling, and adhesion." Proc Natl Acad Sci U S A **97**(7): 3260-3265.

Copley, M. R., P. A. Beer, et al. (2012). "Hematopoietic stem cell heterogeneity takes center stage." Cell Stem Cell **10**(6): 690-697.

Dacquin, R., M. Starbuck, et al. (2002). "Mouse alpha1(I)-collagen promoter is the best known promoter to drive efficient Cre recombinase expression in osteoblast." Dev Dyn **224**(2): 245-251.

Dallas, S. L. and L. F. Bonewald (2010). "Dynamics of the transition from osteoblast to osteocyte." Ann N Y Acad Sci **1192**: 437-443.

Ding, L., T. L. Saunders, et al. (2012). "Endothelial and perivascular cells maintain haematopoietic stem cells." Nature **481**(7382): 457-462.

Doly, J., A. Civas, et al. (1998). "Type I interferons: expression and signalization." Cell Mol Life Sci **54**(10): 1109-1121.

Drissi, H., D. Hushka, et al. (1999). "The cell cycle regulator p27kip1 contributes to growth and differentiation of osteoblasts." Cancer Res **59**(15): 3705-3711.

Druker, B. J. (2002). "Taking aim at Ewing's sarcoma: is KIT a target and will imatinib work?" J Natl Cancer Inst **94**(22): 1660-1661.

Ducy, P., R. Zhang, et al. (1997). "Osf2/Cbfa1: a transcriptional activator of osteoblast differentiation." Cell **89**(5): 747-754.

Ehninger, A. and A. Trumpp (2011). "The bone marrow stem cell niche grows up: mesenchymal stem cells and macrophages move in." J Exp Med **208**(3): 421-428.

Eilers, M. and R. N. Eisenman (2008). "Myc's broad reach." Genes Dev **22**(20): 2755-2766.

Entz-Werle, N., L. Marcellin, et al. (2005). "Prognostic significance of allelic imbalance at the c-kit gene locus and c-kit overexpression by immunohistochemistry in pediatric osteosarcomas." J Clin Oncol **23**(10): 2248-2255.

Essers, M. A., S. Offner, et al. (2009). "IFNalpha activates dormant haematopoietic stem cells in vivo." Nature **458**(7240): 904-908.

Fan, X., D. Fan, et al. (2001). "Increasing membrane-bound MCSF does not enhance OPGL-driven osteoclastogenesis from marrow cells." Am J Physiol Endocrinol Metab **280**(1): E103-111.

Fedde, K. N., L. Blair, et al. (1999). "Alkaline phosphatase knock-out mice recapitulate the metabolic and skeletal defects of infantile hypophosphatasia." J Bone Miner Res **14**(12): 2015-2026.

Felsher, D. W. (2010). "MYC Inactivation Elicits Oncogene Addiction through Both Tumor Cell-Intrinsic and Host-Dependent Mechanisms." Genes Cancer **1**(6): 597-604.

Field, J. K. and D. A. Spandidos (1990). "The role of ras and myc oncogenes in human solid tumours and their relevance in diagnosis and prognosis (review)." Anticancer Res **10**(1): 1-22.

Fisher, D. E., L. A. Parent, et al. (1992). "Myc/Max and other helix-loop-helix/leucine zipper proteins bend DNA toward the minor groove." Proc Natl Acad Sci U S A **89**(24): 11779-11783.

Fleming, H. E., V. Janzen, et al. (2008). "Wnt signaling in the niche enforces hematopoietic stem cell quiescence and is necessary to preserve self-renewal in vivo." Cell Stem Cell **2**(3): 274-283.

Florian, M. C., K. Dorr, et al. (2012). "Cdc42 activity regulates hematopoietic stem cell aging and rejuvenation." Cell Stem Cell **10**(5): 520-530.

Forget, M. A., S. Turcotte, et al. (2007). "The Wnt pathway regulator DKK1 is preferentially expressed in hormone-resistant breast tumours and in some common cancer types." Br J Cancer **96**(4): 646-653.

Franz-Odendaal, T. A., B. K. Hall, et al. (2006). "Buried alive: how osteoblasts become osteocytes." Dev Dyn **235**(1): 176-190.

Fujita, K. and S. Janz (2007). "Attenuation of WNT signaling by DKK-1 and -2 regulates BMP2-induced osteoblast differentiation and expression of OPG, RANKL and M-CSF." Mol Cancer **6**: 71.

Gao, Y., F. Grassi, et al. (2007). "IFN-gamma stimulates osteoclast formation and bone loss in vivo via antigen-driven T cell activation." J Clin Invest **117**(1): 122-132.

Gartel, A. L., X. Ye, et al. (2001). "Myc represses the p21(WAF1/CIP1) promoter and interacts with Sp1/Sp3." Proc Natl Acad Sci U S A **98**(8): 4510-4515.

Gaudio, A., P. Pennisi, et al. (2010). "Increased sclerostin serum levels associated with bone formation and resorption markers in patients with immobilization-induced bone loss." J Clin Endocrinol Metab **95**(5): 2248-2253.

Ge, G., N. S. Seo, et al. (2004). "Bone morphogenetic protein-1/tolloid-related metalloproteinases process osteoglycin and enhance its ability to regulate collagen fibrillogenesis." J Biol Chem **279**(40): 41626-41633.

Glass, D. A., 2nd, P. Bialek, et al. (2005). "Canonical Wnt signaling in differentiated osteoblasts controls osteoclast differentiation." Dev Cell **8**(5): 751-764.

Glass, D. A., 2nd and G. Karsenty (2007). "In vivo analysis of Wnt signaling in bone." Endocrinology **148**(6): 2630-2634.

Gomez-Casares, M. T., E. Garcia-Alegria, et al. (2012). "MYC antagonizes the differentiation induced by imatinib in chronic myeloid leukemia cells through downregulation of p27(KIP1)." Oncogene.

Gossen, M. and H. Bujard (1992). "Tight control of gene expression in mammalian cells by tetracycline-responsive promoters." Proc Natl Acad Sci U S A **89**(12): 5547-5551.

Gowen, M., F. Lazner, et al. (1999). "Cathepsin K knockout mice develop osteopetrosis due to a deficit in matrix degradation but not demineralization." J Bone Miner Res **14**(10): 1654-1663.

Grandori, C., S. M. Cowley, et al. (2000). "The Myc/Max/Mad network and the transcriptional control of cell behavior." Annu Rev Cell Dev Biol **16**: 653-699.

Guise, T. A., K. S. Mohammad, et al. (2006). "Basic mechanisms responsible for osteolytic and osteoblastic bone metastases." Clin Cancer Res **12**(20 Pt 2): 6213s-6216s.

Guney, I., S. Wu, et al. (2006). "Reduced c-Myc signaling triggers telomere-independent senescence by regulating Bmi-1 and p16(INK4a)." Proc Natl Acad Sci U S A **103**(10): 3645-3650.

Guo, J., M. Liu, et al. (2010). "Suppression of Wnt signaling by Dkk1 attenuates PTH-mediated stromal cell response and new bone formation." Cell Metab **11**(2): 161-171.

Gutierrez, G. M., E. Kong, et al. (2008). "Impaired bone development and increased mesenchymal progenitor cells in calvaria of RB1-/- mice." Proc Natl Acad Sci U S A **105**(47): 18402-18407.

Hanahan, D., E. F. Wagner, et al. (2007). "The origins of oncomice: a history of the first transgenic mice genetically engineered to develop cancer." Genes Dev **21**(18): 2258-2270.

Harada, H., S. Tagashira, et al. (1999). "Cbfa1 isoforms exert functional differences in osteoblast differentiation." J Biol Chem **274**(11): 6972-6978.

Harada, S. and G. A. Rodan (2003). "Control of osteoblast function and regulation of bone mass." Nature **423**(6937): 349-355.

Hauge, E. M., D. Qvesel, et al. (2001). "Cancellous bone remodeling occurs in specialized compartments lined by cells expressing osteoblastic markers." J Bone Miner Res **16**(9): 1575-1582.

Hay, E., E. Laplantine, et al. (2009). "N-cadherin interacts with axin and LRP5 to negatively regulate Wnt/beta-catenin signaling, osteoblast function, and bone formation." Mol Cell Biol **29**(4): 953-964.

Hesse, E., H. Saito, et al. (2010). "Zfp521 controls bone mass by HDAC3-dependent attenuation of Runx2 activity." J Cell Biol **191**(7): 1271-1283.

Hoeppner, L. H., F. J. Secreto, et al. (2009). "Wnt signaling as a therapeutic target for bone diseases." Expert Opin Ther Targets **13**(4): 485-496.

Hoffman, B., A. Amanullah, et al. (2002). "The proto-oncogene c-myc in hematopoietic development and leukemogenesis." Oncogene **21**(21): 3414-3421.

Holmen, S. L., C. R. Zylstra, et al. (2005). "Essential role of beta-catenin in postnatal bone acquisition." J Biol Chem **280**(22): 21162-21168.

Horiuchi, K., N. Amizuka, et al. (1999). "Identification and characterization of a novel protein, periostin, with restricted expression to periosteum and periodontal ligament and increased expression by transforming growth factor beta." J Bone Miner Res **14**(7): 1239-1249.

Hornick, J. L. and C. D. Fletcher (2002). "Immunohistochemical staining for KIT (CD117) in soft tissue sarcomas is very limited in distribution." Am J Clin Pathol **117**(2): 188-193.

Hu, H., M. J. Hilton, et al. (2005). "Sequential roles of Hedgehog and Wnt signaling in osteoblast development." Development **132**(1): 49-60.

Ichii, M., M. B. Frank, et al. (2012). "The canonical Wnt pathway shapes niches supportive of hematopoietic stem/progenitor cells." Blood **119**(7): 1683-1692.

Ikeda, A. K., D. R. Judelson, et al. (2010). "ABT-869 inhibits the proliferation of Ewing Sarcoma cells and suppresses platelet-derived growth factor receptor beta and c-KIT signaling pathways." Mol Cancer Ther **9**(3): 653-660.

Iwamoto, M., K. Yagami, et al. (1993). "Expression and role of c-myc in chondrocytes undergoing endochondral ossification." J Biol Chem **268**(13): 9645-9652.

Jacobs, J. J., B. Scheijen, et al. (1999). "Bmi-1 collaborates with c-Myc in tumorigenesis by inhibiting c-Myc-induced apoptosis via INK4a/ARF." Genes Dev **13**(20): 2678-2690.

Jacquin, C., D. E. Gran, et al. (2006). "Identification of multiple osteoclast precursor populations in murine bone marrow." J Bone Miner Res **21**(1): 67-77.

Jaworski, M. (2009). The role of myc in bone and in the hematopoietic stem cell niche. Ph.D., EPFL - ÉCOLE POLYTECHNIQUE FÉDÉRALE DE LAUSANNE.

Jho, E. H., T. Zhang, et al. (2002). "Wnt/beta-catenin/Tcf signaling induces the transcription of Axin2, a negative regulator of the signaling pathway." Mol Cell Biol **22**(4): 1172-1183.

Judson, I. (2010). "New treatments for sarcoma." Clin Adv Hematol Oncol **8**(4): 244-246.

Kang, D. C., R. V. Gopalkrishnan, et al. (2004). "Expression analysis and genomic characterization of human melanoma differentiation associated gene-5, mda-5: a novel type I interferon-responsive apoptosis-inducing gene." Oncogene **23**(9): 1789-1800.

Kaplan, R. N., B. Psaila, et al. (2006). "Bone marrow cells in the 'pre-metastatic niche': within bone and beyond." Cancer Metastasis Rev **25**(4): 521-529.

Kaplan, R. N., S. Rafii, et al. (2006). "Preparing the "soil": the premetastatic niche." Cancer Res **66**(23): 11089-11093.

Karsenty, G. (2000). "Role of Cbfa1 in osteoblast differentiation and function." Semin Cell Dev Biol **11**(5): 343-346.

Karsenty, G., H. M. Kronenberg, et al. (2009). "Genetic control of bone formation." Annu Rev Cell Dev Biol **25**: 629-648.

Kataoka, K., T. Ono, et al. (2012). "S100A7 promotes the migration and invasion of osteosarcoma cells via the receptor for advanced glycation end products." Oncol Lett **3**(5): 1149-1153.

Kato, G. J., W. M. Lee, et al. (1992). "Max: functional domains and interaction with c-Myc." Genes Dev **6**(1): 81-92.

Kato, H., O. Takeuchi, et al. (2006). "Differential roles of MDA5 and RIG-I helicases in the recognition of RNA viruses." Nature **441**(7089): 101-105.

Kato, M., M. S. Patel, et al. (2002). "Cbfa1-independent decrease in osteoblast proliferation, osteopenia, and persistent embryonic eye vascularization in mice deficient in Lrp5, a Wnt coreceptor." J Cell Biol **157**(2): 303-314.

Kawai, T. and S. Akira (2006). "TLR signaling." Cell Death Differ **13**(5): 816-825.

Khosla, S., J. J. Westendorf, et al. (2008). "Building bone to reverse osteoporosis and repair fractures." J Clin Invest **118**(2): 421-428.

Kim, J., J. H. Lee, et al. (2008). "Global identification of Myc target genes reveals its direct role in mitochondrial biogenesis and its E-box usage in vivo." PLoS One **3**(3): e1798.

Kim, M., T. Nakamoto, et al. (2008). "A new ubiquitin ligase involved in p57KIP2 proteolysis regulates osteoblast cell differentiation." EMBO Rep **9**(9): 878-884.

Kim, S. W., P. D. Pajevic, et al. (2012). "Intermittent parathyroid hormone administration converts quiescent lining cells to active osteoblasts." J Bone Miner Res **27**(10): 2075-2084.

Knoepfler, P. S., P. F. Cheng, et al. (2002). "N-myc is essential during neurogenesis for the rapid expansion of progenitor cell populations and the inhibition of neuronal differentiation." Genes Dev **16**(20): 2699-2712.

Knudson, A. G. (2001). "Two genetic hits (more or less) to cancer." Nat Rev Cancer **1**(2): 157-162.

Krishnan, V., H. U. Bryant, et al. (2006). "Regulation of bone mass by Wnt signaling." J Clin Invest **116**(5): 1202-1209.

Kulig, P., T. Kantyka, et al. (2011). "Regulation of chemerin chemoattractant and antibacterial activity by human cysteine cathepsins." J Immunol **187**(3): 1403-1410.

Lai, S. L., A. J. Chien, et al. (2009). "Wnt/Fz signaling and the cytoskeleton: potential roles in tumorigenesis." Cell Res **19**(5): 532-545.

Lander, A. D., J. Kimble, et al. (2012). "What does the concept of the stem cell niche really mean today?" BMC Biol **10**: 19.

Lane, S. W., S. M. Sykes, et al. (2010). "The Apc(min) mouse has altered hematopoietic stem cell function and provides a model for MPD/MDS." Blood **115**(17): 3489-3497.

Laurenti, E., B. Varnum-Finney, et al. (2008). "Hematopoietic stem cell function and survival depend on c-Myc and N-Myc activity." Cell Stem Cell **3**(6): 611-624.

Laurenti, E., A. Wilson, et al. (2009). "Myc's other life: stem cells and beyond." Curr Opin Cell Biol **21**(6): 844-854.

Lee, K. S., H. J. Kim, et al. (2000). "Runx2 is a common target of transforming growth factor beta1 and bone morphogenetic protein 2, and cooperation between Runx2 and Smad5 induces osteoblast-specific gene expression in the pluripotent mesenchymal precursor cell line C2C12." Mol Cell Biol **20**(23): 8783-8792.

Li, J., I. Sarosi, et al. (2000). "RANK is the intrinsic hematopoietic cell surface receptor that controls osteoclastogenesis and regulation of bone mass and calcium metabolism." Proc Natl Acad Sci U S A **97**(4): 1566-1571.

Li, X., Y. Zhang, et al. (2005). "Sclerostin binds to LRP5/6 and antagonizes canonical Wnt signaling." J Biol Chem **280**(20): 19883-19887.

Li, Z., S. Van Calcar, et al. (2003). "A global transcriptional regulatory role for c-Myc in Burkitt's lymphoma cells." Proc Natl Acad Sci U S A **100**(14): 8164-8169.

Lian, J. B. and G. S. Stein (1992). "Concepts of osteoblast growth and differentiation: basis for modulation of bone cell development and tissue formation." Crit Rev Oral Biol Med **3**(3): 269-305.

Liu, H., D. C. Radisky, et al. (2012). "MYC suppresses cancer metastasis by direct transcriptional silencing of alphav and beta3 integrin subunits." Nat Cell Biol **14**(6): 567-574.

Liu, W., S. Toyosawa, et al. (2001). "Overexpression of Cbfa1 in osteoblasts inhibits osteoblast maturation and causes osteopenia with multiple fractures." J Cell Biol **155**(1): 157-166.

Lorenzo, J., M. Horowitz, et al. (2008). "Osteoimmunology: interactions of the bone and immune system." Endocr Rev **29**(4): 403-440.

Lundberg, P., S. J. Allison, et al. (2007). "Greater bone formation of Y2 knockout mice is associated with increased osteoprogenitor numbers and altered Y1 receptor expression." J Biol Chem **282**(26): 19082-19091.

Luo, H., Q. Li, et al. (2005). "c-Myc rapidly induces acute myeloid leukemia in mice without evidence of lymphoma-associated antiapoptotic mutations." Blood **106**(7): 2452-2461.

Luu, H. H., R. Zhang, et al. (2004). "Wnt/beta-catenin signaling pathway as a novel cancer drug target." Curr Cancer Drug Targets **4**(8): 653-671.

Lymperi, S., A. Ersek, et al. (2011). "Inhibition of osteoclast function reduces hematopoietic stem cell numbers in vivo." Blood **117**(5): 1540-1549.

Mackie, E. J., Y. A. Ahmed, et al. (2008). "Endochondral ossification: how cartilage is converted into bone in the developing skeleton." Int J Biochem Cell Biol **40**(1): 46-62.

Mansour, A., G. Abou-Ezzi, et al. (2012). "Osteoclasts promote the formation of hematopoietic stem cell niches in the bone marrow." J Exp Med **209**(3): 537-549.

Martin, J. W., J. A. Squire, et al. (2012). "The genetics of osteosarcoma." Sarcoma **2012**: 627254.

Martin, J. W., M. Zielenska, et al. (2011). "The Role of RUNX2 in Osteosarcoma Oncogenesis." Sarcoma **2011**: 282745.

Matsumoto, A., S. Takeishi, et al. (2011). "p57 is required for quiescence and maintenance of adult hematopoietic stem cells." Cell Stem Cell **9**(3): 262-271.

Matsuyama, S., M. Iwadate, et al. (2003). "SB-431542 and Gleevec inhibit transforming growth factor-beta-induced proliferation of human osteosarcoma cells." Cancer Res **63**(22): 7791-7798.

McGary, E. C., K. Weber, et al. (2002). "Inhibition of platelet-derived growth factor-mediated proliferation of osteosarcoma cells by the novel tyrosine kinase inhibitor STI571." Clin Cancer Res **8**(11): 3584-3591.

Meyer, N. and L. Z. Penn (2008). "Reflecting on 25 years with MYC." Nat Rev Cancer **8**(12): 976-990.

Miao, D. and A. Scutt (2002). "Histochemical localization of alkaline phosphatase activity in decalcified bone and cartilage." J Histochem Cytochem **50**(3): 333-340.

Miiji, L. N., A. S. Petrilli, et al. (2011). "C-kit expression in human osteosarcoma and in vitro assays." Int J Clin Exp Pathol **4**(8): 775-781.

Miller, C. W., A. Aslo, et al. (1990). "Frequency and structure of p53 rearrangements in human osteosarcoma." Cancer Res **50**(24): 7950-7954.

Mohseny, A. B., P. C. Hogendoorn, et al. (2012). "Osteosarcoma models: from cell lines to zebrafish." Sarcoma **2012**: 417271.

Molyneux, S. D., M. A. Di Grappa, et al. (2010). "Prkar1a is an osteosarcoma tumor suppressor that defines a molecular subclass in mice." J Clin Invest **120**(9): 3310-3325.

Monroe, D. G., M. E. McGee-Lawrence, et al. (2012). "Update on Wnt signaling in bone cell biology and bone disease." Gene **492**(1): 1-18.

Morrison, S. J., K. R. Prowse, et al. (1996). "Telomerase activity in hematopoietic cells is associated with self-renewal potential." Immunity **5**(3): 207-216.

Mulligan, L. M., G. J. Matlashewski, et al. (1990). "Mechanisms of p53 loss in human sarcomas." Proc Natl Acad Sci U S A **87**(15): 5863-5867.

Nagasawa, T., Y. Omatsu, et al. (2011). "Control of hematopoietic stem cells by the bone marrow stromal niche: the role of reticular cells." Trends Immunol **32**(7): 315-320.

Namlos, H. M., S. H. Kresse, et al. (2012). "Global gene expression profiling of human osteosarcomas reveals metastasis-associated chemokine pattern." Sarcoma **2012**: 639038.

Nelson, W. J. and R. Nusse (2004). "Convergence of Wnt, beta-catenin, and cadherin pathways." Science **303**(5663): 1483-1487.

Nesbit, C. E., J. M. Tersak, et al. (1999). "MYC oncogenes and human neoplastic disease." Oncogene **18**(19): 3004-3016.

Neve, A., A. Corrado, et al. (2011). "Osteoblast physiology in normal and pathological conditions." Cell Tissue Res **343**(2): 289-302.

Niini, T., L. Lahti, et al. (2011). "Array comparative genomic hybridization reveals frequent alterations of G1/S checkpoint genes in undifferentiated pleomorphic sarcoma of bone." Genes Chromosomes Cancer **50**(5): 291-306.

Nilsson, J. A. and J. L. Cleveland (2003). "Myc pathways provoking cell suicide and cancer." Oncogene **22**(56): 9007-9021.

Nishimori, S., Y. Tanaka, et al. (2001). "Smad-mediated transcription is required for transforming growth factor-beta 1-induced p57(Kip2) proteolysis in osteoblastic cells." J Biol Chem **276**(14): 10700-10705.

Noll, J. E., S. A. Williams, et al. (2012). "Tug of war in the haematopoietic stem cell niche: do myeloma plasma cells compete for the HSC niche?" Blood Cancer J **2**: e91.

Ogawa, M. (1993). "Differentiation and proliferation of hematopoietic stem cells." Blood **81**(11): 2844-2853.

Olsen, B. R., A. M. Reginato, et al. (2000). "Bone development." Annu Rev Cell Dev Biol **16**: 191-220.

Onder, T. T., P. B. Gupta, et al. (2008). "Loss of E-cadherin promotes metastasis via multiple downstream transcriptional pathways." Cancer Res **68**(10): 3645-3654.

Ono, N., K. Nakashima, et al. (2007). "Constitutively active parathyroid hormone receptor signaling in cells in osteoblastic lineage suppresses mechanical unloading-induced bone resorption." J Biol Chem **282**(35): 25509-25516.

Otto, F., A. P. Thornell, et al. (1997). "Cbfa a candidate gene for cleidocranial dysplasia syndrome is essential for osteoblast differentiation and bone development." Cell **89**(5): 765-771.

Parfitt, A. M., M. K. Drezner, et al. (1987). "Bone histomorphometry: standardization of nomenclature, symbols, and units. Report of the ASBMR Histomorphometry Nomenclature Committee." J Bone Miner Res **2**(6): 595-610.

Park, I. K., S. J. Morrison, et al. (2004). "Bmi1, stem cells, and senescence regulation." J Clin Invest **113**(2): 175-179.

Park, I. K., D. Qian, et al. (2003). "Bmi-1 is required for maintenance of adult self-renewing haematopoietic stem cells." Nature **423**(6937): 302-305.

Park, S. B., K. W. Seo, et al. (2012). "SOX2 has a crucial role in the lineage determination and proliferation of mesenchymal stem cells through Dickkopf-1 and c-MYC." Cell Death Differ **19**(3): 534-545.

Passegue, E., A. J. Wagers, et al. (2005). "Global analysis of proliferation and cell cycle gene expression in the regulation of hematopoietic stem and progenitor cell fates." J Exp Med **202**(11): 1599-1611.

Pecina-Slaus, N. (2003). "Tumor suppressor gene E-cadherin and its role in normal and malignant cells." Cancer Cell Int **3**(1): 17.

Perry, J. M., X. C. He, et al. (2011). "Cooperation between both Wnt/{beta}-catenin and PTEN/PI3K/Akt signaling promotes primitive hematopoietic stem cell self-renewal and expansion." Genes Dev **25**(18): 1928-1942.

Phan, T. C., J. Xu, et al. (2004). "Interaction between osteoblast and osteoclast: impact in bone disease." Histol Histopathol **19**(4): 1325-1344.

Pietras, E. M., M. R. Warr, et al. (2011). "Cell cycle regulation in hematopoietic stem cells." J Cell Biol **195**(5): 709-720.

Polakis, P. (2000). "Wnt signaling and cancer." Genes Dev **14**(15): 1837-1851.

Purroy, J. and N. K. Spurr (2002). "Molecular genetics of calcium sensing in bone cells." Hum Mol Genet **11**(20): 2377-2384.

Qian, H., N. Buza-Vidas, et al. (2007). "Critical role of thrombopoietin in maintaining adult quiescent hematopoietic stem cells." Cell Stem Cell **1**(6): 671-684.

Ramsay, G. M., G. Moscovici, et al. (1990). "Neoplastic transformation and tumorigenesis by the human protooncogene MYC." Proc Natl Acad Sci U S A **87**(6): 2102-2106.

Rauch, D. A., M. A. Hurchla, et al. (2010). "The ARF tumor suppressor regulates bone remodeling and osteosarcoma development in mice." PLoS One **5**(12): e15755.

Rawadi, G., B. Vayssiere, et al. (2003). "BMP-2 controls alkaline phosphatase expression and osteoblast mineralization by a Wnt autocrine loop." J Bone Miner Res **18**(10): 1842-1853.

Rodda, S. J. and A. P. McMahon (2006). "Distinct roles for Hedgehog and canonical Wnt signaling in specification, differentiation and maintenance of osteoblast progenitors." Development **133**(16): 3231-3244.

Sadikovic, B., P. Thorner, et al. (2010). "Expression analysis of genes associated with human osteosarcoma tumors shows correlation of RUNX2 overexpression with poor response to chemotherapy." BMC Cancer **10**: 202.

Sadler, A. J., O. Latchoumanin, et al. (2009). "An antiviral response directed by PKR phosphorylation of the RNA helicase A." PLoS Pathog **5**(2): e1000311.

Sambandam, Y., K. Sundaram, et al. (2012). "CXCL13 activation of c-Myc induces RANK ligand expression in stromal/preosteoblast cells in the oral squamous cell carcinoma tumor-bone microenvironment." Oncogene.

Scotlandi, K., M. C. Manara, et al. (2003). "C-kit receptor expression in Ewing's sarcoma: lack of prognostic value but therapeutic targeting opportunities in appropriate conditions." J Clin Oncol **21**(10): 1952-1960.

Shiozawa, Y., E. A. Pedersen, et al. (2011). "Human prostate cancer metastases target the hematopoietic stem cell niche to establish footholds in mouse bone marrow." J Clin Invest **121**(4): 1298-1312.

Siegel, P. M. and J. Massague (2003). "Cytostatic and apoptotic actions of TGF-beta in homeostasis and cancer." Nat Rev Cancer **3**(11): 807-821.

Smith, K. N., A. M. Singh, et al. (2010). "Myc represses primitive endoderm differentiation in pluripotent stem cells." Cell Stem Cell **7**(3): 343-354.

Staal, F. J. and W. E. Fibbe (2012). "Wnt cross-talk in the niche." Blood **119**(7): 1618-1619.

Standal, T., M. Borset, et al. (2004). "Role of osteopontin in adhesion, migration, cell survival and bone remodeling." Exp Oncol **26**(3): 179-184.

Stanton, B. R., A. S. Perkins, et al. (1992). "Loss of N-myc function results in embryonic lethality and failure of the epithelial component of the embryo to develop." Genes Dev **6**(12A): 2235-2247.

Suda, T. (2011). "Hematopoiesis and bone remodeling." Blood **117**(21): 5556-5557.

Sugimura, R., X. C. He, et al. (2012). "Noncanonical Wnt signaling maintains hematopoietic stem cells in the niche." Cell **150**(2): 351-365.

Sugiyama, T., H. Kohara, et al. (2006). "Maintenance of the hematopoietic stem cell pool by CXCL12-CXCR4 chemokine signaling in bone marrow stromal cell niches." Immunity **25**(6): 977-988.

Sulzbacher, I., P. Birner, et al. (2007). "Expression of c-kit in human osteosarcoma and its relevance as a prognostic marker." J Clin Pathol **60**(7): 804-807.

Swiecki, M., Y. Wang, et al. (2011). "Type I interferon negatively controls plasmacytoid dendritic cell numbers in vivo." J Exp Med **208**(12): 2367-2374.

Takayanagi, H., S. Kim, et al. (2002). "Signaling crosstalk between RANKL and interferons in osteoclast differentiation." Arthritis Res **4 Suppl 3**: S227-232.

Takeda, K. and S. Akira (2004). "TLR signaling pathways." Semin Immunol **16**(1): 3-9.

Takeda, S., F. Elefteriou, et al. (2002). "Leptin regulates bone formation via the sympathetic nervous system." Cell **111**(3): 305-317.

Taketo, M. M. (2006). "Wnt signaling and gastrointestinal tumorigenesis in mouse models." Oncogene **25**(57): 7522-7530.

Tang, N., W. X. Song, et al. (2008). "Osteosarcoma development and stem cell differentiation." Clin Orthop Relat Res **466**(9): 2114-2130.

Tesio, M. and A. Trumpp (2011). "Breaking the cell cycle of HSCs by p57 and friends." Cell Stem Cell **9**(3): 187-192.

Teti, A. (2011). "Bone development: overview of bone cells and signaling." Curr Osteoporos Rep **9**(4): 264-273.

Trinchieri, G. (2010). "Type I interferon: friend or foe?" J Exp Med **207**(10): 2053-2063.

Trumpp, A., M. Essers, et al. (2010). "Awakening dormant haematopoietic stem cells." Nat Rev Immunol **10**(3): 201-209.

Tsiatis, A. C., M. E. Herceg, et al. (2009). "Prognostic significance of c-Myc expression in soft tissue leiomyosarcoma." Mod Pathol **22**(11): 1432-1438.

Udagawa, N., N. Takahashi, et al. (1999). "Osteoblasts/stromal cells stimulate osteoclast activation through expression of osteoclast differentiation factor/RANKL but not macrophage colony-stimulating factor: receptor activator of NF-kappa B ligand." Bone **25**(5): 517-523.

Udagawa, N., N. Takahashi, et al. (1995). "Interleukin (IL)-6 induction of osteoclast differentiation depends on IL-6 receptors expressed on osteoblastic cells but not on osteoclast progenitors." J Exp Med **182**(5): 1461-1468.

Ueda, T., J. H. Healey, et al. (1997). "Amplification of the MYC Gene in Osteosarcoma Secondary to Paget's Disease of Bone." Sarcoma **1**(3-4): 131-134.

Ullah, Z., C. Y. Lee, et al. (2009). "Cip/Kip cyclin-dependent protein kinase inhibitors and the road to polyploidy." Cell Div **4**: 10.

Urano, T., H. Yashiroda, et al. (1999). "p57(Kip2) is degraded through the proteasome in osteoblasts stimulated to proliferation by transforming growth factor beta1." J Biol Chem **274**(18): 12197-12200.

Vaananen, H. K., H. Zhao, et al. (2000). "The cell biology of osteoclast function." J Cell Sci **113 (Pt 3)**: 377-381.

van der Wath, R. C., A. Wilson, et al. (2009). "Estimating dormant and active hematopoietic stem cell kinetics through extensive modeling of bromodeoxyuridine label-retaining cell dynamics." PLoS One **4**(9): e6972.

Vijayakumar, S., G. Liu, et al. (2011). "High-frequency canonical Wnt activation in multiple sarcoma subtypes drives proliferation through a TCF/beta-catenin target gene, CDC25A." Cancer Cell **19**(5): 601-612.

Villar, V. H., O. Vogler, et al. (2012). "Nilotinib counteracts P-glycoprotein-mediated multidrug resistance and synergizes the antitumoral effect of doxorubicin in soft tissue sarcomas." PLoS One **7**(5): e37735.

Wada, T., T. Nakashima, et al. (2006). "RANKL-RANK signaling in osteoclastogenesis and bone disease." Trends Mol Med **12**(1): 17-25.

Walkley, C. R., R. Qudsi, et al. (2008). "Conditional mouse osteosarcoma, dependent on p53 loss and potentiated by loss of Rb, mimics the human disease." Genes Dev **22**(12): 1662-1676.

Walsh, M. C., N. Kim, et al. (2006). "Osteoimmunology: interplay between the immune system and bone metabolism." Annu Rev Immunol **24**: 33-63.

Wang, Z. Q., J. Liang, et al. (1995). "c-fos-induced osteosarcoma formation in transgenic mice: cooperativity with c-jun and the role of endogenous c-fos." Cancer Res **55**(24): 6244-6251.

Warner, B. J., S. W. Blain, et al. (1999). "Myc downregulation by transforming growth factor beta required for activation of the p15(Ink4b) G(1) arrest pathway." Mol Cell Biol **19**(9): 5913-5922.

Wei, H., M. Q. Zhao, et al. (2008). "Expression of c-kit protein and mutational status of the c-kit gene in osteosarcoma and their clinicopathological significance." J Int Med Res **36**(5): 1008-1014.

Wei, J., Y. Shi, et al. (2012). "miR-34s inhibit osteoblast proliferation and differentiation in the mouse by targeting SATB2." J Cell Biol **197**(4): 509-521.

Weinberg, R. A. (1995). "The retinoblastoma protein and cell cycle control." Cell **81**(3): 323-330.

Weisberg, E., R. D. Wright, et al. (2006). "Effects of PKC412, nilotinib, and imatinib against GIST-associated PDGFRA mutants with differential imatinib sensitivity." Gastroenterology **131**(6): 1734-1742.

Westendorf, J. J., R. A. Kahler, et al. (2004). "Wnt signaling in osteoblasts and bone diseases." Gene **341**: 19-39.

Wilson, A., E. Laurenti, et al. (2008). "Hematopoietic stem cells reversibly switch from dormancy to self-renewal during homeostasis and repair." Cell **135**(6): 1118-1129.

Wilson, A., E. Laurenti, et al. (2009). "Balancing dormant and self-renewing hematopoietic stem cells." Curr Opin Genet Dev **19**(5): 461-468.

Wilson, A., M. J. Murphy, et al. (2004). "c-Myc controls the balance between hematopoietic stem cell self-renewal and differentiation." Genes Dev **18**(22): 2747-2763.

Winkler, I. G., V. Barbier, et al. (2010). "Positioning of bone marrow hematopoietic and stromal cells relative to blood flow in vivo: serially reconstituting hematopoietic stem cells reside in distinct nonperfused niches." Blood **116**(3): 375-385.

Winkler, I. G., N. A. Sims, et al. (2010). "Bone marrow macrophages maintain hematopoietic stem cell (HSC) niches and their depletion mobilizes HSCs." Blood **116**(23): 4815-4828.

Woeckel, V. J., M. Eijken, et al. (2012). "IFNbeta impairs extracellular matrix formation leading to inhibition of mineralization by effects in the early stage of human osteoblast differentiation." J Cell Physiol **227**(6): 2668-2676.

Woeckel, V. J., M. Koedam, et al. (2012). "Evidence of vitamin D and interferon-beta cross-talk in human osteoblasts with 1alpha,25-dihydroxyvitamin D3 being dominant over interferon-beta in stimulating mineralization." J Cell Physiol **227**(9): 3258-3266.

Wu, C. H., J. van Riggelen, et al. (2007). "Cellular senescence is an important mechanism of tumor regression upon c-Myc inactivation." Proc Natl Acad Sci U S A **104**(32): 13028-13033.

Wu, W., X. Zhang, et al. (2007). "1alpha,25-Dihydroxyvitamin D(3) antiproliferative actions involve vitamin D receptor-mediated activation of MAPK pathways and AP-1/p21(waf1) upregulation in human osteosarcoma." Cancer Lett **254**(1): 75-86.

Xiao, G., D. Jiang, et al. (2005). "Cooperative interactions between activating transcription factor 4 and Runx2/Cbfa1 stimulate osteoblast-specific osteocalcin gene expression." J Biol Chem **280**(35): 30689-30696.

Yamaguchi, A., T. Komori, et al. (2000). "Regulation of osteoblast differentiation mediated by bone morphogenetic proteins, hedgehogs, and Cbfa1." Endocr Rev **21**(4): 393-411.

Yamazaki, S., H. Ema, et al. (2011). "Nonmyelinating Schwann cells maintain hematopoietic stem cell hibernation in the bone marrow niche." Cell **147**(5): 1146-1158.

Yang, S. Y., H. Yu, et al. (2007). "High VEGF with rapid growth and early metastasis in a mouse osteosarcoma model." Sarcoma **2007**: 95628.

Yasuda, H., N. Shima, et al. (1999). "A novel molecular mechanism modulating osteoclast differentiation and function." Bone **25**(1): 109-113.

Yin, T. and L. Li (2006). "The stem cell niches in bone." J Clin Invest **116**(5): 1195-1201.

Yook, J. I., X. Y. Li, et al. (2005). "Wnt-dependent regulation of the E-cadherin repressor snail." J Biol Chem **280**(12): 11740-11748.

Yukawa, K., H. Kikutani, et al. (1989). "Strain dependency of B and T lymphoma development in immunoglobulin heavy chain enhancer (E mu)-myc transgenic mice." J Exp Med **170**(3): 711-726.

Zeller, K. I., A. G. Jegga, et al. (2003). "An integrated database of genes responsive to the Myc oncogenic transcription factor: identification of direct genomic targets." Genome Biol **4**(10): R69.

Zeng, H., R. Yucel, et al. (2004). "Transcription factor Gfi1 regulates self-renewal and engraftment of hematopoietic stem cells." EMBO J **23**(20): 4116-4125.

Zhang, C., K. Cho, et al. (2008). "Inhibition of Wnt signaling by the osteoblast-specific transcription factor Osterix." Proc Natl Acad Sci U S A **105**(19): 6936-6941.

Zhang, H., R. Recker, et al. (2010). "Proteomics in bone research." Expert Rev Proteomics **7**(1): 103-111.

Zhou, S., K. Eid, et al. (2004). "Cooperation between TGF-beta and Wnt pathways during chondrocyte and adipocyte differentiation of human marrow stromal cells." J Bone Miner Res **19**(3): 463-470.

Zhou, Z. Q. and P. J. Hurlin (2001). "The interplay between Mad and Myc in proliferation and differentiation." Trends Cell Biol **11**(11): S10-14.

Zhou, Z. Q., C. Y. Shung, et al. (2011). "Sequential and coordinated actions of c-Myc and N-Myc control appendicular skeletal development." PLoS One **6**(4): e18795.

CONTRIBUTIONS

This dissertation would not have been possible without the critical contribution of several individuals.

First of all I would like to thank **Dr. Johannes Keller** for performing all histo-morphometric bone and serum analyses. Johannes is currently performing his own Ph.D. in the group of Professor Dr. Michael Amling at Universitätsklinikum Hamburg-Eppendorf, Institut für Osteologie und Biomechanik.

Many thanks to **Richard van der Wath** who applied mathematic modeling on the HSC data.

Nikolaus Dietlein joined the lab in January 2011. First as a research assistant and since January 2012 as my Master student and helped in several experiments. He is going to start his own Ph.D. in the group of Professor Rodewald at DKFZ in October 2012. **Simone Mumbauer** joined the lab in May 2011 until December 2011 as a research assistant and helped in finding the best antibodies for Western blot analyses.

All flow cytometry cell sorts were performed at Flow Cytometry Core Facility at DKFZ by **Klaus Hexel**, **Jens Hartwig**, **Gelo de la Cruz** and **Dr. Steffen Schmitt** (head of the department). **Tatjana Schmidt** and **Sabine Henze** performed mircoarrays at Genomics and Proteomics Core Facility at DKFZ.

A big thank to our technicians **Katja Müdder**, **Andrea Takacs**, **Corinna Klein** and **Melanie Neubauer** for their help in all animal-related issues and to **Anja Rathgeb** for managing all the mouse lines in the Animal Facility at DKFZ.

My special thanks go to **Stephan Wurzer**, **Armin Ehninger**, **Hind Medyouf** and **Michael Moos** for critically reading the manuscript and having fruitful discussions.

Acknowledgments

Completing a PhD is truly a memorable adventure and without the support of countless people it would have not been the same experience. However, acknowledging everyone is almost an impossible task. I therefore apologize that this list of people is rather short and I could not mention everyone.

Foremost, I would like to express my gratitude to **Andreas** for his supervision and for giving me the opportunity to conduct my Ph.D. in his lab.

Stephan, my Ph.D. twin! I am most grateful that I got to know you. From the beginning we had a good connection to each other and became very good friends. Thanks for sharing this adventure with many critical discussions, coffee, lots of fun and "Amelie"!
… and of course for using the red pen ;) Without you life´s so dull!

I further want to thank all the members of the **Trumpp lab** for discussions, support and technical expertise. In particular I want to thank **Armin** for critical discussions, his technical expertise, for adopting me next to his bench and many laughs, **Hind** for lively discussions and moral support, **Niko** for sharing troublesome times and a lively atmosphere with his encouraging phrases "nice, sweet, ein Traum", **Simon**, **Nina** and **Massimo** for always being up for a beer and **Marina** for her fast action in organizing things.

Last but not least I would like to thank my parents **Horst** and **Jutta** for always backing me up and supporting me, and my craziness. A special thank goes to **André**, I am so proud to have such an amazing and beloved brother. Above all, I am most grateful to my husband **Michael**, for his love, support, understanding and believing always in me, and my future perspectives!